

Taxonomic revision of *Romaleosyrphus* Bigot (Diptera, Syrphidae), including descriptions of seven new species

Kevin M. Moran^{1,2}, Jeffrey H. Skevington^{1,2}

1 Canadian National Collection of Insects, Arachnids and Nematodes, Agriculture and Agri-Food Canada, 960 Carling Avenue, Ottawa, ON K1A 0C6, Canada **2** Carleton University, Department of Biology, 1125 Colonel By Drive, Ottawa Ontario K1S 5B6, Canada

Corresponding author: Kevin M. Moran (syrphidae@kevinmoran.com)

Academic editor: Kurt Jordaens | Received 7 December 2020 | Accepted 10 August 2021 | Published 7 December 2021

<http://zoobank.org/9A026704-2C38-4B2C-9221-534780145848>

Citation: Moran KM, Skevington JH (2021) Taxonomic revision of *Romaleosyrphus* Bigot (Diptera, Syrphidae), including descriptions of seven new species. ZooKeys 1075: 1–32. <https://doi.org/10.3897/zookeys.1075.55862>

Abstract

The genus *Romaleosyrphus* Bigot is reviewed, including the description of seven new species (*R. argosi* Moran, **sp. nov.**, *R. bigoti* Moran, **sp. nov.**, *R. drysus* Moran, **sp. nov.**, *R. nephelaeus* Moran & Thompson, **sp. nov.**, *R. soletluna* Moran & Thompson, **sp. nov.**, *R. vockerothi* Moran & Thompson, **sp. nov.** and *R. woodi* Moran, **sp. nov.**). *Romaleosyrphus arctophiloides* (Giglio-Tos), **comb. nov.** is transferred to *Romaleosyrphus*. *Romaleosyrphus* **stat. rev.** is redefined to represent the monophyletic unit of species within Criorhinina which possess holoptic males, a proximal ventral half of vein C with setae, a broad intersection of vein R₁ with vein C, the distal part of R₄₊₅ beyond M₁ longer than cross-vein h and appressed pile on the abdomen. Descriptions, habitus and genitalia photographs, distributions, and an illustrated key for all nine *Romaleosyrphus* are presented. DNA barcode data are provided for eight of the species with a cytochrome c oxidase subunit I gene tree presented and discussed.

Keywords

Criorhinina, Eristalinae, flower fly, hoverfly, identification key, taxonomy

Introduction

Romaleosyrphus Bigot, 1882 are large flies of the family Syrphidae (Eristalinae, Milesiini, Criorhinina) and are Batesian mimics of *Bombus* Latreille, 1802. Williston (1892) combined the genus with *Crioprora* Osten Sacken, 1878, where it remained until Thompson (1976) combined it with *Criorhina* Meigen, 1822. *Romaleosyrphus* is Neotropical in distribution, with one described species, *R. villosus* Bigot 1882, and appears to be restricted to high elevation cloud forests. Members of this genus possess the classic anteroventrally produced face predominant throughout the subtribe Criorhinina. Little is known of their natural history, with larvae never illustrated or described, but like their relatives, immatures likely live on decaying roots, in rot holes, sap-runs, or decaying wood in general (Speight 2020).

Moran et al. (2021) resurrected *Romaleosyrphus*, as the single Neotropical species sampled was recovered sister to the genus *Matsumyia* Shiraki, 1930. Neotropical species concepts of *Criorhina* s. l. have never been reviewed. Considering this revived generic status, a detailed examination is necessary to explore species membership in the genus and to confirm that separation of *Matsumyia* from the older concept of *Romaleosyrphus* Bigot, 1882 is warranted.

In the present study we provide evidence to justify the split between *Romaleosyrphus* and *Matsumyia*, transfer *Criorhina arctophiloides* (Giglio-Tos, 1892) to *Romaleosyrphus*, describe seven new species of *Romaleosyrphus*, provide habitus and genitalia photographs and distributions for all the species, and provide the first identification key to the group.

Materials and methods

Examined collections

A list of material examined is provided in Suppl. material 1. All specimens are labelled with a unique reference number, either with their unique collection number or in the format KMMXXXX. Label data from the studied individuals were transcribed by hand into the online CNC database and can be accessed at <https://cnc.agr.gc.ca/>. Specimens were borrowed from the following institutions:

AMNH	American Museum of Natural History, New York, USA;
CNC	Canadian National Collection of Insects, Arachnids, and Nematodes, Ottawa, Ontario, Canada;
ECO-TAP-E	Colección Entomológica de la Unidad San Cristóbal de las Casas de El Colegio de la Frontera Sur, México (Philippe Sagot and Rémy Vandame);
EMEC	Essig Museum of Entomology, University of California, Berkeley, California, USA;
INHS	Illinois Natural History Survey, Champaign, Illinois, USA;
MRSN	Museo Regionale di Scienze Naturali, Torino, Italy;
MZH	Finnish Museum of Natural History, Helsinki, Finland;

MZLU	Lund Museum of Zoology, Lund, Sweden;
NHMUK	Natural History Museum UK, London, United Kingdom;
SEMC	Snow Entomological Museum Collection, University of Kansas, Lawrence, Kansas, USA;
UCRC	Entomology Research Museum, Department of Entomology, University of California, Riverside, California, USA;
USNM	National Museum of Natural History, Washington D.C., USA;
WIRC	University of Wisconsin Insect Research Center, Department of Entomology, University of Wisconsin, Madison, Wisconsin, USA.

Specimen photography, measurements, and figures

Morphological terminology follows Cumming and Wood (2017). Morphological features of some species were examined using an Olympus SZ60 and a Zeiss SteREO DiscoveryV12 stereo microscope. Whole habitus photographs of pinned specimens were taken using the base and StackShot parts of Visionary Digital Passport II system, an Olympus OM-D EM-5 Micro 4/3 camera with a 60mm f2.8 macro lens under illumination from a Falcon FLDM-i200 LED dome-light or using a Leica M205-C stereomicroscope equipped with a Leica DFC 450 module and using 0.6× (habitus) and 1.6× (genitalia) lenses. Final images were assembled using Zerene Stacker (<http://zerenesystems.com/cms/stacker>).

Photographs and descriptions are not restricted to primary types and represent our species concepts as a whole.

Male genitalia were detached after relaxation of specimens in a moisture chamber and then macerated in heated lactic acid overnight before examination and photography. Afterwards the lactic acid was deactivated, the genitalia stored in plastic micro vials containing glycerin, and attached to the pin of the dissected specimen.

Specimen measurements were taken using the Leica measurement module in Leica Application Suite (<https://www.leica-microsystems.com/products/microscope-software/p/leica-application-suite/>) and are based upon the smallest and largest specimen of each species. Body measurements represent the distance between the anterior end of the frons and the posterior end of tergite IV. Wing measurements represent the distance between the tegula and the apex of the wing. Maps include points from all specimens examined and were produced using SimpleMappr (<https://www.simplemappr.net/>).

In the description of primary type labels, the contents of each label are enclosed within double quotation marks (“ ”), italics denote handwriting, and the individual lines of data are separated by a double forward slash (//). At the end of each record, between square brackets ([]) and separated by a comma, the number of specimens and sex, the unique identifier or number, and the holding institution are given.

DNA Sequencing

The right mid leg was removed from selected specimens. Legs were processed in house at the Canadian National Collection of Insects (CNC) by Scott Kelso using a modified version of the (Hajibabaei et al. 2005) protocol with custom primers (see Table 1).

Table 1. Cytochrome *c* oxidase I mitochondrial gene primers used in this study.

Primer name	Primer design	Primer sequence
Heb-F	Folmer et al. 1994	GGT CAA CAA ATC ATA AAG ATA TTG G
COI-Fx-A-R	Kelso (in prep.)	CGD GGR AAD GCY ATR TCD GG
COI-Fx-B-F	Kelso (in prep.)	GGD KCH CCN GAY ATR GC
COI-Fx-B-R	Kelso (in prep.)	GWA ATR AAR TTW ACD GCH CC
COI-Fx-C-F	Kelso (in prep.)	GGD ATW TCH TCH ATY YTA GG
COI-780R	Gibson et al. 2011	CCA AAA AAT CAR AAT ARR TGY TG

The primers, COI-Fx-A-R, B-F, B-R, and C-F are designed to sequence the standard animal DNA barcode region in three portions, labeled A, B, and C after the primers, increasing the chance of successfully sequencing heavily fragmented DNA. This enabled DNA barcoding of species for which only older material, typically considered unsuitable for DNA barcoding, was available.

Raw sequence reads were evaluated using Sequencer v5.4.6 (<http://www.genecodes.com/>) and aligned together with downloaded BOLD data using MAFFT v7 (Kato and Standley 2013).

All sequence data obtained are stored online on the BOLD database (www.boldsystems.org). It is publicly accessible in the *Romaleosyrphus* (ROMALEO) dataset available at http://www.boldsystems.org/index.php/Public_SearchTerms?query=DS-ROMALEO.

Molecular data analysis

Neighbor-joining analysis using uncorrected p-distance was used to explore morphological species concepts for ingroup taxa utilizing PAUP v4.0a168 (Swofford 2001). *Blera fallax* (Linnaeus, 1758), *Milesia virginensis* (Drury, 1773), *Temnostoma alternans* Loew, 1864, and *Xylota flavifrons* Walker, 1849, which also belong to the tribe Milesiini, were used as outgroups of Criorhinina. For outgroups inside Criorhinina, we included any described species for which we possessed a DNA barcode. Pairwise distances were calculated using BOLD (see Table 2).

Taxa in the tree are labeled in the following format BOLD Process ID | Taxon Name | Institution Sample ID.

Table 2. Average intraspecific (diagonal) and interspecific (below diagonal) pairwise (p) distances (%) based on the barcode region of the mitochondrial cytochrome *c* oxidase subunit I gene of *Romaleosyrphus*.

	<i>R. arctophi-loides</i>	<i>R. argosi</i>	<i>R. bigoti</i>	<i>R. drysus</i>	<i>R. nephelaeus</i>	<i>R. soletluna</i>	<i>R. villosus</i>
<i>R. arctophi-loides</i>	–						
<i>R. argosi</i>	4.51	–					
<i>R. bigoti</i>	2.95	4.84	–				
<i>R. drysus</i>	4.26	3.05	3.99	–			
<i>R. nephelaeus</i>	3.58	3.31	3.13	2.85	0.97		
<i>R. soletluna</i>	3.68	5.36	3.04	4.52	3.58	0.93	
<i>R. villosus</i>	2.34	5.23	1.55	3.98	3.28	3.45	–
<i>R. vockerothi</i>	2.81	4.71	1.52	3.62	3.50	3.41	2.17

Results

Taxonomy and systematics

Romaleosyrphus Bigot, 1882

Figures 1–3

Romaleosyrphus Bigot, 1882a: 159. –Bigot (1882b): cxxix; –Bigot (1883): 356. Type species: *Romaleosyrphus villosus* Bigot, 1882 by original designation.

Rhomaleosyrphus Rye, 1884: 10. –Kertész (1910): 291. Unjustified emendation of *Romaleosyrphus*.

Crioprora Williston, 1891: 73. –Aldrich (1905): 401. –Coquillett (1910): 528.

Criorhina Thompson, 1976: 118.

Differential diagnosis. *Romaleosyrphus* is separated from *Criorhina* and *Sphecomylia* by the combination of the following characters. Male eye contiguous for ca. 1/2 length of ocellar triangle. Oval shaped postpedical. Broad intersection of vein R_1 with vein C. Proximal ventral half of vein C with setae. Abdominal pile appressed. Male genitalia with phallopodeme keeled and laterally sclerotized, not banana-shaped. It is further distinguished from *Matsumyia* by a distal part of vein R_{4+5} beyond vein M_1 longer than cross-vein h.

Redescription. MALE. Body length: 13.0–17.1 mm. Wing length: 8.0–12.1 mm.

Head. Face black, produced downwards and completely pruinose, concave beneath antenna, tuberculate; gena broad, as broad or broader than long, bare, shiny, pilose posteriorly; anterior tentorial pit short, extending along ventral third of eye, pilose; frontal prominence distinct; frons broad and pruinose; vertex triangular, longer than broad and always pilose; ocellar triangle small; eye bare, contiguous for ca. 1/2 length of ocellar triangle; head oval in shape; length of antenna segments in a 3:3:2 ratio; postpedical oval, with bare arista dorsally placed.

Thorax. Ca. as long as broad, long pilose; postpronotum pilose; proepimeron pilose; anterior anepisternum bare, posterior anepisternum pilose; scutellum without apical sulcus and with ventral pile fringe; katepisternum bare anteriorly, discontinuously pilose posteriorly with broadly separated patches; anepimeron with anterior portion pilose, and dorsomedial and posterior portion bare; katepimeron bare; metathoracic pleuron bare; without hypopleural pile at the base of the posterior thoracic spiracle; meron bare; metathoracic spiracle ca. same size as postpedical; metasternum pilose; postmetacoxal bridge incomplete; plumula simple, elongate, short, not reaching calypter margin; calypter brown.

Legs. Coxae pilose anteriorly, bare posteriorly; hind trochanter sometimes tuberculate in male; metafemur swollen, curved, with large apicoventral ridge and without basiventral setose patch; metatibia transverse apically, rounded basiventrally.

Wing. Cell r_1 open; stigmatic cross vein present; cross-vein r-m at outer 1/4 of cell dm; broad intersection of vein R_1 with vein C (Fig. 3); vein R_{4+5} straight; distance between apices of veins R_1 and R_{2+3} longer than distance between apices of veins R_{2+3} and



Figure 1. *Romaleosyrphus bigoti* sp. nov.



Figure 2. *Romaleosyrphus* distribution.

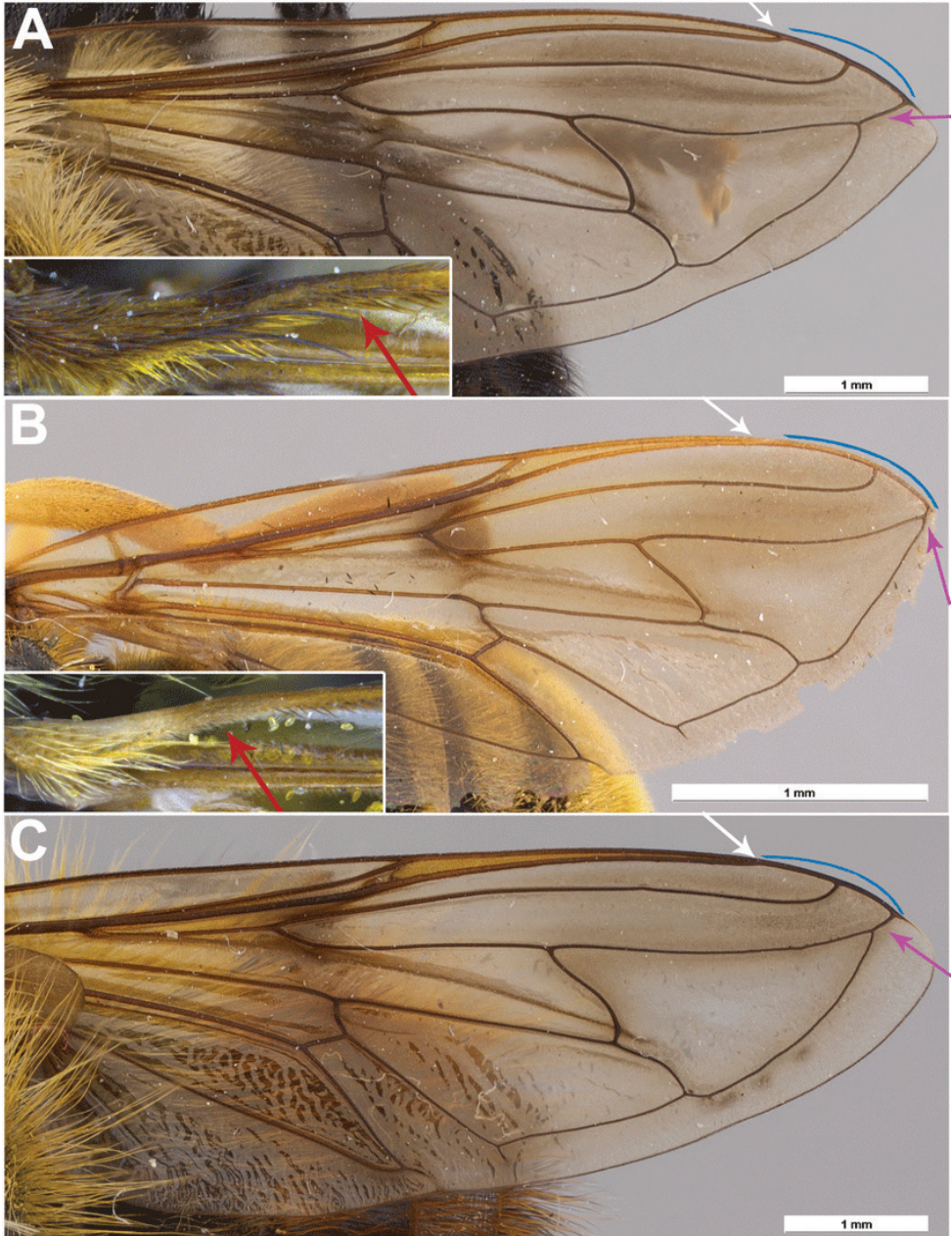


Figure 3. Intersection of vein R_1 with vein C (white), distance between apices of veins R_1 and R_{2+3} and apices of veins R_{2+3} and R_{4+5} (blue), distal vein R_{4+5} (pink) and setosity of proximal ventral half of vein C (red). **A** *Romaleosyrphus bigoti* sp. nov. **B** *Sphecomyia weismanni* (Moran) **C** *Criorhina bubulcus* (Walker).

vein R₄₊₅; distal part of vein R₄₊₅ beyond vein M₁ (hereafter distal vein R₄₊₅) longer than cross-vein h (Fig. 3); vein M₂ absent; vein CuP+CuA short, curved; proximal ventral half of vein C with setae.

Abdomen. Oval, slightly longer than broad, with dense appressed pile.

Male genitalia. Surstyli symmetric; aedeagus segmented, with phallapodeme separated from basiphallus and distiphallus; phallapodeme rounded, not banana-shaped; well-developed ctenidion present in male genitalia.

FEMALE. As male except for the following character states. Eyes widely separated; frons fully brown pruinose; face without pruinosity; metafemur only slightly swollen, never curved or with apicoventral ridge; metatibia never modified; always without tubercle on hind trochanter; wing always less microtrichose with species-specific characters as in species description.

Remarks. Generally, species of *Romaleosyrphus* show little variation in pile color patterns, at least given the limited material we worked with. However, there are a few exceptions. *Romaleosyrphus soletluna* Moran & Thompson, sp. nov. is drastically dimorphic in pile coloration with a mostly orange morph and mostly black morph. The single northern specimen of *Romaleosyrphus arctophiloides* from the Sierra Madre Occidental has fully black pilose legs. This contrasts with the population surrounding Mexico City, from which the type was collected, which have a streak of yellow pile at the base of the fore and mid femora. Finally, pile color on the proepimeron is variable inside multiple species with observed character states being fully yellow, fully black or a mix of the two. We suspect that additional material will likely show proepimeron pile color to be variable in all species.

Key to *Romaleosyrphus* species

- 1 Scutellum entirely black pilose, with only a few posterolateral yellow pile at most; post-alar callus extensively black pilose; male hind tibia as in Fig. 9D; male genitalia as in Fig. 11B ***R. soletluna* Moran & Thompson, sp. nov.**
- Scutellum partially yellow pilose; post-alar callus extensively yellow pilose **2**
- 2 Scutellum entirely rufous or yellow pilose **4**
- Scutellum black pilose medially **3**
- 3 Tergite II–III extensively rufous to yellow pilose; male hind trochanter not tuberculate (Fig. 8A); male hind tibia as in Fig. 9A; male genitalia as in Fig. 11A.....
..... ***R. arctophiloides* (Giglio-Tos)**
- Tergite II black pilose on posterolateral corners; Tergite III black pilose except yellow pilose anteromedially; male unknown but hind trochanter likely tuberculate (Fig. 8B) ***R. woodi* Moran, sp. nov.**
- 4 Tergite III extensively black pilose **6**
- Tergite III extensively rufous to yellow pilose **5**
- 5 Mesonotum entirely yellow to rufous pilose; male hind tibia as in Fig. 9D; male genitalia as in Fig. 11B ***R. soletluna* Moran & Thompson, sp. nov.**
- Mesonotum extensively black pilose medially; male hind tibia as in Fig. 9E; male genitalia as in Fig. 11D ***R. vockerothi* Moran & Thompson, sp. nov.**

- 6 Tergite IV extensively yellow pilose; male hind tibia as in Fig. 9C; male genitalia as in Fig. 11C.....*R. nephelaeus* Moran & Thompson, sp. nov.
 – Tergite IV entirely black pilose.....7
 7 Tergite II without black pile.....9
 – Tergite II with conspicuous black pile8
 8 Tergite II extensively white pilose, extending from anterolateral corners to posteromedial edge..... *R. argosi* Moran, sp. nov.
 – Tergite II black pilose except yellow pilose in anterolateral corners and along the posterior rim*R. drysus* Moran, sp. nov.
 9 Tergite II rufous pilose posteriorly; tergite III rufous pilose anteriorly; male hind tibia as in Fig. 9E; male genitalia as in Fig. 11F.....*R. villosus* Bigot
 – Tergite II without rufous pile; tergite III entirely black pilose; male hind tibia as in Fig. 9B; male genitalia as in Fig. 11E*R. bigoti* Moran, sp. nov.

***Romaleosyrphus arctophiloides* (Giglio-Tos, 1892), comb. nov.**

Figures 4A, 6A, 8A, 9A, 10A, 11A

Crioprora arctophiloides Giglio-Tos, 1892: 7. –Giglio-Tos (1893): 25. –Aldrich (1905): 401. Type locality: Mexico, Angang[ueo] [MRSN]

Penthesilea arctophiloides Kertész, 1910: 286.

Criorhina tapeta Fluke, 1939: 369. –Thompson (1976): 119. Type locality: Mexico City, 10,000 ft. [AMNH]

Criorhina arctophiloides Thompson, 1976: 118.

Material examined. MEXICO. Durango: 14 miles Southwest of El Salto, 23.702772, -105.564053, 2438m, 30.vi.1964, W.R.M. Mason, CNC_Diptera142464 (1♂, CNC); Mexico City, D.F.: San Pedro Atocpan, 19.204792, -99.048853, 2600m, 16.ix.1947, C. Bolivar, CNC_Diptera142465 (1♂, CNC); 1910, USNM_ENT1071372 (1♂, USNM); Mexico: Edo. de Mexico, km. 73rd to Popocatepetel, 19.075366, -98.65902, 3352m, 15.vii.1961, D.H. Janzen, EMEC354664 (1♀, EMEC); Nevado Toluca, 19.110036, -99.753425, 3200m, 11.vii.1951, H.E. Evans, Jeff_Skevington_Specimen52560 (1♂, CNC); 19.110035, -99.753423, 3444m, 11.vii.1951, P.D. Hurd, EMEC354662 (1♂, EMEC); West Slope, Cortez Pass, 19.08569, -98.648296, 2743m, 13.vii.1954, R.R. Dreisbach, KMM0919 (1♂, WIRC); 19.08569, -98.648296; 19.085692, -98.648297, 2743m; -13.vii.1954, CNC_Diptera142466; CNC_Diptera142467 (1♂, 1♀, CNC); Mexico City, 19.42250, -99.14389, 10000ft, vii.1936 (1♂ HT AMNH); Morelos: #17 Lagunas de Zempoala Nat. Park, 19.04828, -99.312179, 2865m, 23.viii.1969, G.W. Byers, KMM0920 (1♂, SEMC); Cuernavaca, 18.924211, -99.221567, 2133m, 29.vii.1961, R. & K. Dreisbach, J_Skevington_Specimen50177 (1♀, ANSP).

Differential diagnosis. Scutellum only partly yellow pilose, black pilose anteriorly and medially. Tergite II–III extensively rufous to yellow pilose. Tergite IV dominantly black pilose, but sometimes with rufous or yellow pile medially or posteriorly. Hind trochanter not tuberculate in male.

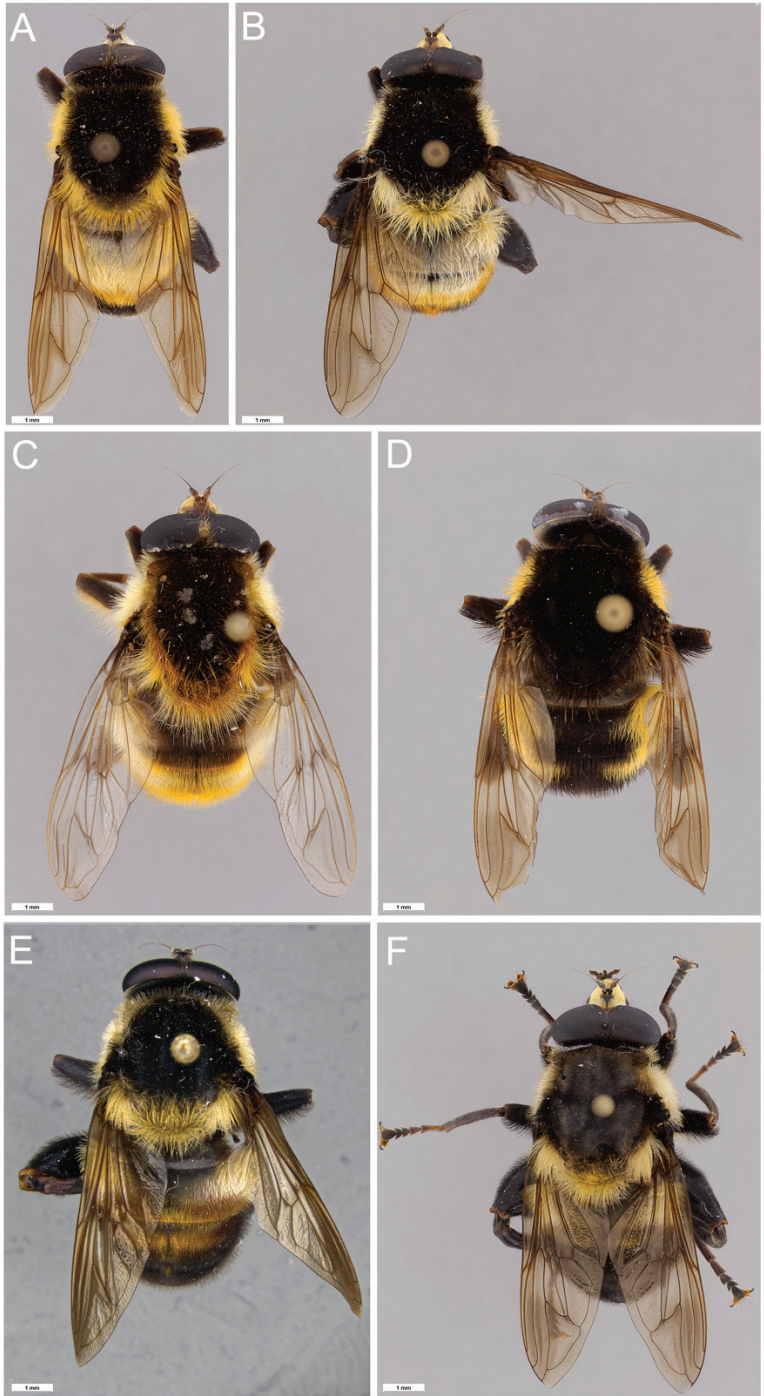


Figure 4. *Romaleosyrphus* dorsal habitus **A:** *Romaleosyrphus arctophiloides* **B:** *Romaleosyrphus vockerothi* sp. nov. **C:** *Romaleosyrphus soletluna* sp. nov. rufous morph **D:** *Romaleosyrphus soletluna* sp. nov. black morph **E:** *Romaleosyrphus villosus* **F:** *Romaleosyrphus bigoti* sp. nov.

Redescription. MALE. Body length: 13.1–14.8 mm. Wing length: 8.6–9.4 mm.

Head. Face shape as in Fig. 10A; face silver or gold pruinose; gena black pilose posteriorly; anterior tentorial pit variable pilose: yellow or black; frons broad, ca. as long as broad at antenna, 2/3 as broad at vertex as at antenna, black pilose and silver-gold pruinose; vertex triangular, longer than broad, black pilose and brown pruinose; postocular setae black; occipital setae variable: yellow or black; antenna reddish orange.

Thorax. Matte black; postpronotum variable pilose: black or mixed black and yellow; scutum black pilose; scutellum yellow pilose, except black pilose anteromedially; postalar callus variable pilose: yellow, black or mixed black and yellow; proepimeron black pilose; posterior anepisternum yellow pilose; katepisternum yellow pilose posteriorly with broadly separated patches; metasternum variable pilose: black, yellow or mixed black and yellow; anepimeron with anterior portion yellow pilose; lower calypter with long black pile.

Legs. Coxae black; femora black except extreme apex of femora; remainder of legs reddish; hind trochanter rounded, not tuberculate as in Fig. 8A; fore and mid-coxae black pilose; hind coxa mixed black and yellow pilose; fore femur black pilose, except occasionally with small mix of yellow pile basally; mid femur fully black pilose or with stretch of yellow pile on posterior side; hind femur black pilose; tibiae and tarsi black pilose; hind tibia as in Fig. 9A.

Wing. Microtrichia absent from following areas: broad anterior margin of cell cua.

Abdomen. Tergites shiny to subshiny black; tergite I with scattered, yellow pile medially, except with short black pile in lateral corners; tergite II with dense yellow pile; tergite III with dense pile which is yellow anteromedially, rufous from anterolateral corners to posteromedial margin and black in posterolateral corners; tergite IV variable, dominantly black pilose, but sometimes with rufous or yellow pile medially or posteriorly; grey pruinosity as follows: tergite I pruinose posteriorly, all of tergite II, tergite III except in posterolateral corners; sternites I–III yellow pilose and not pruinose; sternite IV variable: black or rufous pilose or some mix of the two; pile of postabdomen rufous or yellow.

Male genitalia. (Fig. 11A) Cercus yellowish brown, broader at apex, covered with long yellow pile; surstylus brown, ca. 2 × as long as broad, broadened basally with apical third tapering, directed ventrally and with an acute apex, ventral margin concave, undulated; pile on dorsal surface of surstylus, increasing in length posteriorly; minute spines on ventral surface and apical 3/4th of lateral inner and outer surface.

FEMALE. As male, except for usual sexual dimorphism; microtrichia on wing absent in following areas: broad anterior margin of cell cua, medial area of cell bm, anterior margin in cell dm, small region anteriorly in cell m₄ near cross-vein m-cu.

Distribution. Mexico.

Habitat. Trans-Mexican Volcanic Belt pine-oak forests ecoregion.

Remarks. *Romaleosyrphus arctophiloides* is the only known member of *Romaleosyrphus* in which the hind trochanter is not tuberculate in the male. Although males are not known for *Romaleosyrphus argosi* sp. nov., *R. drysus* sp. nov. and *R. woodi* sp. nov., males of their closest relative in the COI gene tree, *R. nephelaeus* sp. nov., possess

a tuberculate hind trochanter. It is therefore expected that males of these three species also have a tuberculate hind trochanter.

We suspect that a single specimen “CNC_Diptera142464” collected in the Sierra Madre Occidental may represent a distinct species from specimens collected in the Trans-Mexican Volcanic Belt pine-oak forests. Although no genital or discrete morphological differences could be found, the legs of this specimens are fully black pilose while those of all the others have a streak of yellow pile at the base of the fore and mid femora. Unfortunately, while a barcode was obtained for this specimen, no barcode sequences were obtained from specimens from specimens collected in the Trans-Mexican Volcanic Belt pine-oak forests.

***Romaleosyrphus argosi* Moran, sp. nov.**

<http://zoobank.org/0DC38597-3C3D-4846-AB0D-32DB952E3E43>

Figures 5D, 7D

Type locality. GUATEMALA: **San Marcos:** Bojonal Rd., 1.3 km, 14.9333, -91.8667, 1600m.

Types. *Holotype* female, pinned. Original label: “Guatemala: San Marcos // km 1.3, Bojonal Road // 14° 56'N 91° 52'W 1600m // 13-14. vii. 2001 DCH, DY” “Univ. Calif. Riverside // Ent. Res. Museum // UCRC ENT 66852” (UCRC).

Differential diagnosis. Scutellum white pilose. Tergite II extensively white pilose, except with black pile in posterolateral corners. Tergite III black pilose, except with mixed white pile anteromedially. Tergite IV black pilose.

Description. FEMALE. Body length: 12.5 mm. Wing length: 8.1 mm.

Head. Face non-pruinose; gena black pilose anteriorly; anterior tentorial pit black pilose; frons, black pilose and brown pruinose; vertex black pilose and brown pruinose; postocular setae black; occipital setae black; antenna reddish orange.

Thorax. Matte black; postpronotum white pilose; scutum white pilose along margins and black pilose medially; scutellum white pilose; postalar callus white pilose; proepimeron black pilose; posterior anepisternum white pilose; katepisternum white pilose posteriorly with broadly separated patches; metasternum mixed black and white pilose; anepimeron with anterior portion white pilose; lower calypter with long black pile.

Legs. Coxae black; femora black except extreme apex of femora; remainder of legs reddish; fore and mid-coxae black pilose; hind coxa mixed black and white pilose; fore femur black pilose, except small mix of white pile basally; mid femur black pilose, but with stretch of white pile on posterior side; hind femur black pilose; tibiae and tarsi black pilose.

Wing. Microtrichia absent in following areas: cell c along margin of vein Sc running from 2/5 and ending at 4/5 of length of the cell, anterior 1/5 of cell r_1 , cell br except along spurious vein the part right below the start of cell r_{2+3} , all of cell cua except extreme posterior, cell bm, cell cup along the margin of vein CuP in the anterior third of cell, cell m_4 from cross-vein m-cu to end of vein M_4 and in following regions of cell



Figure 5. *Romaleosyrphus* dorsal habitus (cont.) **A** *Romaleosyrphus woodi* sp. nov. **B** *Romaleosyrphus drysus* sp. nov. **C** *Romaleosyrphus nephelaeus* sp. nov. **D** *Romaleosyrphus argosi* sp. nov.

dm: anterior $\frac{1}{4}$, except extreme anterodorsal corner, ventral $\frac{1}{3}$, and broad margin adjacent to vein M_2 .

Abdomen. Tergites shiny to subshiny black; tergite I with scattered, white pile medially, except with short black pile in lateral corners; tergite II with dense white pile which runs diagonally from anterolateral corner until it reaches the posterior margin at a point which is ca. at $\frac{1}{3}$ width of the tergite, remainder of tergite is black pilose; tergite III with black pile except mixed white pile anteromedially; tergite IV with black pile; tergites not distinctly pruinose; sternites I–III white pilose and not pruinose; sternite IV black pilose; pile of postabdomen black.

MALE. Unknown.

Distribution. Guatemala.

Habitat. Central American montane forests ecoregion.

Etymology. Named *argosi*, from the Greek *argos* (white), to highlight the coloration of this species. It is a noun in apposition.

***Romaleosyrphus bigoti* Moran, sp. nov.**

<http://zoobank.org/F9ABF7C4-900A-42A1-9E33-B5D397AC1B39>

Figures 3A, 4F, 6F, 9B, 10B, 11E

Type locality. MEXICO: Chiapas: San Cristóbal de las Casas, Huitepec, 16.7603, -92.6814, 2560m.

Types. *Holotype* male, pinned. Original label: “Mexico-Chiapas // San-Cristobal-de-las-Casas // Huitepec Alt: 2560m. // N16°44’35”/W92°41’17” // 9-02-2009 // SAGOT P. n°7” “Diptera-Brachycera // Syrphidae // Criorhina sp. 1 // Male // Coll. SAGOT P. n°1016” “J. Skevington // Specimen # // 52561” (ECO-TAP-E).

Differential diagnosis. Scutellum yellow pilose. Tergite II completely yellow pilose. Tergite III black pilose. Tergite IV black pilose. Male hind tibia as in Fig. 9B. Male genitalia as in Fig. 11E.

Description. MALE. Body length: 15.2 mm. Wing length: 10.5 mm.

Head. Face shape as in Fig. 10B; face gold pruinose; gena black pilose posteriorly; anterior tentorial pit variable pilose: yellow or black; frons broad, ca. as long as broad at antenna, $\frac{2}{3}$ as broad at vertex as at antenna, black pilose and silver-gold pruinose; vertex triangular, longer than broad, black pilose and brown pruinose; postocular setae black; occipital setae variable: yellow or black; antenna reddish orange.

Thorax. Matte black; postpronotum mixed black and yellow pilose; scutum black pilose; scutellum yellow pilose; postalar callus yellow pilose; proepimeron yellow pilose; posterior anepisternum yellow pilose; katepisternum yellow pilose posteriorly with broadly separated patches; metasternum mixed black and yellow pilose; anepimeron with anterior portion yellow pilose; lower calypter with long black pile.

Legs. Coxae black; femora black except extreme apex of femora; remainder of legs reddish; hind trochanter tuberculate as in Fig. 8B; fore and mid-coxae black pilose; hind coxa mixed black and yellow pilose; fore femur black pilose, except small mix of yellow pile basally; mid femur black pilose, but with stretch of yellow



Figure 6. *Romaleosyrphus* lateral habitus **A** *Romaleosyrphus arctophiloides* **B** *Romaleosyrphus vockerothi* sp. nov. **C** *Romaleosyrphus soletluna* sp. nov. rufous morph **D** *Romaleosyrphus soletluna* sp. nov. black morph **E** *Romaleosyrphus villosus* **F** *Romaleosyrphus bigoti* sp. nov.

pile on posterior side; hind femur black pilose; tibiae and tarsi black pilose; hind tibia as in Fig. 9B.

Wing. Microtrichia absent from following areas: broad anterior margin of cell cua.

Abdomen. Tergites shiny to subshiny black; tergite I with scattered, yellow pile; tergite II with dense yellow pile; tergite III with black pile; tergite IV with black pile; grey pruinosity as follows: tergite I pruinose posteriorly, all of tergite II pruinose; sternites I–III yellow pilose and not pruinose; sternite IV black pilose; pile of postabdomen black.

Male genitalia. (Fig. 11E) Cercus yellowish brown, broader at apex, covered with long yellow pile; surstylus brown, ca. 4 × as long as broad, broadened basally with apical ha1/2lf tapering, directed ventrally and with a rounded apex, ventral margin

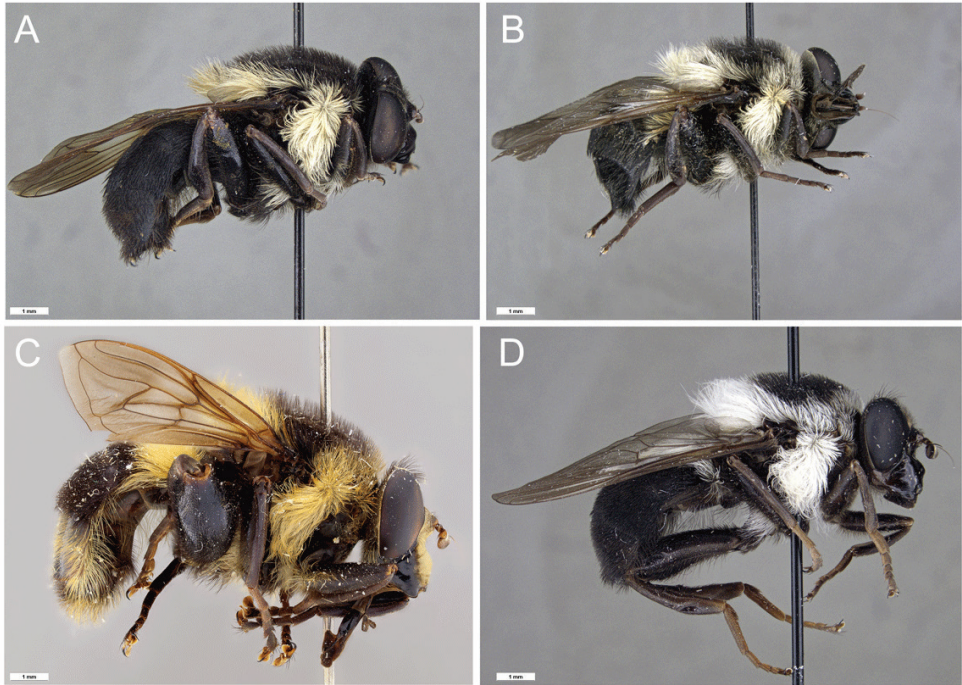


Figure 7. *Romaleosyrphus* lateral habitus (cont.) **A** *Romaleosyrphus woodi* sp. nov. **B** *Romaleosyrphus drysus* sp. nov. **C** *Romaleosyrphus nephelaeus* sp. nov. **D** *Romaleosyrphus argosi* sp. nov.

concave, undulated; pile on dorsal surface of surstylus, increasing in length posteriorly; minute spines on ventral surface and apical 3/4 of lateral inner and outer surfaces.

FEMALE. Unknown.

Distribution. Mexico.

Habitat. Central American pine-oak forests ecoregion.

Etymology. Named after Bigot who erected this genus in 1882.

***Romaleosyrphus drysus* Moran, sp. nov.**

<http://zoobank.org/10B87EF5-2E8A-457F-9F58-AB34F235E66E>

Figures 5B, 7B

Type locality. HONDURAS: La Muralla National Park, vicinity of visitor center, 15.1058, -86.7528, 1460m.

Types. *Holotype* female, pinned. Original label: “HONDURAS: Olancho // La Muralla National Park // vicinity of Visitor Center // 1460 m; 9-13 May 1999 // D.C. Hawks & J. Torres” “Univ. Calif., Riverside // Ent. Res. Museum // UCRC ENT 00035151” (UCRC).

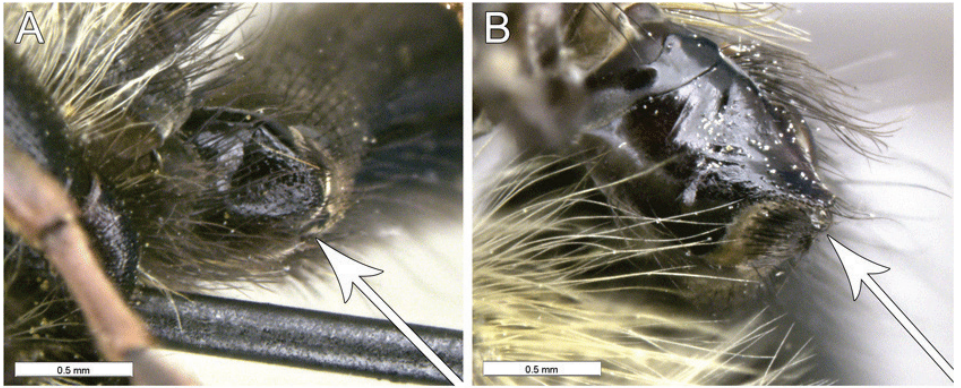


Figure 8. *Romaleosyrphus* 3rd trochanter tubercle **A** *Romaleosyrphus arctophiloides* **B** *Romaleosyrphus villosus*.

Differential diagnosis. Scutellum entirely yellow pilose. Tergite II black pilose except yellow pilose in anterolateral corners and along the posterior rim. Tergite III extensively black pilose.

Description. FEMALE. Body length: 13.4 mm. Wing length: 8.9 mm.

Head. Face non-pruinose; gena black pilose anteriorly; anterior tentorial pit black pilose; frons, black pilose and brown pruinose; vertex black pilose and brown pruinose; postocular setae black; occipital setae black; antenna reddish orange.

Thorax. Matte black; postpronotum yellow pilose; scutum yellow pilose along margins and black pilose medially; scutellum yellow pilose; postalar callus yellow pilose; proepimeron yellow pilose; posterior anepisternum yellow pilose; katepisternum yellow pilose posteriorly with broadly separated patches; metasternum mixed black and yellow pilose; anepimeron with anterior portion yellow pilose; lower calypter with long black pile

Legs. Coxae black; femora black except extreme apex of femora; remainder of legs reddish; fore and mid-coxae black pilose; hind coxa mixed black and yellow pilose; fore femur black pilose, except small mix of yellow pile basally; mid femur black pilose, but with stretch of yellow pile on posterior side; hind femur black pilose; tibiae and tarsi black pilose.

Wing. Microtrichia absent in following areas: cell c along margin of vein Sc running from 2/5 and ending at 4/5 of length of the cell, cell br except along margins of cell and along spurious vein and the part right below the start of vein r_{2+3} , all of cell cua except extreme posterior, ventral half of cell bm, cell m_4 from cross-vein m-cu to end of vein M_4 and cell dm in ventral 1/3 of cell and along broad margin following vein M_2 .

Abdomen. Tergites shiny to subshiny black; tergite I with scattered, yellow pile medially, except with short black pile in lateral corners; tergite II with dense yellow pile on anterior 2/3 and black pile on anterior third; tergite III with black pile; tergite IV with black pile; tergites not distinctly pruinose; sternites I–III yellow pilose and not pruinose; sternite IV black pilose; pile of postabdomen black.



Figure 9. *Romaleosyrphus* male hind tibia **A** *Romaleosyrphus arctophiloides* **B** *Romaleosyrphus bigoti* sp. nov. **C** *Romaleosyrphus nephelaeus* sp. nov. **D** *Romaleosyrphus soletluna* sp. nov. **E** *Romaleosyrphus villosus*.

MALE. Unknown.

Distribution. Honduras.

Habitat. Central American montane forests ecoregion.

Etymology. Named *drysus*, derived from the Greek *drys* for oak, in reference to the high elevation oak forests this species lives in. It is a noun in apposition.

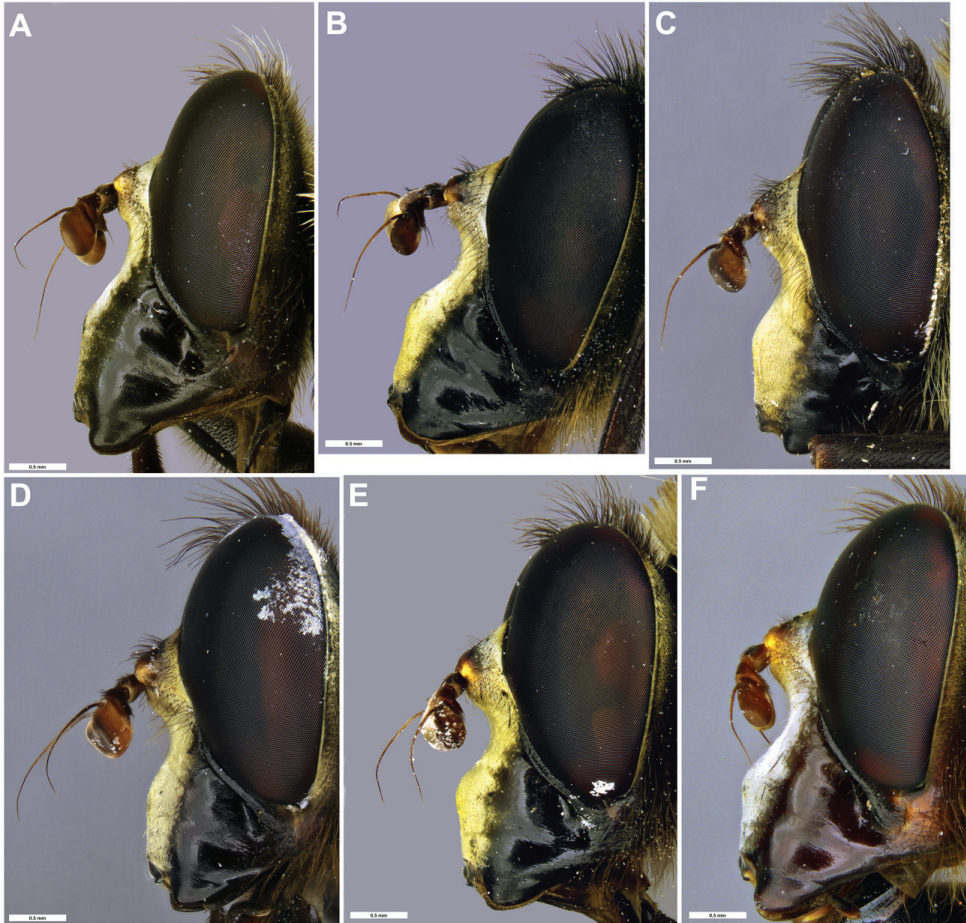


Figure 10. *Romaleosyrphus* male face **A** *Romaleosyrphus arctophiloides* **B** *Romaleosyrphus bigoti* sp. nov. **C** *Romaleosyrphus nephelaeus* sp. nov. **D** *Romaleosyrphus soletluna* sp. nov. **E** *Romaleosyrphus villosus* **F** *Romaleosyrphus vockerothi* sp. nov.

***Romaleosyrphus nephelaeus* Moran & Thompson, sp. nov.**

<http://zoobank.org/E32DF62B-3528-4C3B-8C5F-5B58631C6740>

Figures 5C, 7C, 9C, 10C, 11C

Type locality. EL SALVADOR: Montecristo, 14.3664, -89.3842.

Types. *Holotype* male, pinned. Original label: “4 – 20 – 1978 // Monte Cristo // El Salvador, CA // D. R. Barger” “USNMENT // [BARCODE] // 01087036” (USNM).

Paratypes: EL SALVADOR: Montecristo, 14.36639, -89.38417, D.R. Barger, 20.iv.1978, USNM_ENT1087030; ...USNM_ENT1087058; ...USNM_ENT1087078 (1♂, USNM, 1♂ CNC, 1♂ RMNH); roadside, J.H. Davis, 22.iv.1977, USNM_ENT1087092 (1♂, USNM).

Differential diagnosis. Scutellum completely yellow pilose. Tergite II black pilose, except yellow pilose in anterolateral corners. Tergite III black pilose, although lateral

margins mixed black and yellow. Tergite IV yellow pilose. Male hind tibia as in Fig. 9C. Male genitalia as in Fig. 11C.

Description. MALE. Body length: 13.1–17.2 mm. Wing length: 9.2–12.1 mm.

Head. Face shape as in Fig. 10C; face gold pruinose; gena yellow pilose posteriorly; anterior tentorial pit variable pilose: yellow or black; frons broad, ca. as long as broad at antenna, 2/3 as broad at vertex as at antenna, black pilose and silver-gold pruinose; vertex triangular, longer than broad, black pilose and brown pruinose; postocular setae black; occipital setae yellow; antenna reddish orange.

Thorax. Matte black; postpronotum mixed black and yellow pilose; scutum yellow pilose along margins and black pilose medially; scutellum completely yellow pilose; postalar callus yellow pilose; proepimeron yellow pilose; posterior anepisternum yellow pilose; katepisternum yellow pilose posteriorly with broadly separated patches; metasternum variable pilose: black, yellow, or mixed black and yellow; anepimeron with anterior portion yellow pilose; lower calypter with long black pile.

Legs. Coxae black; femora black except extreme apex of femora; remainder of legs reddish; hind trochanter tuberculate as in Fig. 8B; fore and mid-coxa black pilose; hind coxa mixed black and yellow pilose; fore femur black pilose, except small mix of yellow pile basally; mid femur black pilose, but with stretch of yellow pile on posterior side; hind femur black pilose; tibiae and tarsi black pilose; hind tibia as in Fig. 9C.

Wing. Microtrichia absent from following areas: broad anterior margin of cell cua.

Abdomen. Tergites shiny to subshiny black; tergite I with scattered, yellow pile medially, except with short black pile in lateral corners; tergite II black pilose, except yellow pilose in anterolateral corners; tergite III black pilose, except lateral margins mixed black and yellow; tergite IV yellow pilose; tergites not pruinose; sternites I–III yellow pilose and not pruinose; sternite IV black; pile of postabdomen mixed black and yellow pilose.

Male genitalia. (Fig. 11C) Cercus yellowish brown, broader at apex, covered with long yellow pile; surstylus brown, ca. as long as hypandrium, broadened basally with apical half tapering and directed ventrally with a rounded apex, ventral margin concave, undulated; pile on dorsal surface of surstylus, increasing in length posteriorly; minute spines on ventral surface and apical 3/4 of lateral inner and outer surface.

FEMALE. Unknown.

Distribution. El Salvador.

Habitat. Central American montane forests ecoregion.

Etymology. Named *nephelaeus*, after the Greek *nephele* (cloud), after the high elevation cloud forests in which this genus is found. It is a noun in apposition.

***Romaleosyrphus soletluna* Moran & Thompson, sp. nov.**

<http://zoobank.org/F2961868-C818-47D9-9F7F-07A6916C1674>

Figures 4C, D, 6C, E, 9D, 10D, 11B

Criorhina sp. Ståhls (2006): 25.

Romaleosyrphus sp. MZH Y247 Moran et al. (2021): 30.

Type locality. COSTA RICA, Villa Mills, 9.564227, -83.707515, 3000m.

Types. *Holotype* male, pinned. Original label: "COSTA RICA S José // Villa Mills 3000m // 24.II.87 D. M. Wood" "USNMENT // [BARCODE] // 01261985" (CNC).

Paratypes: COSTA RICA: **Cartago:** 11 mi. S.W. of Cartago, 9.730195, -84.034415, 1920m, C.D. Michner et al., 3.vii.1963, KMM0918 (1♀, USNM); **Guanacaste:** Est. Cacao. Guanacaste, 10.958528, -85.495649, 1200 to 1400m, Steve Marshall, 20.ii.1996, INBIOCRI002239730 (1♂, CNC); **Heredia:** Área de conservación Cordillera Volcánica Central, 9.555000, -83.670000, 1.ii.1990, R. Gerardo, INBIOCRI000154398 (1♂, INBIO); 15.iv.2002, Z. M. Ángel, INB0003945461; INB0003945468 (2♂, INBIO); 10.132, -84.125, 21.iv.2003, Z. M. Ángel, INB0003702365 (1♂, INBIO); Cerro Chompipe, Res. Biol. Chompipe, 10.088, -84.071, 1900m, G. & M. Wood, 17.i.1999, CNC_DIPTERA249643 (1♂, CNC); ...2100m, J.F. Corrales, 1994, INBIOCRI001146848; ...INBIOCRI001146849 (2♂, USNM); Parque Nacional Braulio Carrillo, Estación Barva, 10.133492, -84.121242, 2500m, J.F. Corrales, ii.1990, INBIOCRI000167748 (1♂, EMEC); ...A. Fernández, iii.1990, INBIOCRI00019854 (1♂, USNM); ...G. Rivera & A. Fernández, iii.1990, INBIOCRI000169854 (1♂, USNM); ...x.1989, INBIOCRI000108632 (1♀, USNM); ...xi.1989, INBIOCRI000139986 (1♂, CDFa); ...G. Rivera, ix.1989, INBIOCRI000111238 (1♀, USNM); **Puntarenas:** Área de conservación Arenal, 10.298, -84.793, 1.i.1993, O. Norman, INBIOCRI001369122 (1♂, INBIO); Est. La Casona, Res. Biol. Monteverde, 10.302815, -84.796543, 1520m, N. Obando, iii.1991, INBIOCRI001309535 (1♂, RMNH); Monteverde, Cerro Chomogo, 10.32689, -84.8058, 1800m, D.M. Wood, 22-30.viii.1996, CNC_DIPTERA249644 (1♂, CNC); Monteverde, 10.302815, -84.796543, 1500m, D.M. Wood, 24-28.ii.1991, USNM_ENT01261986 (1♂, USNM); Golfo Dulce, 3km SW. Rincón, 8.670722, -83.514359, 10m, H. Wolda, iii.1991, USNM_ENT1087008 (1♀, USNM); **San José:** Área de conservación La Amistad Pacífico, 9.555000, -83.670000, 13.i.1996, G. R. Billen, INBIOCRI002392420 (1♀, INBIO); 9.459000, -83.553000, 2.iii.1993, Z. M. Angel, INBIOCRI001305894 (1♀, INBIO); Cerro Muerte, 20 km S. Empalme, 9.566582, -83.749957, 2800m, Hanson, 11.vi.1990, USNM_ENT1087023 (1♀, USNM); **PANAMA: Chiriquí:** Guadalupe arriba, 8.871076, -82.550536, H. Wolda, 1.viii-4.ix.1984, USNM_ENT1087055 (1♂, USNM).

Differential diagnosis. Scutum entirely black pilose with at most only with a few anterolateral yellow pili on scutellum or mesonotum entirely yellow to rufous pilose. Male hind tibia as in Fig. 9D. Male genitalia as in Fig. 11B.

Description black morph. MALE. Body length: 13.8–15.3 mm. Wing length: 9.6–10.5 mm.

Head. Face shape as in Fig. 10D; face gold pruinose; gena black pilose posteriorly; anterior tentorial pit black pilose; frons broad, ca. as long as broad at antenna, 2/3 as broad at vertex as at antenna, black pilose and gold pruinose; vertex triangular, longer than broad, black pilose and brown pruinose; postocular setae black; occipital setae black; antenna reddish orange.

Thorax. Matte black; postpronotum mixed black and yellow pilose; scutum black pilose, except sometimes scattered yellow pile along lateral margins; scutellum black

pilose, except with scattered yellow pile along posterior margin; postalar callus black pilose or mixed black and yellow pilose; proepimeron yellow pilose; posterior anepisternum yellow pilose; katepisternum yellow pilose posteriorly with broadly separated patches; metasternum mixed black and yellow pilose; anepimeron with anterior portion yellow pilose; lower calypter with long black pile.

Legs. Coxae black; femora black except extreme apex of femora; remainder of legs reddish; hind trochanter tuberculate as in Fig. 8B; fore and mid-coxae black pilose; hind coxa mixed black and yellow pilose; fore femur black pilose, except small mix of yellow pile basally; mid femur black pilose, but with stretch of yellow pile on posterior side; hind femur black pilose; tibiae and tarsi black pilose; hind tibia as in Fig. 9D.

Wing. Microtrichia absent in following areas: broad anterior margin of cell cua, cell br except along spurious vein and the part right below the start of cell r_{2+3} ;

Abdomen. Tergites shiny to subshiny black; tergite I with scattered, yellow pile; tergite II with dense black pile medially and yellow pile on lateral sides; tergite III with black pile except mixed yellow pile anteromedially and yellow pile in anterolateral corners; tergite IV with black pile; tergites not distinctly pruinose; sternites I–III yellow pilose and not pruinose; sternite IV black pilose; pile of postabdomen black.

Male genitalia. (Fig. 11B) Cercus yellowish brown, broader at apex, covered with long yellow pile. Surstylus brown, ca. 2 × as long as broad, broadened basally with apical half tapering, directed downward and with an acute apex, ventral margin concave, undulated; pile on dorsal surface of surstylus, increasing in length posteriorly; minute spines on ventral surface and apical 3/4 of lateral inner and outer surfaces.

Description rufous morph. MALE. Same as black morph except as follows.

Head. Gena yellow pilose posteriorly; anterior tentorial pit yellow pilose; vertex rufous pilose; postocular setae rufous; occipital setae rufous.

Thorax. Postpronotum rufous pilose; scutum rufous pilose; scutellum rufous pilose; postalar callus rufous pilose.

Legs. Coxae yellow pilose; fore and mid femora yellow pilose; hind femur rufous pilose; tibiae and tarsi black pilose; metasternum yellow pilose.

Abdomen. Tergite II with dense rufous pile medially and yellow pile on lateral sides; tergite III with rufous pile except mixed yellow pile anteromedially and yellow pile in anterolateral corners; tergite IV with rufous pile; sternites I–IV rufous pilose; pile of postabdomen rufous.

FEMALE. As male, except for usual sexual dimorphism; microtrichia on wing absent in following areas: middle third of cell r_1 , cell r_{2+3} along margin of vein R_{2+3} on the anterior third of cell, cell br except along spurious vein and the part right below the start of cell r_{2+3} , all of cell cua except extreme posterior, ventral 2/3 of cell bm, cell cup along the margin of vein CuP in the posterior half, cell m_4 from cross-vein m-cu to end of vein M_2 and cell dm except for a thin line of microtrichia extending from cross-vein bm-m into middle of cell and the margins of cross-vein dm-m.

Distribution. Costa Rica and Panama.

Habitat. Talamancan montane forests (one specimen was collected in lowland rainforest).

Remarks. Color morphs are considered to be intraspecific variation. No morphological differences were found outside of pile coloration in male genitalia or external characters. Additionally, these morphs are not associated with distinct COI haplotypes. It is difficult to argue in favor of interspecific variation without the addition of contradictory genetic evidence or fieldwork showing these morphs do not interbreed.

Etymology. Named *soletluna*, a combination of the Latin words *sol*, for sun, and *luna*, for the moon. It is a reference to the duality of the color morphs in this species. It is a noun in apposition.

***Romaleosyrphus villosus* Bigot, 1882**

Figs 4E, 6E, 8B, 9E, 10E, 11F

Romaleosyrphus villosus Bigot, 1882a: 159. –Bigot (1882b): cxxix. –Bigot (1883): 356. –Williston (1886): 300. **Type locality.** Mexico. [BMNH]
Crioprora villosa Williston, 1891: 73. –Aldrich (1905): 401. –Coquillett (1910): 528. –Kertész (1910): 291.
Criorhina villosa Thompson, 1976: 119.

Material examined. EL SALVADOR. Montecristo, 14.36639, -89.38417, 20.iv.1978, D.R. Barger, USNM_ENT1087039 (1♂, USNM); near Metapán, Montecristo, 14.383639, -89.385111, 2300m, 8-10. v.1971, S. Peck, CNC_Diptera142469 (1♂, CNC); HONDURAS. **Santa Bárbara:** Santa Bárbara 11.5 km S. & 5.6 km W. Peñas Blancas, 14.968983, -88.091211, 1870m, 20.vi.1994, R. Anderson, CNC_Diptera101960 (1♀, CNC); **Francisco Morazán:** San Juancito, 14.220280, -87.0675, 30.iii.1982, R. W. Jones, TAMU-ENTOX0290054 (1♀, TAMU); **Olancho:** Catacamas, 15.83333, -85.85139, 02.iii.1996, R. Cave, MZLU2014394 (1♀ MZLU); MEXICO. **Chiapas:** Tzomtehuizt, near San Cristóbal, 16.833333, -92.633333, 19.v.1969, W.R.M. Mason, CNC_Diptera142472 (1♀, CNC).

Differential diagnosis. Scutellum yellow pilose. Tergite II yellow pilose anteriorly and rufous pilose posteriorly. Tergite III rufous pilose anteriorly and black pilose posteriorly. Tergite IV dominantly black pilose. Male hind tibia as in Fig. 9E. Male genitalia as in Fig. 11F.

Redescription. MALE. Body length: 13.8–15.3 mm. Wing length: 9.9–10.5 mm.

Head. Face shape as in Fig. 10E; face silver or gold pruinose; gena black pilose posteriorly; anterior tentorial pit black pilose; frons broad, ca. as long as broad at antenna, 2/3 as broad at vertex as at antenna, black pilose and silver-gold pruinose; vertex triangular, longer than broad, black pilose and brown pruinose; postocular setae black; occipital setae black; antenna reddish orange.

Thorax. Matte black; postpronotum variable pilose: black or mixed black and yellow; scutum black pilose; scutellum yellow pilose; postalar callus yellow pilose; proepimeron yellow pilose; posterior anepisternum yellow pilose; katepisternum yellow pilose posteriorly with broadly separated patches; metasternum variable pilose:

black, yellow, or mixed black and yellow; anepimeron with anterior portion yellow pilose; lower calypter with long black pile.

Legs. Coxae black; femora black except extreme apex of femora; remainder of legs reddish; hind trochanter tuberculate as in Fig. 8B; fore and mid-coxae black pilose; hind coxa mixed black and yellow pilose; fore femur black pilose, except small mix of yellow pile basally; mid femur black pilose, but with stretch of yellow pile on posterior side; hind femur black pilose; tibiae and tarsi black pilose; hind tibia as in Fig. 9E.

Wing. Microtrichia absent from following areas: broad anterior margin of cell cua;

Abdomen. Tergites shiny to subshiny black; tergite I with scattered, yellow pile; tergite II with dense yellow pile on anterior half and rufous pile on posterior half; tergite III with dense rufous pile on anterior third and black pile on posterior 2/3; tergite IV with black pile; grey pruinosity as follows: tergite I pruinose posteriorly, all of tergite II, tergite III anteriorly; sternites I–III yellow pilose and not pruinose; sternite IV black pilose; pile of postabdomen black.

Male genitalia. (Fig. 11F) Cercus yellowish brown, broader at apex, covered with long yellow pile; surstylus brown, ca. 3 × as long as broad, broadened basally with apical third tapering, directed ventrally and with a rounded apex, ventral margin concave, undulated; pile on dorsal surface of surstylus, increasing in length posteriorly; minute spines on ventral surface and apical 3/4 of lateral inner and outer surfaces.

FEMALE. As male, except for usual sexual dimorphism. Microtrichia on wing absent in following areas: broad anterior margin of cell cua, medial area of cell bm, anteriorly in cell dm.

Distribution. El Salvador, Honduras, and Mexico.

Habitat. Central American pine-oak forests ecoregion.

***Romaleosyrphus vockerothi* Moran & Thompson, sp. nov.**

<http://zoobank.org/E2735672-CD68-4C91-9E5A-71BE2ED6CF8F>

Figs 4B, 6B, 10F, 11D

Type locality. MEXICO: Durango: 14 miles Southwest of El Salto, 23.702771, -105.564051, 2438m.

Types. Holotype male, pinned. Original label: “MEX. Dgo. 14 mi. SW. // El Salto, 8000’ // 26 June 1964 // W. R. M. Mason” “CNC DIPTERA // # 142468” (CNC).

Paratypes: MEXICO: Durango: 14 miles Southwest of El Salto, 23.702771, -105.564051, 2438m, J.F. McAlpine, 26.vi.1964, CNC_Diptera142470 (1♂, RMNH); 30.vi.1964, CNC_Diptera142471 (1♂, CNC); 24 mi. W. La Ciudad, 23.723225, -106.065172, 2133m, J.F. McAlpine, 2.vii.1964, USNM_ENT01261987 (1♂, USNM).

Differential diagnosis. Scutellum completely yellow pilose. Tergites II and III extensively rufous to yellow pilose. Tergite IV dominantly black pilose. Hind trochanter tuberculate in male. Male hind tibia as in Fig. 9E. Male genitalia as in Fig. 11D.

Description. MALE. Body length: 13.8–14.5 mm. Wing length: 9.8–10.5 mm.

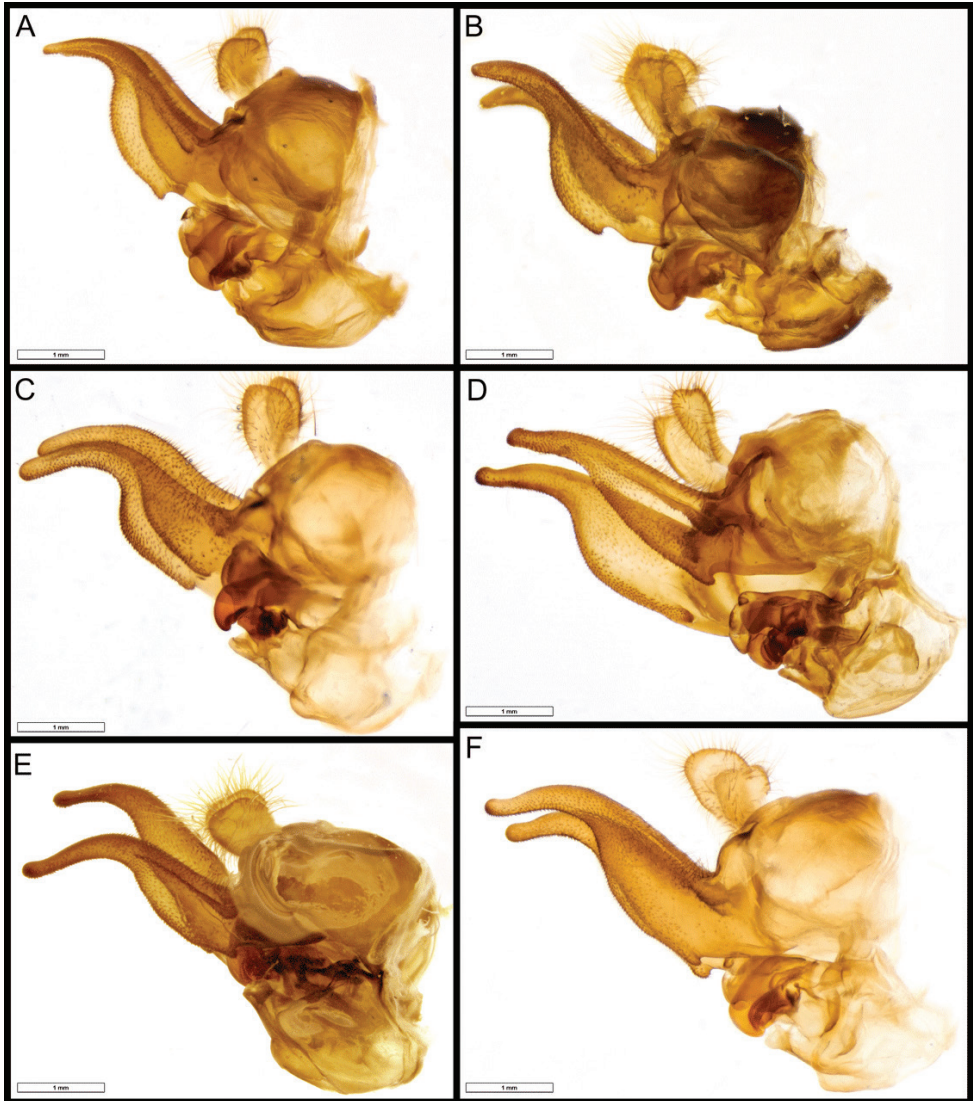


Figure 11. *Romaleosyrphus* male genitalia **A** *Romaleosyrphus arctophiloides* **B** *Romaleosyrphus soletluna* sp. nov. **C** *Romaleosyrphus nephelaeus* sp. nov. **D** *Romaleosyrphus vockerothi* sp. nov. **E** *Romaleosyrphus bigoti* sp. nov. **F** *Romaleosyrphus villosus*.

Head. Face shape as in Fig. 10F; face silver or gold pruinose; gena black pilose posteriorly; anterior tentorial pit black pilose; frons broad, ca. as long as broad at antenna, $2/3$ as broad at vertex as at antenna, black pilose and silver-gold pruinose; vertex triangular, longer than broad, black pilose and brown pruinose; postocular setae black; occipital setae variable: yellow or black; antenna reddish orange.

Thorax. Matte black; postpronotum variable pilose: black or mixed black and yellow; scutum either yellow pilose along margins with black pile medially, or completely

black pilose; scutellum completely yellow pilose; postalar callus variable pilose: yellow, black, or mixed black and yellow; proepimeron black pilose; posterior anepisternum yellow pilose; katapisternum yellow pilose posteriorly with broadly separated patches; metasternum variable pilose: black, yellow or mixed black and yellow; anepimeron with anterior portion yellow pilose; lower calypter with long black pile.

Legs. Coxae black; femora black except extreme apex of femora; remainder of legs reddish; hind trochanter tuberculate as in Fig. 8B; fore and mid-coxae black pilose; hind coxa mixed black and yellow pilose; fore femur black pilose, except small mix of yellow pile basally; mid femur black pilose, but with stretch of yellow pile on posterior side; hind femur black pilose; tibiae and tarsi black pilose; hind tibia as in Fig. 9E.

Wing. Wing completely microtrichose.

Abdomen. Tergites shiny to subshiny black; tergite I with scattered, yellow pile medially, except with short black pile in lateral corners; tergite II with dense yellow pile; tergite III with dense pile which is yellow anteromedially and rufous on the remainder; tergite IV with dense black pile, although sometimes red pilose medially; tergites I–III pruinose; sternites I–III yellow pilose and not pruinose; sternite IV variable: black or rufous pilose or some mix of the two; pile of postabdomen black or rufous.

Male genitalia. (Fig. 11D) Cercus yellowish brown, broader at apex, covered with long yellow pile; surstylus brown, distinctly longer than hypandrium, broadened basally with apical third tapering and not distinctly curved with a rounded apex, ventral margin concave, undulated; pile on dorsal surface of surstylus, increasing in length posteriorly; minute spines on ventral surface and apical 3/4th of lateral inner and outer surface.

FEMALE. Unknown.

Distribution. Mexico.

Habitat. Sierra Madre Occidental pine-oak forests.

Etymology. Named after J. R. Vockeroth in honor of his lifetime of work on Syrphidae and who was the first to recognize characters distinguishing this species from the sympatric *Romaleosyrphus arctophiloides* many years ago.

***Romaleosyrphus woodi* Moran, sp. nov.**

<http://zoobank.org/4DD32215-AD71-459C-9F57-CAFA17A3EAD1>

Figs 5A, 7A

Type locality. MEXICO: Chiapas: 16 mi. west of San Cristóbal, Chiapas, 16.7262, -92.8802.

Types. *Holotype* female, pinned. Original label: “San Christobal. // 16 mi W., Chiapas // MEX., VII-16-57” “UC Berkeley // EMEC // 354663 // [BARCODE]” (EMEC).

Differential diagnosis. Scutellum only partly yellow pilose, black pilose antero-medially. Tergite II black pilose in posterolateral corners. Tergite III black pilose except

yellow pilose anteromedially. Cell r_{2+3} bare along margin of vein R_{4+5} starting from 2/5 of length of cell and ending at cross-vein r-m.

Description. FEMALE. Body length: 13.1 mm. Wing length: 9.1 mm.

Head. Face non-pruinose; anterior tentorial pit black pilose; frons, black pilose and brown pruinose on lateral margins; vertex black pilose and brown pruinose; postocular setae black; occipital setae black; antenna reddish orange.

Thorax. Matte black; postpronotum mixed black and yellow pilose; scutum black pilose, except yellow pilose along lateral margins; scutellum yellow pilose, except black pilose anteromedially; postalar callus yellow pilose; proepimeron black pilose; posterior anepisternum yellow pilose; katepisternum yellow pilose posteriorly with broadly separated patches; metasternum mixed black and yellow pilose; anepimeron with anterior portion yellow pilose; lower calypter with long black pile.

Legs. Coxae black; femora black except extreme apex of femora; remainder of legs reddish; fore and mid-coxae black pilose; hind coxa mixed black and yellow pilose; fore femur black pilose, except small mix of yellow pile basally; mid femur black pilose, but with stretch of yellow pile on posterior side; hind femur black pilose; tibiae and tarsi black pilose.

Wing. Microtrichia absent in following areas: cell c along margin of vein Sc running from 2/5 of length and ending at 4/5 of length of the cell, anterior 1/5 of cell r_1 , r_{2+3} along margin of vein R_{4+5} starting from 2/5 of length and ending at cross-vein r-m, cell br except along spurious vein and the part right below the start of cell r_{2+3} , all of cell cua except extreme posterior, cell bm, cell cup along the margin of vein CuP in the anterior third of cell, cell m_4 from cross-vein m-cu to end of vein M_4 and cell dm in ventral 1/3 of cell and along broad margin following vein M_2 .

Abdomen. Tergites shiny to subshiny black; tergite I with scattered, yellow pile medially, except with short black pile in lateral corners; tergite II with dense yellow pile which runs diagonally from anterolateral corner until it reaches the posterior margin at a point which is ca. at 1/3 of the width of the tergite, remainder of tergite is black pilose; tergite III with black pile except mixed yellow pile anteromedially; tergite IV with black pile; tergites not distinctly pruinose; sternites I–III yellow pilose and not pruinose; sternite IV black pilose; pile of postabdomen black.

MALE. Unknown.

Distribution. Mexico.

Habitat. Central American pine-oak forests ecoregion.

Remarks. The specimen failed to barcode. Most similar in appearance to *Romaleosyrphus drysus* sp. nov. but *R. woodi* sp. nov. differs in having a scutellum which is only partly yellow pilose, instead having black pile anteromedially. Additionally, cell r_{2+3} is bare along the margin of vein R_{4+5} starting from 2/5 the length of cell and ending at cross-vein r-m.

Etymology. Named after dipterologist Monty Wood to honor his passion for flies and whose collecting trips throughout Central and South America provided many critical Syphidae for this as well as other future studies.

Species concepts and DNA barcoding

DNA barcode data (5' end of the COI) were collected for eight of nine morphospecies to provide a database to assist with future identifications of all life stages. Complete barcodes were obtained for all species except *R. woodi* sp. nov. Additional sequences for *Romaleosyrphus* were obtained from the BOLD database.

The rufous and black morphs of *R. soletluna* sp. nov. are not differentiated by COI haplotype showing that coloration should be considered intraspecific variation. The barcode differs by an average pairwise (p) distance of 3.04% from its nearest neighbor *Romaleosyrphus bigoti* sp. nov. It has a maximum intraspecific variation of 0.93% and an average of 0.56%.

Romaleosyrphus arctophiloides is related to the *R. villosus* complex of species (*R. villosus*, *R. vockerothi* sp. nov., *R. bigoti* sp. nov.) with the barcode 2.34% different from the nearest neighbor *Romaleosyrphus villosus*. This is the only known species of *Romaleosyrphus* in which males lack a tubercle on the hind trochanter.

Separation of *R. bigoti* sp. nov. and *R. vockerothi* sp. nov. species from *R. villosus* is supported by DNA barcoding. The barcoded types are 1.52% and 1.55% different from their closest neighbor, respectively. This distance is nearly twice as high as the maximum intraspecific variation seen in *R. soletluna* sp. nov. (0.93%) and *Romaleosyrphus nephelaeus* sp. nov. (0.97%). Morphological differences are found in the shape of the male genitalia as well as the shape of the male hind tibia.

The nearest neighbor of *R. argosi* sp. nov. is *Romaleosyrphus drysus* sp. nov. with the COI barcodes diverging by 3.05%. The nearest neighbor of *Romaleosyrphus drysus* sp. nov. is *Romaleosyrphus nephelaeus* sp. nov. with the COI barcodes diverging by an average of 2.85%. These distinct barcodes along with the unique pile coloration patterns of *Romaleosyrphus argosi* sp. nov. and *Romaleosyrphus drysus* sp. nov. support the recognition of these specimens as new species.

While the type of *R. woodi* sp. nov. failed to produce a barcode, morphological evidence was found in favor of its recognition as a distinct species. The species is most similar in appearance to *Romaleosyrphus drysus* sp. nov. but differs in having a scutellum which is only partly yellow pilose, instead having black pile anteromedially. Additionally, cell r_{2+3} is bare along the margin of R_{4+5} starting from $2/5$ the length of cell and ending at cross-vein r-m.

Discussion

Moran et al. (2021) resurrected *Romaleosyrphus* placing ‘*Romaleosyrphus* sp. MZH Y247’, now known as *Romaleosyrphus soletluna* sp. nov., sister to the genus *Matsumyia*.

In concordance with the neighbor-joining analysis, as well as the multi-gene analysis of Moran et. al (2021), morphological evidence supports the monophyletic origin of these Neotropical species, their relationship with *Matsumyia* and also their separation. The two genera share several characters and are distinguished from members of *Criorhina* and *Sphecomomyia* by: holoptic males, a proximal ventral half of vein C with

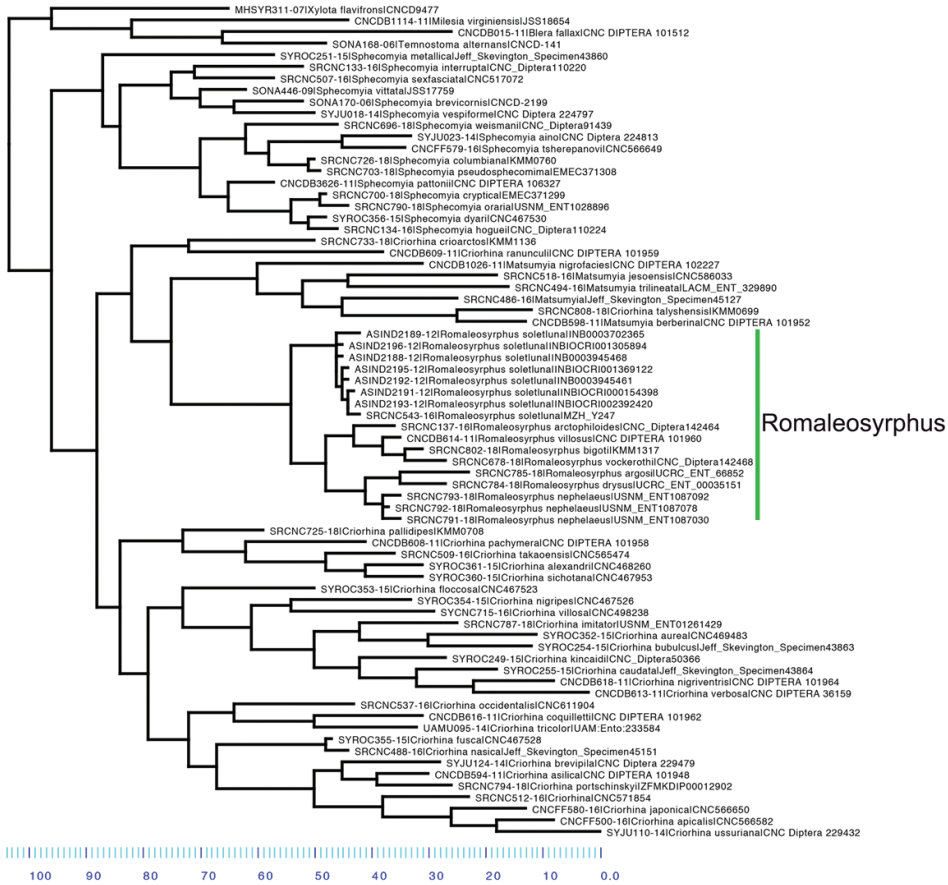


Figure 12. Neighbor-Joining tree based on the barcode region of the mitochondrial cytochrome *c* oxidase subunit I gene.

setae, a broad intersection of vein R_1 with vein C, and appressed hair on the abdomen. Additionally, *Romaleosyrphus* is further distinguished from *Matsumyia* by a distal R_{4+5} longer than cross-vein h. All species of *Matsumyia* examined, as part of an upcoming revision of the genus, however, had a distal R_{4+5} shorter than cross-vein h. *Romaleosyrphus* stat. rev. is therefore redefined to represent the monophyletic unit of species within *Criorhina* which possess these five character states.

Hampered by the rarity of *Romaleosyrphus* and the age of most specimens, more than one sequence was obtained for only two species and neither showed a high degree of intraspecific variation (Fig. 12). DNA barcodes reveal *R. soletluna* sp. nov. is dimorphic in pile coloration and these morphs are not associated with distinct COI haplotypes. The genetic distance between *Romaleosyrphus* species is lower than between species of most other *Criorhina* genera. For example, *Matsumyia* species show a much higher degree of species differentiation both for DNA barcodes and external morphological characters. It is possible that *Romaleosyrphus* diversified more recently. This may explain their less divergent intrageneric morphology and it would be worth investigat-

ing whether speciation coincided with the arrival of *Bombus* in Central America. Fresh material and more markers are needed to test these questions.

The discovery of the larvae of *Romaleosyrphus* would add critical biological knowledge about this genus and their microhabitats. Most likely, immatures live on decaying roots akin to the larvae of *Matsumyia berberina* (Fabricius, 1805), the most closely related species for which larvae is known, as also do larvae of some *Criorhina* species (Speight, 2020). Alternatively, larvae may be associated with rot-holes, sap-runs, or decaying wood in general as in other *Criorhina* species (Speight, 2020).

Moving forward, the authors suspect additional *Romaleosyrphus* species have yet to be discovered considering their apparent rarity and that their high elevation cloud forest habitat is highly conducive to speciation (Bruijnzeel, 2010). Currently, the center of diversity of the genus appears to be either the Central American montane forest ecoregion or the Central American pine-oak forest ecoregion, with three species each. One species each is known from the Sierra Madre Occidental pine-oak forest, the Talamancan montane forests and the Trans-Mexican Volcanic Belt pine-oak forests.

No species have been recorded from several similar ecoregions: Oaxacan, Chiapas, Chimalapas, and the Veracruz montane forests, along with the Sierra Madre de Oaxaca, Sierra Madre Oriental, Sierra Madre del Sur, and the Sierra de la Laguna pine-oak forests. It is also uncertain if the genus extends into the montane pine-oak forest ecoregions of South America. Additional collecting efforts focused on these ecoregions are necessary to discover the extent of *Romaleosyrphus* biodiversity.

Conclusion

Based upon molecular and morphological evidence we redefine *Romaleosyrphus* stat. rev. as the monophyletic unit of species within Criorhinina which possesses holoptic males, a proximal ventral half of vein C with setae, a broad intersection of vein R_1 with vein C, a distal R_{4+5} longer than cross-vein h, and appressed pile on the abdomen. This requires the transfer of *Romaleosyrphus villosus* (Bigot, 1882a) comb. nov. and *Romaleosyrphus arctophiloides* (Giglio-Tos, 1892) comb. nov. to *Romaleosyrphus*.

Acknowledgements

We would like to thank Scott Kelso for his assistance in DNA barcoding many of these specimens. Thanks to Chris Thompson who inspired a love of Syrphidae in the first author, and whose original work formed the foundation for several species concepts. Also, thanks to Jessica Hsiung for her illustration of *Romaleosyrphus* (Figure 1) and Torsten Dikow who mentored and hosted the senior author during his undergraduate internship at the Smithsonian. We also thank our reviewers, as their input resulted in an immensely improved paper. This study was supported by funding to JHS from Agriculture and Agri-Food Canada and a Discovery Grant from the Natural Sciences and Engineering Research Council of Canada.

References

- Aldrich, JM (1905) A catalogue of North American Diptera (or two-winged flies) VL – XLVI. Smithsonian Miscellaneous Collections 46 (2): 1–680. <https://doi.org/10.5962/bhl.title.1681>
- Bigot JMF (1882a) Descriptions de genres et espèces inédits de Syrphidés (3^{ème} partie). Bulletin de la Société Entomologique de France 14: 159–163. <https://biodiversitylibrary.org/page/4241989>
- Bigot JMF (1882b) Diagnoses de genres et espèces inédits de Syrphidés. 3^{ème} partie. Annales de la Société entomologique de France (6)2: 128–129. <https://biodiversitylibrary.org/page/8998058>
- Bigot JMF (1883) Diptères nouveaux ou peu connus. 21e partie, XXXII: Syrphidi (1^{ère} partie). Annales de la Société entomologique de France (6) 3: 221–258. [1883.10.31] <https://biodiversitylibrary.org/page/32548784>
- Bruijnzeel, LA, Scatena FN, Hamilton L (2010) Tropical Montane Cloud Forests: Science for Conservation and Management. Cambridge University Press, 768 pp. <https://doi.org/10.1017/CBO9780511778384>
- Coquillett DW (1910) The Type-Species of the North American Genera of Diptera. Proceedings of the United States National Museum 37: 499–622. <https://doi.org/10.5479/si.00963801.37-1719.499>
- Cumming JM, Wood DM (2017) Adult morphology and terminology. In: Kirk-Spriggs AHS, Sinclair BJ (Eds) Manual of Afrotropical Diptera. Volume 1. Introductory chapters and keys to Diptera families. Suricata 4. South African National Biodiversity Institute, Pretoria, 21–65.
- Folmer O, Black M, Hoeh W, Lutz R, Vrijenhoek R (1994) DNA primers for amplification of mitochondrial cytochrome *c* oxidase subunit I from diverse metazoan invertebrates. Molecular Marine Biology and Biotechnology 3: 294–299.
- Gibson JF, Kelso S, Jackson MD, Kits JH, Miranda GFG, Skevington JH (2011) Diptera-specific polymerase chain reaction amplification primers of use in molecular phylogenetic research. Annals of the Entomological Society of America 104: 976–997. <https://doi.org/10.1603/AN10153>
- Giglio-Tos E (1892) Diagnosi di nuove specie di Ditteri. VI. Bollettino dei musei di zoologia ed anatomia comparata della R. Università di Torino 7(123): 1–7. <https://doi.org/10.5962/bhl.part.12593>
- Giglio-Tos E (1893) Part I. Stratiomyidae – Syrphidae. Torino, 72 pp. [71 pl.]
- Hajibabaei M, deWaard JR, Ivanova NV, Ratnasingham S, Dooh RT, Kirk SL, Mackie PM, Hebert PDN (2005) Critical factors for assembling a high volume of DNA barcodes. Philosophical Transactions of the Royal Society B 360: 1959–1967. <https://doi.org/10.1098/rstb.2005.1727>
- Katoh K, Standley DM (2013) MAFFT multiple sequence alignment software version 7: improvements in performance and usability. Molecular Biology and Evolution 30: 772–780. <https://doi.org/10.1093/molbev/mst010>
- Kertész K (1910) Catalogus dipterorum hucusque descriptorum. VII. Museum Nationale Hungaricum, Budapest, 470 pp. <https://doi.org/10.5962/bhl.title.5147>

- Moran KM, Skevington JH, Kelso S, Mengual X, Jordaens K, Young AD, Ståhls G, Mutin V, Bot S, van Zuijlen M, Ichige K, van Steenis J, Hauser M, van Steenis W (2021) A multi-gene phylogeny of the cristaline flower flies (Diptera: Syrphidae), with emphasis on the subtribe Criorhinina. *Zoological Journal of the Linnean Society* 2021: zlab006. <https://doi.org/10.1093/zoolinlean/zlab006>
- Rye EC (1884) Index to genera and subgenera recorded as new in this volume. *Zoological Record* 19: 1–11.
- Ståhls G (2006) Placement of *Cacoceria* and phylogenetic relationships of the xylotine genera of the tribe Milesiini (Diptera, Syrphidae: Eristalinae) based on molecular characters. *Zootaxa* 1171: 17–29. <https://doi.org/10.11646/zootaxa.1171.1.2>
- Speight MCD (2020) Species accounts of European Syrphidae, 2020. Syrph the Net, the database of European Syrphidae (Diptera) 104: 1–314.
- Swofford DL (2001) PAUP*. Phylogenetic analysis using parsimony (*and Other Methods). 4.0b10 edn. Sinauer Associates, Inc., Sunderland.
- Thompson FC (1999) A key to the genera of the flower flies (Diptera: Syrphidae) of the Neotropical Region including descriptions of new genera and species and a glossary of taxonomic terms. *Contributions on Entomology, International* 3: 322–378.
- Thompson FC, Vockeroth JR, Sedman YS (1976) Family Syrphidae. A catalogue of the Diptera of the Americas south of the United States. Volume 46. Museu de Zoologia, Universidade de São Paulo, São Paulo, 195 pp. <https://doi.org/10.5962/bhl.title.110114>
- Williston SW (1886) Synopsis of the North American Syrphidae. *Bulletin of the United States National Museum* Vol. 31, 335 pp. <https://doi.org/10.5962/bhl.title.40963>
- Williston, SW (1891) Fam. Syrphidae. In: Godman FD, Salvin O (Eds) *Biologia Centrali-Americana – Zoologia – Insecta – Diptera*, Volume 3. Porter RH, London, 1–56. [2 pls] <https://doi.org/10.5962/bhl.title.730>

Supplementary material I

Romaleosyrphus material examined

Authors: Kevin M. Moran, Jeffrey H. Skevington

Data type: species data)

Copyright notice: This dataset is made available under the Open Database License (<http://opendatacommons.org/licenses/odbl/1.0/>). The Open Database License (ODbL) is a license agreement intended to allow users to freely share, modify, and use this Dataset while maintaining this same freedom for others, provided that the original source and author(s) are credited.

Link: <https://doi.org/10.3897/zookeys.1075.55862.suppl1>

Bringing order to a complex system: phenotypic and genotypic evidence contribute to the taxonomy of *Tityus* (Scorpiones, Buthidae) and support the description of a new species

Jairo A. Moreno-González¹, Ricardo Pinto-da-Rocha¹, Jonas E. Gallão²

1 Instituto de Biociências – Universidade de São Paulo, Departamento de Zoologia. Rua do Matão, travessa 14, 321, 005508-900, São Paulo, Brazil **2** Laboratório de Estudos Subterrâneos, Departamento de Ecologia e Biologia Evolutiva, Universidade Federal de São Carlos, Rodovia Washington Luís, km 235, 13565-905 São Carlos, Brazil

Corresponding author: Jairo A. Moreno-González (hansenochrus@gmail.com)

Academic editor: J. A. Ochoa | Received 17 April 2021 | Accepted 11 November 2021 | Published 7 December 2021

<http://zoobank.org/BB034E5C-10CB-4917-9FCD-EF6A72816F6C>

Citation: Moreno-González JA, Pinto-da-Rocha R, Gallão JE (2021) Bringing order to a complex system: phenotypic and genotypic evidence contribute to the taxonomy of *Tityus* (Scorpiones, Buthidae) and support the description of a new species. ZooKeys 1075: 33–75. <https://doi.org/10.3897/zookeys.1075.67459>

Abstract

We present a molecular phylogenetic analysis including a survey for overlooked phenotypic characters. Based on both analysis and characters a new cave-dwelling species is described: *Tityus* (*Tityus*) *spelaeus* **sp. nov.** from the Russão II cave, Posse, state of Goiás, Central Brazil. Characters such as the glandular regions of the female pectinal basal piece and basal middle lamellae of pectines, and the distribution of the ventral setae of telotarsi I–IV proved to be useful to constructing the taxonomy of species and species groups of *Tityus*. The new species is a member of the *Tityus trivittatus* species-group of *Tityus* (*Tityus*) and can be readily recognized by the immaculate coloration pattern and the more developed glandular region on the female pectinal basal piece. In addition, we provide a discussion of the phylogenetic relationships observed within *Tityus*, on the relevance of the new phenotypic characters to the modern taxonomy of the genus *Tityus*, and to the records of Brazilian cave scorpions.

Keywords

Cave, Neotropics, scorpion, South America, state of Goiás

Introduction

Among the Neotropical buthid genera, *Tityus* C. L. Koch, 1836 represents the most diverse genus, with more than 220 species (Francke and Stockwell 1987; Fet and Lowe 2000; Lourenço 2006; Souza et al. 2009; Lourenço 2015). The distribution of the genus is broad, ranging from Dominican Republic to Central Argentina (Francke and Stockwell 1987; Armas and Antún 2004; Souza et al. 2009). *Tityus* contains several species that have been considered dangerous to humans due to their potent venoms and involvement in scorpionism (Lourenço 2011, 2015; Borges and Graham 2016). Nevertheless, despite their richness, wide distribution, and medical importance, a detailed phenotypic study of *Tityus* species is lacking, rendering the genus as one of the most taxonomically problematic in the order (Junior 1932; Fet and Lowe 2000; Souza et al. 2009; Ojanguren-Affilastro et al. 2017b; Moreno-González et al. 2019; Ojanguren-Affilastro et al. 2021).

Great challenges need to be overcome before the taxonomy of *Tityus* can be fully resolved. Currently, the genus is one of the most difficult groups to work with, in view of the large number of species that are phenotypically similar, and the ineffectiveness of the somatic characters used to delimit species-groups. For example, Lourenço (2006) proposed the following five subgenera based on coloration; total size; degree of dilation of the basal middle lamellae of the female pectines; shape of the subaculear tubercle, and development of the fulcra of the pectines: *Tityus (Archaeotityus)* Lourenço, 2006, *Tityus (Atreus)* Gervais, 1843, *Tityus (Brazilotityus)* Lourenço, 2006, *Tityus (Caribetityus)* Armas & Marcano Fondeur, 1992, and *Tityus (Tityus)* Koch, 1836. Ever since, the monophyly of these groups has not been rigorously tested in a phylogenetic framework, and informal taxonomic categories, such as species-groups, are still prevalent (e.g., Borges et al. 2010; Ojanguren-Affilastro et al. 2017b).

Species-level distinctions are also problematic in *Tityus*. For the most part, species are defined based on the following characters: **i)** total body size; **ii)** coloration pattern; **iii)** pectinal tooth number; **iv)** number of oblique rows in the movable finger of pedipalp chela; **v)** morphometric ratios (particularly in males); **vi)** development and array of carinae of metasoma and pedipalp, and **vii)** shape of the subaculear tubercle (e.g., Lourenço 1984, 2002a, 2002b). However, some of these somatic characters, especially the meristic and morphometric characters, frequently overlap among different species, which makes it difficult to set species boundaries (e.g., Prendini 2001; Teruel and García 2008a, 2008b; Moreno-González et al. 2019).

The problems mentioned above, added to the fact that some species were described based on juveniles (e.g., *T. adisi* Lourenço & Pézier, 2002; *T. canopensis* Lourenço & Pézier, 2002), are worsened by the fact that there are few taxonomic publications including thorough phenotypic descriptions that incorporate genotypic data, comparative diagnoses, and imaging of different character states (e.g., pictures under UV light).

There have been a few modern taxonomic revisions of *Tityus*. For example, recently, Moreno-González et al. (2019) tested traditional (e.g., pectinal tooth and movable

finger denticle row counts; morphometric ratios) and new (e.g., glandular region in the pectinal basal piece of females and metasomal macrosetae) phenotypic characters to distinguish among Colombian species of *Tityus* (*Archaeotityus*). On the other hand, few phylogenies have included a small number of terminals of *Tityus* (e.g., Borges et al. 2010; Borges and Graham 2016; Ojanguren-Affilastro et al. 2017a; Ojanguren-Affilastro et al. 2021) and several terminals only once (e.g., Román et al. 2018). These studies have either used Sanger sequences only or analyzed morphological characters together with Sanger sequences (e.g., Esposito et al. 2017, 2018). Ojanguren-Affilastro et al. (2017b) used integrative taxonomy and different sources of evidence, such as Sanger sequences, phenotypic characters, and karyotypes, to support the description of a new species: *Tityus curupi* Ojanguren-Affilastro, Adilardi, Cajade, Ramóarez, Ceccarelli & Mola, 2017 from Northeastern Argentina. More recently, Ojanguren-Affilastro et al. (2021) used phenotypic characters and a molecular phylogeny, based on Sanger sequences, to redescribe *Tityus trivittatus* Kraepelin, 1898 and to describe a new species from Argentina: *Tityus carrilloi* Ojanguren-Affilastro, 2021. However, these efforts are far from sufficient and more contributions incorporating phenotypic and genotypic evidence are urgently needed to improve our current knowledge of *Tityus*.

Cave scorpions

How to classify subterranean organisms based on their restriction/adaptation to the cave habitat has been a matter of debate for a long time (see Trajano and Carvalho 2017 for a review of the most used classification of subterranean organisms). The most popular classification follows Schiner (1854), as emended by Racovitza (1907). It encompasses three categories: troglonexes, troglóphiles, and troglóbites. More recently, Trajano (2012) added metapopulation concepts to the Schiner-Racovitza system as follows: a troglóxene source is a population in epigeal habitats using subterranean resources; a troglóphile source population occurs both in epigeal and hypogeal habitats, and there is gene flow between habitats; a troglóbite source population inhabits exclusively subterranean habitats.

Arachnids (except Solifugae and Thelyphonida) are common in subterranean environments. Cave-dwelling taxa can be found among Acari, Amblypygi, Araneae, Opiliones, Palpigradi, Pseudoscorpiones and, to lesser extent, Ricinulei, Schizomida and Scorpiones (Trajano 1987; Pinto-da-Rocha 1995; Reddell 2012). Few species of scorpions inhabit subterranean habitats compared to other groups mentioned above, but all those scorpions are top predators (Volschenk and Prendini 2008; Reddell 2012).

Troglóbite scorpions are globally rare (Volschenk and Prendini 2008; Sissom and Reddell 2009; Lourenço and Duhem 2010; Reddell 2012; Lourenço and Pham 2013; Gallão and Bichuette 2016). Volschenk and Prendini (2008) redefined the concept of a troglóbite scorpion to species that are restricted to caves and exhibit remarkable troglomorphisms. The following are commonly recognized troglomorph scorpion

features: **i**) reduction or absence of ocelli (median and/or lateral); **ii**) absence of pedal spurs (prolateral and retrolateral); **iii**) reduction of pigmentation and sclerotization; and **iv**) attenuation of legs, pedipalps, and telson vesicle (Volschenk and Prendini 2008). Under this definition, a large proportion of the scorpion species previously recorded to be cave inhabitants fall into the troglaxene or troglophile categories (Lourenço 1981; Lourenço and Francke 1985; Volschenk and Prendini 2008).

Buthidae, the largest scorpion family (~1263 species) (Rein 2021), has few records from subterranean habitats (Volschenk and Prendini 2008; Gallão and Bichuette 2016; Prendini et al. 2021), whereas the buthid genus *Tityus*, the most diverse scorpion genus, has only nine species recorded from caves: *Tityus (Tityus) blaseri* Mello-Leitão 1931 (Brazil) [probably troglophile]; *Tityus (Tityus) confluens bodoquena* Lourenço, Cabral & Ramos, 2004 (Brazil) [troglophile]; *Tityus (Tityus) demangei* Lourenço 1981 (Ecuador) [probably troglaxene]; *Tityus (Tityus) jussarae* Lourenço, 1988 (Ecuador) [troglaxene]; *Tityus (Tityus) grottoedensis* Botero-Trujillo & Flórez, 2014 (Colombia) [probably troglophile]; *Tityus (Atreus) magnimanus* Pocock 1897 (Venezuela) [troglophile or troglaxene]; *Tityus (Tityus) monaguensis* González-Sponga 1974 (Venezuela) [troglophile or troglaxene]; *Tityus (Atreus) obscurus* Gervais 1843 (Brazil) [probably accidental], and *Tityus (Tityus) stigmurus* (Thorell 1876) (Brazil) [majority of records probably accidental, but with troglophile populations in caves of the state of Sergipe (M.E. Bichuette pers. comm.)] (González-Sponga 1974; Lourenço 1981; Trajano 1987; Trajano and Moreira 1991; Pinto-da-Rocha 1995; Lourenço et al. 1997, 2004; Volschenk and Prendini 2008; Lourenço and Duhem 2010; Botero-Trujillo and Flórez 2014). Recently, Prendini et al. (2021) classified *T. grottoedensis* as troglaxene, and *T. demangei*, *T. magnimanus* and *T. monaguensis* as accidental. However, there are scarce field observations on the dependence on and use of subterranean habitats by most *Tityus* species.

In this contribution, we present a phylogenetic hypothesis including a survey for overlooked phenotypical characters. Based on both analysis and characters a new cave-dwelling species is described: *Tityus spelaeus* sp. nov. from Russão II cave, Posse, state of Goiás, Central Brazil. Also, we discuss the phylogenetic relationships observed within *Tityus*, on the relevance of the new phenotypic characters in the modern taxonomy of the genus, and to the records of Brazilian cave scorpions.

Materials and methods

Materials

The type-material of the new species is housed in the Laboratório de Estudos Subterrâneos (**LES/UFSCar**), São Carlos, Brazil (Curator: Dr. Maria E. Bichuette), in the Museu de Zoologia da Universidade de São Paulo (**MZSP**), São Paulo, Brazil (curator: Dr. Ricardo Pinto-da-Rocha), and the Cryo Collection of the Laboratory of Evolution and

Systematics of Arachnids (**IBALCC-RPDR**), Instituto de Biociências, Universidade de São Paulo, São Paulo, SP, Brazil (**IB-USP**). Other materials are listed in Appendix 1.

According to Lourenço (2019) the type material of *Tityus acutidens* Mello-Leitão, 1933 (MNRJ 27781); *Tityus blaseri* Mello-Leitão, 1931 (MNRJ 11282); *Tityus thelyacanthus* Mello-Leitão, 1933 (MNRJ 11280); *Tityus uniformis* Mello-Leitão, 1931 (MNRJ 7041), and *Tityus jeanvellardi* Lourenço, 2001 (MNRJ 7135) were destroyed during the fire that in 2018 consumed the Museu Nacional/ Universidade Federal do Rio de Janeiro (MNRJ). However, about half of the type materials of *Tityus* had been requested on loan, by the first and second authors in 2016 and survived the fire. This loan included all the aforementioned species except for *T. uniformis*, in addition to the following species: *Tityus aba* Candido, Lucas, de Souza, Diaz & Lira-da-Silva, 2005 (MNRJ 7655); *Tityus carvalhoi* Mello-Leitão, 1945 (MNRJ 7043); *Tityus dasyurus fulvipes* Mello-Leitão, 1945 (MNRJ 7051); *Tityus evandroi* Mello-Leitão, 1945 (MNRJ 7049); *Tityus intermedius iophorus* Mello-Leitão, 1931 [= *Tityus thelyacanthus*] (MNRJ 11280); *Tityus kuryi* Lourenço, 1997 (MNRJ 7035); *Tityus maranhensis* Lourenço, de Jesus Junior & Limeira-de-Oliveira, 2006 (MNRJ 11212); *Tityus martinpaechi* Lourenço, 2001 (MNRJ 7077); *Tityus munozi* Lourenço, 1997 (MNRJ 7036, 7136), and *Tityus nematochirus* Mello-Leitão, 1941 (MNRJ 7052). Other types of *Tityus* species not mentioned here and belonging to the MNRJ were destroyed during the fire.

Morphology

Specimens were studied under a Leica MZ75 stereomicroscope with an ocular micrometer. Z-stack pictures under white light and UV light were taken using a Leica MC 170 HD camera. Habitus pictures were taken under white light using a Nikon D3300 digital camera and a 65 mm lens. For Scanning Electron Microscopy (SEM) imaging, a pectine was dissected and cleaned in distilled water with neutral detergent by ultrasound for one minute. After cleaning, the pectine was washed with distilled water and dehydrated via an ethanol concentration gradient (70%, 80%, 90%, 96%, and 100%), giving it 5–15 min in each concentration. Dehydration was completed under critical point drying with the pectine mounted onto a SEM stub using copper tape, after which it was sputter-coated with gold. Stubs were photographed using a Zeiss DSM 940 at Imaging Laboratory of the Instituto de Biociências, Universidade de São Paulo, SP, Brazil (IB-USP). General parameters of pictures were edited with GIMP 2.10 (<http://www.gimp.org/>), whereas the plates were made with INKSCAPE 1.1 (<http://www.inkscape.org/>).

General terminology follows Stahnke (1970) and Sissom et al. (1990), except for metasoma and pedipalp carination (Prendini 2000, 2003a), cheliceral dentition in Buthidae (Vachon 1963), trichobothrial notations (Vachon 1974, 1975), nomenclature of the lateral eyes (Loria and Prendini 2014), sternum shape (Soleglad and Fet 2003), and notation of the ventrosubmedian macrosetal count on the leg telotarsi (Francke 1977). Classification for subterranean species follows Trajano (2012).

Abbreviations

Pedipalp carinae:

D	digital;	DMA	dorsomarginal;	ES	external secondary;
DE	dorsoexternal;	DS	dorsal secondary;	VE	ventroexternal;
DI	dorsointernal;	IM	internomedian;	VI	ventrointernal;
DM	dorsomedian;	EM	externomedian;	SA	secondary accessory.

Mesosoma, metasoma, and telson carinae:

DL	dorsolateral;	ML	median lateral;	VM	ventromedian;
DSM	dorsosubmedian;	VL	ventrolateral;	VSM	ventrosubmedian.

Others:

L	length;	H	height;	W	width.
----------	---------	----------	---------	----------	--------

Taxon sampling

The ingroup taxa comprised 31 terminals of 20 described species of *Tityus* (Table 2). Sequences for 16 terminals were generated for the first time for this study, whereas sequences for 15 other terminals were retrieved from Genbank (Table 2). The type species of three out of five *Tityus* subgenera were included in the analysis: *Tityus* (*Archaeotityus*) (i.e., *Tityus clathratus*); *Tityus* (*Atreus*) (i.e., *Tityus forcipula*), and *Tityus* (*Tityus*) (i.e., *Tityus bahiensis*). The taxon sampling was based on the unpublished results of the first author's Ph.D. dissertation (Moreno-González 2021) and intend to test the phylogenetic placement of *Tityus spelaeus* sp. nov. The tree was rooted using *Isometrus maculatus* (DeGeer 1778) following Esposito et al. (2017, 2018).

Collection of genotypic characters

We extracted genomic DNA from leg tissues using the protocol of Fetzner (1999) and kept voucher specimens in the IBALCC-RPDR. Extractions were quantified using a Thermo Scientific Nanodrop spectrophotometer. Genomic DNA was used as a template to amplify four loci (12S rRNA, 16S rRNA, 28S rRNA, and COI) using universal primers (Table 1) and the protocol described by Pinto-da-Rocha et al. (2014): PCR reactions had a volume of 25 μ L = 13.95 μ L Milli-Q H₂O, 5 μ L PCR buffer (Fermentas), 2 μ L MgCl₂, 1 μ L dNTPs (80 μ M) (Fermentas), 1 μ L primer (0.4 μ M) of each primer, and 0.05 μ L GoTaq DNA polymerase (Fermentas). To amplify 28S, we added 1.25 μ L dimethyl sulfoxide (DMSO) to the final solution. We conducted PCR reactions in an Eppendorf Mastercycler gradient thermal cycler with the following set-up (temperature/ time): 95 °C/ 5 min (initial denaturation),

Table 1. List of primers used to amplify DNA sequences of *Tityus* species. Abbreviations: **F** forward **R** reverse **T** temperature.

Locus	Primer	Sequences	Direction	Annealing (T, °C)	Reference
COI	LCO1490-jj2	5'-CHA CWA AYC AYA ARG AYA TYG G	F	49.3–62.0	Astrin et al. (2016)
COI	HCO2198-jj2	5'-ANA CTT CNG GRT GNC CAA ARA ATC A	R	57.9–66.7	Astrin et al. (2016)
12S	12Sai	5'-AAA CTA GGA TTA GAT ACC CTA TTA T	F	52.3	Kocher et al. (1989)
12S	12Sbi	5'-AAG AGC GAC GGG CGA TGT GT	R	64.6	Kocher et al. (1989)
12S	12Sop2r	5'-CCC TTA AAY YTA CTT TGT TAC GAC C	R	50	Pinto-da-Rocha et al. (2014)
16S	16Sbr	5'-CTC CGG TTT GAA CTC AGA TCA	F	57.7	Simon et al. (1994)
16S	16S_F	5'-CGA TTT GAA CTC AGA TCA	F	49.3	Gantenbein et al. (1999)
16S	16Sbr_mod	5'-GTG CAA AGG TAG CAT AAT CA	R	53.7	Gantenbein et al. (1999)
28S	28Sa (Sad3)	5'-GAC CCG TCT TGA AAC ACG GA	F	60.3	Whiting et al. (1997)
28S	28Srd5b	5'-CCA CAG CGC CAG TTC TGC TTA C	R	64.2	Schwendinger and Giribet (2005)
28S	28SBout	5'-CCC ACA GCG CCA GTT CTG CTT ACC	R	68	Schulmeister (2003)

followed by 35 cycles of 95 °C/ 30s (denaturation), 30s at different temperatures for each set of primers (annealing) (see Table 1), and 72 °C/ 60s (extension), ending with 72 °C/ 7 min (final extension) and an infinite hold of 4 °C (cooling). For specimens and markers that did not amplify, we used Phusion High-Fidelity DNA Polymerase Taq (Finnzymes), following the manufacturer's protocol for 1 µL DNA extract. For COI degenerated primers, we used a touch-down PCR with the parameters proposed by Astrin et al. (2016).

PCR amplifications were checked using electrophoresis of agarose gel (2% agarose). Positive amplifications were purified using Agencourt Ampure XP (Beckman Coulter), then quantified using a Thermo Scientific NanoDrop spectrophotometer. We prepared sequencing reactions with the BigDye Terminator v3.1 Cycle Sequencing Kit (Applied Biosystems), precipitated PCR products with sodium acetate, and sequenced using an ABI PRISM 3100 Genetic Analyzer/HITACHI (Applied Biosystems). Sequence editing (e.g., primer trimming) and contiguous sequence generation were made on AB1 files using Geneious R11 (<http://www.geneious.com>). Consensus sequences were checked against the NCBI nucleotides database using the BLAST algorithm to detect for possible contaminations. Sequences without contamination were grouped into FASTA files separated by loci, and then inspected to detect potential reverse complemented sequences.

Phylogenetic analysis

Sequence alignment

Ribosomal gene and intron sequences (12S rDNA, 16S rDNA, and 28S rDNA) were aligned using the E-INS-i algorithm of MAFFT (Katoh and Standley 2013). Protein-coding gene sequences (Cytochrome *c* Oxidase I- COI) were aligned using the L-INS-i algorithm. The COI alignment was translated and inspected for stop codons using Geneious R11 (<http://www.geneious.com>). A single concatenated matrix composed of

Table 2. List of terminals, voucher specimens, and sequences (GenBank accession numbers indicated) used in the phylogenetic analysis of *Tityus*. (*) Sequence already available on GenBank before the outset of this study. Abbreviations: NA, not applicable.

Species	Subgenus	Voucher	12S	16S	28S	COI
<i>Isometrus maculatus</i> (DeGeer, 1778)	NA	AMNH LP 1798	KY981825.1*	KY981921.1*	KY982111.1*	KY982207.1*
<i>Tityus argentinus</i> Borelli, 1899	<i>Tityus</i>	MACN Ar 35705	NA	KY674452*	KY674474*	KY674493*
<i>Tityus bahiensis</i> (Perty, 1833)	<i>Tityus</i>	IBALCC RPDR 00281	OK493267	OK493246	OK493233	OK561906
<i>Tityus blaseri</i> Mello-Leitão, 1931	<i>Tityus</i>	IBALCC RPDR 00027	OK493254	OK493248	OK493221	OK561901
<i>Tityus blaseri</i> Mello-Leitão, 1931	<i>Tityus</i>	IBALCC RPDR 00114	OK493256	OK493238	OK493223	OK561904
<i>Tityus braziliae</i> Lourenço & Eickstedt, 1984	<i>Tityus</i>	IBALCC RPDR 00168	OK493258	OK493239	OK493225	OK561902
<i>Tityus braziliae</i> Lourenço & Eickstedt, 1984	<i>Tityus</i>	IBALCC RPDR 00169	OK493259	OK493250	OK493226	OK561894
<i>Tityus braziliae</i> Lourenço & Eickstedt, 1984	<i>Tityus</i>	IBALCC RPDR 00199	OK493262	OK493242	OK493228	OK561907
<i>Tityus carvilloi</i> Ojanguren-Affilastro, 2021	<i>Tityus</i>	MACN Ar 35713	NA	KY674461*	KY674483*	KY674501*
<i>Tityus carvalhoi</i> Mello-Leitão, 1945	<i>Tityus</i>	MACN Ar 35708	NA	KY674455*	KY674477*	KY674495*
<i>Tityus charreyroni</i> Vellard, 1932	<i>Tityus</i>	IBALCC RPDR 00112	OK493255	OK493237	OK493222	OK561903
<i>Tityus clathratus</i> C. L. Koch, 1844	<i>Archaeotityus</i>	IBALCC RPDR 00192	OK493261	OK493241	NA	OK561895
<i>Tityus confuensis</i> Borelli, 1899	<i>Tityus</i>	MACN Ar 35709	NA	KY674456*	KY674478*	KY674496*
<i>Tityus curupi</i> Ojanguren-Affilastro et al. 2017	<i>Tityus</i>	MACN Ar 35693	NA	KY674422*	KY674430*	KY674438*
<i>Tityus curupi</i> Ojanguren-Affilastro et al. 2017	<i>Tityus</i>	MACN Ar 35694	NA	KY674423*	KY674431*	KY674439*
<i>Tityus curupi</i> Ojanguren-Affilastro et al. 2017	<i>Tityus</i>	MACN Ar 35695	NA	KY674424*	KY674432*	KY674440*
<i>Tityus curupi</i> Ojanguren-Affilastro et al. 2017	<i>Tityus</i>	MACN Ar 35723	NA	KY674421*	KY674429*	KY674437*
<i>Tityus curupi</i> Ojanguren-Affilastro et al. 2017	<i>Tityus</i>	MACN Ar 35724	NA	KY674457*	KY674479*	KY674497*
<i>Tityus forcipula</i> (Gervais, 1843)	<i>Atreus</i>	IBALCC RPDR 00256	OK493264	OK493251	OK493230	OK561898
<i>Tityus obscurus</i> (Gervais, 1843)	<i>Atreus</i>	IBALCC RPDR 00236	OK493263	OK493243	OK493229	OK561905
<i>Tityus panguana</i> Kovařík et al. 2015	<i>Tityus</i>	IBALCC RPDR 00268	OK493265	OK493244	OK493231	OK561908
<i>Tityus potameis</i> Lourenço & Giupponi, 2004	<i>Tityus</i>	IBALCC RPDR 00275	OK493266	OK493245	OK493232	OK561899
<i>Tityus sastrei</i> Lourenço & Flórez, 1990	<i>Atreus</i>	IBALCC RPDR 00382	OK493268	OK493252	OK493234	OK561897
<i>Tityus serrulatus</i> Lutz & Mello, 1922	<i>Tityus</i>	IBALCC RPDR 00016	OK493253	OK493247	OK493220	OK561900
<i>Tityus soratensis</i> Kraepelin, 1912	<i>Tityus</i>	MACN Ar 35712	NA	KY674460*	KY674482*	KY674500*
<i>Tityus spelaeus</i> sp. nov.	<i>Tityus</i>	IBALCC RPDR 00116	OK493257	OK493249	OK493224	NA
<i>Tityus stigmurus</i> (Thorell, 1876)	<i>Tityus</i>	IBALCC RPDR 00170	OK493260	OK493240	OK493227	OK561896
<i>Tityus uruguayensis</i> Borelli, 1901	<i>Tityus</i>	MACN Ar 35714	NA	KY674425*	KY674433*	KY674442*
<i>Tityus uruguayensis</i> Borelli, 1901	<i>Tityus</i>	MACN Ar 35715	NA	KY674462*	KY674484*	KY674502*
<i>Tityus uruguayensis</i> Borelli, 1901	<i>Tityus</i>	MACN Ar 35716	NA	KY674426*	KY674434*	KY674443*
<i>Tityus uruguayensis</i> Borelli, 1901	<i>Tityus</i>	MACN Ar 35717	NA	KY674427*	KY674435*	KY674444*
<i>Tityus uruguayensis</i> Borelli, 1901	<i>Tityus</i>	MACN Ar 35718	NA	KY674428*	KY674436*	KY674445*

all sequences was created using SequenceMatrix (Vaidya et al. 2011) and exported as a NEXUS file. The final file was visualized and edited in Geneious R11, where leading and trailing gaps were substituted by ‘N’ since they most probably corresponded to differential sequencer reading starting and ending points.

Tree search

Tree search was conducted in IQTREE using the maximum likelihood (ML) criterion (Minh et al. 2020), with the command line: “*iqtree -s matrix.nex -st DNA -spp partitions.nex -pre matrix.nex -m MFP -bb 1000 -ninit 1000 -nt 3*”. Molecular evolution models were selected for each partition based on the BIC value criterion. Ultrafast

Bootstrap values were calculated in IQTREE after 1000 replications. Tree files were edited with Figtree v1.4.4 (<https://github.com/rambaut/figtree/>) and INKSCAPE 1.1 (<http://www.inkscape.org/>).

Results

Phylogenetic relationships

The tree log-likelihood score was -12896.086. The best-fit models per molecular partition were TIM2+F+G4 (12S), TIM2+F+I+G4 (16S), TNe+R2 (28S), and TIM+F+I+G4 (COI). Based on the phylogenetic hypothesis that was obtained (Figs 1–3), the subgenus *Tityus* (*Tityus*), as currently defined, is polyphyletic and composed of at least three main lineages: one lineage includes the species-groups *T. bahiensis* (ultrafast bootstrap value (Ubst)= 74), *T. stigmurus* (Ubst= 100), and *T. trivittatus* (Ubst= 50), a second lineage corresponds to the *T. bolivianus* species-group (Ubst= 41), and a third lineage is that of the species *T. sastrei* (Figs 1–3). In order to arrive at a monophyletic *Tityus* (*Tityus*), it will be necessary to remove the *T. bolivianus* species-group from this subgenus and transfer *T. sastrei* to *Tityus* (*Atreus*) (Figs 1–3). We transferred *T. sastrei* to *Tityus* (*Atreus*), but think that additional data are needed to propose an appropriate subgeneric designation of the *T. bolivianus* species-group.

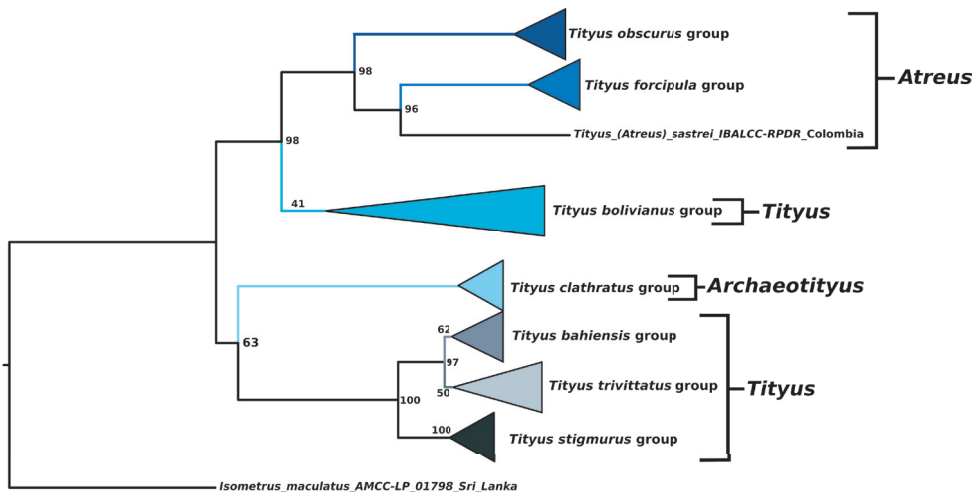


Figure 1. Phylogeny of *Tityus* representatives from South America obtained by analysis of DNA sequences (12S rDNA, 16S rDNA, 28S rDNA, and Cytochrome *c* Oxidase I- COI). Maximum likelihood tree (Log-likelihood= -12896.086), showing species-groups and subgenera. Values on nodes correspond to ultrafast-bootstrap (Ubst) values.

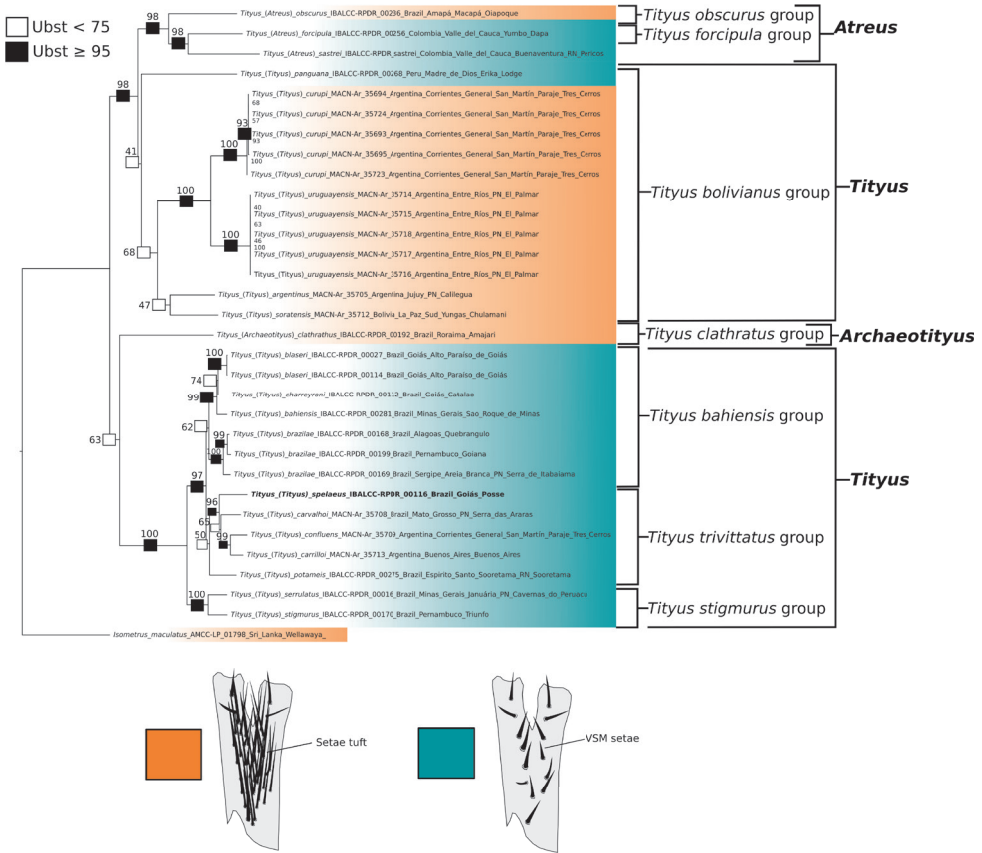


Figure 2. Phylogeny of *Tityus* representatives from South America obtained by analysis of DNA sequences (12S rDNA, 16S rDNA, 28S rDNA, and Cytochrome *c* Oxidase I- COI), showing the distribution of the characters states of the ventral setae of telotarsi I–IV (orange: an irregularly distributed tuft of setae (type I); turquoise: two ventro-submedian rows of setae (type II)) across different *Tityus* subgenera and species-groups. Boxes on branches and associated values correspond to ultrafast-bootstrap (Ubst) values. Observations= *Tityus (Tityus) spelaeus* sp. nov. is marked in bold.

Tityus (Archaeotityus) was recovered as the sister group (Ubst= 63) of a clade containing three *Tityus (Tityus)* species-groups (*T. bahiensis*, *T. stigmurus*, and *T. trivittatus* species-groups). On the other hand, a new species here described, *Tityus (Tityus) spelaeus* sp. nov., was recovered as a member of the *T. trivittatus* species-group (Ubst= 87) and is closely related to *T. carrilloi*, *T. carvalhoi*, and *T. confluens* (Figs 2, 3). Similarly, *Tityus (Atreus)* was recovered as polyphyletic with one clade composed of *T. (Atreus) forcipula*, *T. (Atreus) sastrei*, and *T. (Atreus) obscurus* (Ubst= 98), and another clade composed of *T. (Atreus) brazilae* (Ubst= 100) which is nested inside the *T. bahiensis* species-group (Figs 1–3). Therefore, to make *Tityus (Atreus)* a monophyletic group, *T. brazilae* is here formally transferred to the *T. bahiensis* species-group of *Tityus (Tityus)* (Figs 2, 3). Finally, the *T. bolivianus* species-group appeared as the sister group (Ubst= 98) of the clade composed of *Tityus (Atreus)* (Figs 2, 3).

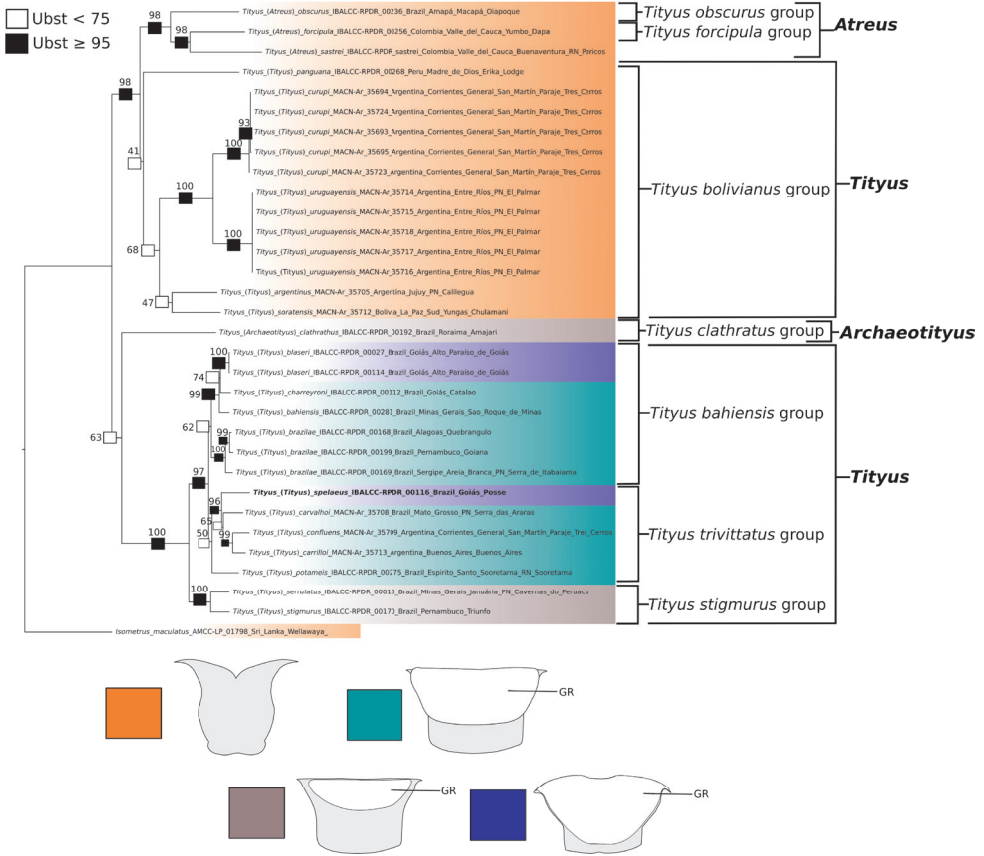


Figure 3. Phylogeny of *Tityus* representatives from South America obtained by analysis of DNA sequences (12S rDNA, 16S rDNA, 28S rDNA, Cytochrome *c* Oxidase I), showing distribution of the characters states exhibited by the female basal pectinal piece (orange: GR absent; grey: medium-sized GR; turquoise: relatively large GR; blue: very large GR) across different *Tityus* subgenera and species-groups. Boxes on branches and associated values correspond to ultrafast-bootstrap (Ubst) values. Observations=*Tityus (Tityus) spelaus* sp. nov. is marked in bold. Abbreviations= GR, glandular region.

Phenotypic characters

Ventral setae of telotarsi I–IV

We observed that the distribution of the ventral setae of telotarsi I–IV in *Tityus* can exhibit two states: **i**) an irregularly distributed tuft of setae (type I) (Figs 2, 4C, D, G, H) or **ii**) two ventro-submedian rows of setae (type II) (Figs 2, 4A, B, E, F, I–L) (Table 3). According to our phylogenetic hypothesis (Fig. 1) and a comprehensive total evidence analysis (e.g., Moreno-González 2021), the distribution of ventral macrosetae on telotarsi is highly homoplastic (Figs 2, 4; Table 3). For example, species-groups such as *T. bahiensis*, *T. bolivianus* [in part: *T. panguana*], *T. forcipula*, *T. stigmurus*, and *T. trivittatus*, and the species *T. sastrei* share ventral setation type II on telotarsi I–IV (Fig. 2; Table 3). Other species-groups such as *T. bolivianus*, *T. clathratus*, and *T. obscurus* exhibit ventral

Table 3. Phenotypic characters useful for the taxonomy of *Tityus*. (***) Species here transferred to the indicated subgenus; ventral macrosetae distribution on telotarsi I–IV: **Type I**= tuft of irregularly distributed macrosetae. **Type II**= two discrete ventrosubmedian rows of macrosetae. Abbreviations: BML, basal middle lamellae; D, dilated; NA, not applicable; ND, not dilated; PBP, pectinal basal piece.

Species	Subgenus	Species Group	Telotarsal setae	Females	
				PBP gland	BML
<i>Isometrus maculatus</i> (DeGeer, 1778)	NA	NA	Type II	Absent	ND
<i>Tityus argentinus</i> Borelli, 1899	<i>Tityus</i>	<i>T. bolivianus</i>	Type I	Absent	D= semicircular
<i>Tityus babiensi</i> (Perty, 1833)	<i>Tityus</i>	<i>T. babiensi</i>	Type II	First 2/3 of the anterior region	ND
<i>Tityus blaseri</i> Mello-Leitão, 1931	<i>Tityus</i>	<i>T. babiensi</i>	Type II	More than first 2/3 of the anterior region	ND
<i>Tityus braziliae</i> Lourenço & Eickstedt, 1984***	<i>Tityus</i>	<i>T. babiensi</i>	Type II	First 2/3 of the anterior region	ND
<i>Tityus carrilloi</i> Ojanguren-Affilastro, 2021	<i>Tityus</i>	<i>T. trivittatus</i>	Type II	First 2/3 of the anterior region	ND
<i>Tityus carvalhoi</i> Mello-Leitão, 1945	<i>Tityus</i>	<i>T. trivittatus</i>	Type II	First 2/3 of the anterior region	ND
<i>Tityus charreyroni</i> Mello-Leitão, 1933	<i>Tityus</i>	<i>T. babiensi</i>	Type II	First 2/3 of the anterior region	ND
<i>Tityus clathratus</i> C. L. Koch, 1844	<i>Archaeotityus</i>	<i>T. clathratus</i>	Type I	First anteromedian third	ND
<i>Tityus confluentis</i> Borelli, 1899	<i>Tityus</i>	<i>T. trivittatus</i>	Type II	First 2/3 of the anterior region	ND
<i>Tityus curupi</i> Ojanguren-Affilastro et al. 2017	<i>Tityus</i>	<i>T. bolivianus</i>	Type II	Absent	D= suboval
<i>Tityus forcipula</i> (Gervais, 1843)	<i>Atreus</i>	<i>T. forcipula</i>	Type II	Absent	D= suboval
<i>Tityus obscurus</i> Gervais, 1843	<i>Atreus</i>	<i>T. obscurus</i>	Type I	Absent	D= semicircular
<i>Tityus panguana</i> Kovařík et al. 2015	<i>Tityus</i>	<i>T. bolivianus</i>	Type II	Absent	D= semicircular
<i>Tityus potameis</i> Lourenço & Giupponi, 2004	<i>Tityus</i>	<i>T. trivittatus</i>	Type II	First 2/3 of the anterior region	ND
<i>Tityus sastrei</i> Lourenço & Flórez, 1990***	<i>Atreus</i>	NA	Type II	Absent	D= semicircular
<i>Tityus serrulatus</i> Lutz & Melo, 1922	<i>Tityus</i>	<i>T. stigmurus</i>	Type II	First anteromedian third	ND
<i>Tityus soratensis</i> Kraepelin, 1912	<i>Tityus</i>	<i>T. bolivianus</i>	?	Absent	D= semicircular
<i>Tityus spelaeus</i> sp. nov.	<i>Tityus</i>	<i>T. trivittatus</i>	Type II	More than first 2/3 of the anterior region	ND
<i>Tityus stigmurus</i> (Thorell, 1876)	<i>Tityus</i>	<i>T. stigmurus</i>	Type II	First anteromedian third	ND
<i>Tityus trivittatus</i> Kraepelin, 1898	<i>Tityus</i>	<i>T. trivittatus</i>	Type II	First 2/3 of the anterior region	ND
<i>Tityus uruguayensis</i> Borelli, 1901	<i>Tityus</i>	<i>T. bolivianus</i>	Type I	Absent	D= semicircular

setation type I on telotarsi I–IV (Fig. 2; Table 3). Morphological variations of this character were not observed within the same species or species-group (except for *T. panguana* in the *T. bolivianus* species-group, which exhibited ventral setation type II). However, both *Tityus* (*Atreus*) and *Tityus* (*Tityus*) exhibited the two character states (Fig. 2).

Development of pectinal basal piece and basal middle lamellae of female pectines

The pectinal basal piece of female exhibits the following character states within the examined terminals of *Tityus*: **i**) absence of glandular region (Figs 3, 5E, F, 6A, B; Table 3); **ii**) presence of a relatively large glandular region, occupying a large area of anterior two thirds of the anteromedian region (Figs 3, 5A, B; Table 3); **iii**) presence of a medium-sized glandular region, occupying the anterior third, but absent from the anterolateral margins (Figs 3, 5C, D, 6C, D; Table 3), and **iv**) presence of a very large glandular region, occupying beyond the anterior two thirds of the medial region (Figs 3, 6E, F; Table 3). According to our phylogenetic hypothesis (Fig. 1) and a comprehensive total evidence analysis (e.g., Moreno-González 2021), the character states exhibited by the glandular region of the female pectinal basal piece are highly homoplastic (Figs 3, 5, 6; Table 3).

However, it is noteworthy that in some *Tityus* (*Atreus*) (i.e., *Tityus forcipula* see Fig. 5E, F and *T. obscurus* see Fig. 6A, B species-groups and *T. sastrei*) and in the

Tityus bolivianus species-group, both of which lack a glandular region on the female pectinal basal piece (Fig. 3; Table 3), exhibit dilated middle basal lamellae with glandular regions in the female pectines (Table 3). Conversely, *Tityus* (*Archaeotityus*) (i.e., *T. clathratus* species-group) (Figs 3, 5C, D) and *Tityus* (*Tityus*) (i.e., *T. bahiensis* (Fig. 5A, B), *T. stigmurus* (Fig. 6C, D), and *T. trivittatus* (Fig. 6E, F) species-groups) present well-developed glandular regions on the female pectinal basal piece (Fig. 3; Table 3), but do not exhibit dilatation of the middle basal lamellae of the female pectines (Table 3). Finally, it is worth mentioning that males of *Tityus* species do not exhibit glandular regions on the pectinal basal piece, with the exception of some species of the *T. androcottoides* species-group (i.e., *T. rebierei*- also females).

Taxonomy

Family Buthidae C. L. Koch, 1837

Genus *Tityus* C. L. Koch, 1836

Tityus C. L. Koch 1836: 33.

Subgenus *Tityus* (*Tityus*) C. L. Koch, 1836

Tityus (*Tityus*): Lourenço (2006): 57, 58, 60, figures 3–6, 10–13, 22.

Type species. *Scorpio bahiensis* Perty, 1833 by monotypy.

Comments. This subgenus currently includes, among others, all species assigned to the *T. bahiensis* Mello-Leitão, 1945; *T. bolivianus* Kraepelin, 1895; *T. stigmurus* Mello-Leitão, 1945, and *T. trivittatus* Mello-Leitão, 1945 species-groups, according to the classification proposal of Lourenço (2006). In addition to *T. braziliae* Lourenço & Eickstedt, 1984, here transferred to this subgenus (see Discussion). On the other hand, *Tityus sastrei* Lourenço & Flórez, 1990 belongs to *Tityus* (*Atreus*) and is excluded from *Tityus* (*Tityus*) (see Discussion). Finally, according to previous hypotheses and our data, the *T. bolivianus* Kraepelin, 1895 species-group forms an independent clade outside *Tityus* (*Tityus*), but additional studies, including the study of the type species of this group, are required to propose a formal taxonomic decision.

Tityus spelaeus sp. nov.

<http://zoobank.org/3AE5D4E6-C2F1-47A7-9768-046B09B2FF48>

Figures 1–8; Tables 3–5

Type material. BRAZIL: State of Goiás: **Holotype.** Adult female from Posse, Russão II cave, 14°05'05.3"S, 46°23'07.1"W, 01.iv.2007, R. Pinto-da-Rocha leg. (MZSP 74633). **Paratypes.** Four adult female paratypes, same data as the holotype (MZSP

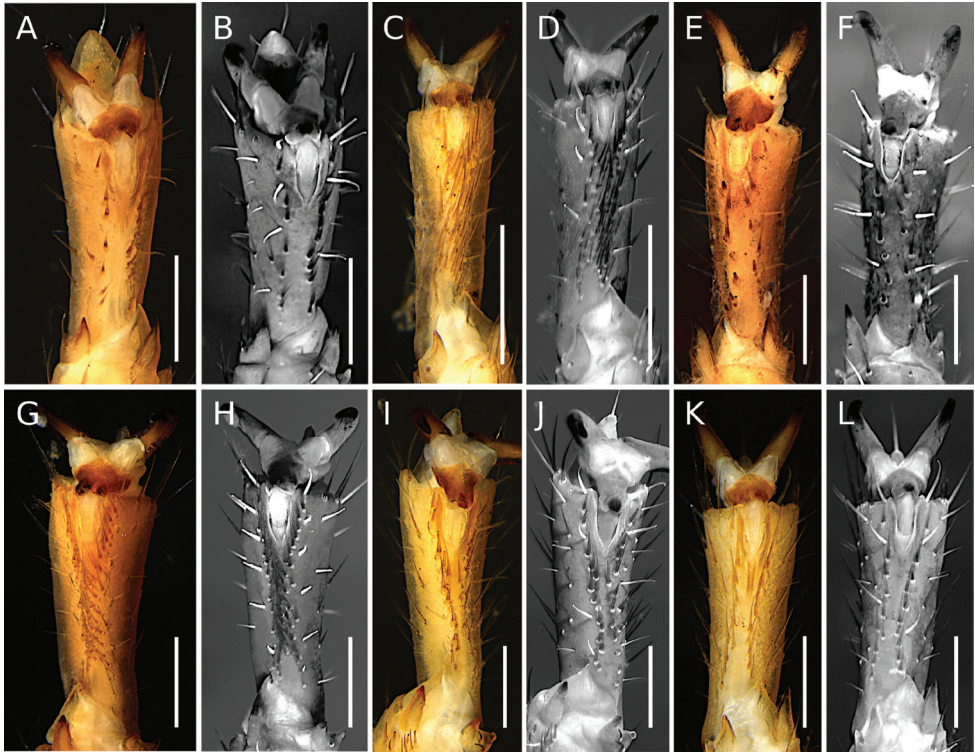


Figure 4. *Tityus* C. L. Koch, 1836, telotarsi IV, showing ventral macrosetae **A, C, E, G, I, K** white light **B, D, F, H, J, L** UV light **A, B** *Tityus (Tityus) braziliae* Lourenço & Eickstedt, 1984 (type II) (MZSP 75619) **C, D** *Tityus (Archaeotityus) clathratus* C. L. Koch, 1844 (type I) (MZSP 31468) **E, F** *Tityus (Atreus) forcipula* (Gervais, 1843) (type II) (MZSP) **G, H** *Tityus (Atreus) obscurus* Gervais, 1843 (type I) (MNRJ 07610) **I, J** *Tityus (Tityus) serrulatus* Lutz & Mello, 1922 (type II) (MZSP 28205) **K, L** *Tityus (Tityus) spelaeus* sp. nov. (MZSP 74633) (type II). Observations = telotarsi I–IV ventral setae distribution: Type I = tuft of irregularly distributed setae. Type II = two discrete ventrosubmedian rows of setae. Scale bars: 500 μ m.

74634); eight adult females, same locality as the holotype, 23.iv.2015, J. E. Gallão & C. C. de Paula leg. (LES/UFSCar 14668; LES/UFSCar 14669; LES/UFSCar 14670; LES/UFSCar 14671; LES/UFSCar 14672; LES/UFSCar 14673); four adult females, same locality as the holotype, 01.iv.2007, R. Pinto-da-Rocha et al. (MZSP 52228, 52229, 52230, 52231).

Etymology. The species epithet is a derivative form of the Greek noun, σπήλαιον (Latin: caverna), which means cave, in reference to the subterranean habitat where *Tityus spelaeus* has an established population. It is a noun in apposition.

Diagnosis. (Based on female). This species belongs to the *Tityus trivittatus* species-group (Figs 2, 3). Among members of the group distributed in Brazil (*T. carvalhoi* Mello-Leitão, 1945; *T. charreyroni* Vellard, 1932; *T. confluens* Borelli, 1899; *T. fasciolatus* Pessoa, 1935; *T. jeanvillardii* Lourenço, 2001; *T. karaja* Lourenço, 2016; *T. rupestre*

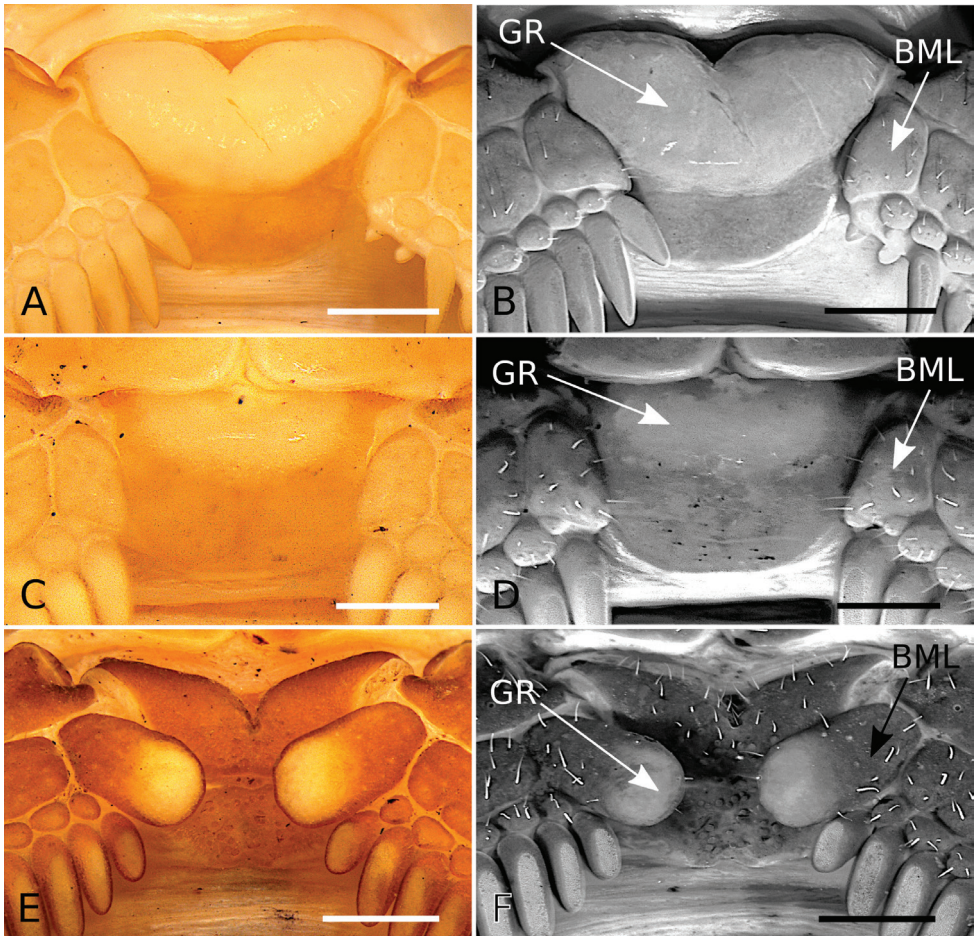


Figure 5. *Tityus* C. L. Koch, 1836, female pectinal basal piece and basal middle lamellae of the pectines, showing glandular regions **A, C, E** White light **B, D, F** UV light **A, B** *Tityus (Tityus) braziliae* Lourenço & Eickstedt, 1984 (MZSP 75619) **C, D** *Tityus (Archaeotityus) clathratus* C. L. Koch, 1844 (MZSP 31468) **E, F** *Tityus (Atreus) forcipula* (Gervais, 1843) (MZSP). Abbreviations: BML, basal middle lamellae; GR, glandular region. Scale bars: 500 μ m.

Lourenço, 2019; *T. sylviae* Lourenço, 2005, and *T. trivittatus* Kraepelin, 1898), *Tityus spelaesus* sp. nov. can be readily recognized. *Tityus spelaesus* sp. nov.; *T. carvalhoi*; *T. charreyroni*; *T. confluens*; *T. fasciolatus*; *T. rupestre*, and *T. trivittatus* share a subaculear tubercle small, and acute, pointing towards the tip of the aculeus (Fig. 12A). In contrast, *T. jeanvellardi*; *T. karaja*, and *T. sylviae* exhibit a small and coarse subaculear tubercle that points either towards the tip of the aculeus (*T. sylviae*) or towards the middle of the aculeus (*T. jeanvellardi* and *T. karaja*).

On the other hand, *Tityus spelaesus* sp. nov. and *T. sylviae* share a very large glandular region occupying beyond the anterior two thirds of the medial region of the pectinal basal piece of female pectines (Figs 6E, F, 11). In *T. carvalhoi*; *T. charreyroni*;

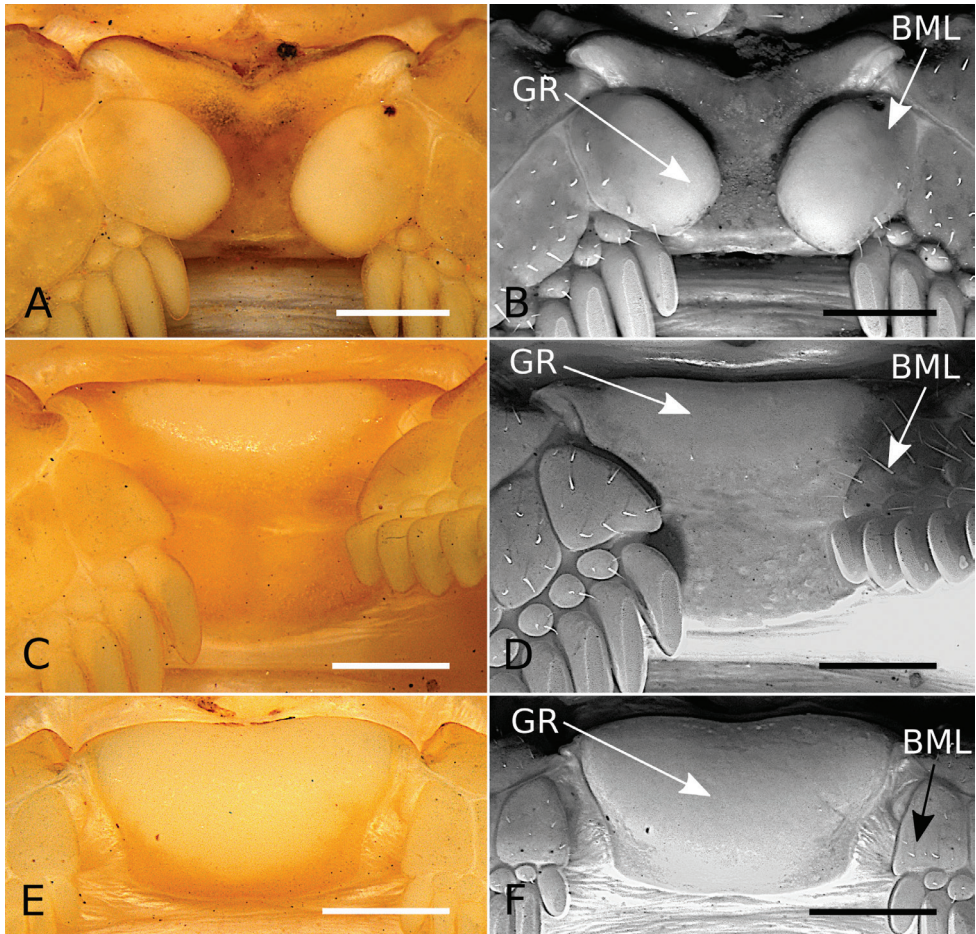


Figure 6. *Tityus* C. L. Koch, 1836, female pectinal basal piece and basal middle lamellae of the pectines, showing glandular regions **A, C, E** White light **B, D, F** UV light **A, B** *Tityus (Atreus) obscurus* Gervais, 1843 (MNRJ 07610) **C, D** *Tityus (Tityus) serrulatus* Lutz & Mello, 1922 (MZSP 28205) **E, F** *Tityus (Tityus) spelaeus* sp. nov. (MZSP 74633). Abbreviations: BML, basal middle lamellae; GR, glandular region of the pectinal basal piece. Scale bars: 500 μ m.

T. confluens; *T. fasciolatus*, and *T. trivittatus* (females of *T. jeanvillardii*; *T. karaja* and *T. rupestre* are unknown) the glandular region occupies a large area of anterior two thirds of the anteriomedian region of the pectinal basal piece of female pectines (e.g., Fig. 5A, B).

Finally, *Tityus spelaeus* sp. nov. and *T. karaja* can be readily distinguished from *T. carvalhoi*; *T. charreyroni*; *T. fasciolatus*; *T. jeanvillardii*; *T. rupestre*; *T. sylviae*, and *T. trivittatus*, based on the presence of residual spots on tergites (Figs 7, 13), and having the carapace (Figs 7, 8A) and cheliceral manus immaculate (Fig. 8A). In contrast, *T. charreyroni*; *T. confluens*; *T. fasciolatus*; *T. jeanvillardii*; *T. rupestre*; *T. sylviae*, and *T. trivittatus* have the carapace and tergites moderately covered with brownish spots and the cheliceral manus with reticulations (except *T. jeanvillardii* that exhibit a cheliceral manus immaculate).

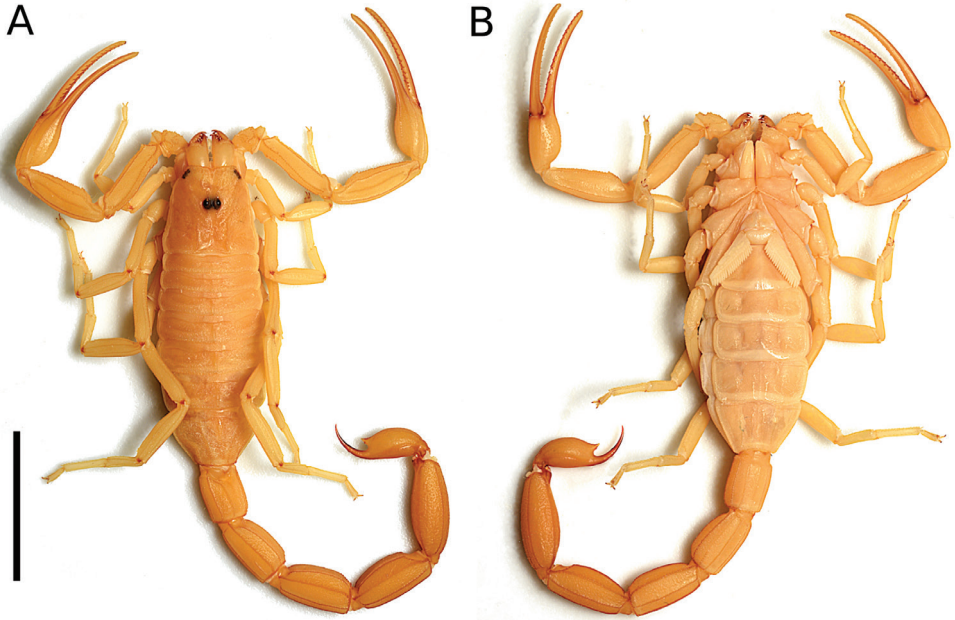


Figure 7. *Tityus (Tityus) spelaeus* sp. nov., female holotype (MZSP 74633) **A** dorsal view **B** ventral view. Scale bars: 10 mm.

Remarks. In an unpublished comprehensive phylogenetic analysis of *Tityus* (Moreno-González 2021), the *Tityus trivittatus* species-group was one of the most morphologically homogeneous species-groups of the genus. In fact, no somatic character of the morphological matrix (~164 chars) was optimized as a synapomorphy in the nodes within the clade representing the *Tityus trivittatus* species-group. Instead, those nodes were solely supported by unambiguous molecular synapomorphies. It is worth mentioning that, although coloration patterns presented high levels of homoplasy, they also showed significant differences at the species level, and the diagnosis of *Tityus spelaeus* sp. nov. is based on this background knowledge. Nonetheless, additional studies including molecular and phenotypical evidence of poorly described species from the Central region of Brazil are required to untangle the phylogeny of this cryptic species complex.

On the other hand, *Tityus karaja* Lourenço, 2016 was described based on a single male collected in 1929 in the region that corresponds to the northern portion of the state of Goiás, Brazil. According to the brief description of Lourenço (2016), *Tityus karaja* could share a similar body coloration pattern to that of *T. spelaeus*. However, given that the male of *T. karaja* is almost a hundred years old, the coloration needs to be corroborated with fresh specimens. Despite this, according to Lourenço's (2016: fig. 5) illustration, the subaculear tubercle of *T. karaja* is conical, small, and coarse, pointing towards the middle of the aculeus, whereas in *T. spelaeus* sp. nov. it points towards the tip of the aculeus (Fig. 12A).

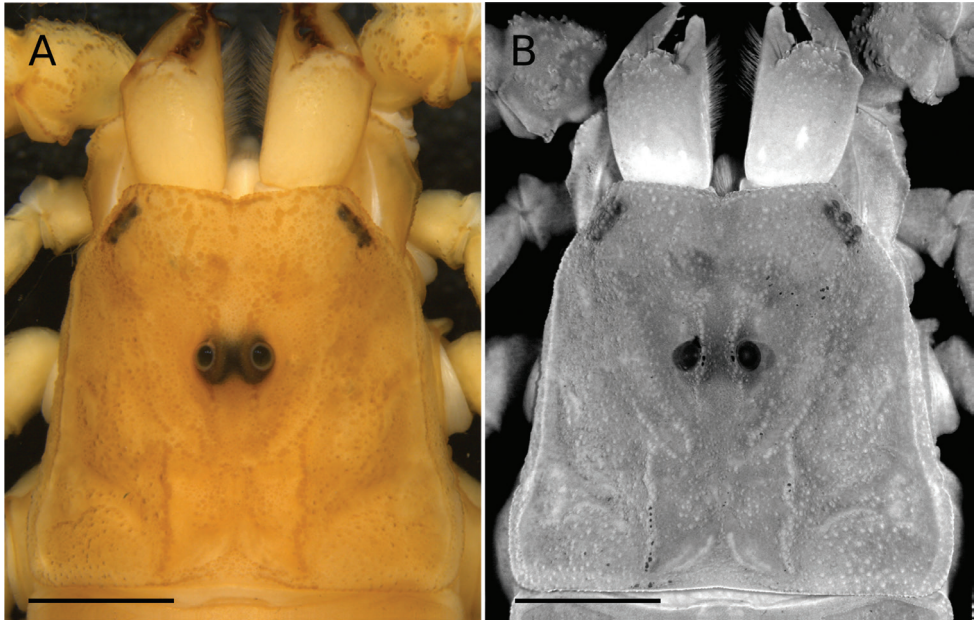


Figure 8. *Tityus (Tityus) spelaeus* sp. nov., female holotype (MZSP 74633), carapace, dorsal view **A** white light **B** UV light. Scale bars: 2 mm.

Description. Based on the female holotype (MZSP 74633). Male unknown.

Total length. Female: 53.52 mm (measurements in Table 4).

Coloration. General pattern (in ethanol 70%) (Fig. 7): light yellow, without variegated pigmentation. **Carapace** (Figs 7A, 8A): light yellow; lateral and median eyes, surrounded by black variegated pigments. **Chelicerae** (Figs 7A, 8A): coxa and hand light yellow, without pigments; fingers, dark reddish-brown. **Mesosoma, coxosternal region, pedipalps, legs** (Fig. 7A, B): all light yellow. **Metasoma** (Fig. 7A, B): segments light yellow, progressively becoming darker towards the telson. **Telson** (Fig. 7A, B): dark yellow; aculeus dark reddish-brown. Live coloration pattern (Fig. 13A–C) similar to that of preserved specimens, except for mesosoma with a faint brown median stripe crossing all tergites, telson light reddish-brown, pedipalp chela fingers and metasomal segments IV–V dark reddish-brown.

Morphology. Carapace (Fig. 2B): densely covered with fine granulation and few coarse granules; anterior margin with deep median notch; anterior median carinae only feebly marked over anterior 1/3; central lateral, central median, lateral ocular, posterior, posterior median and superciliary carinae, all well-marked; and furrows (anterior median, anterior marginal, central transverse, lateral ocular, superciliary, posterior transverse, posterior lateral and posterior marginal), all well-marked; ocular tubercle well-marked, located on the anterior half of carapace; median eyes separated by about 0.53 ocular diameters; with three pairs of lateral eyes and two pairs of lateral micro-ocelli.

Chelicerae (Fig. 8B): dentition characteristic of the family Buthidae (Vachon 1963), densely covered with setae over the internal and ventral surfaces.

Pedipalps: Chela, short and slender (female, L/W = 5.5). Orthobothriotaxitic pattern Type A, femur with alfa configuration (hand: Eb3:Eb2:Eb1:Esb:Est:Et, fixed finger: eb:esb:est:et:db:dt:it). **Femur** (Fig. 9A) with five carinae: VI, DI, DE, and VE crenulate, EM serratocrenulate, complete and pronounced, with intercarinal areas densely covered with fine granulation and few coarse granules. **Patella** (Fig. 9B, C) with seven carinae: VI, VE, DI, DE, and EM complete and crenulate; DM incomplete and crenulate; IM complete and serratocrenulate, with a short spiniform granule near the segment base; with intercarinal areas densely covered with fine granulation. **Chela** (tibia) (Fig. 10A–C) with eight carinae: VI, VE, D, DS, DMA, IM, and ES, complete and crenulate; SA, incomplete and crenulate, only present on the anterior half of the hand. Pedipalp movable and fixed fingers without basal lobe (Fig. 10A). Movable finger with 17–17 rows.

Coxosternal region (Fig. 7B): Sternum with posterior depression, outer ridge, and apical button, well-marked; sclerite covered with fine granulation, and few setae, except for the coxapophyses I–II, which are smooth; genital operculum longitudinally divided, composed of two sub-triangular plates.

Pectines (Fig. 11). Pectinal basal piece sub-rectangular and covered with a large and raised glandular region occupying beyond the anterior two thirds of the antero-medial region (Figs 6E, F, 11A, B; Table 3); pectinal tooth count of 19–22. Marginal lamellae, median lamellae, and fulcra moderately covered with setae (Fig. 5C). Basal middle lamellae, not dilated (Figs 6E, F, 11C). Pectinal tooth peg sensillae rectangular in cross-section, with a narrow distal opening (Fig. 11D, E).

Legs: Carinae present; intercarinal areas with sparse fine granulation; ventral telotarsal macrosetae acute and fine, arranged in two ventrosubmedian rows (Fig. 4K, L); telotarsi, counts of ventral macrosetae in the left (L) and right (R) legs on prolateral (pro) and retrolateral (retro) rows of legs I to IV (L (pro/retro) R (pro/retro)): 7/6 7/7: 7/7 7/7: 9/8 9/10: 10/10 9/11. Claws short and symmetrical.

Mesosoma: Tergites I–VI, moderately covered with fine granulation and few coarse granules; pre-tergites well defined, with median carina visible on the posterior margin of the post-tergites; tergite VII with DSM and DL carinae complete and crenulate, and median carina composed of a crenulate anteromedian eminence present on the anterior half of the post-tergite. Sternites densely covered with fine granulation; sternites III–VI with a pair of elliptic spiracles on the posterior half, which are progressively larger; sternite V with a hyaline subtriangular area on the posterior margin; sternite VI with VSM carinae crenulate, present on posterior half; sternite VII with VSM and VL carinae crenulate, present on posterior two thirds.

Metasoma (Fig. 12C, D): Segments II–V short and robust (L/W ratio: II = 1.9; III = 1.9; IV = 2.0; V = 2.5); segment V not incrassate (Fig. 12C). Segments I–II (Fig. 12C, D) with 10 complete carinae, parallel to one another and crenulate (paired DSM, DL, ML, VL, and VSM), ML of segment II represented by coarse granules on posterior two thirds, intercarinal areas densely covered with fine granulation;

Table 4. Measurements (mm) of *Tityus spelaeus* sp. nov.

Structure	Measure	Measurements (mm)																
		Female holotype MZSP 74633	Female paratype # 1 MZSP 74633	Female paratype # 2 MZSP 74633	Female paratype # 4 MZSP 74633	Female paratype # 5 MZSP 74633	Female paratype MZSP 52228	Female paratype MZSP 52229	Female paratype MZSP 52230	Female paratype MZSP 52231	Female paratype LES014668	Female paratype LES014669	Female paratype LES014670	Female paratype LES014671	Female paratype LES014672	Female paratype LES014673	Female paratype LES014673	
Total length	–	53.52	51.29	57.89	51.06	51.70	48.30	49.64	51.41	49.90	57.98	53.69	53.84	54.19	54.40	50.75	52.02	54.29
Carapace	length	6.00	5.84	6.40	5.68	5.68	5.57	5.57	5.71	5.57	6.45	5.83	5.98	6.06	6.20	5.57	5.73	6.07
Carapace	anterior width	4.08	3.76	4.32	3.84	3.84	3.71	3.57	3.86	3.71	3.33	3.08	3.09	3.13	3.28	2.89	3.01	3.10
Carapace	posterior width	6.64	6.48	7.12	6.24	6.24	6.00	5.57	6.29	5.71	6.53	6.09	6.08	6.10	6.32	5.84	5.92	6.21
Carapace	eye diameter	0.45	0.48	0.48	0.45	0.45	0.40	0.40	0.43	0.47	0.47	0.44	0.44	0.46	0.43	0.40	0.41	0.43
Carapace	interocular distance	0.53	0.50	0.55	0.48	0.48	0.47	0.47	0.50	0.53	0.54	0.53	0.49	0.54	0.55	0.54	0.47	0.59
Carapace	ocular diada width	1.20	1.28	1.36	1.20	1.20	1.13	1.17	1.20	1.17	1.26	1.21	1.24	1.21	1.23	1.13	1.18	1.19
Tergite I	length	1.12	1.08	1.08	1.00	1.00	1.00	1.07	1.00	0.87	1.24	1.16	1.18	1.16	1.14	1.09	1.01	1.17
Tergite II	length	1.44	1.28	1.52	1.24	1.24	1.27	1.27	1.27	1.00	1.50	1.32	1.44	1.42	1.35	1.23	1.31	1.41
Tergite III	length	1.76	1.60	1.88	1.56	1.68	1.47	1.73	1.60	1.67	1.88	1.77	1.68	1.61	1.68	1.64	1.67	1.76
Tergite IV	length	2.20	2.00	2.32	2.08	2.04	1.87	2.00	2.07	1.93	2.35	2.16	2.20	2.01	2.10	1.94	2.00	2.06
Tergite V	length	2.32	2.20	2.60	2.28	2.24	2.07	2.20	2.20	2.33	2.52	2.44	2.34	2.33	2.28	2.19	2.28	2.38
Tergite VI	length	2.68	2.40	2.84	2.44	2.52	2.27	2.40	2.40	2.53	2.74	2.56	2.58	2.48	2.51	2.44	2.47	2.56
Tergite VII	length	3.88	3.96	4.20	3.80	3.84	3.60	3.80	4.07	3.80	4.60	4.09	4.06	4.05	4.11	4.01	3.83	4.28
Mesosoma	total length (tergites)	15.40	14.52	16.44	14.40	14.56	13.53	14.47	14.60	14.13	16.83	15.50	15.48	15.06	15.17	14.54	14.57	15.62
Metasoma I	length	3.55	3.55	3.75	3.55	3.55	3.30	3.50	3.60	3.50	4.00	3.67	3.63	3.66	3.71	3.49	3.56	3.84
Metasoma I	width	2.85	2.85	2.95	2.35	2.85	2.50	2.70	2.90	2.70	2.99	2.83	2.79	2.88	2.86	2.78	2.76	2.85
Metasoma I	height	2.60	2.65	2.65	2.85	2.85	2.40	2.50	2.50	2.50	2.83	2.62	2.62	2.66	2.70	2.43	2.50	2.63
Metasoma II	length	4.55	4.40	4.80	4.35	4.50	4.20	4.30	4.50	4.30	4.97	4.57	4.67	4.69	4.71	4.32	4.57	4.64
Metasoma II	width	2.75	2.70	3.05	2.20	2.75	2.40	2.60	2.70	2.60	3.02	2.75	2.82	2.84	2.89	2.69	2.72	2.77
Metasoma II	height	2.75	2.70	2.95	2.70	2.85	2.40	2.50	2.60	2.50	2.73	2.54	2.45	2.51	2.59	2.44	2.48	2.60
Metasoma III	length	5.20	5.00	5.50	4.90	5.00	4.70	4.80	5.00	4.90	5.44	5.19	5.10	5.28	5.21	4.68	4.96	5.05
Metasoma III	width	2.85	2.70	3.20	2.25	2.80	2.40	2.70	2.70	2.60	3.09	2.77	2.79	2.83	2.88	2.67	2.79	2.95
Metasoma III	height	2.90	2.60	3.00	2.85	2.85	2.40	2.40	2.50	2.60	2.81	2.53	2.54	2.60	2.63	2.52	2.50	2.58
Metasoma IV	length	5.75	5.50	6.50	5.50	5.60	5.20	5.40	5.60	5.50	6.25	5.88	5.81	5.80	5.87	5.51	5.79	5.82
Metasoma IV	width	2.85	2.75	3.25	2.25	2.85	2.50	2.60	2.80	2.60	3.10	2.77	2.77	2.87	2.87	2.68	2.77	2.86
Metasoma IV	height	2.85	2.50	3.12	2.85	2.85	2.30	2.40	2.50	2.40	2.77	2.55	2.51	2.49	2.64	2.59	2.51	2.58
Metasoma V	length	6.83	6.57	7.74	6.70	6.76	6.00	6.10	6.50	6.30	7.24	6.74	6.67	6.93	6.92	6.43	6.58	6.84
Metasoma V	width	2.93	2.60	3.25	2.86	2.93	2.30	2.50	2.60	2.40	2.91	2.57	2.58	2.59	2.63	2.49	2.57	2.59
Metasoma V	height	2.73	2.54	3.12	2.80	2.86	2.30	2.40	2.60	2.40	2.69	2.82	2.50	2.48	2.58	2.41	2.51	2.61
Metasoma	length	25.88	25.02	28.29	25.00	25.41	18.70	19.30	20.20	19.60	27.90	26.05	25.88	26.36	26.42	24.43	25.46	26.19
Telson	vesicle length	3.84	3.77	4.23	3.77	3.77	3.40	3.40	3.70	3.50	3.57	3.41	3.38	3.46	3.51	3.33	3.37	3.43
Telson	vesicle width	2.21	1.95	2.28	1.95	1.95	1.80	1.90	2.00	1.90	2.10	1.96	1.93	2.05	2.11	1.88	1.89	2.03
Telson	vesicle height	2.15	2.08	2.28	2.08	2.02	1.80	1.90	2.00	1.90	2.17	2.01	2.00	2.10	2.12	1.90	1.97	2.11
Telson	aculeus length	2.80	2.67	2.99	2.67	2.67	2.50	2.60	2.70	2.60	2.68	2.54	2.53	2.63	2.56	2.52	2.49	2.57
Telson	total length	6.24	5.92	6.76	5.98	6.05	5.80	5.50	5.90	5.70	6.80	6.31	6.50	6.71	6.61	6.21	6.26	6.41

Structure	Measure	Measure																
		Female holotype	Female paratype # 1	Female paratype # 2	Female paratype # 4	Female paratype # 5	Female paratype											
		MZSP 74633	MZSP 74633	MZSP 74633	MZSP 74633	MZSP 74633	MZSP 52228	MZSP 52229	MZSP 52230	MZSP 52231	LES014668	LES014669	LES014670	LES014671	LES014672	LES014673	LES014673	LES014673
Metasoma+	total length	32.12	30.93	35.05	30.98	31.46	29.20	29.60	31.10	30.20	34.70	32.36	32.38	33.07	33.03	30.64	31.72	32.60
Telson	length	6.18	5.98	6.70	6.18	6.11	5.60	5.80	6.00	5.90	6.96	6.46	6.51	6.76	6.72	6.39	6.41	6.61
Femur	width	1.50	1.56	1.76	1.69	1.56	1.40	1.50	1.50	1.50	1.75	1.56	1.61	1.62	1.64	1.54	1.60	1.60
Patella	length	6.76	6.70	7.28	6.44	6.57	6.00	6.00	6.20	6.30	6.68	6.10	6.12	6.54	6.31	5.78	6.01	6.21
Patella	width	2.08	2.02	2.02	2.08	2.02	1.80	1.90	2.00	1.90	2.12	1.88	1.93	2.01	2.00	1.85	1.90	1.94
Chela	length	11.50	11.10	13.00	11.57	10.50	10.40	10.60	11.20	10.90	12.26	11.28	11.25	11.75	11.77	10.79	11.08	11.63
Chela	width	2.60	2.00	2.47	2.34	2.10	1.80	2.00	2.00	1.90	2.32	2.04	1.96	2.06	2.08	1.90	2.01	2.02
Chela	height	2.10	2.10	2.73	2.21	2.10	1.80	2.00	2.10	2.00	2.10	1.81	1.85	1.92	1.95	1.84	1.82	1.93
Chela	movable finger length	8.00	7.20	8.97	7.80	7.20	7.00	7.00	7.40	7.30	8.29	7.62	7.61	8.01	8.02	7.45	7.51	7.99
Chela	fixed finger length	6.80	6.40	7.67	6.89	6.20	6.20	6.10	6.60	6.40	7.07	6.55	6.74	7.05	6.91	6.17	6.89	6.92
Chela	palm length	4.00	3.80	4.68	4.16	3.90	3.40	3.70	3.70	3.70	4.14	4.11	4.09	4.16	4.15	3.92	4.03	4.03

segments III–IV (Fig. 12C, D) with eight complete carinae, parallel to one another and crenulate (paired DSM, DL, VL, and VSM), intercarinal areas densely covered with fine granulation; segment V (Fig. 12C, D) with five complete carinae, crenulate (VM, paired DSM, and VL: DSM carinae feebly marked), intercarinal areas moderately covered with fine granulation and few coarse granules. Segments II–IV (Fig. 12C) with DSM carinae feebly marked, composed of evenly sized granules, without enlarged distoterminal granule.

Metasomal macrosetae: Segments I–IV each with two pairs of VSM macrosetae (2/2): pair of VSM1 located on the anterior third, and pair of VSM2 located near posterior margin of segment; and with two pairs of VL macrosetae (2/2): pair of VL1 located near anterior margin of segment, and pair of VL2 located on posterior two thirds of segment. Segment V with two pairs of VSM macrosetae (2/2), two pairs of VL macrosetae (2/2), and a single pair of ML macrosetae (1/1); pairs of VSM1 and VL1 located near anterior margin of segment; pair of VL2 located on posterior two thirds of segment, and pair of ML1 located dorsolaterally behind the DSM carinae near posterior margin of segment; anal arch with two pairs of setae on the intercrestral area: one pair of VSM macrosetae (1/1) and one pair of VL macrosetae (1/1).

Telson (Fig. 12A, B): Vesicle suboval, not elongated (L/H= 1.8), dorsal surface smooth, lateral surfaces with shallow longitudinal furrow; with VM, paired VSM, VL, and DL carinae, vestigial. Subaculear tubercle large, conical, with spiniform apex directed towards the distal region of the aculeus (Fig. 12A); subaculear tubercle with ventral pair of small, rounded granules, pointing towards the basal portion of the aculeus; aculeus strongly curved, shorter than vesicle and with ventral groove.

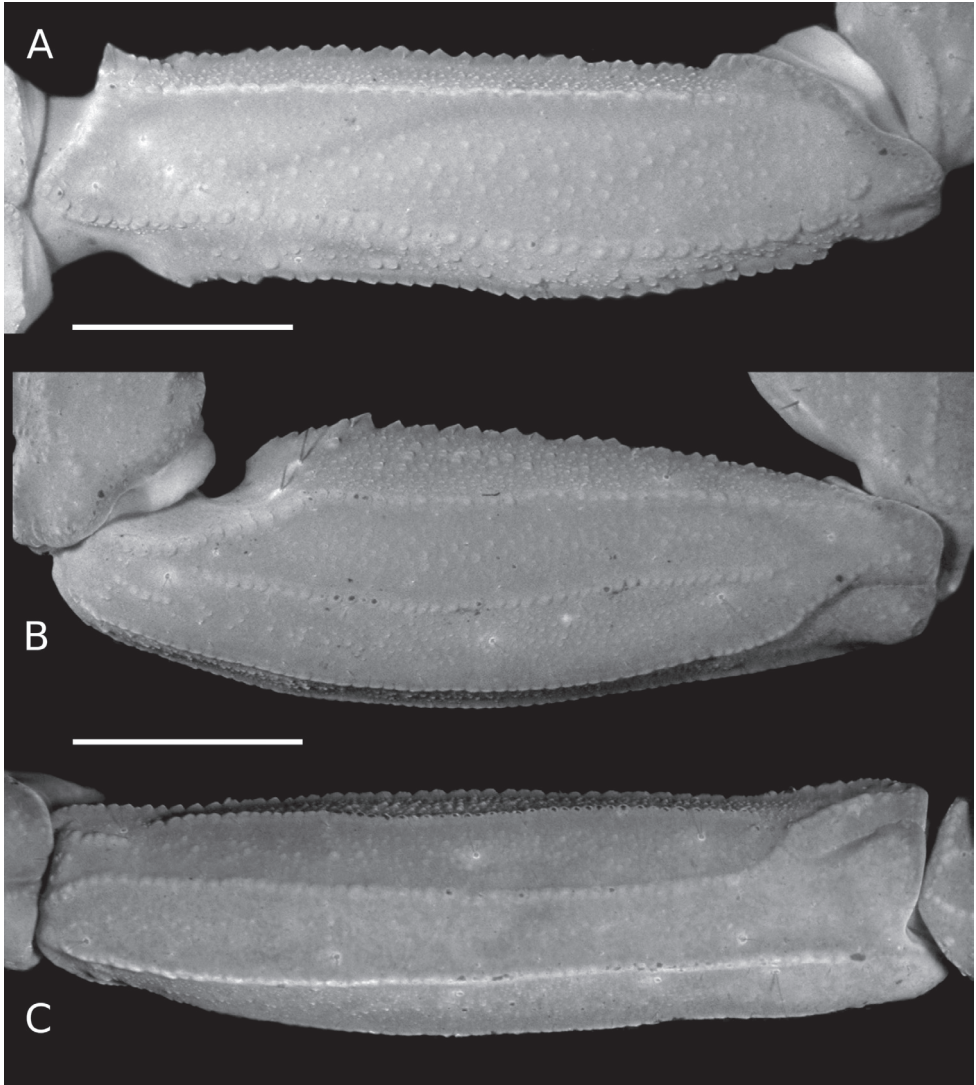


Figure 9. *Tityus (Tityus) spelaeus* sp. nov., female holotype (MZSP 74633), right pedipalp segments **A** femur, dorsal view **B, C** patella **B** dorsal view **C** external view. Scale bars: 1.5 mm.

Variability (females). **Morphometrics.** Total length (including telson): 48.30–57.98 mm (n= 17, mean= 52.70, standard deviation (SD)= 2.66). Chela L/W ratio: 4.42–5.78 (n= 17, mean= 5.44, SD= 0.37). Metasomal segment I L/W ratio: 1.24–1.51 (n= 17, mean= 1.30, SD= 0.06). Metasomal segment V L/W ratio: 2.31–2.68 (n= 17, mean 2.52, SD= 0.12). Telson vesicle L/H: 1.63–1.89 (n= 17, mean= 1.76, SD= 0.09). **Meristics.** Pectinal tooth count: 19–22 (n= 34, mode= 20). Number of movable finger oblique granular rows: 16–18 (n= 34, mode= 18). Metasomal macrosetae count: (n= 17): 2/2 VSM and 2/2 VL macrosetae on segments I–IV, 3/3 VSM and 2/2 VL macrosetae on segment V. However, one specimen (LES/UFSCar 14668) lost VSM1

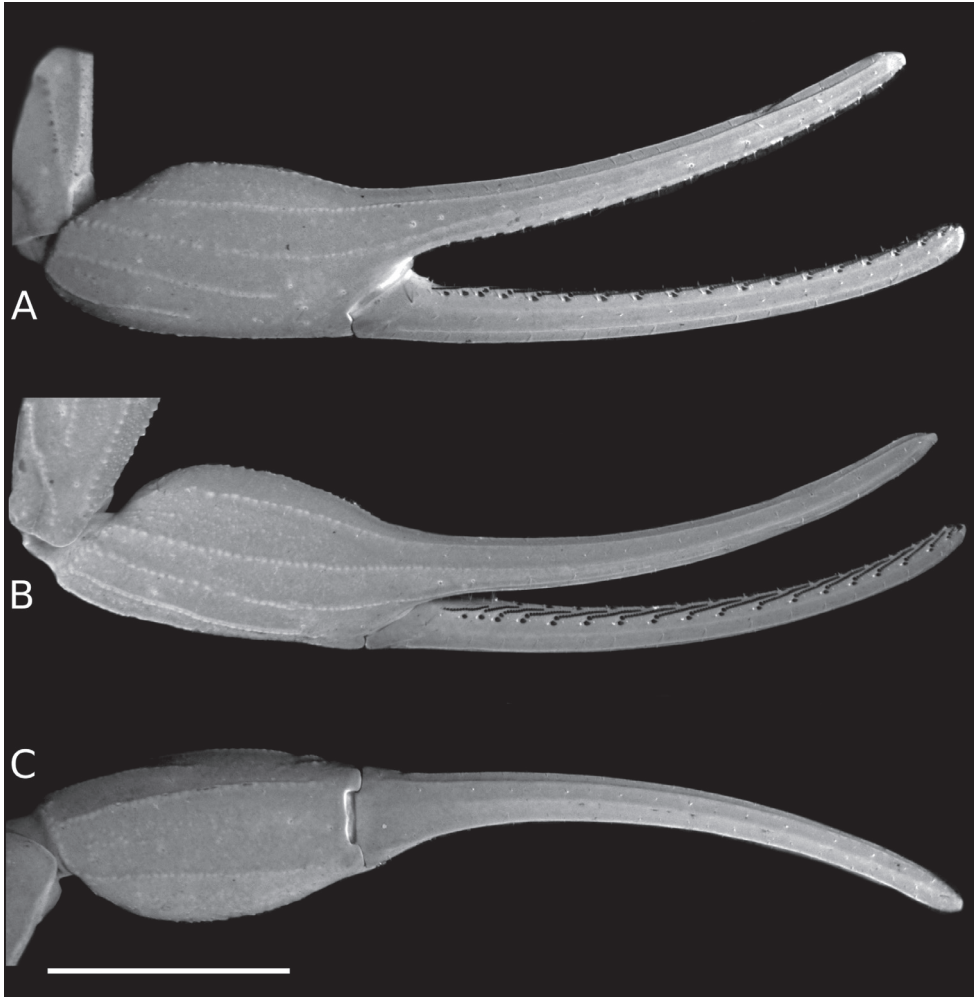


Figure 10. *Tityus (Tityus) spelaeus* sp. nov., female holotype (MZSP 74633), chela **A** external view **B** dorsal view **C** ventral view. Scale bar: 3 mm.

on segment II, a second specimen (LES/UFSCAR 14669) lost VL1 on segment II, and a third specimen (LES/UFSCAR 014673) lost one VSM1 on segment I. Variation in the count of telotarsal ventrosubmedian setae is presented in Table 5.

Natural history. Russão II cave is formed by limestone (a karstified type of rock), located in Posse municipality, the northeastern state of Goiás, Central Brazil. This karst region is part of the Bambuí geomorphological group, the large geomorphological group in Brazil, occurring in states of Bahia, Goiás, Minas Gerais, and Tocantins. Russão II cave is inserted on the Cerrado morphoclimatic domain (Ab'Saber 1977), and the climate is tropical semi-humid (Nimer 1979). There is a stream crossing the cave although there are no surface drainages nearby (Tencatt and Bichuette 2017). Russão II cave is located on private property, and in addition surface habitats are under

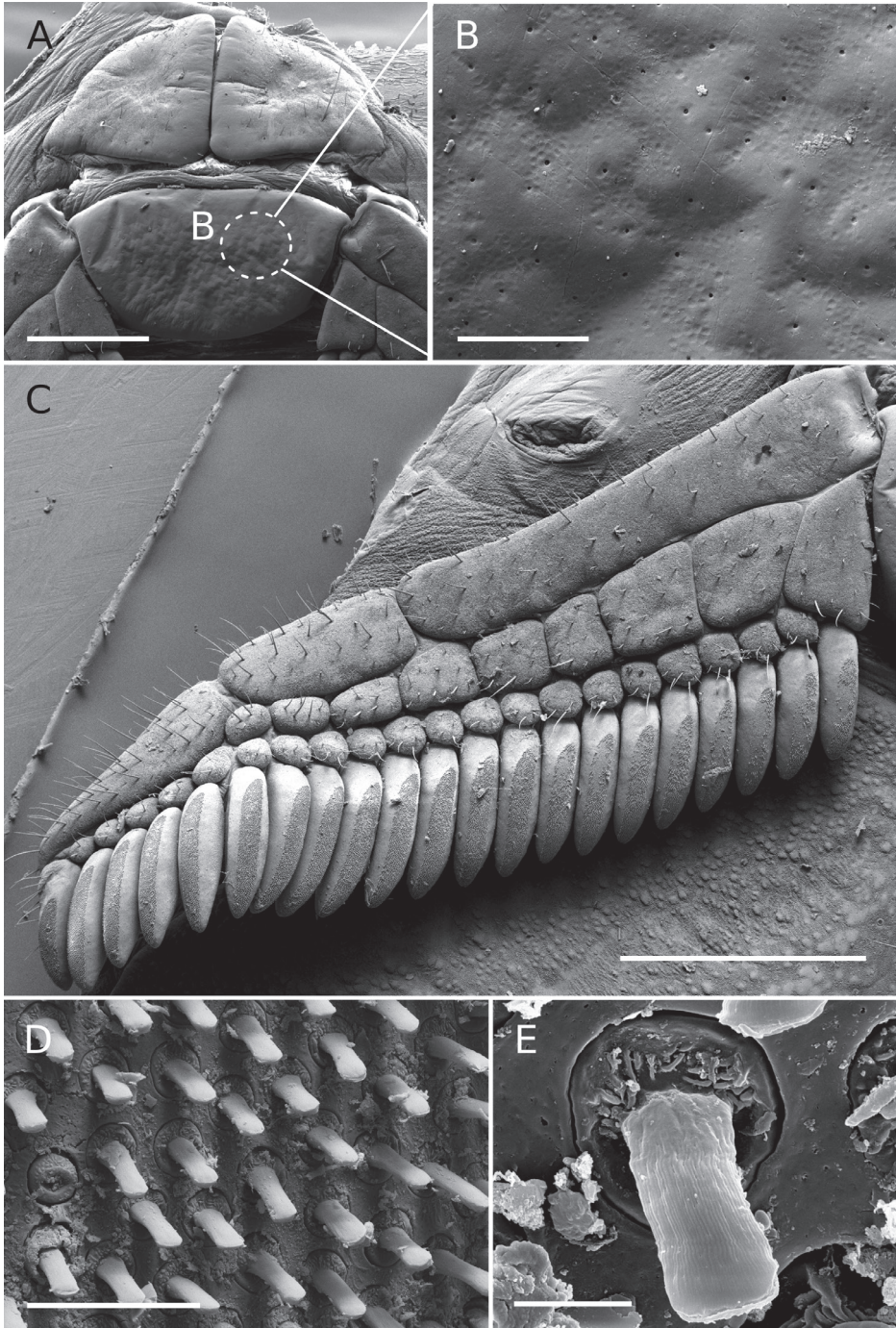


Figure 11. *Tityus (Tityus) spelaeus* sp. nov., female paratype (MZSP 74633) genital area and pectines **A** genital operculum and pectinal basal piece **B** closeup of the pectinal basal piece, showing cuticular pores on glandular region **C** right pectine **D** peg sensillae, distribution **E** closeup of a peg sensilla. Scale bars: 800 μm (**A**); 60 μm (**B**); 1000 μm (**C**); 20 μm (**D**); 3 μm (**E**).

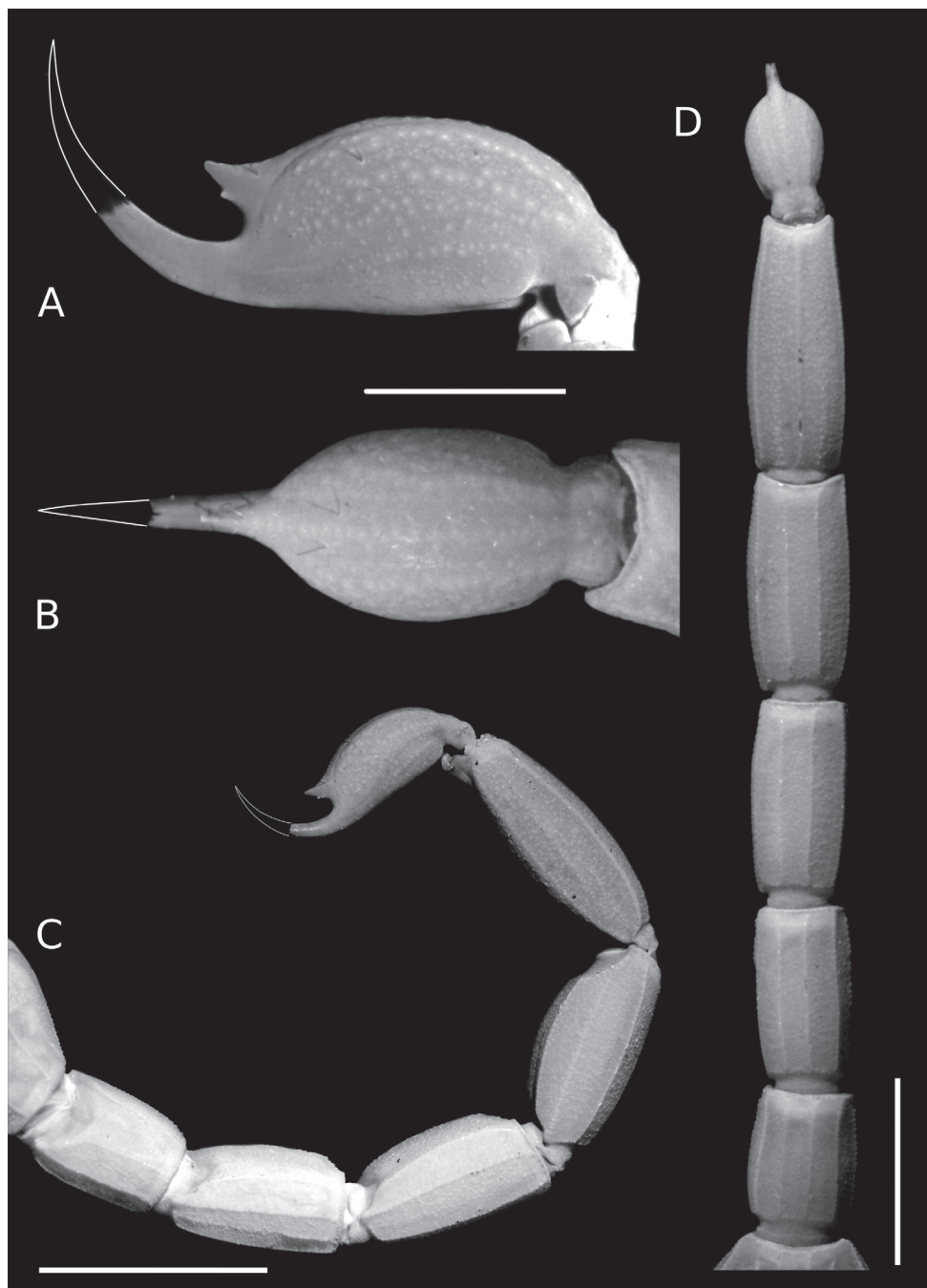


Figure 12. *Tityus (Tityus) spelaeus* sp. nov., female holotype (MZSP 74633), metasoma and telson **A, B** telson **A** lateral view **B** ventral view **C, D** metasoma **C** lateral view **D** ventral view. Scale bars: 2 mm (**A, B**); 5 mm (**C, D**).

Table 5. Variation in the number of macrosetae of the ventrosubmedian setal rows on telotarsi I–IV across paratypes of *Tityus spelaeus* sp. nov. Abbreviations: L, left leg; Pl, prolateral row; Rl, retrolateral row; R, right leg.

Telotarsus	MZSP 74634 (1)		MZSP 74634 (2)		MZSP 74634 (3)		MZSP 74634 (4)	
	L(Pl/Rl)	R(Pl/Rl)	L(Pl/Rl)	R(Pl/Rl)	L(Pl/Rl)	R(Pl/Rl)	L(Pl/Rl)	R(Pl/Rl)
I	8/7	8/7	6/7	8/6	8/7	7/8	6/7	6/7
II	7/8	8/7	8/8	8/9	8/8	7/8	8/8	8/7
III	8/8	7/8	8/7	8/9	10/8	8/9	6/8	8/7
IV	10/10	10/10	10/10	-	9/12	10/9	10/10	10/11
Telotarsus	MZSP 52228		MZSP 52230		MZSP 52229		MZSP 52231	
	L(Pl/Rl)	R(Pl/Rl)	L(Pl/Rl)	R(Pl/Rl)	L(Pl/Rl)	R(Pl/Rl)	L(Pl/Rl)	R(Pl/Rl)
I	6/6	-	7/8	7/6	7/6	7/7	6/7	6/8
II	7/7	7/8	7/7	8/7	9/6	7/7	8/7	7/8
III	9/7	8/8	7/8	8/7	7/6	10/8	6/6	8/8
IV	-	10/12	10/11	9/8	10/10	11/10	10/8	10/10
Telotarsus	LES 14668		LES 14669		LES 14670		LES 14671	
	L(Pl/Rl)	R(Pl/Rl)	L(Pl/Rl)	R(Pl/Rl)	L(Pl/Rl)	R(Pl/Rl)	L(Pl/Rl)	R(Pl/Rl)
I	8/7	8/7	8/9	8/8	9/8	6/7	8/8	9/9
II	8/7	8/7	10/9	9/8	9/8	10/7	9/9	8/8
III	8/8	9/8	9/10	9/9	9/8	8/8	9/9	9/9
IV	11/11	11/10	10/11	10/11	10/10	10/10	12/12	10/11
Telotarsus	LES 14672		LES 14673-1		LES 14673-2		LES 14673-3	
	L(Pl/Rl)	R(Pl/Rl)	L(Pl/Rl)	R(Pl/Rl)	L(Pl/Rl)	R(Pl/Rl)	L(Pl/Rl)	R(Pl/Rl)
I	9/8	8/8	8/8	8/8	8/9	9/8	8/8	9/9
II	9/8	8/8	8/9	8/8	10/9	9/8	8/8	8/8
III	9/9	10/9	9/9	8/8	9/9	10/10	9/9	9/8
IV	10/11	11/12	11/10	11/10	12/12	11/12	12/11	11/12

impact from pollution through the discharge of domestic sewage, deforestation of surroundings for cattle pasture, and small mining projects (Tencatt and Bichuette 2017). Russão II cave, like other caves in the region, has no legal protection under Brazilian environmental laws. The cave has a significant amount of bat guano piles and a large cricket population that is preyed upon by scorpions. In the aphotic zone of Russão II cave, the temperature was 30.04 °C, the relative humidity of the air was 72.02%.

This species was studied in the past by Outeda-Jorge et al. (2009) who reported a litter size of two scorpionlings, but under laboratory conditions (Fig. 13A–C), another two females had a litter of four scorpionlings, and both females were fed upon their litter (Fig. 13A, B). The population of *Tityus spelaeus* sp. nov. at the Russão cave is well-established (Fig. 8A, B). During a one-hour-long visit to the cave in 2007, more than 20 live scorpions were observed on the ground and walls (Fig. 14A, B). In another two-hour visit in 2015, 32 individuals were counted, both adults and juveniles.

Discussion

Phylogenetic patterns within *Tityus*

Our phylogenetic results (Figs 1–3) are similar to those of previous studies (i.e., Ojanguen-Affilastro et al. 2017a). In our analysis using molecular evidence, we found that *Tityus* (*Tityus*) is polyphyletic and *Tityus* (*Atreus*) is paraphyletic (Figs 1–3). This agrees with previously published *Tityus* phylogenies, which found discrepancies in the sub-

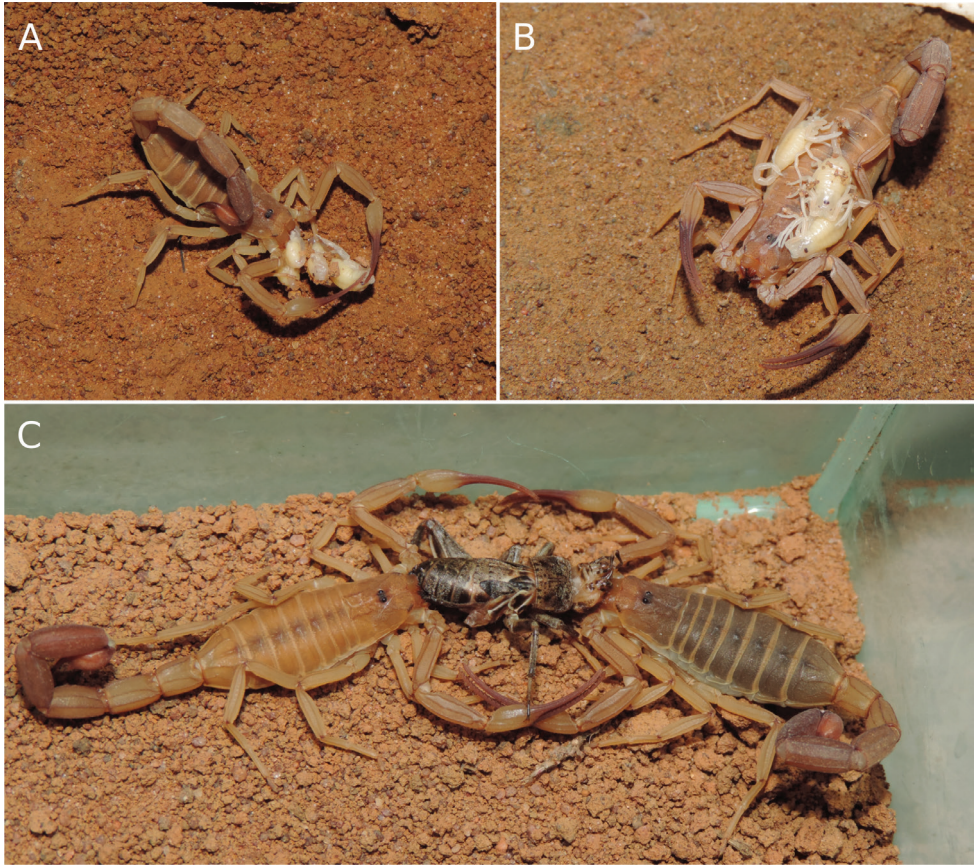


Figure 13. *Tityus (Tityus) spelaeus* sp. nov., female paratypes under laboratory conditions **A**, **B** female paratype with scorpionlings **A** feeding upon scorpionlings **B** litter on female's back **C** specimens feeding on a cricket.

generic classification of the genus proposed by Lourenço (2006). In the molecular phylogeny of Ojanguren-Affilastro et al. (2017a), which incorporated 18 *Tityus* terminals representing three subgenera, *Tityus (Tityus)* was found to be polyphyletic, with one clade containing *T. bahiensis*, *T. stigmurus*, and *T. trivittatus* species-groups as the sister group of *Tityus (Archaeotityus)*, and another clade consisting of the *T. bolivianus* species-group as the sister group of *Tityus (Atreus)*. Our results are highly consistent with those results (Figs 1–3), since we also recovered *Tityus (Tityus)* (here including *T. braziliae*) as the sister group of *Tityus (Archaeotityus)*, and *Tityus (Atreus)* (here including *T. sastrei*) as the sister group of the *T. bolivianus* species-group [referred to as *Tityus (Tityus)- T. bolivianus* species-group in Ojanguren-Affilastro et al. (2017a)].

More recently, Román et al. (2018) analyzed 51 terminals of 26 species [including 22 *Tityus (Atreus)* species] and recovered the *T. obscurus* species-group as paraphyletic. However, their study had a problem, because Román et al. (2018) mixed up members of the *T. androcottoides* species-group with members of the *T. obscurus* species-group. In

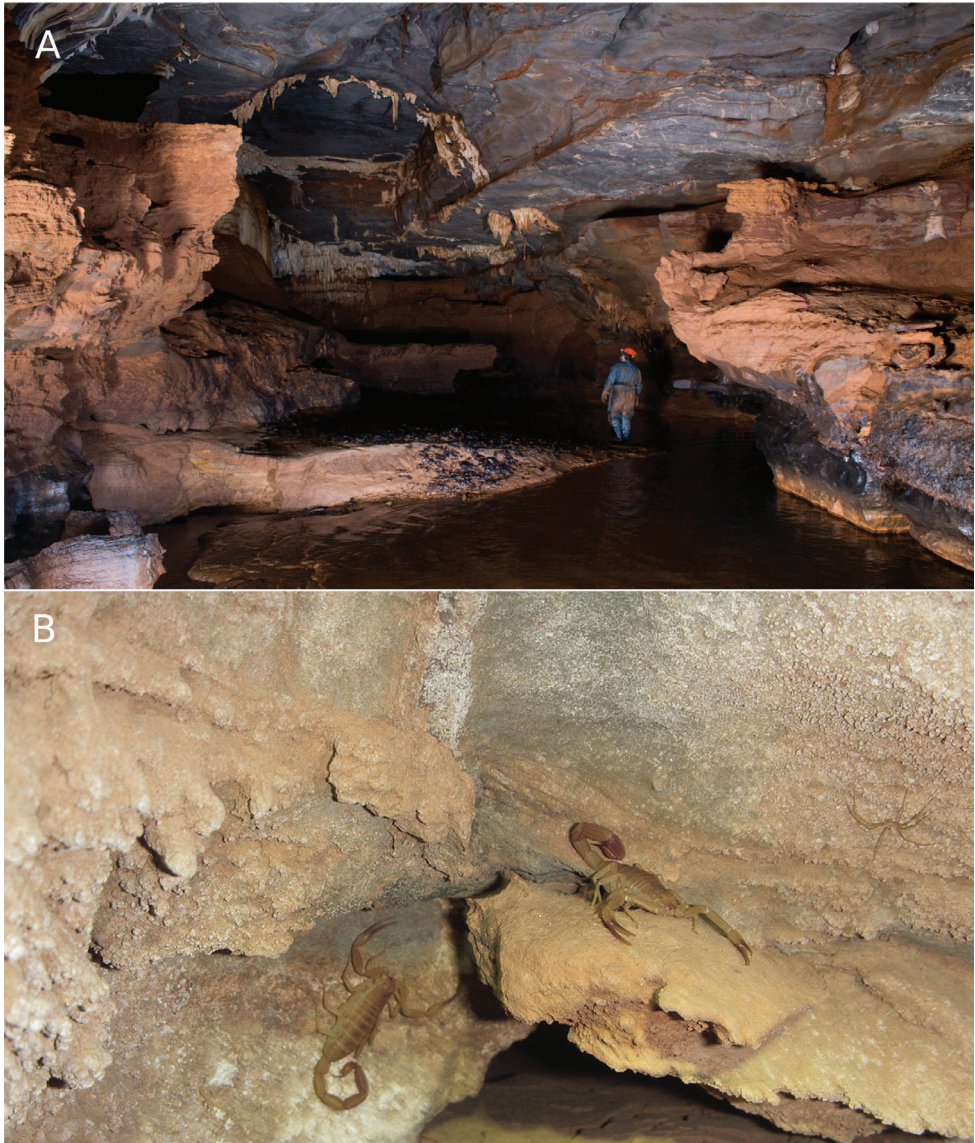


Figure 14. Habitat of *Tityus (Tityus) spelaeus* sp. nov. in the Russão cave **A** inside landscape of the cave **B** females on the cave walls.

reality, Román et al. (2018) recovered a monophyletic *T. obscurus* species-group and a polyphyletic *T. androcottoides* species-group (mostly composed of Venezuelan species). In our hypothesis, *Tityus (Atreus)* was recovered as monophyletic upon transfer of *Tityus (Tityus) sastrei* to *Tityus (Atreus)* (Figs 1–3).

Finally, other aspects were not challenged by several authors, such as the consensus about *Tityus (Archaeotityus)* (i.e., *T. clathratus* species-group) being the sister clade of

the remaining groups of *Tityus*. Indeed, this notion was discussed and supported by several authors during the last 75 years (Mello-Leitão 1945; Lourenço 1999, 2002a, 2002b; Borges et al. 2010). Some have assumed without any phylogenetic support that the small size, large subaculear tubercle, and cryptic coloration patterns of *Tityus* (*Archaeotityus*) scorpions are plesiomorphic character states (e.g., Lourenço 1999). Nevertheless, the phylogenetic analysis of Ojanguren-Affilastro et al. (2017a) recovered *Tityus* (*Archaeotityus*) as the sister group of a clade composed of some *Tityus* (*Tityus*) terminals, not the sister group of all *Tityus* subgenera, something that we also recovered in our results (Figs 1–3). Likewise, Borges et al. (2012) found a close relationship between the toxin composition of the *T. clathratus* and *T. stigmurus* species-groups. Based on a comprehensive phylogenetic analysis of *Tityus* (*Archaeotityus*) carried (Moreno-González 2021) and the results of this investigation, *Tityus* (*Archaeotityus*) cannot be considered as the sister clade of other *Tityus* subgenera or species-groups, as previously believed.

On the position of *Tityus brazilae* Lourenço & Eickstedt, 1984

In the original description of *Tityus brazilae* Lourenço & Eickstedt, 1984 the species was associated with *Tityus costatus* (Karsch, 1879) (referred to as *Tityus dorsomaculatus* Lutz & Mello, 1922) mainly due to the similar coloration pattern of the body of both species (Lourenço and Eickstedt 1984). However, Lourenço and Eickstedt (1984) also mentioned that the slender and elongated male pedipalp of *T. brazilae* is very common among some Amazonian species such as *Tityus obscurus* Pocock, 1897. Lourenço (2002b: 167) argued: “The fact I have included *Tityus brazilae* in the *Tityus asthenes* species-group, may surprise some readers because this species presents a pattern of pigmentation which excludes it from the group of dark or blackish scorpions. I based my decision, however, on the general morphology of the species and on the type of sexual dimorphism it displays.” Lourenço (2006) ended up including *Tityus brazilae* in the subgenus *Tityus* (*Atreus*).

It is worth mentioning that the slender and elongated shape of the male pedipalp has been demonstrated to be a highly homoplastic character state that evolved independently at least four times within *Tityus* (Moreno-González, 2021). For this reason, the shape of the male pedipalp must be used with caution and used in conjunction with other morphological characters and molecular data, such as those proposed in this paper, to correctly classify *Tityus* species into species-groups.

For example, the position of *Tityus brazilae* into the *Tityus obscurus* species-group (previously the *Tityus asthenes* species-group) of the subgenus *Tityus* (*Atreus*) is contradicted by our molecular and morphological evidence (e.g., Figs 1–3). In fact, *Tityus brazilae* exhibits some character states shared by all members of the *Tityus bahiensis* species-group of the subgenus *Tityus* (*Tityus*) (plus all the members of the *Tityus stigmurus* and *Tityus trivittatus* species-groups) such as: **i**) ventral macrosetae of telotarsi I–IV distributed in two ventrosubmedian rows (type II) (Fig. 4A, B), **ii**) basal middle lamellae of female pectines not dilated and without glandular regions (Fig. 5A, B), and **iii**) female

pectinal basal piece with a well-developed glandular region (Fig. 5A, B). In contrast, all the members of the *Tityus obscurus* species-group exhibit: **i**) telotarsi I–IV ventral macrosetae irregularly distributed in a tuft (type I) (Fig. 4G, H), **ii**) basal middle lamellae of female pectines dilated (subcircular) and with glandular regions (Fig. 6A, B), and **iii**) female pectinal basal piece without glandular region whatsoever (Fig. 6A, B).

On the position of the *Tityus bolivianus* species-group and *Tityus sastrei* Lourenço & Flórez, 1990

Lourenço (2006) assigned all the species of the *Tityus bolivianus* species-group and the species *Tityus sastrei* to the subgenus *Tityus* (*Tityus*). This decision was based on a combination of morphological characters that, according to Lourenço (2006), allow the diagnosis of *Tityus* (*Tityus*): **i**) total body length between 50–80 mm, **ii**) coloration pattern pale yellow to dark brownish frequently with confluent or longitudinal spots, **iii**) pectines with 15–26 teeth, **iv**) movable finger with 15–18 dorsal oblique rows of granules, and **v**) subaculear tubercle frequently acute.

Given the results of our phylogenetic analysis, previous hypotheses (Ojanguren-Affilastro et al. 2017a), and the phenotypic characters explored in this paper (i.e., the ventral macrosetae of telotarsi, the female pectinal piece glands, and the basal middle lamellae of female pectines), it seems that the *Tityus bolivianus* species-group and *Tityus sastrei* are not part of *Tityus* (*Tityus*) (Figs 2, 3). According to our observations, *Tityus* (*Tityus*) presents well-developed glandular areas in the pectinal basal piece of females (e.g., Figs 3, 5A, B, C, D, 6C, D, E, F; Table 3) and do not exhibit dilation and glandular region in the basal middle lamellae of female pectines (e.g., Figs 3, 5A, B, C, D, 6C, D, E, F; Table 3). Whereas, in terminals such as members of the *Tityus bolivianus* group and in *Tityus sastrei*, glandular areas are absent in the pectinal basal piece of females (e.g., Fig. 3; Table 3) and the basal middle lamellae of female pectines are always dilated and exhibit glandular areas (Table 3). Consequently, *Tityus sastrei* was transferred to *Tityus* (*Atreus*), whereas the *Tityus bolivianus* species-group awaits for an appropriate subgeneric designation based on a broader phylogenetic analysis of *Tityus* (i.e., Moreno-Gonzalez, 2021)

Phenotypic characters

Distribution of ventral setae of telotarsi I–IV

The leg telotarsi ventral setation has been a very commonly used phenotypic character to define genera and/or assist species diagnoses in families such as Bothriuridae, Chactidae, Diplocentridae, and Vaejovidae (e.g., Lourenço 2002a, 2002b; Prendini 2003b; Mcwest 2009). However, it has been a neglected morphological character in the taxonomy of all the New World buthid genera, including *Tityus*. For instance, after being used in an identification key of *Tityus* species presented by Kraepelin (1895), the distribution of the ventral macrosetae of the telotarsi was never again used for spe-

cies identification. In fact, very few descriptions of *Tityus* species have described the distribution of the ventral macrosetae of telotarsi I–IV (e.g., Ojanguren-Affilastro et al. 2017b), and none have implemented existing interspecific variations into modern taxonomic diagnoses or identification keys.

It is particularly interesting to note that the *Tityus* species that have ventral setae tufts on the telotarsi, for instance members of the *Tityus* (*Archaeotityus*) or the *T. obscurus* species-group of *Tityus* (*Atreus*), tend to be more strongly associated with vegetation and trees, and some are more prone to climb up to the top of the trees. On the contrary, species with two ventrosubmedian rows of setae, for instance some members of *Tityus* (*Atreus*), such as species in the *T. forcipula* species-group and *T. sastrei*, have a stronger association with bark, lower vegetation, rotten logs, and soil in general, but not with the canopy. However, after a SEM survey of the ventral setal distribution of telotarsi I–IV across different species of *Tityus* (Moreno-González, 2021), no significant differences were found in the ultrastructure of the setae from tufts (type I) or the ventrosubmedian rows (type II). Both setae have a striated surface and no other obvious modifications, much like setae from other body regions.

This previously ignored morphological character has sometimes been proved useful to assist taxonomic delimitations, even outside the genus *Tityus*. For example, Esposito et al. (2017, 2018) included the ventral setae of telotarsi in their morphological matrix, although they did not use it to assist the diagnoses of Centruroidinae genera. However, according to our observations, the distribution of the ventral macrosetae of telotarsi do not significantly vary between legs or species of the same species-group, nor are these sex- or maturity dependent, thus representing an informative characters for the recognition of Centruroidinae genera: type I in *Centruroides* Marx, 1890, *Physoctonus* Mello-Leitão, 1934, and *Rhopalurus* Thorrell, 1876; type II in *Heteroctenus* Pocock, 1893, *Jaguajir* Esposito, Yamaguti, Souza, Pinto-da-Rocha & Prendini, 2017, *Ischnotelson* Esposito, Yamaguti, Souza, Pinto-da-Rocha & Prendini, 2017, and *Troglophopalurus* Lourenço, Baptista & Giupponi, 2004. For this reason, we consider it is important to incorporate this character into the diagnoses of New World buthid taxa.

The basal piece and basal middle lamellae of the female pectines

The sexual dimorphism of the basal pectinal piece and the glands that it sometimes carries are characters that have been neglected in the taxonomy of *Tityus*. Here we continued the exploration of the pectinal piece morphology started by Moreno-González et al. (2019), including additional species-groups and subgenera of *Tityus*.

The glandular region of the pectinal basal piece of female has far too often been an overlooked morphological character in taxonomic and systematic contributions dealing with buthid taxa. Moreno-González et al. (2019) suggested, for the first time, that the presence of a glandular region on the pectinal basal piece of female is a useful character for the recognition of *Tityus* (*Archaeotityus*). In the present contribution, we discovered that the evaluation of the morphology of the pectinal basal piece of females helps make taxonomic decisions at the species and species-group levels. In the analyzed

terminals of *Tityus*, we detected four character states for the presence and development of the glandular region on the basal piece (see Results). Those character states were very congruent with the topology (Fig. 3) (i.e., Moreno-González 2021). For this reason, we consider that the pectinal basal piece provides valuable information, and we urge all incoming species descriptions to incorporate a detailed description of this structure and to use it in the construction of comparative taxonomic diagnoses when relevant.

On the other hand, the dilatation exhibited by the basal middle lamellae of the female pectines has been a widely used character in the taxonomy of *Tityus* (e.g., Lourenço 2000, 2002a, 2002b). It is worth noting that, when these lamellae are dilated, there is no glandular region in the pectinal basal piece, except in the *T. androcottooides* species-group of *Tityus* (*Atreus*). In this group, the basal pectinal piece may bear a glandular region in both sexes (e.g., *T. rebierei*), something not previously reported in any other study. It is possible that these glandular regions could play a crucial role in chemical communication, but specific studies are needed to evaluate this hypothesis.

Cuticular (exocrine) glandular regions are a very common feature in a broad spectrum of arthropod groups (e.g., Coleoptera, Hemiptera, Hymenoptera, Isoptera, Lepidoptera, and Orthoptera) (Costa-Leonardo et al. 2009; Schiestl 2010; Richard and Hunt 2013; Pelosi et al. 2014; Blomquist et al. 2020). However, in *Tityus* species, the glandular function of these regions, present on the pectinal basal plate and basal middle lamellae of the female pectines, and the sternites of both sexes, remains unexplored. Nevertheless, all these regions exhibit a high density of cuticular pores when compared to other body parts (e.g., Fig. 11A, B), which leads us to think that they may secrete chemicals. But again, more studies are required to corroborate this hypothesis.

On cave-dwelling scorpions from Brazil

Species of two scorpion families occur in Brazilian caves, Bothriuridae Simon, 1880 and Buthidae (Trajano 1987; Trajano and Moreira 1991; Gnaspini and Trajano 1994; Pinto-da-Rocha 1995; Cordeiro et al. 2014). Few specimens of Bothriuridae have been recorded in Brazilian caves, with *Bothriurus araguayae* Vellard 1934 having been recorded from caves in the states of São Paulo (Iporanga municipality) and Minas Gerais (Itacarambi municipality), and *Thestylus aurantiurus* Yamaguti and Pinto-da-Rocha, 2003 from one granitic cave in the state of São Paulo (Bichuette et al. 2017). Considering their burrowing habits, coupled with the few records in caves, Bothriuridae species probably are accidental fauna in subterranean habitats.

Representatives of Buthidae are more found in Brazilian caves, with at least eight species having been recorded, belonging to the genera *Tityus* and *Troglohopalurus* (Lourenço et al. 1997; Esposito et al. 2017). One undoubtedly troglobitic species, *Troglohopalurus translucidus* Lourenço, Baptista and Giupponi 2004, is known from sandstone caves in Chapada Diamantina, state of Bahia. Two other species are probably accidental, *Tityus* (*Atreus*) *obscurus* and *Ischnotelson peruassu* Esposito, Yamaguti,

Souza, Pinto-da-Rocha and Prendini 2017, each with records from caves in the states of Pará (Altamira region) and Minas Gerais (Itacarambi region), respectively (authors, pers. obs.). Some other species are trogliphiles, such as *Tityus (Tityus) blaseri* which lives in caves and epigeal habitats in the state of Goiás, *Tityus (Tityus) confluens* Borelli 1899 in caves and epigeal habitats in the states of Mato Grosso and Mato Grosso do Sul, *Tityus (Tityus) stigmurus* (Thorell 1876) which is widely distributed in northeastern Brazil with facultative cave populations in the state of Sergipe and the new species here described, *Tityus (Tityus) spelaeus* sp. nov. The biospeological classification of *Troglophopalurus lacraui* (Lourenco and Pinto-da-Rocha 1997) remains contentious due to it having cave populations in the state of Bahia and one epigeal record (of its junior synonym *Rhopalurus brejo* Lourenço, 2014) from Crato in the state of Ceará (Esposito et al. 2017). Based on those records, Esposito et al. (2017) classified *Troglophopalurus lacraui* as a trogliphile, a classification also followed by Prendini et al. (2021).

As expected, trogliphilic populations are found more often inside caves than in epigeal habitats due to differences in the dynamics of species. They are generally more numerous in subterranean habitats (Trajano and Carvalho 2017) and, for that reason, collecting in epigeal habitats to find trogliphilic populations with low densities on the surface is advisable (Trajano and Carvalho 2017).

Trogliphiles and troglonexes are both found in epigeal and subterranean environments, and, since individuals can move between them, it is not easy to distinguish between these two categories. One strong piece of evidence for trogliphilic populations is the presence of individuals of all ages distributed along with the subterranean environment throughout different annual cycles (Bichuette and Trajano 2006; Trajano and Carvalho 2017). In both visits to Russão II cave (2007 and 2015), we found individuals of *T. spelaeus* sp. nov. of different ages, including juveniles of the second instar and pregnant females, distributed in all terrestrial zones of the cave, which signal that the new species is a trogliphile.

No individuals of *T. spelaeus* sp. nov. have been found in the epigeal habitat to date. However, *Tityus spelaeus* sp. nov., does not show any troglomorphisms, such as elongated appendices, reduction of visual organs, low degree of sclerotization or depigmentation. The use of clues like troglomorphisms to assume that a species is troglobitic become valid when analyzed within a phylogenetic framework, which can show that these features are autapomorphic states of troglobites (Trajano and Carvalho 2017). So, we believe that the new scorpion described here is a trogliphile, and it is noteworthy that the surroundings of the Russão II cave are severely modified for cattle pastures and urban growth (Tencatt and Bichuette 2017).

Also, it is worth mentioning that trogliphiles are not less adapted to subterranean environment than troglobites in what is considered a continuum of cave adaptation (Trajano and Carvalho 2017), just as troglobites do not represent an evolutionary dead-end, with some known cases of endogenous scorpions having evolved from troglobitic ancestors (Prendini et al. 2010).

Acknowledgements

We are grateful to Alex S. Valdarnini (Grupo Pierre Martin de Espeleologia – GPME) for the photography of Russão II cave. Eleonora Trajano and Maria E. Bichuette (UFSCar) helped during one field trip to the cave. We also thank Maria E. Bichuette for the valuable information on scorpions in Brazilian caves. This work was supported by the Fundação de Amparo à Pesquisa do Estado de São Paulo (FAPESP) (under Grant 2015/18376–2 to JAMG, and project Dimensions US–BIOTA–São Paulo 2013/50297–0, and 2010/08459–4), NSF–DOB 1343578, NASA and Conselho Nacional de Desenvolvimento Científico e Tecnológico (CNPq under Grant 142276/2013–8 to JEG, and 457413/2014–0). We thank C. C. de Paula for the help during the 2015 fieldwork and to ICMBIO for the collecting permits. Finally, we are grateful to Andrés Ojanguren-Affilastro (MACN) and Ricardo Botero (AMNH) for their useful comments and suggestions that allowed us to improve this manuscript.

References

- Ab'Saber NA (1977) Os domínios morfoclimáticos na América do Sul. *Geomorfologia* 52: 1–21.
- Armas LFD, Antún AJA (2004) Adiciones al género *Tityus* C. L. Koch, 1836 en República Dominicana, con la descripción de dos especies nuevas. *Revista Ibérica de Arcnología* 10: 53–64.
- Astrin JJ, Höfer H, Spelda J, Holstein J, Bayer S, Hendrich L, Huber BA, Kielhorn K-H, Krammer H-J, Lemke M (2016) Towards a DNA barcode reference database for spiders and harvestmen of Germany. *PLoS ONE* 11: e0162624. <https://doi.org/10.1371/journal.pone.0162624>
- Bichuette ME, Trajano E (2006) Morphology and distribution of the cave knifefish *Eigenmannia vicentespelaea* Triques, 1996 (Gymnotiformes: Sternopygidae) from Central Brazil, with an expanded diagnosis and comments on subterranean evolution. *Neotropical Ichthyology* 4: 99–105. <https://doi.org/10.1590/S1679-62252006000100011>
- Bichuette ME, Nascimento AR, Von Schimonsky DM, Gallão JE, Resende LPA, Zepon T (2017) Terrestrial fauna of the largest granitic cave from Southern Hemisphere, southeastern Brazil: A neglected habitat. *Neotropical Biology and Conservation*. 12: 75–90. <https://doi.org/10.4013/nbc.2017.122.01>
- Blomquist GJ, Tittiger C, Jurenka R (2020) Cuticular hydrocarbons and pheromones of arthropods. In: *Hydrocarbons, oils and lipids: diversity, origin, chemistry, and fate. Handbook of Hydrocarbon and Lipid Microbiology*. Springer Nature, Switzerland, 213–244. https://doi.org/10.1007/978-3-319-90569-3_11
- Borges A, Graham MR (2016) Phylogenetics of scorpions of medical importance. In: Gopalakrishnakone P, Calvete JJ (Eds), *Venom Genomics and Proteomics. Toxinology*. Springer Netherlands, Dordrecht, 81–104. https://doi.org/10.1007/978-94-007-6416-3_36
- Borges A, Jowers MJ, Bónoli S, De Sousa L (2012) Scorpions from the primeval subgenus *Archaeotityus* produce putative homologs of *Tityus serrulatus* toxins active on voltage-gated sodium channels. *Journal of Venomous Animals and Toxins including Tropical Diseases* 18: 432–440. <https://doi.org/10.1590/S1678-91992012000400012>

- Borges A, Bermingham E, Herrera N, Alfonzo MJ, Sanjur OI (2010) Molecular systematics of the neotropical scorpion genus *Tityus* (Buthidae): The historical biogeography and venom antigenic diversity of toxic Venezuelan species. *Toxicon* 55: 436–454. <https://doi.org/10.1016/j.toxicon.2009.09.011>
- Botero-Trujillo R, Flórez E (2014) A new species of *Tityus* (Scorpiones, Buthidae) from El Edén Cave, Colombia. *Zootaxa* 3796: 108–120. <https://doi.org/10.11646/zootaxa.3796.1.5>
- Cordeiro LM, Borghezán R, Trajano E (2014) Subterranean biodiversity in the serra da Bodoquena karst area, paraguay river basin, Mato Grosso do Sul, Southwestern Brazil. *Biota Neotropica* 14: 1–28. <https://doi.org/10.1590/1676-06032014011414>
- Costa-Leonardo AM, Casarin FE, Lima JT (2009) Chemical communication in Isoptera. *Neotropical Entomology* 38: 1–6. <https://doi.org/10.1590/S1519-566X2009000100001>
- Espósito LA, Yamaguti HY, Souza CA, Pinto-Da-Rocha R, Prendini L (2017) Systematic revision of the neotropical club-tailed scorpions, *Physoctonus*, *Rhopalurus*, and *Troglophopalurus*, revalidation of *Heteroctenus*, and descriptions of two new genera and three New Species (Buthidae: Rhopalurusinae). *Bulletin of the American Museum of Natural History* 415: 1–136. <https://doi.org/10.1206/0003-0090-415.1.1>
- Espósito LA, Yamaguti HY, Pinto-da-Rocha R, Prendini L (2018) Plucking with the plectrum: phylogeny of the New World buthid scorpion subfamily Centruroidinae Kraus, 1955 (Scorpiones: Buthidae) reveals evolution of three pecten-sternite stridulation organs. *Arthropod Systematics & Phylogeny* 76: 87–122.
- Fet V, Lowe G (2000) Family Buthidae C. L. Koch, 1837. In: *Catalog of the Scorpions of the World*. The New York Entomological Society, New York, 54–286.
- Fetzner Jr JW (1999) Extracting high-quality DNA from shed reptile skins: a simplified method. *Biotechniques* 26: 1052–1054. <https://doi.org/10.2144/99266bm09>
- Francke OF (1977) Scorpions of the genus *Diplocentrus* from Oaxaca, Mexico (Scorpionida, Diplocentridae). *Journal of Arachnology* 4: 145–200.
- Francke OF, Stockwell SA (1987) Scorpions (Arachnida) from Costa Rica. *Special Publications The Museum of Texas Tech University, Austin*, 63 pp. <https://doi.org/10.5962/bhl.title.156482>
- Gallão JE, Bichuette ME (2016) On the enigmatic troglobitic scorpion *Troglophopalurus translucentus*: distribution, description of adult females, life history and comments on *Rhopalurus lacrau* (Scorpiones: Buthidae). *Zoologia (Curitiba)* 33: 1–13. <https://doi.org/10.1590/s1984-4689zool-20150193>
- Gantenbein B, Fet V, Largiadèr CR, Scholl A (1999) First DNA phylogeny of *Euscorpium* Thorell, 1876 (Scorpiones, Euscorpidae) and its bearing on taxonomy and biogeography of this genus. *Biogeographica (Paris)* 75: 49–65.
- Gnaspini P, Trajano E (1994) Brazilian cave invertebrates, with a checklist of troglomorphic taxa. *Revista Brasileira de Entomologia* 38: 549–584.
- González-Sponga MA (1974) Dos nuevas especies de alacranes del género *Tityus* en las cuevas venezolanas (Scorpionida: Buthidae). *Boletín de la Sociedad Venezolana de Espeleología* 5: 55–72.
- Junior SDTP (1932) Considerações a respeito da systematica geral do genero *Tityus* e do *Tityus bahiensis* em particular. *Revista de Agricultura* 7: 295–306.
- Katoh K, Standley DM (2013) MAFFT multiple sequence alignment software version 7: improvements in performance and usability. *Molecular Biology and Evolution* 30: 772–780. <https://doi.org/10.1093/molbev/mst010>

- Kocher TD, Thomas WK, Meyer A, Edwards SV, Pääbo S, Villablanca FX, Wilson AC (1989) Dynamics of mitochondrial DNA evolution in animals: amplification and sequencing with conserved primers. *Proceedings of the National Academy of Sciences* 86: 6196–6200. <https://doi.org/10.1073/pnas.86.16.6196>
- Kraepelin K (1895) Nachtrag zu Theil I der Revision der Scorpione. *Jahrbuch der Hamburgischen Wissenschaftlichen Anstalten* 12: 73–96.
- Loria SF, Prendini L (2014) Homology of the lateral eyes of scorpiones: A six-ocellus model. *PLoS ONE* 9: 1–30. <https://doi.org/10.1371/journal.pone.0112913>
- Lourenço WR (1981) Scorpions cavernicoles de l'Equateur: *Tityus demangei* n. sp. et *Ananteris ashmolei* n. sp. (Buthidae): *Trogloayosicus vachoni* n. gen., n. sp. (Chactidae), Scorpion troglobie. *Bulletin du Museum national d'histoire naturelle. Section A: Zoologie, biologie et ecologie animales* 2: 635–662.
- Lourenço WR (1984) Analyse taxonomique des scorpions du groupe *Tityus clathratus* Koch, 1845 (Scorpiones, Buthidae). *Bulletin du Muséum national d'histoire naturelle. Section A, Zoologie, biologie et écologie animales* 6: 349–360.
- Lourenço WR (1999) Origines et affinités des scorpions des Grandes Antilles: le cas particulier des éléments de la famille des Buthidae. *Biogeographica* 75: 131–144.
- Lourenço WR (2000) Synopsis of the colombian species of *Tityus* Koch (Chelicerata, Scorpiones, Buthidae), with descriptions of three new species. *Journal of Natural History* 34: 449–461. <https://doi.org/10.1080/002229300299561>
- Lourenço WR (2002a) 4.9 Scorpiones. In: *Amazonian Arachnida and Myriapoda. Faunistica* N° 24. Pensoft Publishers, Sofia-Moscow, 399–438.
- Lourenço WR (2002b) Scorpions of Brazil. *Les éditions de l'If Paris*, 304 pp.
- Lourenço WR (2006) Une nouvelle proposition de découpage sous-générique du genre “*Tityus*” C.L. Koch, 1836 (Scorpiones, Buthidae). *Boletín de la Sociedad Entomológica Aragonesa* 39: 55–67.
- Lourenço WR (2011) The distribution of noxious species of scorpions in Brazilian Amazonia: the genus *Tityus* CL Koch, 1836, subgenus *Atreus* Gervais, 1843 (Scorpiones, Buthidae). *Entomologische Mitteilungen aus dem Zoologischen Museum Hamburg* 15: 287–301.
- Lourenço WR (2015) What do we know about some of the most conspicuous scorpion species of the genus *Tityus*? A historical approach. *Journal of Venomous Animals and Toxins Including Tropical Diseases* 21: 1–12. <https://doi.org/10.1186/s40409-015-0016-9>
- Lourenço WR (2016) Une nouvelle espèce de *Tityus* CL Koch, 1836 (Scorpiones: Buthidae), collectée par Jean A. Vellard dans l'ancien Etat de Goiás, aujourd'hui Tocantins, Brésil. *Revista Ibérica de Aracnología*: 75–78.
- Lourenço WR (2019) New insights on the scorpion species of the “*Tityus trivittatus* group” of subgenus *Tityus* CL Koch, 1836 (Scorpiones: Buthidae). *Revista Ibérica de Aracnología*: 119–125.
- Lourenço WR, Eickstedt VRD von (1984) Descrição de uma espécie nova de *Tityus* coletada no Estado da Bahia, Brasil (Scorpiones, Buthidae). *Journal of Arachnology* 12: 55–60.
- Lourenço WR, Francke OF (1985) Révision des connaissances sur les scorpions cavernicoles (troglobies) (Arachnida, Scorpions). *Mémoires Biospéologiques* 12: 3–7.
- Lourenço WR, Pinto-da-Rocha R (1997) A reappraisal of the geographic distribution of the genus *Rhopalurus* Thorell (Scorpiones, Buthidae) and description of two new species. *Biogeographica* 73: 181–191.

- Lourenço WR, Duhem B (2010) Buthid scorpions found in caves; a new species of *Isometrus* Ehrenberg, 1828 (Scorpiones, Buthidae) from southern Vietnam. *Comptes Rendus – Biologies* 333: 631–636. <https://doi.org/10.1016/j.crvi.2010.05.005>
- Lourenço WR, Pham DS (2013) First record of a cave species of *Euscorpiops* Vachon from Viet Nam (Scorpiones, Euscorpiidae, Scorpiopinae). *Comptes Rendus – Biologies* 336: 370–374. <https://doi.org/10.1016/j.crvi.2013.06.005>
- Lourenço WR, Knox MB, Magalhães ED (1997) Redescription of *Tityus blaseri* (Scorpiones: Buthidae) from Goiás, Brazil. *Revista de Biología Tropical* 45: 1579–1582.
- Lourenço WR, Cabral BC, Ramos EB (2004) Confirmation of *Tityus confluens* Borelli, 1899 (Scorpiones, Buthidae) in Brazil and description of a new subspecies from the State of Mato Grosso do Sul. *Boletín de la Sociedad Entomológica Aragonesa* 34: 27–30.
- Mcwest KJ (2009) Tarsal spinules and setae of vaejovid scorpions (Scorpiones: Vaejovidae). *Zootaxa* 2001: 1–126.
- Mello-Leitão C de (1945) Escorpiões sul-americanos. *Arquivos do Museu Nacional* 40: 7–468.
- Minh BQ, Schmidt HA, Chernomor O, Schrempf D, Woodhams MD, Von Haeseler A, Lanfear R (2020) IQ-TREE 2: New models and efficient methods for phylogenetic inference in the genomic era. *Molecular Biology and Evolution* 37: 1530–1534. <https://doi.org/10.1093/molbev/msaa015>
- Moreno-González JA, González OR, Flórez DE (2019) Taxonomic revision of the Colombian *Tityus* (*Archaeotityus*) (Scorpiones, Buthidae) species: A morphological and morphometric approach, with a description of a new species. *Zootaxa* 4660: 1–94. <https://doi.org/10.11646/zootaxa.4660.1.1>
- Moreno-González JA (2021) Phylogenetic analysis of the *Tityus clathratus* species-group and other species-groups and subgenera of *Tityus* (Scorpiones: Buthidae) based on molecular and morphological characters [In portuguese: Análise filogenética do grupo de espécies *Tityus clathratus* e outros grupos e subgêneros de *Tityus* (Scorpiones: Buthidae) baseada em caracteres moleculares e morfológicos]. Ph.D. dissertation. Universidade de São Paulo, São Paulo, 250 pp.
- Nimer E (1979) *Climatologia do Brasil*. Vol. 4. Rio de Janeiro: SUPREN.
- Ojanguren-Affilastro AA, Adilardi RS, Mattoni CI, Ramírez MJ, Ceccarelli FS (2017a) Dated phylogenetic studies of the southernmost American buthids (Scorpiones; Buthidae). *Molecular Phylogenetics and Evolution* 110: 39–49. <https://doi.org/10.1016/j.ympev.2017.02.018>
- Ojanguren-Affilastro AA, Adilardi RS, Cajade R, Ramírez MJ, Ceccarelli FS, Mola LM (2017b) Multiple approaches to understanding the taxonomic status of an enigmatic new scorpion species of the genus *Tityus* (Buthidae) from the biogeographic island of Paraje Tres Cerros (Argentina). *PLoS ONE* 12: 1–24. <https://doi.org/10.1371/journal.pone.0181337>
- Ojanguren-Affilastro AA, Kochalka J, Guerrero-Orellana G, Garcete-Barrett B, Roodt AR, Borges A, Ceccarelli S (2021) Redefinition of the identity and phylogenetic position of *Tityus trivittatus* Kraepelin 1898, and description of *Tityus carrilloi* n. sp. (Scorpiones; Buthidae), the most medically important scorpion of southern South America. *Revista del Museo Argentino de Ciencias Naturales, nueva serie* 23: 27–55. <https://doi.org/10.22179/REVMACN.23.714>
- Outeda-Jorge S, Mello T, Pinto-da-Rocha R (2009) Litter size, effects of maternal body size, and date of birth in South American scorpions (Arachnida: Scorpiones). *Zoologia (Curitiba)* 26: 43–53. <https://doi.org/10.1590/s1984-46702009000100008>

- Pelosi P, Iovinella I, Felicioli A, Dani FR (2014) Soluble proteins of chemical communication: an overview across arthropods. *Frontiers in Physiology* 5: e320. <https://doi.org/10.3389/fphys.2014.00320>
- Pinto-da-Rocha R (1995) Sinopse da fauna cavernícola do Brasil (1907–1994). *Papéis Avulsos de Zoologia* 39: 61–173.
- Pinto-da-Rocha R, Bragagnolo C, Marques FB, Antunes Junior M (2014) Phylogeny of harvestmen family Gonyleptidae inferred from a multilocus approach (Arachnida: Opiliones). *Cladistics* 30: 519–539. <https://doi.org/10.1111/cla.12065>
- Prendini L (2000) Phylogeny and classification of the superfamily Scorpionoidea Latreille 1802 (Chelicerata, Scorpiones): An exemplar approach. *Cladistics* 16: 1–78. <https://doi.org/10.1006/clad.1999.0127>
- Prendini L (2001) Further additions to the scorpion fauna of Trinidad and Tobago. *Journal of Arachnology* 29: 173–188. [https://doi.org/10.1636/0161-8202\(2001\)029\[0173:FATTSF\]2.0.CO;2](https://doi.org/10.1636/0161-8202(2001)029[0173:FATTSF]2.0.CO;2)
- Prendini L (2003a) Discovery of the male of *Parabuthus muelleri*, and implications for the phylogeny of *Parabuthus* (Scorpiones: Buthidae). *American Museum Novitates* 3408: 1–24. [https://doi.org/10.1206/0003-0082\(2003\)408%3C0001:DOTMOP%3E2.0.CO;2](https://doi.org/10.1206/0003-0082(2003)408%3C0001:DOTMOP%3E2.0.CO;2)
- Prendini L (2003b) Revision of the genus *Lisposoma* Lawrence, 1928 (Scorpiones: Bothriuridae). *Insect Systematics & Evolution* 34: 241–264. <https://doi.org/10.1163/187631203788964764>
- Prendini L, Francke OF, Vignoli V (2010) Troglomorphism, trichobothriotaxy and typhlochactid phylogeny (Scorpiones, Chactoidea): more evidence that troglobitism is not an evolutionary dead-end. *Cladistics* 26: 117–142. <https://doi.org/10.1111/j.1096-0031.2009.00277.x>
- Prendini L, Ehrenthal VL, Loria SF (2021) Systematics of the relictual Asian scorpion family Pseudochactidae Gromov, 1998, with a review of cavernicolous, troglobitic, and troglomorphic scorpions. *Bulletin of the American Museum of Natural History* 453: 1–149. <https://doi.org/10.1206/0003-0090.453.1.1>
- Racovitza EG (1907) Essai sur les problemes biospeologiques. *Archives des Maladies du Coeur et des Vaisseaux 4e serie* 6: 371–48.
- Reddell JR (2012) Spiders and related groups. In: *Ecosystems of the World, Subterranean Ecosystems*. Elsevier Academic Press, Amsterdam, 554–564. <https://doi.org/10.1016/b978-0-12-814124-3.00118-7>.
- Rein JO (2021) The Scorpion Files. Trondheim: Norwegian University of Science and Technology. <https://www.ntnu.no/ub/scorpion-files/>
- Richard F-J, Hunt JH (2013) Intracolony chemical communication in social insects. *Insectes Sociaux* 60: 275–291. <https://doi.org/10.1007/s00040-013-0306-6>
- Román JP, García F, Medina D, Vásquez M, García J, Graham MR, Romero-Alvarez D, Pardal PP de O, Ishikawa EAY, Borges A (2018) Scorpion envenoming in Morona Santiago, Amazonian Ecuador: Molecular phylogenetics confirms involvement of the *Tityus obscurus* group. *Acta Tropica* 178: 1–9. <https://doi.org/10.1016/j.actatropica.2017.10.014>
- Schiestl FP (2010) The evolution of floral scent and insect chemical communication. *Ecology Letters* 13: 643–656. <https://doi.org/10.1111/j.1461-0248.2010.01451.x>

- Schiner JR (1854) Fauna der Adelsberger-, Luegger-, und Magdalenen- Grotte. In: Die Grotten und Höhlen von Adelsberg, Lueg, Planina und Laas. Braunmüller, Wien, 231–272.
- Schulmeister S (2003) Simultaneous analysis of basal Hymenoptera (Insecta): introducing robust-choice sensitivity analysis. *Biological Journal of the Linnean Society* 79: 245–275. <https://doi.org/10.1046/j.1095-8312.2003.00233.x>
- Schwendinger PJ, Giribet G (2005) The systematics of the south-east Asian genus *Fangensis* Rambla (Opiliones: Cyphophthalmi: Stylocellidae). *Invertebrate Systematics* 19: 297–323. <https://doi.org/10.1071/IS05023>
- Simon C, Frati F, Beckenbach A, Crespi B, Liu H, Flook P (1994) Evolution, weighting, and phylogenetic utility of mitochondrial gene sequences and a compilation of conserved polymerase chain reaction primers. *Annals of the Entomological Society of America* 87: 651–701. <https://doi.org/10.1093/aesa/87.6.651>
- Sissom WD, Reddell JR (2009) Cave scorpions of Mexico and the United States. *Texas Memorial Museum Speleological Monographs* 7: 19–32.
- Sissom WD, Polis GA, Watt DD (1990) Field and laboratory methods. In: *The Biology of Scorpions*. Stanford University Press, California, 445–461.
- Soleglad ME, Fet V (2003) High-level systematics and phylogeny of the extant scorpions (Scorpiones: Orthosterni). *Euscorpius* 11: 1–56. <https://doi.org/10.18590/euscorpius.2003.vol2003.iss11.1>
- Souza CARDE, Candido DM, Lucas SM, Brescovit AD (2009) On the *Tityus stigmurus* complex (Scorpiones, Buthidae). *Zootaxa* 38: 1–38.
- Stahnke HL (1970) Scorpion nomenclature and mensuration. *Entomological News* 81: 297–316.
- Tencatt LFC, Bichuette ME (2017) *Aspidoras mephisto*, new species: the first troglobitic Callichthyidae (Teleostei: Siluriformes) from South America. *PLoS ONE* 12: e0171309. <https://doi.org/10.1371/journal.pone.0171309>
- Teruel R, García LF (2008a) Rare or poorly known scorpions from Colombia. I. Redescription of *Tityus macrochirus* Pocock, 1897 (Scorpiones: Buthidae). *Euscorpius* 63: 1–11. <https://doi.org/10.18590/euscorpius.2008.vol2008.iss63.1>
- Teruel R, García LF (2008b) Rare or poorly known scorpions from Colombia. II. Redescription of *Tityus columbianus* (Thorell, 1876) (Scorpiones: Buthidae). *Euscorpius* 64: 1–14. <https://doi.org/10.18590/euscorpius.2008.vol2008.iss64.1>
- Trajano E (1987) Fauna cavernícola brasileira: composição e caracterização preliminar. *Revista Brasileira de Zoologia* 3: 533–561. <https://doi.org/10.1590/S0101-81751986000400004>
- Trajano E (2012) Ecological classification of subterranean organisms. In: White WB, Culver DC (Eds) *Encyclopedia of Caves* (Second Edition). Academic Press, Amsterdam, 275–277. <https://doi.org/10.1016/B978-0-12-383832-2.00035-9>
- Trajano E, Moreira JRA (1991) Estudo da fauna de cavernas da Província Espeleológica Arenítica Altamira-Iraituba, Pará. *Revista Brasileira de Zoologia* 51: 13–29.
- Trajano E, Carvalho MR (2017) Towards a biologically meaningful classification of subterranean organisms: a critical analysis of the Schiner-Racovitza system from a historical perspective, difficulties of its application and implications for conservation. *Subterranean Biology* 22: 1–26. <https://doi.org/10.3897/subtbiol.22.9759.figure1>
- Vachon M (1963) De l'utilité, en systématique, d'une nomenclature des dents des chélicères chez les Scorpions. *Bulletin du Muséum national d'Histoire naturelle, Paris*: 161–166.

- Vachon M (1974) Etude des caractères utilisés pour classer les familles et les genres de Scorpions (Arachnides). 1. La trichobothriotaxie en arachnologie. Sigles trichobothriax et types de trichobothriotaxie chez les Scorpions. Bulletin du Muséum national d'Histoire naturelle, Paris 140: 857–958.
- Vachon M (1975) Sur l'utilisation de la trichobothriotaxie du bras des pédipalpes des Scorpions (Arachnides) dans le classement des genres de la famille des Buthidae Simon. Comptes Rendus des séances de l'Académie des Sciences, Paris, série D 281: 1597–1599.
- Vaidya G, Lohman DJ, Meier R (2011) SequenceMatrix: concatenation software for the fast assembly of multi-gene datasets with character set and codon information. Cladistics 27: 171–180. <https://doi.org/10.1111/j.1096-0031.2010.00329.x>
- Volschenk ES, Prendini L (2008) *Aops oncodactylus*, gen. et sp. nov., the first troglobitic urodacid (Urodacidae: Scorpiones), with a re-assessment of cavernicolous, troglobitic and troglomorphic scorpions. Invertebrate Systematics 22: 235–257. <https://doi.org/10.1071/IS06054>
- Whiting MF, Carpenter JC, Wheeler QD, Wheeler WC (1997) The Strepsiptera problem: phylogeny of the holometabolous insect orders inferred from 18S and 28S ribosomal DNA sequences and morphology. Systematic Biology 46: 1–68. <https://doi.org/10.1093/sysbio/46.1.1>

Appendix I

Voucher samples from which material was examined for morphological study and Sanger loci were sequenced. The vouchers are deposited in the following collections: the Ambrose Monell Cryocollection (**AMCC**) of the American Museum of Natural History (**AMNH**), New York (curator: Dr. Lorenzo Prendini); the Instituto de Biotecnologías, Arachnology Laboratory Cryo-Collection (**IBALCC**) (curator: Dr. Ricardo Pinto da Rocha); the Museum National d'Histoire Naturelle (**MNHN**), Paris, France (curator: Dr. Mark Judson); the Museu Nacional/ Universidade Federal do Rio de Janeiro (**MNRJ**), Rio de Janeiro, Brazil (curator: Dr. Adriano B. Kury); the Museu de Zoologia da Universidade de São Paulo (**MZSP**), São Paulo, Brazil (curator: Dr. Ricardo Pinto da Rocha); the Museu de aracnología, Universidade Federal de Minas Gerais (**UFMG**), Belo Horizonte, Brazil (curator: Dr. Adalberto Santos).

***Isometrus maculatus* (DeGeer, 1778):** BRAZIL: adult male, without locality data, xii.1954 (MZSP 87742). State of Pará: adult male, Belém, 1984 (MNRJ 7041); adult female, Belém-Brasília highway km 91, 15.viii-20.x.1959 (MZSP 8743). SRI LANKA: adult male and adult female, Wellawaya, 24.ii.2000, D. Huber (AMCC [LP 1798])

***Tityus annae* Lourenço, 1997:** BRAZIL, state of Paraíba/ Pernambuco: adult female (holotype), 1895, Gounelle (MNHN-RS-0818).

***Tityus argentinus* Borelli, 1899:** ARGENTINA, Salta province: two adult females, Calilegua National Park- Águas Negras section [Parque Nacional de Calilegua- Seccional Águas Negras], 23°45'38.16"S, 64°51'0.79"W, 7.xii.2008, A. Ojanguren-Affilastro & C. I. Mattoni (UFMG 15906).

- Tityus blaseri* Mello-Leitão, 1931:** BRAZIL, state of Goiás: subadult female (holotype), Veadeiros, Rio São Miguel, 11.ii.1882, Blaser (MNRJ 11282); adult female, Alto Paraíso de Goiás, entrance Cristal waterfall [Entrada Cachoeira Cristal], 14°05.583'S, 47°30.547'W, 5.iv.2009, F. Marques & S. Outeda-Jorge (IBALCC-RPDR 00027); subadult female, same data (IBALCC-RPDR 00114/ MZSP 31125).
- Tityus bahiensis* (Perty, 1833):** BRAZIL, state of Minas Gerais: adult male and subadult female, Serra do Rola Moça National Park [Parque Estadual Serra do Rola Moça], 20°5"S, 44°2"W, 2.xii.2004, A. A. Azevedo (UFMG 4076); adult female, RPPN Cachoeira Cerradão, São Roque de Minas, -20.22797, -46.3869, 2.v.2014, R. Pinto-da-Rocha & F. Marques (IBALCC-RPDR 00281).
- Tityus blaseri* Mello-Leitão, 1931:** BRAZIL, state of Goiás: adult female, Alto Paraíso de Goiás, pathway to Cristal waterfall [cachoeira Cristal], 05.iv.2009, S. Outeda-Jorge & F. Marques (IBALCC-RPDR 00027, 00114).
- Tityus braziliae* Lourenço & Eickstedt, 1984:** BRAZIL, state of Pernambuco: adult female, Engenho Água, Serra dos Mascarenhas, 07°36'S, 35°23'W, 24–25.vii.2010, M. B. da Silva & A. M. Souza (MZSP 75619); adult male, Goiana, 29.v.2008, H. Yamaguti, T. Porto & M. B. da Silva (IBALCC-RPDR 00199). State of Sergipe: adult male, Serra de Itabaina National Park [Parque Nacional Serra de Itabaina], 10°45'07"S, 37°20'27"W, 28.vi.2009, R. Pinto-da-Rocha (IBALCC-RPDR 00169).
- Tityus carrilloi* Ojanguren-Affilastro, 2021:** PARAGUAY: two males and three females, Asunción, xi.1944 (MZSP 21772).
- Tityus charreyroni* Mello-Leitão, 1933:** BRAZIL, state of Goiás: subadult female, Catalão, 12°11.755'S, 47°57.189'W, 4.iv.2009, S. Outeda-Jorge & F. Marques (IBALCC-RPDR 00112); adult female, Piranhas, 20.iv.2008 (UFMT 00340). State of Mato Grosso: adult female and four juveniles, urban area, Pontal do Araguaia, 27.iv.2007, Neivander (UFMT 00343); adult female, same locality data, 14.v.2007, Neivander (UFMT 00338); adult female, João de Barro, Torixoreu, 2010, Silvana (UFMT 00341).
- Tityus clathratus* C. L. Koch, 1844:** BRAZIL, state of Roraima: adult male and 10 adult females, Alto Alegre, 3°00'10"N, 61°18'08"W, 10.xi.2008, H. Yamaguti & R. Pinto-da-Rocha (MZSP 31468); adult female, Amajari, Vila Tepequém, 11.xi.2008, H. Yamaguti & R. Pinto-da-Rocha (IBALCC-RPDR 00192).
- Tityus confluens* Borelli, 1899:** BRAZIL, state of Mato Grosso do Sul: adult female, Gruta Pitangueiras, Bonito, 22.x.2002, E. Trajano et al., pitfall- 40 m away from the entrance (MZSP 23943).
- Tityus costatus* (Karsch, 1879):** BRAZIL, state of Minas Gerais: adult female, Fazenda Montes Claros, 19°47'S, 42°8'W, iv.2001, W. J. Cassimiro (UFMG 4088); adult female, same locality, 18.xi.2000, W. J. Cassimiro (UFMG 4077); adult female, same locality data, 18.ix.1999, W. P. Martins (UFMG 4081). State of Espírito Santo: adult male, Biological Reserve Córrego do Veado [Reserva Biologica Córrego do Veado], 18°21.280'S, 40°08.165'W, 13.vi.2011, H. Yamaguti et al. Leg., pitfall (MZSP 42883). State of Rio de Janeiro: adult female, Mangaratiba, viii.2017, D. Álvarez (MZSP).

***Tityus forcipula* (Gervais, 1843):** COLOMBIA, Risaralda department: three adult males and two adult females, Santuario, San Rafael Plains Natural Regional Park (Planes de San Rafael), 5°7'34"N, 76°0'26.4"W, 2158 m a.s.l., 17.x.2012, J. A. Moreno (MZSP). Valle del Cauca department: adult female, Yumbo, Dapa, Bocatoma del Acueducto, 17–18.viii.2016, J. A. Moreno (IBALCC-RPDR 00256).

***Tityus gasci* Lourenço, 1981:** FRENCH GUIANA: adult male (holotype), South of French Guiana, 1975, J. P. Gasci (MNHN-RS-7921). *Tityus nelsoni* Lourenço, 2005: BRAZIL, Amazonas state: adult female (paratype) and adult male (holotype), São Gabriel da Cachoeira, 5–30.iii.1992, E. Soares (MNHN-RS-8619, MNHN-RS-8618).

***Tityus obscurus* Gervais, 1843:** BRAZIL: state of Pará: three adult males and two adult females, posto 8- sismografo, Altamira, 14.iv.2009 (MNRJ 07610). state of Amapá: juvenile, Oiapoque–Tumucumaque, Saur Maripa, 17.iii.2015, D. Chirivi & J. Murienne (IBALCC-RPDR 00236).

***Tityus panguana* Kovařík, Teruel, Lowe & Friedrich, 2015.** PERU, Madre de Dios department: adult male, Erika Lodge, Rio Alto, 30 min on boat from Atoleya, 7–8.xii.2004, J. A. Ochoa (IBALCC-RPDR 00268).

***Tityus pintodarochai* Lourenço, 2005:** BRAZIL, state of Paraná: adult female (holotype), Vilha Velha National Park [Parque Estadual de Vilha Velha], 28.i.1973, J. Garzoni (MNHN-RS-6567).

***Tityus potameis* Lourenço & Giupponi, 2004.** BRAZIL, state of Espírito Santo: adult female, Sooretama Biological Reserve [Reserva Biologica Sooretama], trilha da sede, 19°03'23.5"S, 40°08'51.7"W, 02.vi.2011, H. Yamaguti (IBALCC-RPDR 00275).

***Tityus raquelae* Lourenço, 1987:** BRAZIL, state of Pará: adult male and adult female (paratypes), Tefé, Mathan (MNHN-RS-0825).

***Tityus rionegrensis* Lourenço, 2006:** BRAZIL, state of Amazonas: adult male (holotype), between São Gabriel da Cachoeira and 'Pico da Neblina', Rio Negro region, ii.1970, Rain Forest, in canopy, J. Lacroix (MNHN-RS-8643).

***Tityus sastrei* Lourenço & Flórez, 1990.** COLOMBIA, Valle del Cauca department: adult female, Buenaventura, vía al mar, Pericos Natural Reserve [Reserva Natural Pericos], 8.xii.2018, J. A. Moreno & N. Herreño (IBALCC-RPDR 00382).

***Tityus serrulatus* Lutz & Melo, 1922:** BRAZIL, state of Bahía: two adult females, between Mucugé and Igatu, 22.i.2007, C. Mattoni, R. Pinto-da-Rocha & H. Yamaguti (MZSP 28205). State of Minas Gerais: adult male, Cavernas do Peruçu National Park [Parque Nacional Cavernas do Peruçu], Januária, -15.12383, -44.24111, 4–25.i.2009, R. S. Recoder & M. Teixeira Jr. (IBALCC-RPDR 00016); adult female, Grande Sertão Veredas National Park [Parque Nacional Grande Setão Veredas], 15°11'12.1"S, 45°42'39.9"W, 6.ii.2018, D. Álvarez, manual capture (IBALCC-RPDR 00336).

***Tityus spelaeus* Moreno-González, Pinto-da-Rocha & Gallão, 2021.** BRAZIL, state of Goiás: adult female, Posse, Russão II cave, 1.iv.2007, R. Pinto-da-Rocha et al. (IBALCC-RPDR 00116).

***Tityus stigmurus* (Thorell, 1876)** BRAZIL, state of Pernambuco: adult female, Triunfo, 9.vii.2009, R. Pinto-da-Rocha, C. Bragagnolo & M. B. da Silva (IBALCC-RPDR 00170); adult female, Vitória de Santo Antão, 08°07'S, 35°23"W, 28.v.2008, H. Yamaguti, W. Porto & M. B. da Silva (IBALCC-RPDR 00218); adult male, Exu, 07°26'44"S, 39°44'21"W, 1.vi.2008, H. Yamaguti, W. Porto & M. B. da Silva (IBALCC-RPDR 00219);

***Tityus sylviae* Lourenço, 2005:** BRAZIL, state of Amazonas: adult female (paratype), Jaú National Park [Parque Nacional do Jaú], Seringalzinho, pitfall, together with *Tityus dinizi* and *Tityus silvestris*, 01°52'34"S, 61°35'15"W, 1–8.viii.2001, I. Ghizoni Jr. (MNHN-RS-8620).

***Tityus trivittatus* Kraepelin, 1898.** BRAZIL, state of São Paulo: one adult male, Linhares, Fazenda Cupido, 2.x.1944, Schubart (MZSP 21775). State of Paraná: two females, Palmeira, xii.1852, Schubart (MZSP 21768).

Addendum to a minimalist revision of Costa Rican Braconidae: 28 new species and 23 host records

Michael J. Sharkey¹, Austin Baker^{1,2}, Kathryn McCluskey³,
Alex Smith⁴, Suresh Naik⁵, Sujeevan Ratnasingham⁵,
Ramya Manjunath⁵, Kate Perez⁵, Jayme Sones⁵, Michelle D'Souza⁵,
Brianna St. Jacques⁵, Paul Hebert⁵, Winnie Hallwachs³, Daniel Janzen³

1 *The Hymenoptera Institute, 116 Franklin Ave., Redlands, CA, 92373, USA* **2** *Department of Entomology, University of California, Riverside, CA 92521, USA* **3** *Department of Biology, University of Pennsylvania, Philadelphia, PA 19104-6018, USA* **4** *Department of Integrative Biology, University of Guelph and Biodiversity Institute of Ontario, Guelph, Canada* **5** *Centre for Biodiversity Genomics, University of Guelph, Guelph, Canada*

Corresponding author: Michael J. Sharkey (msharkey@uky.edu)

Academic editor: K. van Achterberg | Received 26 July 2021 | Accepted 26 September 2021 | Published 7 December 2021

<https://zoobank.org/3202711B-0DEF-4B4D-95A5-36FF1D233FA4>

Citation: Sharkey MJ, Baker A, McCluskey K, Smith A, Naik S, Ratnasingham S, Manjunath R, Perez K, Sones J, D'Souza M, Jacques BS, Hebert P, Hallwachs W, Janzen D (2021) Addendum to a minimalist revision of Costa Rican Braconidae: 28 new species and 23 host records. *ZooKeys* 1075: 77–136. <https://doi.org/10.3897/zookeys.1075.72197>

Abstract

Twenty-nine species are treated, most of which have host caterpillar and food plant records, and all but one are new to science. The first host record for the agathidine genus *Amputoearinus* is given. *Gnathopleura josequesadai* Sharkey, **sp. nov.** is reported as a hyperparasitoid of fly larvae, the first such record for the genus. The following new species are diagnosed primarily using COI barcode data; Sharkey is the authority for all: Agathidinae: *Aerophilus davidwagneri*, *Aerophilus fundacionbandorum*, *Aerophilus nicklaphami*, *Lytopylus davidstopaki*, *Lytopylus davidschindeli*; Alysiinae: *Gnathopleura josequesadai*; Braconinae: *Bracon andreamezae*, *Bracon franklinpaniaguai*, *Bracon rafagutierrezii*, *Bracon guillermoblancoi*, *Bracon oscar-masisi*, *Bracon pauldimaurai*, *Bracon shebadimaurae*, *Sacirema karendimaurae*; Cheloninae: *Chelonius minor-zunigai*; Homolobinae: *Homolobus stevestroudi*; Macrocentrinae: *Macrocentrus michaelstroudi*; Orgilinae: *Stantonia gilbertfuentesii*; Rhysipolinae: *Rhysipolis stevearsoni*; Rogadinae: *Aleiodes kaydodgeae*, *Aleiodes kerrydresslerae*, *Aleiodes josesolanoi*, *Aleiodes juniorporrasi*, *Aleiodes rociocheverri*, *Aleiodes ronaldzunigai*, *Choreborogas jesseausubeli*, *Triraphis doncombi*, and *Yelicones mayrabortillae*.

Keywords

Accelerated taxonomy, BIN code, conservation, COI DNA barcode, Hymenoptera, Ichneumonoidea, parasitoid host associations, tri-trophic interaction.

Introduction

The purpose of this research is to diagnose and name 28 new species of Costa Rican braconids. We deal with braconid subfamilies: Agathidinae, Braconinae, Cheloninae, Macrocentrinae, Orgilinae, Proteropinae, Rhysipolinae, and Rogadinae. Of these 28 species, 23 are reared from host caterpillars and their food plants are documented. This is an addendum to Sharkey et al. (2021a) where 403 species were diagnosed by using COI DNA barcode sequences. Zamani et al. (2020) criticized our barcoding approach and responses to their criticisms can be found in Sharkey et al. (2021a and 2021b).

We briefly describe the fate of large monographs that treat small portions of hyper-diverse Neotropical ichneumonoids by exemplifying the Sharkey (1988) revision of *Alabagrus* (Braconidae) and the Dasch (1974) revision of *Mesochorus* (Ichneumoniidae). We emphasize that in these two publications the keys and descriptions required enormous time, effort, and expense; they are little used; and when they are used, the results are usually erroneous. This makes them useless or even detrimental to the taxonomy and understanding of these groups.

According to a search in Google Scholar (May 2021), the *Alabagrus* revision has 32 citations and the *Mesochorus* revision has 39. The majority of the citations are geographical surveys that simply copy the distributional records that are in these papers. For example, Rodríguez-Berrío et al. (2009) surveyed the literature for all Ichneumoniidae occurring in Peru and included a number of species cited as being present in Peru by Dasch (1974); the keys and descriptions were not employed.

Only four publications dealing with Neotropical *Alabagrus* employed the key of Sharkey (1988); in three of these cases the specimens were identified by or checked by Sharkey himself. The quality of the identifications in one of these, Leathers and Sharkey (2003), was reported in Sharkey et al. (2018, 2021a), and our self-criticisms are repeated here. Leathers and Sharkey (2003) used the key and also had access to identified specimens. Nonetheless, of the 17 species that they reported to occur in Costa Rica, none are now realized to occur in Costa Rica because they only live elsewhere, and Costa Rican undescribed species were mistaken for them. These are *Alabagrus albispina*, *A. imitatus*, *A. juchuy*, *A. kagaba*, *A. latisoma*, *A. latreillei*, *A. maya*, *A. mojos*, *A. nahuatl*, *A. nigrilitus*, *A. pachamama*, *A. paruyana*, *A. parvifaciatus*, *A. semialbus*, *A. tricarinatus*, *A. tripartitus*, and *A. warrau*. Furthermore, five of the species reported by Leathers and Sharkey (2003) were found to be composed of species complexes as determined by a combination of morphological, barcode, and host data. These five are *Alabagrus cocto*, *A. englishi*, *A. pecki*, *A. roibasi*, and *A. yaruro* (Sharkey et al. 2018). There is no reason to believe that the other two publications in which Sharkey played a role in identification

of specimens of *Alabagrus* (Braet 2002, Cauich-Kumul 2012) are any better, despite his being the world authority on identification of Agathidinae. The sole publication in which Sharkey did not play a role in identification was one dealing with the Brazilian fauna (Yamada et al. 2006). In this publication 21 species of *Alabagrus* were identified. Of these, ten of the holotypes are from Mexico or Central America and one is from the United States. The likelihood of any of these occurring in Brazil is extremely low and yet they probably fit the key in Sharkey (1988). We estimate there to be many more than 1,000 species of *Alabagrus* in the Americas; the probability of the undescribed species fitting the key is therefore obviously high. A key that deals with only 10% of the fauna is all but useless, and if all of the species were described, the key would be more than 1,000 couplets long; impossible to work with. A key of this length would preclude accurate identifications due to user error or location inaccuracies (e.g., a Brazilian specimen that looks like a Mexican specimen has a high probability of being a different species).

In summary, in the 30-plus years since the publication of the morphology-based revision of *Alabagrus*, only one person other than Sharkey has used the key to arrive at a determination for Neotropical species, and in that instance most of the identifications are probably incorrect. It took Sharkey more seven years to produce the 1988 revision, and it is worse than useless because it is full of misleading information on species limits and species distributions, owing to misidentifications. Some might argue for an integrative approach, such as the revision of *Alabagrus* by Sharkey et al. (2018), but what is the point of including morphological descriptions, which tend to be lengthy and time-consuming to produce, when the COI barcode is the only reliable source for identification (barring much more expensive and complex multi-gene information)?

There are many genera of ichneumonoids that contain hundreds or thousands of species in the Neotropics, but few of these have been revised for the entire area. One of these exceptions, besides Sharkey (1988), is the revision of Neotropical *Mesochorus* (Dasch 1974), a genus of hyperparasitoid Ichneumonidae. Dasch treated what he considered to be 245 Neotropical species, and like the Sharkey revision of *Alabagrus*, few publications have used his keys or descriptions to identify specimens of *Mesochorus*; we have located three. Of all of the 245 species of Neotropical *Mesochorus* that he treated, 30 were recorded from Costa Rica. Based on the 172 BINs of Costa Rican *Mesochorus* presently on BOLD (March 2, 2021), we estimate that there are approximately 688 species in Costa Rica. These species are almost exclusively from the Area de Conservación Guanacaste, from rearings that have been conducted exclusively in the provinces of Guanacaste and Alajuela (Janzen and Hallwachs 2011). Given this estimate, the odds of a Costa Rican specimen being in Dasch's (1974) key is 4.4%. The fact that these large revisions are not useful is not the result of poor workmanship, nor is it that the readers are poorly trained. In fact, the only users are highly trained taxonomists specializing in Ichneumonoidea. The keys are not used simply because they do not work. Not only are the species concepts poor with many species having similar morphology, but the revisions deal with such a small portion of the total number of species that the odds of a specimen in hand being in the key is remote.

Materials and methods

Delimiting species

We received considerable critical feedback after the publication of Sharkey et al. (2021a). One of the most common criticisms directed at our approach is that barcodes in general, and BINs in particular, are not capable of delimiting species. This was dealt with at length in Sharkey et al. (2021a); nonetheless in an effort to avoid further confusion, we describe in detail below the process we go through to arrive at species limits or at the least, species central tendencies. BIN is an abbreviation for Barcode Index Number and an article by Ratnasingham and Hebert (2013) describes how and why the BIN algorithm was developed. They describe the BIN system as a means of forming Operational Taxonomic Units (OTUs) based on divergence in COI sequences. In essence, the BIN is like a unit tray of specimens believed to be monospecific by similarity of contained barcodes rather than appearance. They clearly state that no system like this can be perfect, “Any algorithmic approach based on the analysis of sequence diversity in a single gene region will be an imperfect tool for the discrimination of closely related species as they will be overlooked because of their low sequence divergence.” (Ratnasingham and Hebert 2013: 2).

We start a revision by grouping our specimens into unit trays based on their BIN placements. The specimens in each tray are then investigated for general morphological consistency, and inconsistent specimens are flagged. This is followed by an inspection of a NJ tree that we generate on the BOLD website using only those specimens with full or almost full barcodes, i.e., barcodes with 500–658 base pairs. We carefully examine the branching pattern of the specimens in each BIN. If there is any clumping or any outliers in the tree of the specimens within a BIN, we look at the rearing host data and microgeography, if it is available. We also look at the morphology of the specimens, to see if they differ significantly and check for concordance between these three data sources. If these data sources are consistent with the hypothesis that any cluster of branches represents a separate species within the BIN, we consider this possibility based on the degree of difference in morphology, sequence divergence, and host use. We then build a new NJ tree that includes shorter barcodes to place those specimens into species formulated in the previous step and to add new species that may not be represented by specimens with full barcodes. Finally, we look at the morphology and host data of the nearest neighbors for each BIN. If these do not differ morphologically, we might consider this to be a case where a pair of BINs split a species. This, of course, depends on the degree of COI divergence. To date, we have found no such case. Specimens that fail to barcode, are contaminated, or are otherwise not barcodeable, are excluded from consideration, but the specimen and its record are retained. There are times when a reared specimen is obviously conspecific with others reared from the same host species but not currently barcodeable, and therefore, they are only retained for ecological analyses, such as what fraction of caterpillars were killed by that parasitoid.

Co-author Janzen estimates that the BIN algorithm lumps two or more sympatric species of Costa Rican Lepidoptera within a BIN at a rate of ~ 10%. And in those cas-

es, almost invariably the multiple species are evident by genitalic differences, caterpillar food plant, microgeography, and/or extremely slight differences in coloration. He also has not come across a case in which a species is split into more than one BIN, although this is certainly possible through within-species barcode polymorphisms. Thus, the BIN algorithm can be described as conservative. The 403 new species in Sharkey et al. (2021a) were grouped into 395 BINs with only three “multi-species” BINs, for a 2% BIN “error” rate. Error is in quotes here because the barcodes do separate the species, but the BINs do not in these few cases.

In the following paragraphs we give an empirical example of how we arrive at species delimitations; we do not say “species limits” because these geobiological limits have not been explored further than ACG, or Costa Rica, or the Neotropics. BIN BOLD:ACK7466, treated in Sharkey et al. (2021a), is a BIN with multiple species, and there are also a handful of examples in the literature (e.g., Hebert et al. 2004; Janzen et al. 2017). In this BIN, BOLD:ACK7466, we have what are probably 11 species, nine of which we have described, and one is in the current publication. Each of these 11 species matches a distinctive set of host caterpillars yet are fully sympatric, just as was the case for 6 of the first 11 sympatric species found to be described as a single species, *Astraptus fulgerator* (Hesperiidae) (Hebert et al. 2004). To help discover potential species within a BIN, the first NJ tree that we build employs only those sequences with complete or almost complete barcodes, e.g., > 500bp. The portion of the tree that contains the specimens of BIN BOLD:ACK7466 is presented in Figure 1. The reason for using almost complete barcodes at this stage is to base our decisions on the highest quality data. A quick look at the tree (Fig. 1) shows that there are a number of specimens with identical sequences that cluster together on different branches of the tree. We investigate each cluster individually. For example, the two specimens of *M. michaelstroudi* sp. nov. (branch A at the top of the tree in Figure 1) are consistent with the hypothesis of being a separate species because: 1. They have the same barcode sequence, which is quite divergent from other members of the clade. 2. Their hosts are the same crambid, *Phaedropsis leialis*DHJ03, and no other specimens in the BIN attack members of this genus. 3. These two specimens are morphologically different from all others in the BIN, the details of which are in the diagnosis in the species treatment; “In the morphological key for the species in this BIN, *Macrocentrus michaelstroudi* keys to *M. gustavogutierrezii*. *Macrocentrus michaelstroudi* differs in having pale basal flagellomeres, contrasting with the melanic basal flagellomeres of *M. gustavogutierrezii* (Sharkey et al. 2021a).

Within the cluster of specimens identified as *Macrocentrus geoffbarnardi* (Fig.1, branch B) we have the same situation as in *M. michaelstroudi*, so we compare with the specimens on the branch with specimens of *M. fredsingeri* (Fig. 1, branch C). Here we have two clusters (C1 and C2) that are joined on a relatively long branch. Members of branches C1 and C2 are all parasitoids of *Neurophyseta clymenalis*DHJ03. (*N. clymenalis*DHJ03 is the interim name for a species, probably unnamed, that is similar to *N. clymenalis*). The specimens on C1 cannot be separated from those on C2 on morphological grounds. However, the entity (C1 + C2) can be separated on morphological grounds from all of the other specimens in BIN BOLD:ACK7466. Finally, no other

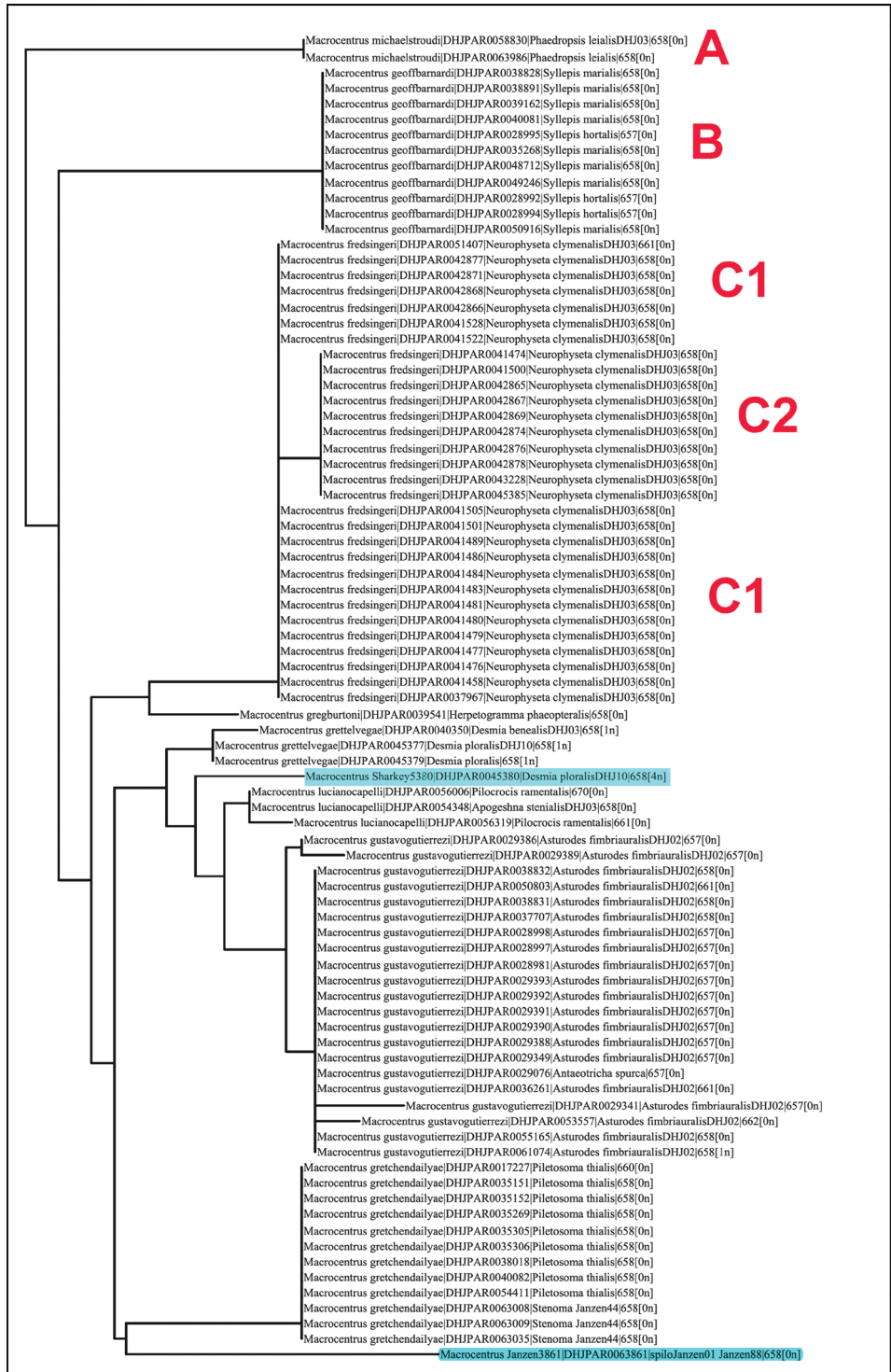


Figure 1. NJ tree of *Macrocentrus* BIN BOLD:ACK7466.

specimens in the BIN are parasitoids of species of *Neurophyseta*. Therefore, we considered the entire cluster (C1 + C2) as one species. If further examination or data suggest that it is two, then one more will be also described. Similar arguments were used to delimit the other nine species in the BIN (Fig. 1). The specimens highlighted in blue (Fig. 1) represent probable new species that have not yet crossed the desk of author Sharkey because they are still in the barcoding pipeline.

The next step in our process is to add specimens to the analysis with less COI data, i.e., shorter COI barcodes. This often produces a “noisier” NJ tree. Here we just show a small segment of the NJ tree to make our point (Fig. 2). The highlighted terminals have shorter barcodes and are new to the tree of Figure 1. Neither falls in the large homogeneous polytomy of *M. gustavogutierrezii*, and this is not uncommon for specimens with shorter barcodes. Specimens of this sort are looked at more carefully both morphologically and biologically and may or may not be included in the paratype series. In this case the two specimens share the same host, which is unique to the species, and do not differ morphologically in a substantive way.

By this stage we have examined the membership of each BIN to determine whether there is one or more species in the BIN. The final step before species description is to investigate the nearest neighbor of each BIN to ensure that they differ morphologically and/or biologically. To date, all BINs examined for Braconidae have differed from their neighboring BINs. The nearest neighbor can be found on the BOLD website. For example, to find the nearest neighbor of BIN BOLD:ACK6477, we search for that BIN on the BOLD database and are taken to a page that includes the information in Figure 3. In this case the nearest neighbor to BIN:BOLD:ACK6477 is *Macrocentrus iangauldi*, which occupies BIN BOLD:ABY7812. Specimens in the two BINs are then compared to ensure that they differ morphologically and biologically, which they do. We stated earlier that the BIN algorithm failed to be mono-specific at a rate of 2% in the treatment by Sharkey et al. (2021a), but it is worth noting that the barcode sequences themselves did not fail. Even when there are multiple species within a BIN, the COI sequences differentiated the included species as seen in Figure 1; these results are corroborated by host data and morphology.

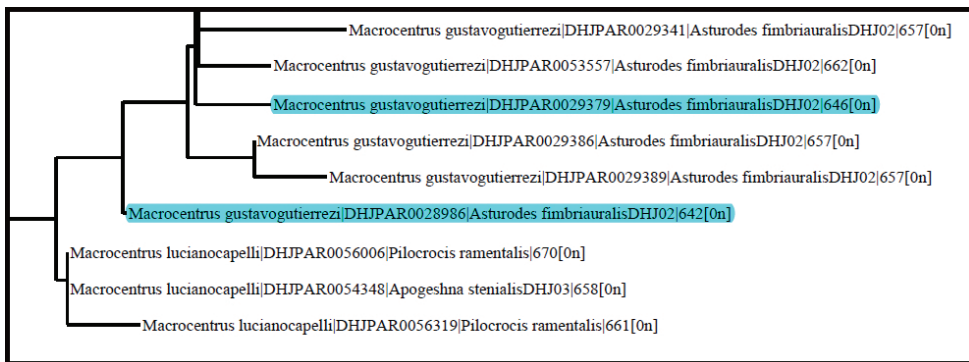


Figure 2. Portion of the NJ tree generated from BOLD showing additions of sequences with barcodes shorter than 650bp. These are highlighted in blue.

NEAREST NEIGHBOR (NN) DETAILS			
Nearest BIN URI:	BOLD:ABY7812	Average Distance:	0.16% (p-dist)
Member Count:	7	Maximum Distance:	0.31% (p-dist)
Nearest Member:	ACGBA1803-12	Distance Variance:	0.01% (p-dist)
Nearest Member Taxonomy:	Arthropoda, Insecta, Hymenoptera, Braconidae, Macrocentrinae, Macrocentrus, <u>Macrocentrus iangauldi</u>		

Figure 3. A portion of the webpage on BOLD for BIN BOLD:ACK7466.

In contrast to COI barcode diagnostics, we have found cases in which morphology cannot discriminate species that are clearly diagnosed by COI barcodes. Of the 86 species treated in the revision of *Alabagrus* by Sharkey et al. (2018) there were three species that could not be separated morphologically but were clearly delimited based on host data and COI sequence data. The final couplet for this group from the key by Sharkey et al. (2018) is as follows:

- 102 A** Forewing with yellowish or clear area extending to the 2nd submarginal cell .
..... *A. roibasi*
- 102 B** Forewing entirely infusate, or if with yellowish or clear area basally, it does not extend to 2nd submarginal cell (we cannot distinguish the following 3 species morphologically)
..... *A. jennyphillipsae*; *A. isidrochaconi*; *A. jeanfrancoislandryi*

Figure 4 is a portion of the tree of highest posterior probability (from Sharkey et al. 2018) based on COI data showing the relationships of these three species (indicated with a red dot). The NJ tree produced by BOLD indicates slightly different relationships but, as with the Bayesian tree, the three morphologically indistinguishable species are not sister species nor are they nearest neighbors by any definition of that concept. We may have made different decisions if these lineages shared hosts or formed a monophyletic clade and were represented by very few sequences.

Specimens and generic placements

As with those of Sharkey et al. (2021a), most of the species described here were collected by rearing wild-caught host caterpillars in ACG in northwestern Costa Rica (Janzen and Hallwachs 2016). Holotypes of all newly described species are deposited in the insect collection of the Canadian National Collection of Insects, Ottawa. Paratypes and all other specimens are currently deposited in the Centre for Biodiversity Genomics in the Biodiversity Institute of Ontario at the University of Guelph.

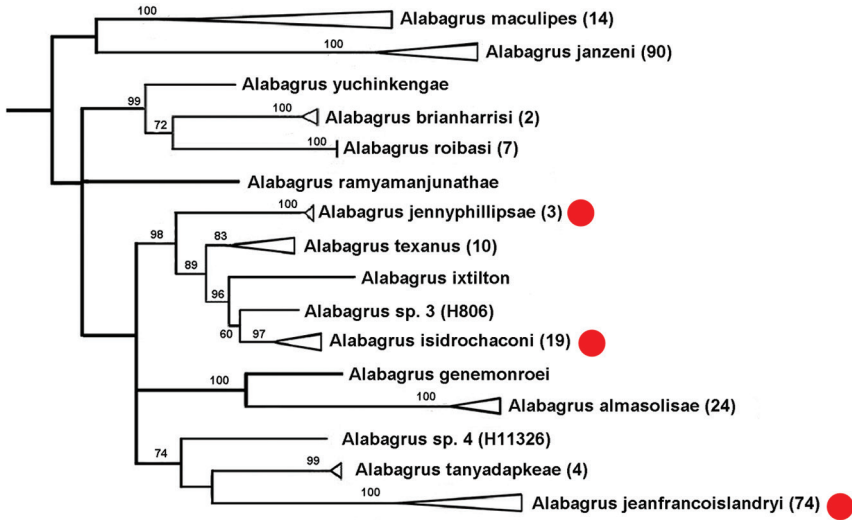


Figure 4. Portion of the tree of highest posterior probability from a 10 million-generation Bayes analysis of COI. The numbers of specimens of each species are collapsed (when possible) into single terminals (terminal triangles), with the number of specimens/OTUs for each collapsed species in parentheses. The length of the triangles represents the branch length from the node to the tip of the longest branch for that species. The numbers above the branches are the posterior probabilities $\times 100$. The red dots indicate the three species that could not be differentiated morphologically. Modified from Sharkey et al. (2018).

Identification of specimens to the subfamily level can be achieved using the key by Sharkey (1997). Keys to the genera of the species treated here are found in Sharkey et al. (2021a) and references therein. However, identification to any level is best acquired by obtaining COI barcodes and submitting them to BOLD. Instructions on how to do this are included below.

Some host species treated here are awaiting full identification and are given interim names. For example, *Antaeotricha* Janzen233 is identified to the genus *Antaeotricha* by classical morphology-based criteria and to Janzen233 by barcode and ecological information. However, no formal scientific species name is available until a barcode-match is obtained with an existing holotype or until it is described as new, or interim matched morphologically with a described species by a taxonomic specialist, which may take decades. Equally, *Antaeotricha* radicalis EPR03 is also an interim name based on what the species looks like, however, it is not a scientific name. It temporarily retains the information that this species is recognized by similarity with its look-alike, *A. radicalis*, before barcoding and associating it with other ecological data. Finally, a name such as gelJanzen01 Janzen407 signifies a caterpillar in the family Gelechiidae for which even a generic name is not obtainable at present.

DNA extraction and sequencing

Molecular work was carried out at the CBG using their standard protocols. A leg of each frozen-then-oven-dried specimen was destructively sampled for DNA extraction

using a glass fiber protocol (Ivanova et al. 2006). Extracted DNA was amplified for a 658-bp region near the 5' terminus of the cytochrome *c* oxidase subunit I (COI) gene using standard insect primers LepF1 (5'-ATTCAACCAATCATAAAGATATTGG-3') and LepR1 (5'-TAAACTTCTGGATGTCCAAAAAATCA-3') (Ivanova and Grainger 2007). If initial amplification failed, additional amplifications were conducted following the established protocols using internal primer pairs: LepF1–C113R (130 bp) or LepF1–C_ANTMR1D (307 bp) and MLepF1–LepR1 (407 bp) to generate shorter overlapping sequences. Amplified products were sequenced using Sanger technology, though the most recent were sequenced by SEQUEL II. Specimens that “failed” barcoding are not included here unless otherwise indicated. When included, they are usually identified by unambiguous morphological and ecological information equally possessed by others from ACG in that species.

Barcode sequences presented in the species descriptions herein are a consensus of the barcode sequences of all included individuals, meaning base pairs that differ between conspecific specimens are replaced by IUPAC ambiguity codes.

Databases

Voucher codes are presented for all holotype specimens (and all other barcoded individuals) treated herein. All host caterpillars are individually vouchered to their individual records (yy-SRNP-xxxxx). Codes beginning with DHJPARxxxxxxx are for the parasite (or hyperparasite) specimens reared from the caterpillar; therefore, each wasp carries two voucher codes, one for the rearing (host) record and one for the wasp itself. The SRNP voucher codes are from the Janzen and Hallwachs' database (<http://janzen.sas.upenn.edu/caterpillars/database.lasso>). Specimen voucher codes beginning with BIOUG are from the BOLD database (<http://www.boldsystems.org>), and most of the specimens obtained from ACG Malaise traps have this prefix. The DHJPAR and their associated SRNP codes can also be found on the BOLD database. The abundant collateral information obtainable from these two databases complements the species treatments. See Sharkey et al. (2021a) for a brief introduction to what to look for and how the two databases supplement the species treatments herein.

The BOLD database can be used to identify specimens using the following steps: 1. Navigate to the identification tab of the BOLD Systems database (http://www.boldsystems.org/index.php/IDS_OpenIdEngine). 2. Paste the COI sequence of the query organism (in forward orientation) into the query box and search against the appropriate library (e.g., All Barcode Records on BOLD, Species Level Barcode Records, etc.). 3. The search results page shows the top hits based on % similarity starting with the closest matches. This page also provides additional information to help verify the identity of a match, such as links to the BIN where specimen data (including images) can be found, a distribution map, and a tree-based identification tool. 4. Use the Tree-Based Identification button to generate a neighbor-joining tree and find the query taxon (name in red). This allows you to visualize how distant the query sequence is from the closest matches.

Taxonomic account

Agathidinae

A key to the genera of the New World can be found in Sharkey et al. (2021a). Agathidines are cosmopolitan and exclusively koinobiont endoparasitoids of caterpillars. They emerge from the host after the caterpillar is full-grown and has begun to spin or has already spun a cocoon.

Aerophilus davidwagneri Sharkey, sp. nov.

<http://zoobank.org/DA927AD6-EB95-45B2-8570-F29BB42F9968>

Diagnostics. Figure 5.

BOLD data. BIN: BOLD:ACJ2677; nearest neighbor: *Aerophilus bradzlotnicki* BOLD:ACA4771; distance to nearest neighbor is 3.9%. Consensus barcode: AATTTTATATTTTATTTTGGGAATTTGAGCAGGAATTGTAGGATTATCAATAAGAATAATAATTCGAATAGAATTAAGAATAGTAGGTAATTTAATTGGTAATGATCAAATTTATAATAGAATTTGTTCTGCTCATGCTTTTTGTAA-TAATTTTTTTTATAGTTATAACCAATTATAATTGGAGGATTTGGTAATTGATTAGTACCCTTAATATTAGGAGGTCCTGATATAGCTTTTCCTCGAATAAATAATATRAGATTTTGATTATTAATTCCTTCATTATTATTATTAATTTAAGATCTTTARTTAATATTGGTGTAGGTAAGTACTGGATGAAGTGTACCCTCCTTTATCATTAATAATAAGACATAATGGAATATCAGTAGATTAGCTATTTTTCTTTACATATTGCAGGTATTCATCAATTATAGGAGCAATTAATTTATTACAATATATAAATATATGAATAATTAATGTAAAAATTGATAAAATACCTTTAATAATTTGATCAATTTTTATTCTGC-TATTTTATTATTATTATCTTTACCTGTTTTAGCTGGTGCTATT-CTATATTATTAAGTATCGAAATTTAAATACTAGATTTTTTTGATCCTACAGGAGGAGGAGATCCAATTTTATATCAACATTTATTT.

Morphological data. This species can be morphologically distinguished from its nearest neighbor by having the mesosoma entirely black (Fig. 5) compared to having large orange patches on the lateral sides (Sharkey et al. 2011: figs 3, 4).

Holotype ♀: Costa Rica: Alajuela, Area de Conservación Guanacaste, Sector San Cristobal, Cementerio Viejo, 570 m, 10.88111 -85.38889; host caterpillar collection date: 27/ii/2013, parasitoid eclosion: 19/iii/2013; depository CNC, holotype voucher code: DHJPAR0051912.

Holotype host data. *Polyortha* Janzen226 (Tortricidae) feeding on *Desmopsis schippii* (Annonaceae). Host caterpillar voucher code 13-SRNP-972

Paratype. Hosts are all the same as that of the holotype: DHJPAR0054734, DHJPAR0055235, DHJPAR0051139, DHJPAR0051915, DHJPAR0055516, DHJPAR0054741, DHJPAR0055237, DHJPAR0054728, DHJPAR0055233.

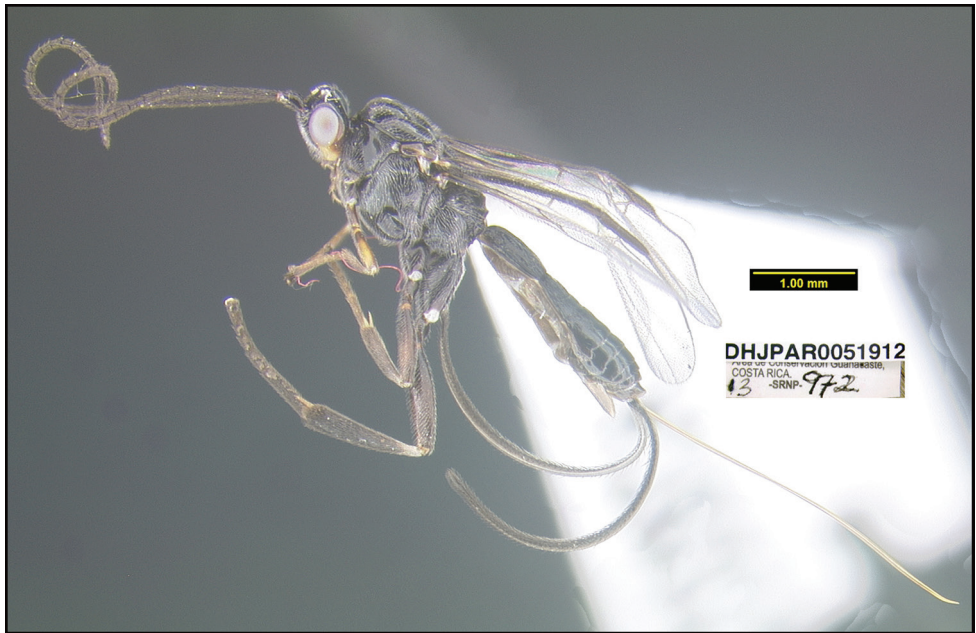


Figure 5. *Aerophilus davidwagneri*, holotype.

Etymology. *Aerophilus davidwagneri* is named in honor of David Wagner of the University of Connecticut, Storrs, Connecticut, USA, for his recent work as an environmental activist for a healthier global climate and wild biodiversity.

***Aerophilus fundacionbandorum* Sharkey, sp. nov.**

<http://zoobank.org/A73266E4-1332-4185-816A-4AD9EEDACEC4>

Diagnostics. Figure 6.

BOLD data. BIN: BOLD:ACN0950; nearest neighbor: *Aerophilus calcareatus* BOLD:AAU4711; distance to nearest neighbor is 5.81%. Consensus barcode
 AATTTTATATTTTATTTTGGAAATTTGATCTGGTATTTTAGGAT-
 TATCAATAAGAATCATTATTCGTATAGAATTAAGATTAGGGGGTAATT-
 TAATTGGTAATGATCAAAATTTATAATAGAATTGTTCTGCTCATGCTTTT-
 GTAATAATTTT'TTTTATAGTTATACCGATTATAATTGGAGGATTTG-
 GAAATTGATTAGTTCCTTTAATGTTAGGAGGTCCAGATATGGCCTTTC-
 CACGRATAAATAATAAGATTTTGATTATTAATTCCTTCATTAAC'TTT-
 ATTAATTTTAAGATCAATATTAATGTTGGTGTAGGTACGGGATGAAC-T-
 GTYTATCCTCCCTTATCATTAATATAAGTCATAGAGGAATATCTGTA-
 GATTTAGCAATTTT'TCTTTACATAYTGCTGGAATTTCTTCTATTATAG-
 GAGCAATAAATTTTATTACTACAATTATTAATATATGRATAATAAATG-
 TAAAAATTGATAAAATACCTTTATTGGTATGATCTATTTTATTCTGC-



Figure 6. *Aerophilus fundacionbandorum*, holotype.

TATTTTATTATTATTATCTTTACCAGTATTAGCTGGGGCTATTCTATATT-
ATTAAGTATCGAAATTTAAATCTAGATTTTTTTGATCCTTCTGGAGGAG-
GAGATCCAATTTTATATCAACACTTATTT

Morphological data. *Aerophilus fundacionbandorum* keys to *A. macadamiae* in Sharkey et al. (2011). *Aerophilus fundacionbandorum* differs in many ways. One of the most obvious is its wide, sharply angled, median propodeal areola (Fig. 6). In *A. macadamiae* the areola is gradually narrowed anteriorly. *A. fundacionbandorum* can be morphologically distinguished from its nearest neighbor, *A. calcaratus*, by its more heavily sculptured first metasomal tergum. It is mostly striate in *A. fundacionbandorum* and mostly smooth in *A. calcaratus* (Sharkey et al. 2016: figs 12, 13).

Holotype ♀: Costa Rica: Guanacaste, Area de Conservación Guanacaste, Sector Pitilla Bullas, 440 m, 10.98670 -85.38503; host caterpillar collection date: 07/x/2013, parasitoid eclosion: 12/xi/2013; depository CNC, holotype voucher code: DHJ-PAR0054494.

Holotype host data. *Loxiorhiza unitula* (Thyrididae) feeding on *Schnella guianensis* (Fabaceae), caterpillar voucher code 13-SRNP-71694.

Paratype. Same host species as that of holotype DHJPAR0054547.

Etymology. *Aerophilus fundacionbandorum* is named in honor of the BAND Foundation of the USA, in recognition of its decades of support for growth and development of Costa Rica's Área de Conservación Guanacaste and most recently for adding 85 more hectares to ACG of original forest, Bosque Transición, lying on the nearly extinct fusion of dry forest with rain forest (<http://www.gdpcf.org/content/introducing-bosque-transición>).

***Aerophilus nicklaphami* Sharkey, sp. nov.**

<http://zoobank.org/5C52FDA0-10E1-4152-9EE5-4D7BFE64516E>

Diagnostics. Figure 7.

BOLD data. BIN: BOLD:ACT7814; nearest neighbor: *Aerophilus colleenhitchockae* BOLD:ACA4890; distance to nearest neighbor is 5.16%. Consensus barcode: AATTTTATATTTTATTTTGGAAATTTGATCTGGAATTTTAGGATTATCAATAAGAATAATTATTCGTATAGAATTAAGATTAA-GGGGCAATTTAATTGGAAATGATCAAATTTATAATAGAGTTGTTCTGCTCATGCTTTTGTATAATTTTATAGTTATACCAATTATGATTGGGGGTTTGGTAATTGATTAATTCCTTTAATATTAGGAGGTC-CAGATATAGCATTTCCTCGTATAAATAATATAAGATTTTGATTATTAATTCCTTCTTTATTTTATTAATTTAAGTTCAATATTAATATTGGAGTAGGTACAGGATGAACTGTTTATCCTCCTTTATCATTAATATAAGACACAGAGGAATATCTGTAGATTTAGCAATTTTCTTTACATATTGCTGGAATTTCTTCTATATAGGGGCAATAAATTTATTAATAATAATAATAATAATAACGTAATAAATTTGATAAATAACCTTTATTAGTATGATC-CATTTTATTTCTGCTATTTTATTATTATCTTTACCAGTATTGGCTGGAGCTATTCTATATTATTAACAGATCGAAATTTAAATCTAGATTCCTTGATCCTTCAGGGGGAGGAGATCCTATTTTATATCAACATTTATTT

Morphological data. This species keys to *A. jessicadimauroae* in Sharkey et al. (2011), but *A. nicklaphami* differs in many ways. Two of the most obvious are the wide sharply angled median propodeal areola and the sharp lateral longitudinal carinae on the first metasomal median tergite. In *A. jessicadimauroae* the areola is gradually narrowed anteriorly and the carinae are not sharp.

This species can be morphologically distinguished from its nearest neighbor, *Aerophilus colleenhitchockae*, by having the hind coxa and femur entirely brown (Fig. 7) compared to mostly black (Sharkey et al. 2011: figs 5, 6).

Holotype ♀: Costa Rica: Alajuela, Area de Conservación Guanacaste, Sector Rincon Rain Forest Sendero Anonas, 405 m, 10.90527 -85.27881; host caterpillar collection date: 18/iii/2014, parasitoid eclosion: 02/v/2014; depository CNC, holotype voucher code: DHJPAR0055983.

Holotype host data. *Tebenna* Janzen02 (Choreutidae) feeding on *Ficus citrifolia* (Moraceae), caterpillar voucher code: 14-SRNP-41346.

Etymology. *Aerophilus nicklaphami* is named in honor of Nick Lapham of the BAND Foundation of the USA, in recognition of his decades of support for growth



Figure 7. *Aerophilus nicklaphami*, holotype.

and development of Costa Rica's Área de Conservación Guanacaste, Costa Rica, and most recently adding 85 more hectares to ACG of original forest, Bosque Transición, lying on the nearly extinct fusion of dry forest with rain forest (<http://www.gdpcf.org/content/introducing-bosque-transición>).

Amputoearinus alafumidus Lindsay & Sharkey, 2006

Diagnostics. Figure 8.

BOLD data. There is no BIN for this specimen because the barcode is too short to merit a BIN code. The short barcode follows:

ATATTTATTTAATTTTTTGGAAATTTGATCAGG-ATTTTAGGATTAT-
CAATAAGAATAATTATTCGTATAGAATTAAGAATGGGGGGAAATTT-
TATTGGTAATGATCAAATTTATAATAGAATTGTT-CTGCTCATGCATT-
TATTATAATTTTTTTTAAAGTTATACCAATTATAATTGGAGGATTTG-
GAAATTGATTAATTCCTTTAATATTAGGGGGCCAGAAAAAGCTTTCCC-
CCGAATAAATAATATAAAATTTTGAT

Morphological data. This specimen was identified based on morphological criteria from the key in Lindsay and Sharkey (2006).

Reared specimen: ♀: Costa Rica: Guanacaste, Area de Conservación Guanacaste, Sector Del Oro, Puente Mena, 280 m, 11.04562 -85.45742; host caterpillar collection



Figure 8. *Amputoearinus alafumidus*, holotype.

date: 11/07/2007, parasitoid eclosion: 27/07/2007; depository CNC, voucher code: DHJPAR0028287.

Reared specimens host data: *Dysodia spissicornis* (Thyrididae) a leaf-roller feeding on *Heisteria concinna* (Olacaceae), caterpillar voucher code: 07-SRNP-22487.

Note. This is the first host record for this wasp genus.

***Lytopylus davidstopaki* Sharkey, sp. nov.**

<http://zoobank.org/B88988CF-D2D5-4B57-ACC5-B3D5A8E7A2DF>

Diagnostics. Figure 9.

BOLD data. BIN: BOLD:ACJ2185; nearest neighbor: *Lytopylus davidschindeli* BOLD:ACB1289; distance to nearest neighbor is 2.56%. Consensus barcode: AATTTTATATTTTATATTTGGTATTTGATCAGGAATTTTAGGTT-

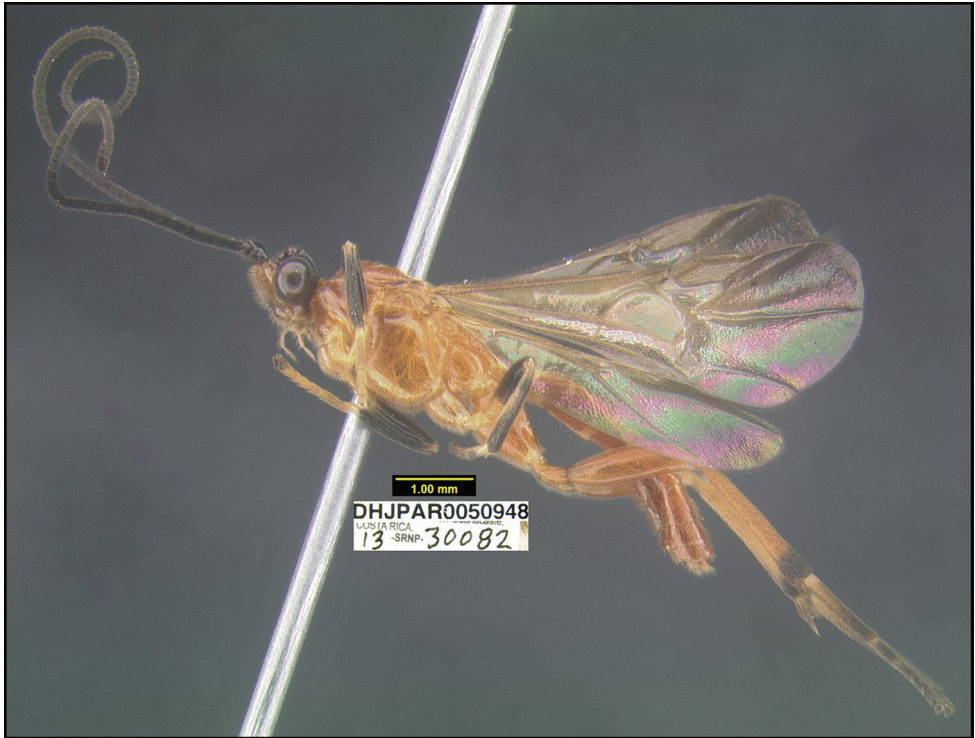


Figure 9. *Lytopylus davidstopaki*, holotype.

TATCATTAAAGATTAATTATTTCGAATAGAATTAAGAATTGGTGAAATT-
 TAATTGGAAATGATCAAATTTATAATAGAATTGTTACTGCTCATGCTTT-
 TATTATAATTTTTTTTATAGTTATACCAATTATAATTGGAGGATTTGG-
 TAATTGATTAATTCCTTTATTATTAGGAGGTCCTGATATAGCTTTCC-
 CTCGAATAAATAATATAAGATTTTGATTATTAATTCCTTCATTATTATT-
 ATTAATTTTAAGATCTTTAATTAATATTGGTG TAGGTACAGGATGAACA-
 GTTTATCCTCCATTATCTTTAAATATAAGTCATAGTGGTATATCTGTA-
 GATATAGCAATTTTTCTTTACATATTGCTGGAATTTCTTCAATTATAG-
 GAGCTATAAATTTTATTACTACTATTATAAATATATGAATTTTAAATT-
 TAAAATTTGATAAAATACCTTTATTAGTTTGATCAATTTTAATTACAG-
 CAATTTTATTATTATTATCATTACCAGTTTAGCTGGAGCTATTACTAT-
 ATTATTAAGTATCGAAATTTAAATACAAGATTTTTTGATCCTTCAGGAG-
 GAGGAGATCCAATTTTATATCAACATTTATTT

Morphological data. This species keys to *L. youngcheae* in Kang et al. (2017) but differs in many ways. The easiest to see is that the hind coxae and bases of hind femora are partly black in *L. youngcheae* and entirely orange in *L. davidstopaki*. This species can be morphologically distinguished from its nearest neighbor, *Lytopylus davidschindeli*, by having its mesosoma and coxae entirely tan (Fig. 9) compared to entirely black or dark brown (Fig. 10).

Holotype ♂: Costa Rica: Guanacaste, Area de Conservación Guanacaste, Sector Pitilla, Sendero Laguna, 680m, 10.9888 -85.42336; host caterpillar collection date: 10/i/2013, parasitoid eclosion: 01/ii/2013; depository CNC, holotype voucher code: DHJPAR0050948.

Holotype host data. elachJanzen01 Janzen527 (Depressariidae) feeding on *Calatola costaricensis* (Metteniusaceae), caterpillar voucher code: 13-SRNP-30082.

Paratype. Same host species as that of the holotype, DHJPAR0050946, DHJPAR0057411.

Etymology. *Lytopylus davidstopaki* is named in honor of David Stopak of the Editorial Office of the Proceedings of the National Academy of Sciences (PNAS), in recognition of his decades of editorial understanding and accepting the strange research emerging from the biodiversity inventory of Costa Rica's Área de Conservación Guanacaste.

***Lytopylus davidschindeli* Sharkey, sp. nov.**

<http://zoobank.org/5006423F-2393-4963-9EE1-8423DC2CE954>

Diagnostics. Figure 10.

BOLD data. BIN: BOLD:ACB1289; nearest neighbor: *Lytopylus davidstopaki* BOLD:ACJ2185; distance to nearest neighbor is 2.56%. Consensus barcode AATTTTATATTTTATATTTGGAATTTGATCAGGAATTTTAGGATTATCATTAAGATTAATTATTCGAATAGAATTAAGAATTGGAGGAAATTTAATTGGTAATGATCAAATTTATAACAGAATTGTAAGTCTCATGCTTTTATTATAATTTTTTTTATAGTTATAACCAATTATAATTGGAGGATTTGGAAATTTGATTAATTCCTTTAATATTAGGAGGTCCTGATATAGCTTTTCCTCGAATAAATAATATAAGATTTTGATTATTAATTCCTTCATTATATTATTAATTTAAGGTCTTTAATTAATATTGGAGTAGGAACAGGATGAACAGTTATCCTCCTTTATCTTTAAATATAAGTCATAGTGGTATATCTGTAGATATGGCAATTTTTTCTTTACATATTGCTGGAATTTCTTCAATTATAGGAGCTATAAATTTTATTAATAATTTGATCAATTTTAAATTACAGCAATTTTATTATTATCATACCAGTTTAGCTGGTGCTATTACTATATTATTAAGTATGATCGAAATTTAAATACAAGATTTTTTGATCCATCAGGAGGAGGAGATCCAATTTTATATCAACATTTATTT

Morphological data. This species keys to *L. angelagonzalezae* in Kang et al. (2017) and differs in many respects. The most evident is that the propodeum of *Lytopylus davidschindeli* is almost completely smooth with the central areola barely indicated. This species can be morphologically distinguished from its nearest neighbor, *Lytopylus davidstopaki*, by having the mesosoma and coxae entirely black or dark brown (Fig. 10) compared to entirely tan (Fig. 9).

Holotype ♂: Costa Rica: Guanacaste, Area de Conservación Guanacaste, Sector Cacao, Estación Cacao, 1150 m, 10.92691 -85.46822; host caterpillar collection date: 06/iii/2012, parasitoid eclosion: 02/iv/2012; depository CNC, holotype voucher code: DHJPAR0049050.



Figure 10. *Lytopylus davidschindeli*, holotype.

Holotype host data. elachJanzen01 Janzen185 (Depressariidae) feeding on *Prunus annularis* (Rosaceae), caterpillar voucher code:12-SRNP-35088.

Etymology. *Lytopylus davidschindeli* is named in honor of David Schindel of the greater Washington, D.C. area and formerly the US National Science Foundation for his decades of understanding the unconventional traits of the biodiversity inventory of Costa Rica's Área de Conservación Guanacaste.

Alysiinae

The key by Wharton (1997) is outdated but it is the only available key to Alysiinae genera of the New World. Members of the subfamily are parasitoids of cyclorrhaphous Diptera.

***Gnathopleura josequesadai* Sharkey, sp. nov.**

<http://zoobank.org/0D07C3EF-ED94-4933-BD2F-33F027916C6A>

Diagnostics. Figure 11.

BOLD data. BIN: BOLD:AAE0055; nearest neighbor: *Gnathopleura* sp. BOLD:AEF6891; distance to nearest neighbor is 7.99%. Consensus barcode GTATTATATTTTATATTTGGTATTTGAGCTGGTATAGTAGGGTTATC-TATAAGATTAATTATTCGGTTAGAATTAGGTATACCTGGRTCTTTAT-TAATAAATGATCAAATTTATAATAGTATAGTAACAGCYCATGCATTT-GTCATAATTTTTTTTATAGTTATACCTGTAATAATTGGTGGATTTGG-TAATTGATTAGTTCCTTTAATGTTAGGATCTCCTGATATAGCTTTCCCAC-GAATAAATAATATAAGATTTTGACTTTTAATCCATCTTTATTGTTATT-ATTATTAAGAAGAGTATTAATATTGGTGTAGGAACAGGGTGAACAGTT-TATCCACCTTTATCGTCAGGAATTGGTCATAGAGGGATTTCTGTTGATT-TAGCTATTTTTCTTTACATTTGGCTGGKGTATCYTCAATTATAGGGGT-TATTAATTTTTAACTACAATTTTTAATATAAAAATCTTGCATGATTAATAA-GATCAGTTAAGGTTATTTATTTGATCTATTTAATTACAGCTATTTTAT-TATTATATCTTTACCTGTTTTAGCAGGTGCAATTACAATATTATTAAC-TGATCGAAATTTAAATACTACTTTTTTTGATTTTTTCAGGTGGTGGGGATC-CAATTTTTATTCAACATTTATTT

Morphological data. *Gnathopleura josequesadai* keys to *G. cariosa* in Wharton (1980) but differs in many ways. For example, the first flagellomere is approximately equal in length to the second flagellomere in *G. cariosa* but much shorter than the second in *G. josequesadai*. This species can be morphologically distinguished from its nearest neighbor by the carina separating the propodeum from the metapleuron. This is rough and complete in *G. josequesadai* (Fig. 11) and smooth and restricted to the posterior 1/3 in the specimen in BIN BOLD:AEF6891.

Holotype ♀: Costa Rica: Guanacaste, Area de Conservación Guanacaste, Sector Santa Rosa, Sendero Natural, 290 m, 10.836 -85.613; host caterpillar collection date: 08/vi/2008, parasitoid eclosion: 11/vii/2008; depository CNC, holotype voucher code: DHJPAR0028304.

Holotype host data. Hyperparasitoid of the fly *Leschenaultia* Wood30DHJ01 (Tachinidae) which is a primary parasitoid of *Pachyliaficus* (Sphingidae) feeding on *Maclura tinctoria* (Moraceae). Including the holotype, five specimens were reared from the fly puparia parasitizing the caterpillar, voucher code 08-SRNP-13289. The host flies were identified from their surviving sibs, one of which is DHJPAR0027924 of BIN BOLD:ACE9310.

Paratype. Reared from the same caterpillar as the holotype DHJPAR0028038, DHJPAR0028039, DHJPAR0028040, DHJPAR0028041.

Etymology. *Gnathopleura josequesadai* is named in honor of José Ramón Quesada Mora, the manager of the 2020–21 BioAlfa Malaise traps for the Hacienda Baru Wildlife Refuge, Costa Rica.

Note. This is the first species of *Gnathopleura* confirmed to be a hyperparasitoid.



Figure 11. *Gnathopleura josequesadai*, holotype.

Braconinae

Braconines are mostly primarily idiobiont parasitoids of Coleoptera and Lepidoptera, but use many other insect orders as well. A key to the Braconinae genera of the New World is in Sharkey et al. (2021a).

Bracon andreamezae Sharkey, sp. nov.

<http://zoobank.org/C8FD7E7C-5289-4EF6-A9F0-BC1C493AEBBD>

Diagnostics. Figures 12, 13.

BOLD data. BIN: BOLD:AAJ8891; nearest neighbor: *Bracon franklinpaniaguai* BOLD:ACK6897; distance to nearest neighbor is 5.64%. Consensus barcode: TATATTATATTTTATACTTGGTATTTGATCTGGTATAATTGGTT-TATCAATAAGTTTAATTATTTCGGTTAGAATTAAGAATACCAGGAAGTT-TATTAAGTAATGATCAAATTTATAATAGAATAGTTACAGCACATGCTTTT-GTAATAATTTTTTTATAGTTATACCAGTGATATTAGGAGGGTTTGG-

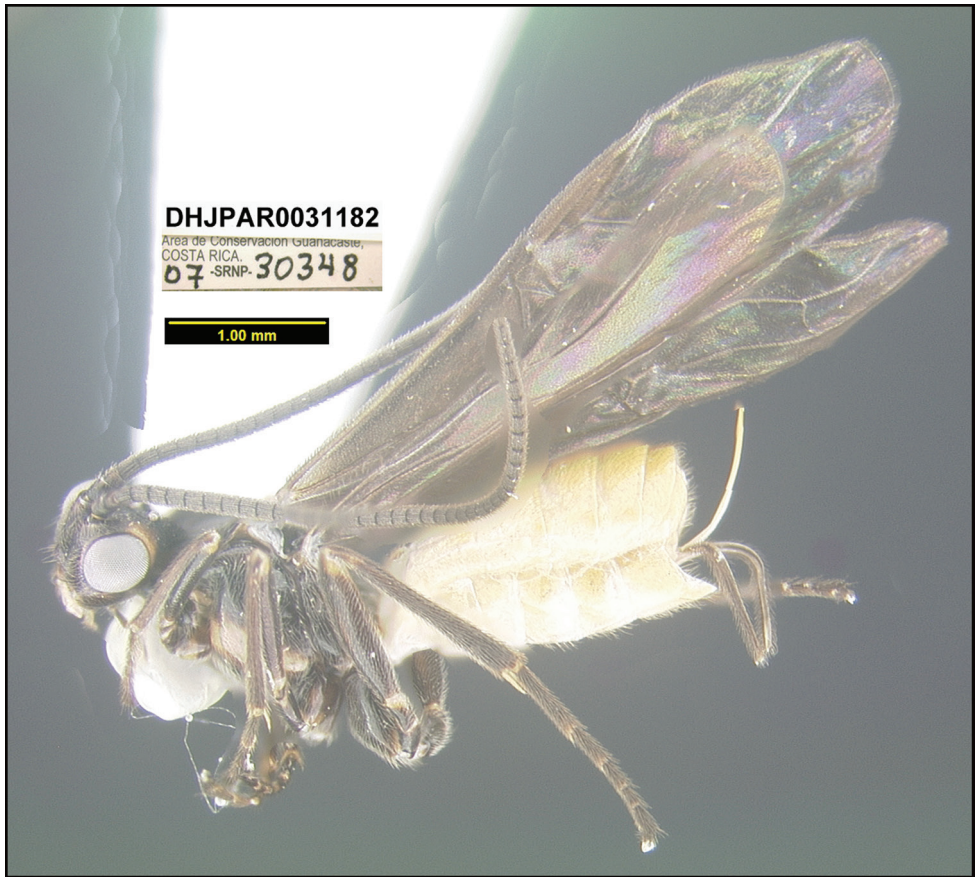


Figure 12. *Bracon andreamezae*, holotype.

TAATTGATTAATCCCTTTAATATTTGGGATCTCCTGATATAGCTTTTCCTC-
 GAATAATAATATAAGATTTTGATTAATTCCTTCATTAATTTTATTAAT-
 ATTAAGAAGAATATTAATGTAGGAGTGGGTACTGGTTGAACATTTATC-
 CTCCATTATCTTCTAACTTAGGGCATAGAGGTGTATCTGTTGATTTAGC-
 TATTTTTCTTTACATTTAGCTGGTATTTTCATCTATTATAGGTTCAAT-
 TAATTTTATTTCTACAATTTTAAATATAACATTTATTAATATTTAAATTA-
 GATCAATTAACCTTATTTATTTGATCAATTTTATTACAACATTTTAT-
 TATTATATCTTTACCTGTTTTAGCAGGAGCTATTACTATATTATTAAC-
 TACTGAAATTTAAATACTTCATTTTTTGATTTTTCTGGAGGAGGGGATC-
 CAATTTTATTTCAACATTTATTT

Morphological data. This species can be morphologically distinguished from its nearest neighbor by having the metasoma dorsally entirely yellow and the mesepisternum dorsally black (Fig. 12) compared to the metasoma dorsally black and the mesepisternum entirely yellow-orange in *B. franklinpaniaguai* (Fig. 14).

Holotype ♀: Costa Rica: Guanacaste, Area de Conservación Guanacaste, Sector Pitilla, Sendero Laguna, 680 m, 10.9888 -85.42336; host caterpillar collection date:



Figure 13. Communal and jointly constructed cocoon of at least 56 sibling larvae of *Bracon andreamezae*, one of which is DHJPAR0031182, displaying adult exit holes through the tough silk roof of the same consistency as the floor of the chamber; multiple wasps exited through a single hole. This species of wasp has been reared only twice among 1,391 rearings of solitary *Yanguna cosyra* caterpillars for more than 34 years.

02/i/2007, parasitoid eclosion: 20/i/2007; depository CNC, holotype voucher code: DHJPAR0031182.

Holotype host data. 07-SRNP-30348 *Yanguna cosyra* (Hesperiidae) feeding on *Chrysochlamys glauca* (Clusiaceae). The species is a gregarious parasitoid; the holotype is one of 56 specimens that emerged from the host, caterpillar voucher code: 07-SRNP-30348.

Paratype. Ten specimens, reared from the same caterpillar as the holotype, were mounted and designated as paratypes (DHJPAR0066400 to DHJPAR0066409), depository CNC.

Etymology. *Bracon andreamezae* is named in honor of Ministra Andrea Meza Murillo of the Ministerio de Recursos Naturales y Energía de Costa Rica (MINAE) in recognition of her taking on this difficult ministerial task mid-government.

***Bracon franklinpaniaguai* Sharkey, sp. nov.**

<http://zoobank.org/45DC951E-E7E0-4C69-9518-E2628FAA99DE>

Diagnostics. Figure 14.

BOLD data. BIN: BOLD:ACK6897; nearest neighbor: *Bracon alejandromasisi* BOLD:AAA5367; distance to nearest neighbor is 4.49%. Consensus barcode:

ATATTATATTTTTTATTTGGAATTTGAGCTGGAATAATTGGTTTAT-
 CAATAAGATTAATTATTCGTTTAGAATTAGGTATAACCAGGTAGTTTAT-
 AGGTAATGATCAAATTTATAATAGTATAGTTACAGCTCATGCTTTT-
 GTAATAATTTTTTTTATAGTTATAACCAGTAATATTAGGAGGATTTG-
 GAAATTGATTAATTCCTTTAATATTAGGAGCTCCTGATATAGCTTTTC-
 CTCGAATAAATAATATAAGATTTTGGTTATTAATTCCTTCATTAATTTTAT-
 TATTATTAAGAAGAATATAAATGTTGGTGTAGGGACAGGTTGAACTATT-
 TATCCTCCTTTATCATCTAGGTTAGGTCATGGAGGTATATCTGTTGATT-
 TAATTATTTTTTTCTTTACATTTAGCTGGTATTTTCATCTATTATAGGATC-
 TATTAATTTTATTACTACAATTTTAAATATGCATTTATTAATATTAAGT-
 TAGATCAATTAECTTTATTTATTTGATCAATTTTTATTACAACCTATTTTAT-
 TATTATATCTTTACCTGTATTAGCAGGAGCTATTACTATATTTAACT-
 GATCGAAATTTAAATACTTCATTTTTTTGATTTTTCTGGAGGTGGGGATC-
 CAATTTTATTTCAACATTTATTT

Morphological data. This species can be morphologically distinguished from its nearest neighbor by having the mesepisternum entirely orange-yellow, lateral sides of the head orange-yellow, and yellow fore- and mid-tibiae and femora (Fig. 14) compared to the mesepisternum entirely black, head entirely black, and all tibiae and femora black in *B. alexandromasisi* (Sharkey et al. 2021a: fig. 31).

Holotype ♂: Costa Rica: Guanacaste, Area de Conservación Guanacaste, Sector Pitilla, Pasmompa, 440 m, 11.019 -85.41; host caterpillar collection date: 09/xii/2004, parasitoid eclosion: 28/xii/2004; depository CNC, holotype voucher code: DHJPAR0029032.

Holotype host data. *Fountainea confusa* (Nymphalidae) feeding on *Croton billbergianus* (Euphorbiaceae), caterpillar voucher code: 04-SRNP-56695.

Paratype. Eight specimens reared from the same host specimen as the holotype were mounted and designated as paratypes (DHJPAR0066410 to DHJPAR0066417), depository CNC.

Etymology. *Bracon franklinpaniaguai* is named in honor of Vice-Minister Franklin Paniagua Alfaro of the Ministerio de Recursos Naturales y Energía de Costa Rica (MI-NAE) in recognition of his taking on this difficult task mid-government.

***Bracon rafagutierrezii* Sharkey, sp. nov.**

<http://zoobank.org/0093066D-6B8F-4674-9D40-9538CD2ECE5C>

Diagnostics. Figure 15.

BOLD data. BIN: BOLD:ACB1290; nearest neighbor: *Bracon* sp.BOLD:AAV0639; distance to nearest neighbor is 2.24%. Consensus barcode: GATTTTATATTTTTTATTTGGTATATGAGCAGGTATAGTTGGTTTAT-
 CAATAAGGTTAATTATTCGATTAGAATTAGGTATAACCTGGGAGTTTAC-
 TAGGTAATGATCAAATTTATAATAGTATAGTGACTGCTCATGCTTTTATT-
 ATAATTTTTTTTATAGTTATAACCTGTAATATTAGGAGGATTTGGTAATT-



Figure 14. *Bracon franklinpaniaguai*, holotype.

GATTAATTCCTTTAATATTAGGAGCTCCAGATATAGCTTTTCCTCGTT-
 TAAATAATATAAGATTTTGTTATTATTTCCCTCTTTAATTTTATTATT-
 ATTAAGAAGAATTTTAAATGTTGGTGTAGGTACTGGGTGAACAATATACC-
 CACCTTTGTCATCTAGATTAGGTCATAGAGGGTTATCTGTTGATTTAGC-
 TATTTTTTCTTTACATTTAGCTGGGGTTTCTTCTATTTTAGGTTTCAGT-
 TAATTTTATTACAACAATTTTAAATATACATTTATTAATATTTAAAATTA-
 GATCAATTAACCTTTATTAATTTGATCAATTTTATTACAACCTATTTTAT-
 TATTATTATCTTTACCTGTTTTAGCTGGTGCTATTACTATATTATTAACA-

GATCGAAATTTAAATACTTCTTTTTTTTGATTTTTCTGGTGGAGGGGATC-
CTATTTTATTCAACATTTATTT

Morphological data. This species can be morphologically distinguished from its nearest neighbor by having all femora dark brown and the metasoma dark brown dorsally starting at the third tergum (Fig. 15) compared to all femora yellow and the metasoma yellow to light brown dorsally.

Holotype ♀: Costa Rica: Alajuela, Area de Conservación Guanacaste, Sector Rincon Rain Forest, Palomo, 96 m, 10.962 -85.28; host caterpillar collection date: 05/iii/2012, parasitoid eclosion: 18/iii/2012; depository CNC, holotype voucher code: DHJPAR0049049.

Holotype host data. *Cosmorrhyncha albistrigulana* (Tortricidae) feeding on *Dialium guianense* (Fabaceae). This is one of the only two species of *Bracon* reared by us that is solitary; the ten species treated by Sharkey et al. (2021a) are all gregarious. It was reared from a very small caterpillar; caterpillar voucher code: 12-SRNP-67398.

Etymology. *Bracon rafagutierrez* is named in honor of SINAC Director Rafa Gutiérrez Rojas of the Ministerio de Recursos Naturales y Energía de Costa Rica (MINAE) in recognition of his taking on this difficult task mid-government.



Figure 15. *Bracon rafagutierrez*, holotype.

***Bracon guillermoblancoi* Sharkey, sp. nov.**

<http://zoobank.org/2E651361-5D12-419B-8A55-A2504505C00E>

Diagnostics. Figure 16.

BOLD data. BIN: BOLD:AAT8852; nearest neighbor: *Bracon* sp. BOLD:AED7502; distance to nearest neighbor is 8.17%. Consensus barcode: TATTTTATATTTT-TATTTGGTATATGATCAGGAATAATTGGTTTATCAATAAGTTAATTATTC-GATTAGAATTAGGGATACCTGGAAGATTATTAGGTAATGATCAAATT-TATAATAGAATAGTTACAGCTCATGCTTTTATTATAATTTTTTTTATAGT-TATACCAATTATATTAGGAGGATTTGGGAATTGATTAATTCCTTTAATATT-AGGAGCTCCTGATATAGCTTTTCCTCGTTAAATAATATAAGATTTTGAT-TATTAATTCCTTCATTAACCTTATTATTATTAAGAAGAATTTTAAATGTAG-



Figure 16. *Bracon guillermoblancoi*, holotype.

GTGTAGGAAGTGGGTGAACAATGTATCCTCCATTATCATCTAATTTAGGT-CATAGAGGTTTATCTGTAGATTTAGCTATTTTTTCTTTACATTTAGCTG-GAATTTCTTCTATTATAGGTTCAATAAATTTTATTACTACTATTTTAAATATA-CATTTAAAAATATTTAAAACCTTGATCAATTAACGTTATTAATTTGATCTATTTT-TATTACTACAATTTTGTATTATTATCTTTACCTGTTTTAGCTGGGGCAAT-TACTATACTATTAACCTGATCGAAATTTAAATACTTCATTTTTTT-GATTTTTCTGGGGGAGGAGACCCAATTTATTCCAACATTTATTT.

Morphological data. There is only one low-quality image on BOLD for the nearest neighbor, but the p-distance makes it doubtful that it is conspecific.

Holotype ♀: Costa Rica: Guanacaste, Area de Conservación Guanacaste, Sector Mundo Nuevo, Mamones, 365 m, 10.771 -85.429; host caterpillar collection date: 01/viii/2010, parasitoid eclosion: 12/viii/2010; depository CNC, holotype voucher code: DHJPAR0040470.

Holotype host data. *Dysodia sica* (Thyrididae) feeding on *Piper marginatum* (Piperaceae). This is one of the only two species of *Bracon* reared by us that is solitary; the ten species treated by Sharkey et al. (2021a) are all gregarious. It was reared from a very small caterpillar; caterpillar voucher code: 10-SRNP-56246.

Etymology. *Bracon guillermoblancoi* is named in honor of Guillermo Blanco, the BioAlfa Malaise traps manager for Parque Nacional Isla del Coco, ACMIC (Área de Conservación Marino Isla del Coco), Costa Rica.

***Bracon oscarmasisi* Sharkey, sp. nov.**

<http://zoobank.org/48249926-80DE-4AB4-98E2-D204D3A3CFB7>

Diagnosics. Figures 17, 18.

BOLD data. BIN: BOLD:AAY4686; nearest neighbor: *Bracon* sp. BOLD:AEF4783; distance to nearest neighbor is 6.09%. Consensus barcode: AGTTTTGTATTTTTTATTTGGTATATGAGCTGGTATAGTTGGTTTTAT-CAATAAGTTTAATTATTCGTTTAGAGTTAGGTATACCTGGAAGTTT-ATTAGGTAATGATCAAATTTATAATAGAATAGTTACAGCTCATGCTTTT-GTTATAATTTTTTTTATAGTTATACCTGTTATAATTGGAGGATTTGG-TAATTGATTAATTCCTTTAATATTAGGAGCTCCTGATATAGCTTTTC-CTCGAATAAATAATATGAGATTTTGGTTATTAGTTTCCTTCATTAACCT-TATTATTATTAAGTAGAATTTTAAATGTAGGGGTAGGTACAGGTTG-GACAATATATCCACCTTTATCTTCAAGTTTAGGTCATAGAGGGTTATCT-GTTGATTTAGCTATTTTTTCTTTACATTTAGCTGGTGTTTCTTCAAT-TATAGGGGCAATAAATTTTATTACTACTATTTTAAATATGCATTTATTAAT-ATTTAAATTTAGATCAGTTAACTTTATTAGTTTGATCAATTTTTTATTACTAC-TATTTTATTATATTATCTTTACCTGTTTTAGCAGGAGCAATTACAATAT-TATTAACCTGATCGAAATTTAAATACTTCTTTTTTTGATTTTTTCAGGAG-GTGGAGATCCTATTTATTTCACATTTATTT.



Figure 17. *Bracon oscarmasisi*, holotype.



Figure 18. *Bracon oscarmasisi*, remains of pupal chamber of host caterpillar, *Anadasmus Janzen25*.

Morphological data. This species can be morphologically distinguished from its nearest neighbor by having the hind femur dark brown (Fig. 17) compared to yellow.

Holotype ♂: Costa Rica: Guanacaste, Area de Conservación Guanacaste, Sector Mundo Nuevo, Punta Plancha, 420 m, 10.742 -85.427; host caterpillar collection date: 17/x/2010, parasitoid eclosion: 28/x/2010; depository CNC, holotype voucher code: DHJPAR0041854.

Holotype host data. Gregarious parasitoid of *Anadasmus Janzen25* (Depressariidae) feeding on *Mespilodaphne veraguensis* (Lauraceae); four specimens emerged from the host, caterpillar voucher code: 10-SRNP-56886.

Paratype. Two males, same data as holotype (DHJPAR0066418, DHJPAR0066419) depository CNC.

Etymology. *Bracon oscarmasisi* is named in honor of Oscar Masis, the BioAlfa Malaise traps manager for Parque Nacional Los Quetzales, ACOPAC (Área de Conservación Pacífico Central), Costa Rica.

***Bracon pauldimaurai* Sharkey, sp. nov.**

<http://zoobank.org/723581AA-45CD-4F42-9AB1-CED38EBEA383>

Diagnostics. Figure 19.

BOLD data. BIN: BOLD:AEF4305; nearest neighbor: *Bracon* sp. BOLD:ACG3693; distance to nearest neighbor is 9.62%. Consensus barcode: TGTTT-TATATTTTTTATTTGGTATATGAGCTGGGATACTAGGTCTATCAATAA-GATTAATTATCCGACTAGAGCTCGGAATACCGGGAAGTTTACTTG-GTAATGACCAAATTTACAATAGAATAGTAACAGCTCATGCTTTTGTA-ATAATTTTTTTTATAGTTATACCTGTAATAGTAGGAGGATTTGGAAATT-GACTATTACCTTTAATATTAGGAGCCCCTGATATAGCATTTCCTCGTT-TAAATAATATAAGATTTTGATTACTTATTCCTTCCCTAACTTTATTATTAA-TAAGAAGAATTTTAAATGTAGGAGTAGGGACTGGATGAACAGTTTATC-CTCCTTTATCCTCTTCACTAGGTCATAGAGGGTTATCAGTTGATTTG-GCTATTTTTTCTTTACATATTGCAGGAATTTCCCTCAATTTTGGGGGC-TATTAACCTTTATTTCAACTATTTTAAATATACATTTATTAATTTTAAAAC-TAGATCAACTAACATTATTAATTTGATCAATTTTATTACAGCTATTTTAT-TATTATTATCTTTACCAGTATTAGCAGGAGCTATCACAATATTATTAAC-CGATCGAAATTTAAATACATCTTTTTTTGATTTTTTCAGGAGGGGGTGAC-CCAATTTTATTTCAACATTTATTT.



Figure 19. *Bracon pauldimaurai*, holotype.

Morphological data. This species can be morphologically distinguished from its nearest neighbor by having large portions of the mesoscutum and mesepimeron brown (Fig. 19) compared to entirely black.

Holotype ♀: Costa Rica: Guanacaste, Area de Conservación Guanacaste, Sector Cacao, Sendero Cima, 1460 m, 10.933 -85.457, 23/iii/2009, Malaise trap, depository CNC, holotype voucher code: DHJPAR0051516.

Etymology. *Bracon pauldimaurai* is named in honor of Paul Dimaura of Boston, Massachusetts for his decades of support of the University of Pennsylvania in general and D. H. Janzen's position as a professor of conservation biology specifically.

***Bracon shebadimaurae* Sharkey, sp. nov.**

<http://zoobank.org/E87C71B3-2C89-4EB5-AFE9-47FD75A1C533>

Diagnostics. Figure 20.

BOLD data. BIN: BOLD:ADW8464; nearest neighbor: *Bracon* sp. BOLD:AEB6448; distance to nearest neighbor is 4.81%. Consensus barcode: TTTATATTTTTTATTTGGTATATGAGCAGGAATATTAGGATTATCACTAAGTTTAAATTATTCGTTTAGAATTAGGGATACCTGGAAGATTATTAGGTAATGATCAAATTTATAATAGTATAGTTACAGCTCATGCATTTGTTATAATTTTTTTTTATAGTTATACCAGTAATATTAGGAGGATTTGGTAATTGATTATTACCTTTAATATTAGGGGCTCCTGATATAGCTTTCCCACGAATAAATAATATAAGATTTTGGTTAATTATCCCTTCTTTAATTTTATTATTAATAAGAAGAATTTTAAATGTAGGAGTAGGAACAGGTTGAACAGTTTATCCTCCTTTATCATCTTCATTAGGGCATAGTGGGTTATCTGTTGATTTAGCTATTTTTTCTTTACATATTGCAGGAATTTCTTCAATTATAGGTTCAATTAATTTTATTACTACTATTTTAAATACATTTTATTTAAATTTAAATTTAGATCAATTAACATTATTAATTTGATCTATTTTATCACAACTATTTTACTTTTATTATCTTTACCAGTTTTAGCGGGGGGAATTTACTATATTATTAACAGATCGTAATTTAAATACATCATTTTTTGATTTTTCTGGAGGGGGAGATCCTGTTTTATTTC AACATTTATT.

Morphological data. No images of the unnamed nearest neighbor are available.

Holotype ♀: Costa Rica: Guanacaste, Area de Conservación Guanacaste, Sector Pailas Dos, PL12-1, 828 m, 10.7642 -85.335, 14/v/2015, Malaise trap, depository CNC, holotype voucher code: BIOUG44786-F08, GenBank accession MW627534.

Etymology. *Bracon shebadimaurae* is named in honor of Sheba Dimaura of Boston, Massachusetts for her decades of support of the University of Pennsylvania in general and D. H. Janzen's position as a Professor of Conservation Biology.

***Sacirema karendimaurae* Sharkey, sp. nov.**

<http://zoobank.org/5BE4D1E3-9F52-444D-8F49-AC0130EEE9FF>

Diagnostics. Figure 21.



Figure 20. *Bracon shebadimaurae*, holotype.

BOLD data. BIN: BOLD:ADY0104; nearest neighbor: *Sacirema* sp. BOLD:AEH2057; distance to nearest neighbor is 2.24%. Consensus barcode: TTTATATTTTTTATTGGGATATGATCTGGTATATTAGGTTTATCAATAAGTTTAATTATTCGATTAGAACTTGAATACCATCAAGTTTATTAACAAATGATCAAATTTATAATA-



Figure 21. *Sacirema karendimaurae*, holotype.

GAATAGTAACTGCCCATGCATTGTCATAATTTTTTTTTATAGTTATAACCAAT-TATAATTGGTGGATTTGGAAATTGATTAATTCCTTTAATATTAAGAGCTC-CAGATATAGCTTTCCCTCGTATAAATAATATAAGTTTTTGATTACTAATTC-CTTCTTTAATAATATTAATTTAAGAAGAATTATTAATACAGGTGTAGG-TACTGGTTGAACAGTTTACCCTCCTTTATCTTCTTCTATAGGACATAGAG-GAATTTCAGTTGATTTAGCAATTTTTTCTTTACATTTAGCTGGAGCTTC-CTCAATTATAGGGTCTATTAATTTTATTTCAACTATTAATATAACGACTT-TATTTAATAAAAATAGATCAATTAACATTATTAATTTGATCTATTTTTATTAC-TACAATTTTATATTATTATCATTACCAGTTCTAGCTGGGGCAATCACAAAT-ATTATTAACAGATCGAAATTTAAATACTACTTTTTTTTGATTTTTTCAGGAG-GTGGGGATCCAATTTTATTCCAACACTTAT.

This species differs from the three described species of *Sacirema* (Papp 2007) in many ways. The easiest to see is that none of the other three species has a predominantly yellow meso- and metasoma. The generic placement of this species is somewhat uncertain as are those of other specimens in the group of braconine genera with a medial area of the face delimited by longitudinal grooves or ridges.

Morphological data. No images of the unnamed nearest neighbor are available, and when it is described, it should be carefully compared to *Sacirema karendimaurae*.

Holotype ♂: Costa Rica: Guanacaste, Area de Conservación Guanacaste, Sector Pailas Dos, PL12-3, 820 m, 10.7631 -85.3344, 08/i/2015, Malaise trap, depository CNC, holotype voucher code: BIOUG44686-A07. GenBank accession MW627576.

Etymology. *Sacirema karendimaurae* is named in honor of Karen Dimaura of Boston, Massachusetts for her decades of support of the University of Pennsylvania in general and D. H. Janzen's position as a professor of conservation biology.

Cheloninae

Cheloninae are egg-larval parasitoids of Lepidoptera. A key to the genera of the New World is included in Sharkey et al. (2021a).

Chelonus minorzunigai Sharkey, sp. nov.

<http://zoobank.org/6B54FDAF-3228-4F7D-B0B8-8B61B5FDBD6C>

Diagnostics. Figure 22.

BOLD data. BIN: BOLD:AEB3509; nearest neighbor: *Chelonus jeffmilleri* BOLD:ACF0845; distance to nearest neighbor is 4.81%. Consensus barcode: AATATTATATTTTGTTTTGGGAATTTGGAGTGGGAATAATAGGTTTATCATTAAAGATTAATAATTCGTATAGAATTAAGAAGTGTAATAAGATTATTTATAATGATCAATTATATAATAGAGTTGTAACATAACATGCTTTTATTATAATTTTTTTTATAGTTATACCTTTAATAATTGGAGGATTTGGAAATTGATTAATTCCTTTAATATTAGGATTATCTGATATAAATTTTTTCCTCGAATAAATAATATAAGATTTTGATTATTAATTCCTTCAATTATTTTATTAATTATAGGAGGGTTTGTTAATATAGGAGCTGGGACAGGATGAACAGTTTATCCTCCATTATCATTATTAATAGGTCATAGAGGAGTTTCAGTAGATTATCTATTTTTTCTTTACATTTAGCAGGAGTTTCATCTATTATAGGATCAATTAATTTTATTGTTACTATTATAAACTTTGATTACATTATAAAATATATAGATAAATACCCATTATTTGTTTGATCAGTTTTTATTACAACACTATTTTATTATTATTATCATTACCAGTTTTGGCTGGTGCAATTACTATGTTATTAAGAGATCGAAATTTAAATACAAGATTTTTTGATCCATCAGGAGGAGGAGATCCTGTATTATACCAACATTTGTTT.

Morphological data. This species can be morphologically distinguished from its nearest neighbor by having the hind tibia entirely black (Fig. 22) whereas that of *C. jeffmilleri* has a light brownish yellow patch near the base of the hind tibia, which is otherwise black (Sharkey et al. 2021a: 164, fig. 101).

Holotype ♀: Costa Rica: Guanacaste, Area de Conservación Guanacaste, Sector Cacao, Estación Cacao, 1150 m, 10.9269 -85.4682; host caterpillar collection date: 07/iii/2019, parasitoid eclosion: 31/iii/2019; depository CNC, holotype voucher code: DHJPAR0064501, GenBank accession: MW627562.

Holotype host data. 19-SRNP-35166 *Desmia benealis* (Crambidae) feeding on *Hamelia patens* (Rubiaceae), caterpillar voucher code: 19-SRNP-35166.

Paratype. Same host data as holotype, DHJPAR0064500, DHJPAR0064502, depository CNC.

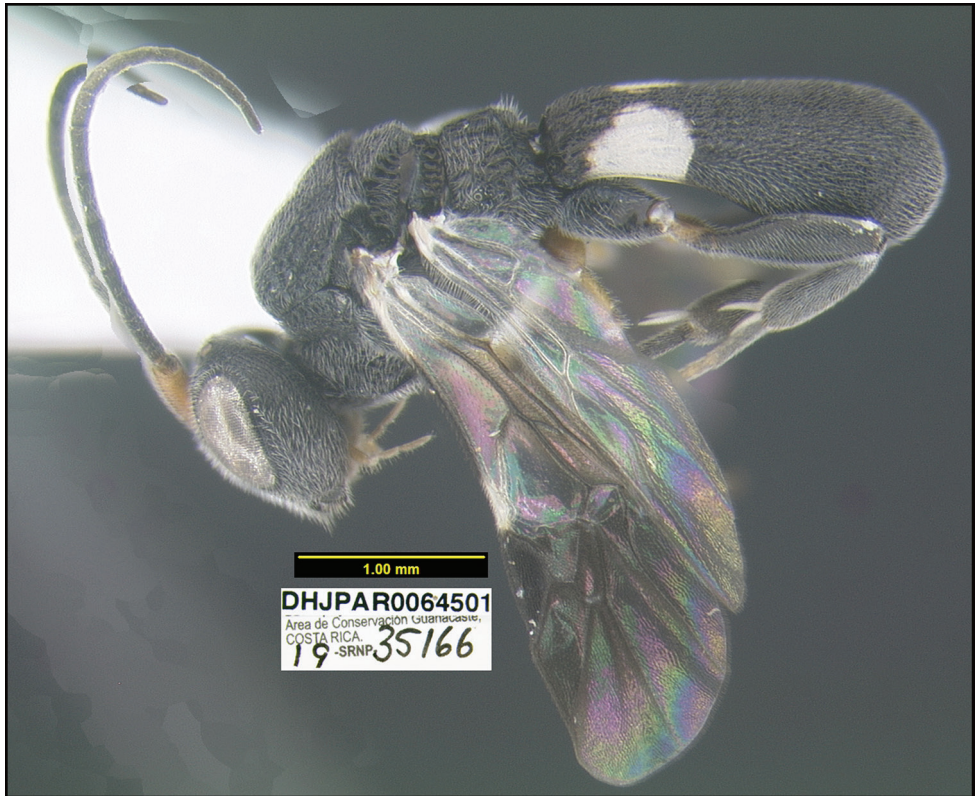


Figure 22. *Chelonus minorzunigai*, holotype.

Etymology. *Chelonus minorzunigai* is named in honor of Minor Zúñiga Siles, the BioAlfa Malaise traps manager for Estación Esquinas, Parque Nacional Tortuguero, ACTO (Área de Conservación Tortuguero), Costa Rica.

Homolobinae

Members of Homolobinae are endoparasitoids of lepidopteran larvae. A key to the genera of the New World is included in Sharkey et al. (2021a).

Homolobus stevestroudi Sharkey, sp. nov.

<http://zoobank.org/D21DFA7D-C461-4F83-9521-79A1E9982771>

Diagnostics. Figures 23, 24.

BOLD data. BIN: BOLD:AAA7060. The nearest neighbor: *Homolobus* sp. BOLD:ACM2462 is separated by a p-distance of only 1.12%. Consensus barcode: TATTTTATATTTTATATTTGGAATTTGAGCTGGAATTTTAGGTA-

TATCAATAAGAATTATTATTTCGAATAGAATTAAGAATACCAGGTAATT-
 TAATTGGTAACGATCAAATTTATAATAGTATTGTTACTGCTCATGCATT-
 TATTATAATTTTTTTTATAGTTATAACCAATTATAATTGGAGGGTTTG-
 GAAATTGATTAATTCCTTTAATATTAGGATGTGTTGATATAGCTTTTC-
 CTCGAATAAATAATATAAGATTTTGATTATTAATCCATCATTAATTTTAT-
 TAATTTAAGAAGAATTTTAAATGTTGGTGTTGGTACTGGATGAACT-
 GTTTATCCTCCTTTATCTTTAAATATTGGTCATGGAGGTTTATCTGTT-
 GATTTAGCTATTTTTCTTTACATTTAGCTGGAATTTCTTCAATTATAG-
 GAGCTATTAATTTTATTACTACTATTTTAAATATACGATCTAATTTAAT-
 TACAATAGATAAAATTTCTTTATTAAGTTGATCAATTTAATTACTG-
 TAATTTTATTATTATTATCTTTACCAGTTTATAGCTGGGGCTATTACAAT-
 ATTATTAACTGATCGTAATTTAAATACATCTTTTTTTTGATCCATCTGGTG-
 GAGGGGATCCAATTTTATATCAACATTTATTT.

Morphological data. The specimen keys to *Homolobus infumator* in van Achterberg's (1979) key and is very similar morphologically. Subtle differences include the shape of vein R1a of the hind wing, which is longer in *H. stevestroudi* and the size of the basal tooth of the hind tarsal claws, which are longer in *H. stevestroudi*. The convincing difference can be found by looking at the NJ tree produced from the BOLD



Figure 23. *Homolobus stevestroudi*, holotype.



Figure 24. Tough-walled silk cocoon of *Homolobus stevestroudi*. Note shiny surface of the inside visible just inside the cut off right-hand end. That hard smooth surface makes the cocoon wall extremely tough and difficult to penetrate with an insect pin. The terminal circular cut exit hole is characteristic of most genera of large bodied ACG Braconidae and many small ones as well.

website; *H. stevestroudi* is found in its own BIN, far removed from any other species of *Homolobus* and particularly distant from specimens identified as *H. infumator* from Norway. The type locality of *H. infumator* is England. All nine specimens in the unnamed nearest neighbor are from Canada. They might represent the same species as the Costa Rican specimens, but more sampling will need to be done between Canada and Costa Rica to confirm or refute. There are no obvious morphological differences based on the BOLD images of the Canadian specimens.

Holotype ♂: Costa Rica: Guanacaste, Area de Conservación Guanacaste, Sector Cacao, Sendero Toma Agua, 1140 m, 10.928 -85.467; host caterpillar collection date: 23/iv/2009, parasitoid eclosion: 18/v/2009; depository CNC, holotype voucher code: DHJPAR0035530, GenBank accession: MW627552.

Holotype host data. *Pherotesia minuisca* (Geometridae) feeding on *Zygia palmana* (Fabaceae), caterpillar voucher code: 09-SRNP-35488.

Etymology. *Homolobus stevestroudi* is named in honor of Steve Stroud as the primary supporter of the BioAlfa Malaise trapping at the Hacienda Barú Wildlife Refuge, Savegre, ACOPAC, Costa Rica, as well as decades of support for the Area de Conservación Guanacaste.

Macrocentrinae

Members of all genera are koinobiont endoparasitoids of caterpillars from a wide range of families. Most are solitary, but several gregarious species are known. A key to the genera of the New World is in Sharkey et al. (2021a).

Macrocentrus michaelstroudi Sharkey, sp. nov.

<http://zoobank.org/6E04139A-E5D6-4F29-BC63-DBD88D4EBADA>

Diagnostics. Figure 25.

BOLD data. This is the eighth species to be described in BIN BOLD:ACK7466.
 Consensus barcode: TGTTTTATATTTTTTATTAGGTATTTGATGTG-
 GATTAGTAGGTTTATCTTTAAGGTTACTTATTCGGTTAGAGTTGA-
 GAAATTTAGGAAGATTATTAGGTAATGATCAAATTTATAATGTAGTT-
 GTTACTATACATGCTTTTATTATAATTTTTTTTATGGTGATACCT-
 ATTATAATTGGAGGTTTTGGAAATTGATTAATCCCTTAATATTAG-
 GAGCTCCTGATATAGCTTCCCTCGTATAAATAATATAAGATTTTGATT-
 ATTAATTCCTTCTTTGTTATTAATTAATAAGAGGATTTATTATAGTTG-
 GTAGTGGAACCTGGGTGAACTATATATCCTCCTTTAAGTTCTT-

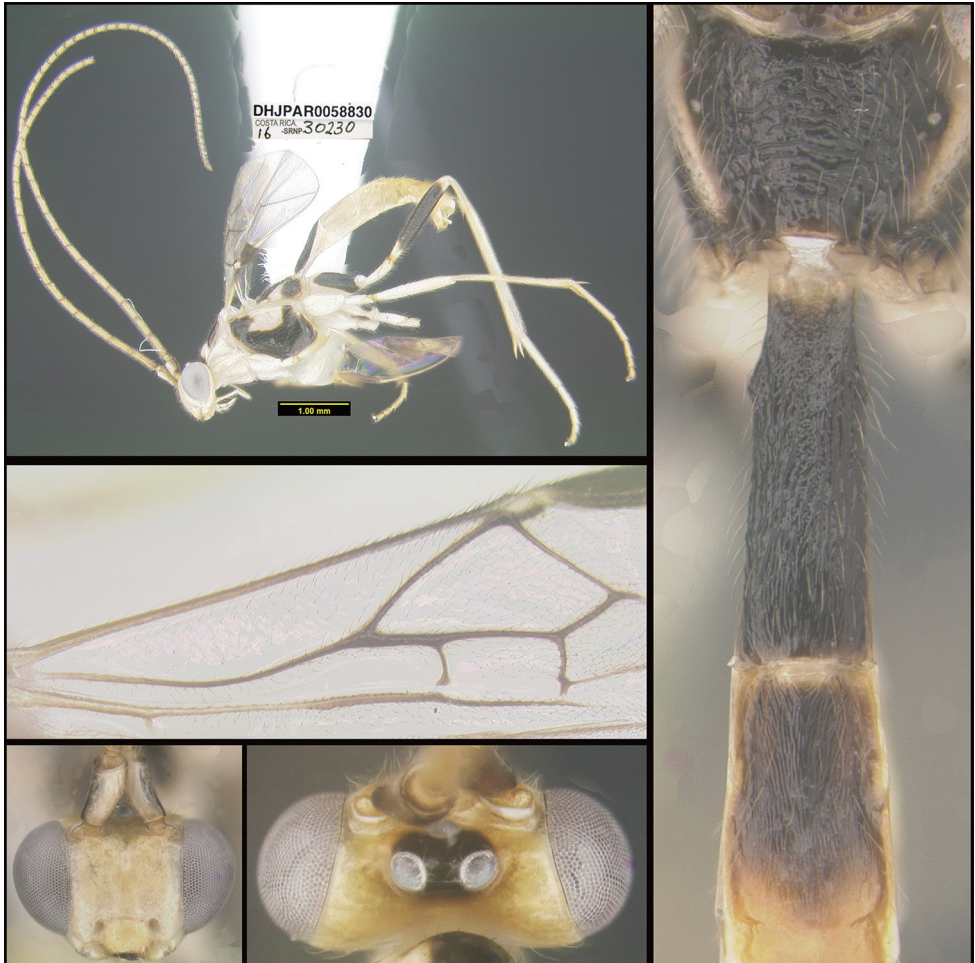


Figure 25. *Macrocentrus michaelstroudi*, holotype.

TAATTGGGCATAGAAGGTTTTCTGTTGATATAGTAATTTTTTTCTT-
TACATTTAGCAGGGGTTTTCTTCAATTATAGGAGCTATTAATTTTATTA-
CAACAATTTTAAATATAAAAATTAATTT---TAAAATTAGATCAGATTATAT-
TATTTGTATGATCTGTATTAATTACTIONGCTTTTTTTATTATTACTTTCTT-
TACCTGTTTTGGCAGGAGGAATTACTIONTATATATTAACAGATCGTAAT-
TTAAATACTTCTTTTTTTTGATTTTTTCAGGAGGGGGAGATCCTGTTT-
TATTTCAACACTTATTT.

Morphological data. In the morphological key to the species in this BIN (Sharkey et al. 2021a), *Macrocentrus michaelstroudi* will key to *M. gustavogutierrezii*. *Macrocentrus michaelstroudi* differs in its pale basal flagellomeres, contrasting with the melanic basal flagellomeres of *M. gustavogutierrezii*. The host caterpillar also differs from those of *M. gustavogutierrezii*. It belongs to the group of species with vein M+Cu of the forewing distinctly widened apically.

Holotype ♂: Costa Rica: Guanacaste, Area de Conservación Guanacaste, Sector Pitilla, Sendero Rotulo, 510 m, 11.0135 -85.4241; host caterpillar collection date: 22/i/2016, parasitoid eclosion: 01/iii/2016; depository CNC, holotype voucher code: DHJPAR0058830, GenBank accession: MW627584.

Holotype host data. *Phaedropsis leialis*DHJ03 (Crambidae) feeding on *Gouania lupuloides* (Rhamnaceae), caterpillar voucher code: 16-SRNP-30230.

Etymology. *Macrocentrus michaelstroudi* is named in honor of Michael Stroud Bonilla as the primary supporter of the BioAlfa Malaise trapping at the Hacienda Baru Wildlife Refuge, Savegre, ACOPAC, Costa Rica, as well as decades of support for the Area de Conservación Guanacaste.

Orgilinae

Members of all genera are koinobiont endoparasitoids of caterpillars. A key to the genera of the New World can be found in Sharkey et al. (2021a).

Stantonina gilbertfuentesii Sharkey, sp. nov.

<http://zoobank.org/6058EB69-E85F-4CFB-8771-92DD917FA191>

Diagnostics. Figure 26.

BOLD data. BIN: BOLD:AEC3983; nearest neighbor: *Stantonina miriamzunzae* BOLD:ACB1896; distance to nearest neighbor is 4.47%. Consensus barcode: TATATTGTATTTTTTTGTTTTGGTATATGGTCTGGGGTGTTAGGTTTAT-
CACTAAGTTTAATTAATTCGTATAGAATTAGGTCAAATTTGGTTCATT-
TATTGGAAATGATCAAATTTATAATAGTATTGTTACTTCTCATGCTTT-
TATTATAATTTTTTTTATAGTTATGCCTATTATAAATTGGGGGGTTTTG-
GAAATTGATTGATTCCTTTAATATTAGGAAGTGTTGATATAGCTTTCC-
CTCGAATAAATAATAAGATTTTGATTATTAATTCCTTCTTTAATATT-
ATTAATTTTAAGAGGATTTATAAATATTGGTGTAGGTACAGGATGAACA-



Figure 26. *Stantonia gilbertfuentesii*, holotype.

GTTTACCCTCCTTTATCATTAAATGTTAGTCATATAGGAATTTCTGTAGATATAGCTATTTTTCATTACATTTGGCTGGTATTTCTTCAATTATAGGTGCTATTAATTTTATTGTTACTATTATAAATATACGAAATTATGGGGTATTAATAGATAAAAATTAGATTATTATCATGATCAATTTTAATTACAGCTATTTTATTATTGTTATCTTTACCTGTGTTAGCTGGTGCTATTACAATATTGTTAACTGACCGTAATTTAAATACATCCTTTTTTGGATCCTGCTGGAGGAGGGGATCCTATTTTATATCAACATTTATTT

Morphological data. This species can be morphologically distinguished from its nearest neighbor by having the first metasomal tergite uniformly pale yellowish-orange and the mesoscutum uniformly yellowish-orange (Fig. 26), contrasting with the first metasomal tergite darkening apically and melanic patches on each of the three mesoscutal lobes in *S. miriamzunzae* (Sharkey et al. 2021a: 502, fig. 354).

Holotype ♂: Costa Rica: Guanacaste, Area de Conservación Guanacaste, Sector Rincon Rain Forest, 369 m, 10.969 -85.32; host caterpillar collection date: 07/ix/2019, parasitoid eclosion: 28/ix/2019; depository CNC, holotype voucher code: DHJPAR0065133, GenBank accession: MW627539.

Holotype host data. *Casandria* Poole01 (Erebidae) feeding on *Vismia baccifera* (Hypericaceae), caterpillar voucher code: 19-SRNP-46256. Erebidae is a new host-family record for *Stantonia*.

Etymology. *Stantonia gilbertfuentesi* is named in honor of Gilbert Fuentes of the Organización de Estudios Tropicales of Costa Rica in recognition of his decades of intensive management of the OET library of tropical publications.

Rhysipolinae

Members of the subfamily are thought to be solitary, koinobiont ectoparasitoids of caterpillars. A diagnosis for the subfamily is included in Sharkey et al. (2021a).

Rhysipolis stevearonsoni Sharkey, sp. nov.

<http://zoobank.org/B5D5C71B-6810-4120-976F-D30A453FF262>

Diagnostics. Figure 27.

BOLD data. BIN: BOLD:ADA0151; nearest neighbor: *Rhysipolis* sp. BOLD:ADL9389; distance to nearest neighbor is 2.91%. Consensus barcode: TG-TATTATATTTTATTATTGGAATTTGATCTGGAATAGTAGGTTTGTC-TATGAGTTTAATTATTCGTTTAGAGTTAGGTATAACCCGGTAGTTTGT-TATTTAATGATCAGATTTATAATACGATAGTTACAGCTCATGCTTT-TATTATAATTTTTTTATAGTGATACCTGTAATGATTGGGGGGTTTGG-TAATTGGTTAGTTCCATTAATGTTGGGGGCTCCTGATATAGCTTTTC-CTCGTATGAATAATATAAGATTTTGATTATTAATTCCTTCTTTAATTTTAT-TATTTTTGAGGGGATTAGTAAATGTTGGGGTAGGTAAGTACTGGATGAACA-GTTTATCCTCCTTTATCTTCTTCTATAGGTCATAGAGGTATTTCTGTT-GATTTGGCTATTTTTCTTTACATTTAGCTGGTATTTCTTCTATTATAG-GAGCTATTAATTTATTTCAACAATTTTAATATGTGTTTATATTTCAAT-TAATATAGATCAAATTAGTTTATTTATTTGATCTATTTTGATTACT-GCTTTTTTATTATTGTTGTCTTTACCTGTTTTGGCAGGGGCTATTACTA-TATTGTTAACGGATCGAAATTTAAATACTTCATTTTTTGATTTTTCTGG

Morphological data. This species can be morphologically distinguished from its nearest neighbor by having its mesoscutum entirely black (Fig. 27) compared to partially orange-brown.

Holotype ♀: Costa Rica: Guanacaste, Área de Conservación Guanacaste, Sector San Cristobal, Estación San Gerardo, 575 m, 10.8801 -85.389, 04/viii/2014, Malaise trap, depository CNC, holotype voucher code: BIOUG28483-E12, GenBank accession MW627555.

Paratype. BIOUG27682-G07.

Etymology. *Rhysipolis stevearonsoni* is named in honor of Steve Aronson of San Jose, Costa Rica, in recognition of decades of concern and involvement with the betterment of Costa Rica's positive relationship with its wild environment, and specifically with providing broadband internet to Área de Conservación Guanacaste as the first Costa Rican Área de Conservación to be so facilitated.



Figure 27. *Rhyssipolis stevearonsi*, holotype.

Rogadinae

Members of all genera are koinobiont endoparasitoids of caterpillars from a wide range of families. A key to the genera of the New World is in Sharkey (2021a).

Aleiodes kaydodgeae Sharkey, sp. nov.

<http://zoobank.org/B8C158F4-07CA-4776-91B7-D7507870695F>

Diagnostics. Figure 28.

BOLD data. BIN: BOLD:AEB2985; nearest neighbor: *Aleiodes* sp. BOLD:AAV6245; distance to nearest neighbor is 10.74%. Consensus barcode: AGTATTGTATTTTTTATTTGGTATATGAGCTGGAATAGTTGGTTTATC-TATAAGATTAATTATTCGGTTAGAATTAAGAGTTGGGGGGAGAGTCT-TAAAAAATGATCAGATTTATAAYGGTATAGTAACTTTGCATGCTTTT-GTAATAATTTTTTTTATAGTTATACCTATTATATTAGGAGGGTTTG-GAAATTGGTTAGTTCCTTTAATATTGAGAGCTCCAGATATAGCTTTC-



Figure 28. *Aleiodes kaydodgeae*, holotype.

CCTCGAATAAATAATATAAGATTTTGATTATTAATTCCATCTTTTTTTTTT-
TATTATTGATTAGAGGTGTTATTAATTCAGGRGTAGGAACAGGTT-
GAACAATATATCCTCCTCTTTCTTTATTAATTGGTCATGATGGAATTTCT-
GTAGATATATCAATTTTTTCTTTACATTTAGCAGGAGCTTCTTCCAT-
TATAGGTTCAATTAATTTTATTTCTACTATTTTTAATATAAAAATTA AAA-
GATTTAAAATTAGATCAAGTTTCTTTATTTGTTTGATCTATTTTAATTA-
CAACAATTTTATTATTGTTATCTTTACCTGTTTTAGCGGGGGCAATTAC-
TATATTATTGACTGATCGAAACTTAAATACAAGATTTTTTGATTTTGCTG-
GAGGAGGGGATCCAATTTTATTTCAACATTTGTTT.

Morphological data. This species can be morphologically distinguished from its nearest neighbor by having the base of the stigma brown (Fig. 28), contrasting with yellow in the nearest neighbor.

Holotype ♀: Costa Rica: Guanacaste, Area de Conservación Guanacaste, Sector Brasilia, Gallinazo, 360 m, 11.0183 -85.372; host caterpillar collection date: 10/vii/2019, parasitoid eclosion: 23/vii/2019; depository CNC, holotype voucher code: DHJPAR0064529, GenBank accession: MW627545.

Holotype host data. *Isogona* Poole07 (Erebidae) feeding on *Celtis iguanaea* (Ulmaceae), caterpillar voucher code: 19-SRNP-65351.

Paratype. DHJPAR0065341.

Etymology. *Aleiodes kaydodgeae* is named in honor of Kay Dodge of Costa Rica's Nicoya Peninsula today, original and decades long facilitator of ACG support from Peter Wege (RIP) of the Wege Foundation of Grand Rapids, Michigan, USA.

***Aleiodes kerrydresslerae* Sharkey, sp. nov.**

<http://zoobank.org/273165E1-C8BD-43E8-8EED-75004A28DD99>

Diagnostics. Figure 29.

BOLD data. BIN: BOLD:AEF3944; nearest neighbor: *Aleiodes* sp. BOLD:AAG1309; distance to nearest neighbor is 8.29%. Consensus barcode: AGTATTATATTTTATTGGAATATGAGCAGGAATAATTGGGATATCAATAAGTTAATAATCCGATTAGAATTAAGAACAAATGGAAGAATCTTAAAAAATGATCAAATTTATAATGGTATGGTAACTTTACATGCCTTTATATAATTTTTTTATAGTAATACCAATTATAATTGGAGGATTTGGAAATTGATTAATTCCTTTAATATTAGGAGCTCCTGACATAGCTTTCCCACGTATAAATAATATAAGATTTTGATTACTAATACCTTCTTTAATACTTTTATTACTTTAGAGGAATAATTAATACCGGGGTAGGAACAGGATGAACTATATATCCCCCTTTATCATCACTAATTGGACATAATGGAATTCAGTAGATATATCTATTTTTCTTTACACCTTGCAGGGGCTTCTTCAATTATAGGAGCAATCAACTTCATTTCAACTATTTTAAATATAAATATTATAACAATAAAATAGATCAAATTATACTATTAATTTGATCTATTTAAATTACTACAATCCTTTTATTATATCTTTACCAGTATTAGCAGGAGCAATTACTATATTACTAACA-GATCGAAATTTAAATACAAGATTTTTTGACTTTTCAGGGGGAGGAGACCCTATTTTATTCCAACATCTTTTT.

Morphological data. This species can be morphologically distinguished from its nearest neighbor by its pale stigma (Fig. 29), which is mostly melanic in the nearest neighbor.

Holotype ♂: Costa Rica: Guanacaste, Area de Conservación Guanacaste, Sector Pitilla, Bullas, 440 m, 10.98670 -85.38503; host caterpillar collection date: 25/i/2019, parasitoid eclosion: 13/ii/2019; depository CNC, holotype voucher code: DHJ-PAR0063995, GenBank accession: MW627548.

Holotype host data. *Anomis gentilis* (Erebidae) feeding on *Peltaea ovata* (Malvaceae), caterpillar voucher code:19-SRNP-70250.

Paratype. DHJPAR0063970.

Etymology. *Aleiodes kerrydresslerae* is named in honor of Kerry Dressler for her life career of deep and intense work and interest in the taxonomy of orchids, and of supporting Bob Dressler's enthusiasm for the same.

***Aleiodes josesolanoi* Sharkey, sp. nov.**

<http://zoobank.org/2A3DC697-674E-4EB5-AE11-A15680375504>

Diagnostics. Figure 30.

BOLD data. BIN: BOLD:AEB1913; nearest neighbor: *Aleiodes* sp. BOLD:AAM5681; distance to nearest neighbor is 2.24%. Consensus barcode: AATTTTATATTTTTTATTGTTTATGAGCAGGAATAATTGGGATATCAATAAGATTAATTAATTCGATTAGAATTAAGAACTAGAGGTAGAATTTTAAAAAATGATCAAATTTATAACGGCATAGTAACTTTACATGCATTATTATAATTTTTTTTATAGTAATACCATTATAATTGGAGGGTTTG-



Figure 29. *Aleiodes kerrydresslerae*, holotype.

GAAATTGATTAATYCCTCTAATATTAGGAGCCCCTGATATAGCATTTC-
 CTCGAATAAATAATATAAGATTTTGATTACTAATTCATCATTAATATTTT-
 TATTAATTAGAGGAATTATTAATACAGGTGTAGGAACAGGATGAACAATA-
 TATCCTCCATTATCTTCATTAATTTGGACATAATAGAATTTTCAGTTGATA-
 TATCAATTTTTCTTTACATATAGCAGGTGCTTCATCAATTATAGGAGCT-



Figure 30. *Aleiodes josesolanoi*, holotype.

ATTAATTTTATTTCAACAATTTTCAATATAAACTTAATAAAAATCAAATA-GAYCAAATTATATTATAGTTTGATCAGTTTTAATTACAGCCATTTTAT-TATTACTTTCATTACCTGTTTTAGCAGGAGCAATCACTATATRTTAAC-CGACCGTAACTTAAATACAAGTTTTTTTGATTTTTCAGGAGGAGGAGA-TCCTATTTTATTTCCAACATTTATT.

Morphological data. The nearest neighbor is a sole specimen from Canada. There is no image available on BOLD but due to the distribution, conspecificity is doubtful.

Holotype ♀: Costa Rica: Guanacaste, Area de Conservación Guanacaste, Sector Del Oro, Meteorológico, 590 m, 11.002 -85.4617; host caterpillar collection date: 25/vi/2019, parasitoid eclosion: 15/vii/2019; depository CNC, holotype voucher code: DHJPAR0064517, GenBank accession: MW627567.

Holotype host data. *Herbita medama* (Geometridae) feeding on *Dendropanax arboreus* (Araliaceae), caterpillar voucher code: 19-SRNP-20457.

Paratype. DHJPAR0064001 (DHJPAR0062033 not barcoded), host data *Prenesta scyllalis* feeding on *Forsteronia spicata* (Apocynaceae), depository CNC.

Etymology. *Aleiodes josesolanoi* is named in honor of Jose Andrés Solano, the Bio-Alfa Malaise traps manager for Estación El Ceibo, Parque Nacional Braulio Carrillo, ACC, Costa Rica.

***Aleiodes juniorporrasi* Sharkey, sp. nov.**

<http://zoobank.org/474FE466-BEF5-4451-8623-252D716F6B6F>

Diagnostics. Figure 31.

BOLD data. BIN: BOLD:AAV7490; nearest neighbor: *Aleiodes* sp. BOLD:AAV6239, from French Guiana; distance to nearest neighbor is 8.65%. Consensus barcode. AATTTTATATTTTTTATTTGGTTTATGGTCAGGAATAATTGGCATGTCATAAGATTAATTATTTCGATTAGAATTAAGAACGAGAGGTTAGAATTTTAAAAAATGACCAAATTTATAATGGCATAGTAACCTTTACATGCATTTATTTATAATTTTTTTTATAGTAATACCAATTATAATTTGGTGGGTTTGGAAATTTGATTAATTCCTTTAATATTTAGGAGCCCCTGATATAGCATTTCCCTCGTATAAATAATATAAGATTTTGATTATTAATCCCATCACTAATATTTTTTATTGATTAGAGGTATTATTAATACAGGAGTAGGGACAGGATGAACTATATATCTCCCCCTATCTTCCTTAATTGGCCATAATAGAATATCAGTTGATATATCAATTTTTTCTCTCCATATAGCTGGAGCCTCATCAATCATAGGAGCAATTAATTTTCATCTCAACAATTTTAAACATAAATCTAATAAAAATTTAAAATAGACCAAATTATACTATTAGTATGGTCAGTTTTAATTACAGCTATTTTATTACTTTTCATTACCTGTTTTAGCAGGAGCAATTACAATATTTAACTGACCGTAATTTAAATACAAGATTTTTTTGATTTTTTCAGGAGGAGGGGACCCCATTTTTATTCCAACATTTATTT.

Morphological data. This species can be morphologically distinguished from its nearest neighbor by its uniformly colored hind legs (Fig. 31), compared to hind femur darker than remaining leg segments in the nearest neighbor.



Figure 31. *Aleiodes juniorporrasi*, holotype.

Holotype ♀: Costa Rica: Alajuela, Guanacaste Area de Conservación, Sector Rincon Rain Forest, Sendero Aura, 432 m, 10.9654 -85.3239; host caterpillar collection date: 04/vii/2019, parasitoid eclosion: 31/vii/2019; depository CNC, holotype voucher code: DHJPAR0064521, GenBank accession: MW627570.

Holotype host data. geoJanzen01 Janzen7158 (Geometridae) feeding on *Serjania schiedeana* (Sapindaceae), caterpillar voucher code:19-SRNP-27158.

Paratype. BCLDQ01511, Honduras, Malaise-trapped (CNC).

Etymology. *Aleiodes juniorporrasi* is named in honor of Junior Porras Quirós, the BioAlfa Malaise traps manager for Estación Altamira, Parque Nacional Chirripo, ACLAP, Costa Rica.

***Aleiodes rocioecheverri* Sharkey, sp. nov.**

<http://zoobank.org/E8FBEA44-9DE3-4E93-81F8-0CBAD405DB42>

Diagnosics. Figure 32.

BOLD data. BIN: BOLD:AAM5673; nearest neighbor: *Aleiodes* sp. BOLD:AAH8820; distanceto nearestneighbor is 4.03%. Consensus barcode: GTTTATA-TATTTTTTATTTGGGATATGAGCTGGTATATTAGGRTTATCTATAAGGT-TAGTTATYCGTTTAGAATTAAGAAAYTGTGGRAGAGTTTTAAAAAATGAT-CAAATTTATAATGGKATGGTTACATTACATGCTTTTGTAATAATYTTTTT-TATAGTTATACCTATTATAATTGGTGGGTTTGGAAATTGATTAATTCCTT-TAATATTAGGGGCTCCTGATATAGCATTYCCTCGGATAAATAATATGAGA-TTTTGRTTATTAATTCCTTCATTTTTTTTTATTATTAATTAGAGGTGTTAT-TAATTCAGGGGTAGGTACAGGTTGAACAATATACCCTCCCCTTTCTT-TATTAATTGGTCATAATGGTTTATCAGTGGATATATCTATTTTTTCTTTA-CATTTAGCTGGRGCTTCTTCTATTATAGGATCAATTAATTTTATTTC AAC-TATTTTTTAATATAAATTTATTTTATATTA AATTAGATCAGATTTCTT-TATTAGTATGGTCAGTATTAATCACTACTATTTTATTATTTATTTATCTT-TACCTGTTTTTRGCAGGGGCTATTACTATATATTGACTGATCGTAATT-TAAATACAAGATTTTTTTGATTTTTTCGGGGGAGGGGATCCAATTT-TATTTCAACATTTA.

Morphological data. There is no image on BOLD, but the p-distance makes it doubtful that it is conspecific.

Holotype ♀: Costa Rica: Guanacaste, Area de Conservación Guanacaste, Sector San Cristobal, Estación San Gerardo, 575 m, 10.88 -85.389, 18/xi/2013, Malaise trap, depository CNC, holotype voucher code: BIOUG20202-G10, GenBank accession: MW627543.

Other material. BMNHE897799, from Belize deposited in the Natural History Museum (London), based on barcode, not viewed and lacking image on BOLD.

Etymology. *Aleiodes rocioecheverri* is named in honor of Rocio Echeverri of San Jose and Liberia, Costa Rica, in recognition of her lifetime of concern and involvement with the betterment of Costa Rica's positive relationship with its wild environment.



Figure 32. *Aleiodes rociocheverri*, holotype.

***Aleiodes ronaldzunigai* Sharkey, sp. nov.**

<http://zoobank.org/A73F3D24-4F8D-42C3-94F3-EC56B5219C77>

Diagnostics. Figure 33.

BOLD data. BIN: BOLD:AAH8707; nearest neighbor: *Aleiodes* nr. *speciosus* BOLD:AAM4342; distance to nearest neighbor is 2.4%. Consensus barcode: AATTTTATAYTTCATATTTGGAATATGAGCAGGTATAATTGGAATATCAATAAGATTAATTATTCGAATAGAATTAAGAACAAGAGGAAGAATTTTAAAAAATGACCAAATTTATAATGGTATAGTAACTTTGCATGCTTTTATTATAATTTTTTTTATAGTTATAACCARTTATAATTGGGGGATTCGGAAATTGATTAATCCCCTTAATATTAGGGGCCCTGATATAGCATTCCCTC-GAATAAATAATATAAGATTTTGGTTATTAATTCCATCTTTATTATTTTTACTAATAAGAGGTATTATTAATACAGGAGTTGGGACAGGATGAACATATATACCCTCCTTTATCRTCTTTAATTGGACATAATAGAATTTTCARTTGATATGTC AATTTTTCTTTACATTTAGCAGGAGCTTCTTCTATTATAGGRGCAATTAATTTTATTTCAACAATTTTAAATATAAATTTAATAAAAAATTAAATTA-



Figure 33. *Aleiodes ronaldzunicai*, holotype.

GACCAAATTTTCATTGTTAATTTGATCAATTTTAATTACTACTATTTTAT-TATTATATCTTTACCTGTACTAGCAGGAGCAATCACCATATTTATTAAC-TATCGTAACTTAAACACAAGATTTTTTGGATTTTCTGGAGGAGGAGAYC-CAATTTTATTTC AACATTTATT.

Morphological data. No images are available on BOLD for the three specimens in the nearest neighbor, all from Ecuador.

Holotype ♂: Costa Rica: Guanacaste, Area de Conservación Guanacaste, Sector Del Oro, Sendero Puertas, 400 m, 11.01087 -85.48816; host caterpillar collection date: 28/xii/2018, parasitoid eclosion: 07/i/2019; depository CNC, holotype voucher code: DHJPAR0064524, GenBank accession: MW627585.

Holotype host data. geoJanzen01 19-SRNP-20029 (Geometridae) feeding on algae, caterpillar voucher code: 18-SRNP-21223.

Paratype. all males and all with same host as holotype, DHJPAR0064525, DHJPAR0064526, DHJPAR0063992.

Etymology. *Aleiodes ronaldzunicai* is named in honor of Ronald Zúñiga, the Bio-Alfa Malaise traps manager for Parque Ecológico, SINAC, Santo Domingo de Heredia, ACC (Area de Conservación Central), Costa Rica.

***Choreborogas jesseausubeli* Sharkey, sp. nov.**

<http://zoobank.org/20C776D0-74D9-4B3D-B0E0-EE4E117B28CB>

Diagnostics. Figure 34.

BOLD data. BIN: BOLD:AAM5951; nearest neighbor: *Choreborogas* sp. BOLD:ACG8400; distance to nearest neighbor is 2.71%. Consensus barcode:

```
AGTATTGTATTTTTTTTTTTGGTATATGATCAGGTATATTGGGYTTAT-  
CAATAAGGTTAATTATTCGGTTTGAATTAGGGGTTCCCTGGATCATTTT-  
TAGGTAATGATCAGATTTATAATAGAATTGTTACGGCYCATGCCTTG-  
GTTATAATTTTTTTTATGGTTATACCTGTAATAATTGGGGGATTTGG-  
TAATTGATTAATTCCTTTAATATTAGGRGCACCTGATATAGCTTTYCCTC-  
GAATAAATAATATAAGATTTTGGTTATTAATTCCTTCTATTTTGTTATT-  
GTTAGTTAGATCTTTAGTTAATGTTGGGGYAGGTACAGGATGAACAATT-  
TATCCTCCTTTATCTTCRTTAATAGGTCATGGSGGGATTCAGTTGATT-  
TAGCTATTTTTTCTTTACATTTAGCTGGTGCATCATCAATTATAGGTG-  
CAATTAATTTTATTTCTACAATTTTAAATATAAATTTATTTTCAATGAAAAT-
```

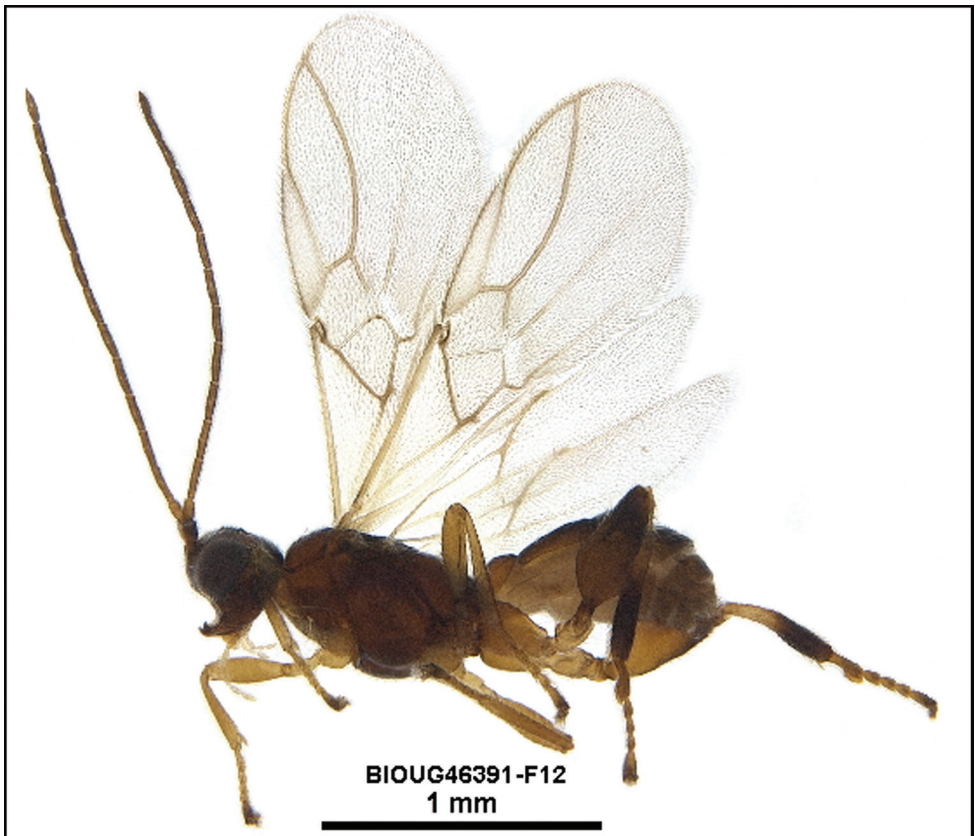


Figure 34. *Choreborogas jesseausubeli*, holotype.

AGATCAAATTATATTATTAGTTTGATCTGTATTAATCACTGCTTTTTTAT-
TATTATTATCATTRCCTGTTTTGGCGGGGGCAATTACTATATTATTATTT-
GATCGTAAAYATTAATAGAACTTTTTTTGATTTTTTCAGGGGGAGGGGATC-
CTATTTTTATTYCAGCATTATT

Morphological data. This species can be morphologically distinguished from its nearest neighbor by its swollen hind basitarsus (Fig. 34), which is much narrower in the nearest neighbor. Males lack the swollen hind femora.

Holotype ♀: Costa Rica: Guanacaste, Area de Conservación Guanacaste, Sector Pailas Dos, PL12-6, 853 m, 10.7637 -85.3331, 04/xii/2014, Malaise trap, depository CNC, holotype voucher code: BIOUG46391-F12, GenBank accession: MW627542.

Paratype. Malaise trapped, BIOUG46544-F12, BIOUG49790-H06, BIOUG07453-F05, BIOUG28810-A07, BIOUG29020-B09.

Other material: BMNHE897774 from Belize is in the same BIN and likely conspecific. There is no image on BOLD and the specimen was not examined.

Etymology. *Choreborogas jesseausubeli* is named in honor of Jesse Ausubel of Rockefeller University, New York, USA, for his very strong support of the germination and early development of DNA barcoding as an identification tool.

***Triraphis doncombi* Sharkey, sp. nov.**

<http://zoobank.org/8228960E-CF6E-4BF9-8C86-696F7EA67FE5>

Diagnostics. Figures 35–37.

BOLD data. BIN: BOLD:AAH8815; nearest neighbor: *Triraphis* sp. BOLD:AAG5003 from Guyana. Distance to nearest neighbor is 6.28%. Consensus barcode: TGTTTTATATTTTTTATTTGGAATTTGAGCTGGTATAGTCGGG-CTGTCTATAAGGTTAATTATTCGGTTAGAATTAAGTATAACCAGGGAGAT-TATTTGGGAATGAYCAGATTTATAATGGTATAGTTACCGCTCATGCTTT-TATTATAATTTTTTTTATGGTAATACCTATTATAATTTGGTGGTTTTG-GAAATTTGATTAATTCATTAATGTTGGGGGCYCCTGATATGGCTTTCC-CTCGTATAAATAATATGAGGTTTTGGTTATTAATTTCCYTCATTGACGT-TATTAATTTAAGGGCTGTAGTTAACGTTGGAGTAGGTAAGTACTGGGT-GAACTTTATATCCYCCCTTATCTTCTTTAGTTGGTCATGGGGGTA-TATCTGTAGATATAGCTATTTTTTCTTTACATTTAGCTGGTGCCTCTTC-TATTATAGGAGTTGTTAATTTTATTTCTACTATTTTTAATATAAAAT-TAATATCAATTAATTTAGATCAAATTAATTTATTTGTTTGATCAGTAT-TAATTACGGCTGTTTTATTATTATTATCTTTACCAGTATTAGCTGGT-GCAATTACTATATTATTGACAGATCGTAATTTAAATACAACATTTTTT-GATTTTTCTGGGGGGGGYGATCCTATTTTATTCCAACATTTATTT

Morphological data. No image of the nearest neighbor is available on BOLD, but the COI distance and geographic distribution suggest that they are not the same species.

Holotype ♀: Costa Rica: Guanacaste, Area de Conservación Guanacaste, Sector Pitilla, Sendero Naciente, 700 m, 10.98705 -85.42816; host caterpillar collection

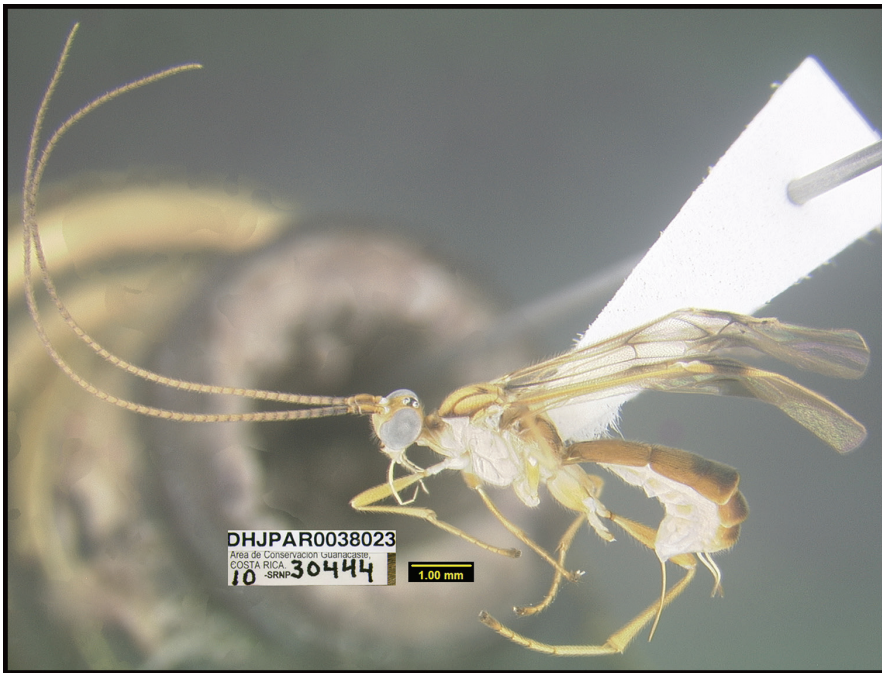


Figure 35. *Triraphis doncombi*, holotype.



Figure 36. White pupa of wasp *Triraphis doncombi* (DHJPAR0038023) visible through the translucent body wall of the parasitized host caterpillar *Euclea mesoamericana* (Limacodidae) in its last instar.

date: 09/ii/2010, parasitoid eclosion: 13/ii/2010; depository CNC, holotype voucher code: DHJPAR0038023. GenBank accession: HQ548697.

Holotype host data. *Euclea mesoamericana* (Limacodidae) feeding on *Thelypteris nicaraguensis* (Thelypteridaceae), caterpillar voucher code: 10-SRNP-30444.

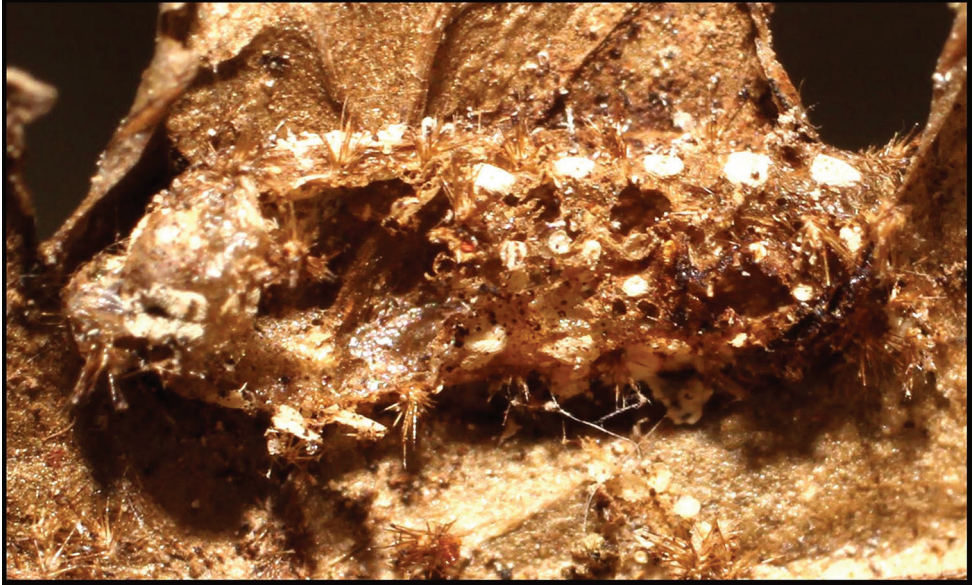


Figure 37. Exit hole, left side, cut by the wasp *Triraphis doncombi* (DHJPAR0038023) to exit the mummified body wall of the parasitized host caterpillar *Euclea mesoamericana* (Limacodidae) in its last instar.

Paratype. BCLDQ0860.

Etymology. *Triraphis doncombi* is named in honor of Dr. Don Comb (RIP), founder of the New England Biolabs and New England Biolabs Foundation, in recognition of his serious and ongoing support for the management and biodiversity conservation of Área de Conservación Guanacaste in northeastern Costa Rica (<http://www.acguanacaste.ac.cr>), through the Guanacaste Dry Forest Conservation Fund (<http://www.acguanacaste.ac.cr>).

***Yelicones mayraboillae* Sharkey, sp. nov.**

<http://zoobank.org/8BE983A2-E1D9-4FB8-AC3C-6E2FB4B5F8AA>

Diagnostics. Figures 38, 39.

BOLD data. BIN: BOLD:AAT9450. Its nearest neighbor on BOLD is identified by D. Quicke as *Yelicones artitus* BOLD:AAM6954; distance to nearest neighbor is 9.2%. Consensus barcode: TGTTTTATATTTTTTATTAGGTATTTGATGTGGATTAGTAGGTTTATCTTTAAGGTTACTTATTCGGTTAGAGTTGAGAAATTTAGGAAGATTATTAGGTAATGATCAAATTTATAATGTAGTTGTTACTATACATGCTTTTTATTATAATTTTTTTTTATGGTGATACCTATTATAATTTGGAGGTTTTGGAAATTGATTAATTCCTTAATATTAGGAGCTCCTGATATAGCTTCCCTCGTATAAATAATATAAGATTTTGATTATTAATTCCTTCTTTGTTATTAATATAATAAGAGGATTTATTATAGTTGGTAGTGGAACCTGGGTGAACTATATATCCTCCTTTAAGTTCTTTAATTGGGCATAGAAGGTTTTCTGTTGATATAGTAATTTTTTCTT-



Figure 38. *Yelicones mayrabortillae*, holotype.

TACATTTAGCAGGGGTTTCTTCAATTATAGGAGCTATTAATTTTATTA-
CAACAATTTTAAATATAAAATTAATTT--TAAAATTAGATCAGATTATAT-
TATTTGTATGATCTGTATTAATTAAGCTTTTTTATTATTACTTTCTT-
TACCTGTTTTGGCAGGAGGAATTAAGTATATTAACAGATCGTAAT-
TTAAATACTTCTTTTTTTGATTTTTTCAGGAGGGGGAGATCCTGTTT-
TATTTCAACACTTATTT.

Morphological data. This species keys to *Y. vilawanae* in the key of Areekul and Quicke (2006). *Yelicones vilawanae* has the apical 0.2 of hind tarsus and apical 0.8



Figure 39. *Yelicones mayrabonillae*, remains of host caterpillar, epipajanzen01 Janzen882 (Pyralidae); note mummified host caterpillar curved into a distinctive “C” shape, characteristic of other species of pyralid caterpillars attacked by species of *Yelicones*.

of hind basitarsus brown. *Yelicones mayrabonillae* has the basal four hind tarsomeres brown and the apical tarsomere yellow. This species can be morphologically distinguished from its nearest neighbor, *Yelicones artitus*, by the color of the hind femur being entirely testaceous (Fig. 38) (apical .04 brown in *Y. artitus*).

Holotype ♀: Costa Rica: Alajuela, Area de Conservación Guanacaste, Sector Rincon Rain Forest, Sendero Venado, 420 m, 10.897 -85.27; host caterpillar collection date: 26/vi/2010, parasitoid eclosion: 03/viii/2010; depository CNC, holotype voucher code: DHJPAR0040351.

Holotype host data. epipajanzen01 Janzen882 (Pyralidae) feeding on *Vochysia guatemalensis* (Vochysiaceae), caterpillar voucher code:10-SRNP-42391.

Etymology. *Yelicones mayrabonillae* is named in honor of Mayra Bonilla as the primary supporter of the BioAlfa Malaise trapping at the Hacienda Baru Wildlife Refuge, Savegre, ACOPAC, Costa Rica, as well as decades of support for the Area de Conservación Guanacaste.

Acknowledgements

We thank reviewers of the manuscript, who may or may not have agreed with our methods. We gratefully acknowledge the unflagging support of the team of ACG parataxonomists who collected and reared the specimens used in this study, and the team of biodiversity managers who protect and manage the ACG forests that are home to these wasps and their caterpillar hosts. The study has been supported by U.S. National Science Foundation grants BSR 9024770 and DEB 9306296, 9400829, 9705072, 0072730, 0515699, and grants from the Wege Foundation, International Conservation Fund of Canada, Jessie B. Cox Charitable Trust, Blue Moon Fund, Guanacaste Dry Forest Conservation Fund, Permian Global, individual donors, and University of Pennsylvania (DHJ&WH). This study has been supported by the Government of Canada through its ongoing support to the Canadian National Collection, and by grants from Genome Canada and Ontario Genomics to PDNH in support of the Centre for Biodiversity Genomics at the University of Guelph, and to the Natural Sciences and Engineering Research Council of Canada.

References

- Areekul B, Quicke DLJ (2006) Systematics of the parasitic wasp genus *Yelicones* Cameron (Hymenoptera: Braconidae: Rogadinae) and revision of the genus from the New World. *Systematics and Biodiversity* 4(3): 255–376. <https://doi.org/10.1017/S1477200005001866>
- Braet Y (2002) Contribution to the knowledge of Agathidinae (Hymenoptera Braconidae) from French Guiana with description of two new species of *Earinus* Wesmael, 1837. *Belgian Journal of Entomology* 4: 41–51.
- Cauich-Kumul R, Delfin-Gonzalez H, Lopez-Martinez V, Sharkey M (2012) Braconid wasps (Hymenoptera: Braconidae) of Northern Yucatan, Mexico: Subfamilies Agathidinae and Doryctinae (excluding *Heterospilus* Haliday). *Journal of the Kansas Entomological Society* 85(3): 186–205. <https://doi.org/10.2317/JKES120212.1>
- Dasch CE (1974) Neotropical Mesochorinae (Hymenoptera: Ichneumonidae). *Memoirs of the American Entomological Institute* 22: 1–509.
- Hebert PDN, Penton EH, Burns JM, Janzen DH, Hallwachs W (2004) Ten species in one: DNA barcoding reveals cryptic species in the neotropical skipper butterfly *Astraptes fulgerator*. *Proceedings of the National Academy of Sciences of the United States of America* 101(41): 14812–14817. <https://doi.org/10.1073/pnas.0406166101>
- Ivanova NV, Grainger CM (2007) CCDB protocols, COI amplification. [accessed 1 July 2019]
- Ivanova NV, Dewaard JR, Hebert PD (2006) An inexpensive, automation-friendly protocol for recovering high-quality DNA. *Molecular Ecology Resources* 6(4): 998–1002. <https://doi.org/10.1111/j.1471-8286.2006.01428.x>
- Janzen DH, Hallwachs W (2011) Joining inventory by parataxonomists with DNA barcoding of a large complex tropical conserved wildland in northwestern Costa Rica. *PLOS ONE* 6(8): e18123. <https://doi.org/10.1371/journal.pone.0018123>

- Janzen DH, Hallwachs W (2016) DNA barcoding the Lepidoptera inventory of a large complex tropical conserved wildland, Area de Conservación Guanacaste, northwestern Costa Rica. *Genome* 59: 641–660. <https://doi.org/10.1139/gen-2016-0005>
- Janzen DH, Burns JM, Cong Q, Hallwachs W, Dapkey T, Manjunath R, Hajibabaei, Hebert PDN, Grishin NV (2017) Nuclear genomes distinguish cryptic species suggested by their DNA barcodes and ecology. *Proceedings of the National Academy of Sciences* 114(31): 8313–8318. <https://doi.org/10.1073/pnas.1621504114>
- Kang I, Chapman EG, Janzen DH, Hallwachs W, Dapkey T, Smith MA, Sharkey MJ (2017) Revision of the species of *Lytopylus* from Area de Conservación Guanacaste, northwestern Costa Rica (Hymenoptera, Braconidae, Agathidinae). *ZooKeys* 721: 93–158. <https://doi.org/10.3897/zookeys.721.20287>
- Leathers J, Sharkey MJ (2003) Taxonomy and life history of Costa Rican *Alabagrus* (Hymenoptera: Braconidae), with a key to world species. *Contributions in Science* 497: 1–82. <https://doi.org/10.5962/p.214390>
- Lindsay C, Sharkey MJ (2006) Revision of the genus *Amputoearinus* (Hymenoptera: Braconidae: Agathidinae) with fourteen new species. *Zootaxa* 1329: 1–27. <https://doi.org/10.11646/zootaxa.1329.1.1>
- Papp J (2007) First survey of the *Sacirema* Quicke species (Hymenoptera: Braconidae: Braconinae). *International Journal of Invertebrate Taxonomy* 18: 507–515.
- Ratnasingham S, Hebert PDN (2013) A DNA-Based Registry for All Animal Species: The Barcode Index Number (BIN) System. *PLoS ONE* 8(8): e66213. <https://doi.org/10.1371/journal.pone.0066213>
- Rodríguez-Berrío A, Bordera S, Sääksjärvi IE (2009) Checklist of Peruvian Ichneumonidae (Insecta, Hymenoptera). *Zootaxa* 2303: 1–44. <https://doi.org/10.11646/zootaxa.2303.1.1>
- Sharkey MJ (1988) A taxonomic revision of *Alabagrus* (Hymenoptera, Braconidae). *Bulletin of the British Museum of Natural History (Ent)* 57(2): 311–437.
- Sharkey MJ (1997) Subfamily key of Braconidae. Agathidinae. In: Wharton RA, Marsh PM, Sharkey MJ (Eds) *Manual of the New World genera of the family Braconidae* (Hymenoptera). International Society of Hymenopterists. Special Publication No. 1. 439, 141–148.
- Sharkey MJ, Chapman EG, Iza de Campos GY (2016) Revision of *Aerophilus* Szépligeti (Hymenoptera, Braconidae, Agathidinae) from eastern North America, with a key to the Nearctic species. *Contributions in Science* 524: 51–110. http://sharkeylab.org/sharkeylab/docs/posts/web/Sharkey_et_al_2016_Aerophilus.pdf
- Sharkey M, Brown B, Baker A, Mutanen M (2021b) A response to Zamani et al. (2020): The omission of critical data in the pursuit of “revolutionary” methods to accelerate the description of species. *ZooKeys* 1033: 191–201. <https://doi.org/10.3897/zookeys.1033.66186>
- Sharkey MJ, Clutts S, Tucker EM, Janzen D, Hallwachs W, Dapkey T, Smith MA (2011) *Lytopylus* Förster (Hymenoptera: Braconidae: Agathidinae) species from Costa Rica, with an emphasis on specimens reared from caterpillars in Area de Conservación Guanacaste. *ZooKeys* 130: 379–419. <https://doi.org/10.3897/zookeys.130.1569>
- Sharkey MJ, Meierotto S, Chapman EG, Janzen DJ, Hallwachs W, Dapkey T, Solis MA (2018) *Alabagrus* Enderlein (Hymenoptera, Braconidae, Agathidinae) species of Costa Rica, with

- an emphasis on specimens reared from caterpillars in Area de Conservación Guanacaste. *Contributions in Science* 526: 31–180. <https://doi.org/10.5962/p.320146>
- Sharkey MJ, Janzen DH, Hallwachs W, Chapman EG, Smith MA, Dapkey T, Brown A, Ratnasingham S, Naik S, Manjunath R, Perez K, Milton M, Hebert P, Shaw SR, Kittel RN, Solis MA, Metz MA, Goldstein PZ, Brown JW, Quicke DLJ, van Achterberg C, Brown BV, Burns JM (2021a) Minimalist revision and description of 403 new species in 11 subfamilies of Costa Rican braconid parasitoid wasps, including host records for 219 species. *ZooKeys* 1013: 1–665. <https://doi.org/10.3897/zookeys.1013.55600.figure403>
- van Achterberg C (1979) A revision of the subfamily Zelinae auct. (Hymenoptera, Braconidae). *Tijdschrift voor Entomologie* 122: 241–479.
- Wharton RA (1980) Review of the Nearctic Alysiini (Hymenoptera, Braconidae) with discussion of generic relationships within the tribe. *University of California publications in entomology* 88:1–112.
- Wharton RA (1997) Alysiinae. In: Wharton RA, Marsh PM, Sharkey MJ (Eds) *Manual of the New World genera of the family Braconidae (Hymenoptera)*. International Society of Hymenopterists. Special Publication No. 1: 85–118.
- Yamada MV, Shimbori EM, Penteadodias AM, Scatolini D (2006) Perfil da fauna de Agathidinae (Ichneumonoidea: Braconidae) da Estação Ecológica de Jataí (Luiz Antônio, SP, Brasil), com especial interesse nas espécies de *Alabagrus* Enderlein. In: Moschini LE, Pires JSR, Santos JE (Eds) *Estudos Integrados em Ecossistemas 3: Estação Ecológica de Jataí*. São Carlos, EdUFSCar, 197–207. ISBN: 85-7600-082-2
- Zamani A, Vahtera V, Sääksjärvi IE, Scherz MD (2020) The omission of critical data in the pursuit of “revolutionary” methods to accelerate the description of species. *Systematic Entomology* 46: 1–4. <https://doi.org/10.1111/syen.12444>

A review of the genus *Hesperosoma* Scheerpeltz (Coleoptera, Staphylinidae, Staphylininae) of China

Yu-Jie Cai¹, Liang Tang¹, Harald Schillhammer²

1 College of Science, Shanghai Normal University, 100 Guilin Road, 1st Educational Building 323 Room, Shanghai, 200234, China **2** Naturhistorisches Museum Wien, Burgring 7, A – 1010 Wien, Austria

Corresponding author: Liang Tang (staphylinidae@shnu.edu.cn)

Academic editor: Volker Assing | Received 27 September 2021 | Accepted 8 November 2021 | Published 7 December 2021

<http://zoobank.org/72BC3720-940B-448A-9522-5CF226FDB5C6>

Citation: Cai Y-J, Tang L, Schillhammer H (2021) A review of the genus *Hesperosoma* Scheerpeltz (Coleoptera, Staphylinidae, Staphylininae) of China. ZooKeys 1075: 137–174. <https://doi.org/10.3897/zookeys.1075.75799>

Abstract

A review of 16 species of *Hesperosoma* Scheerpeltz from China is presented. Five new species are described: *H.* (s.str.) *chenchangchini* **sp. nov.** from Yunnan, *H.* (s.str.) *languidum* **sp. nov.** from Yunnan, *H.* (s.str.) *motuoense* **sp. nov.** from Xizang, *H.* (*Paramichrotus*) *parvioculatum* **sp. nov.** from Hubei, Hunan and *H.* (s.str.) *xizangense* **sp. nov.** from Xizang. Two species are new to China: *H.* (*Paramichrotus*) *brunkei* Schillhammer, 2015 from Yunnan and *H.* (s.str.) *kleebergi* Schillhammer, 2009 from Xizang. Females of *H.* (*Paramichrotus*) *alexpuchneri* Schillhammer, 2009, *H.* (*Paramichrotus*) *guizhouense* Schillhammer, 2018 and *H.* (s.str.) *flavoterminalis* Schillhammer, 2004 are described for the first time. Habitus and diagnostic characters of all species are photographed and a key to Chinese species of *Hesperosoma* is provided.

Keywords

Identification key, new records, new species

Introduction

Hesperosoma Scheerpeltz, 1965 is an Asian genus with 29 known species (Schillhammer 2004, 2009, 2015, 2018) in the subtribe Anisolinina Hayashi, 1993 of the tribe Staphylinini. The species of this genus may be easily distinguished from members of related genera (*Philomyceta*, *Hesperoschema*) by segment 2 of maxillary palpi less dis-

tinctly or hardly dilated, abdominal tergites III–V with medio-basal depression laterally bordered by more or less distinct oblique ridges (abdominal tergites III–VI with medio-basal depression laterally bordered by more or less distinct oblique ridges in *Philomyceta* and segment 2 of maxillary palpi comparatively slender in *Hesperoschema*) (Schillhammer 2004). The genus is currently subdivided into two subgenera, *Hesperosoma* Scheerpeltz, 1965 and *Paramichrotus* Naomi, 1982. The major differences separating the two subgenera are in the shape of aedeagus and the body colouration: with aedeagus symmetrical and fore body always with a certain amount of reddish colour on the elytra or pronotum in *Paramichrotus*, while the aedeagus is asymmetrical and fore-body with metallic tint throughout in *Hesperosoma* (Schillhammer 2015).

Up to now, nine species of the genus have been recorded from China. In this paper, five new species are described and two species are new country records for China. Thus, the total number of *Hesperosoma* in China is increased to 16. The members of the subgenus *Hesperosoma* are distributed in mountainous areas of southwest China, while the members of the subgenus *Paramichrotus* are widely distributed in southern China. (Fig. 1).

The species of the genus *Hesperosoma* can be usually found in undisturbed forests. Microhabitats include leaf litter, decaying logs and ground-based debris in woodlands with mixed shrub and grassland (Schillhammer, 2004, 2009, 2015, 2018; Hu et al. 2020). Based on our collecting experiences, the species of the subgenus *Paramichrotus* prefer rotten material, especially rotten bamboos, where they hunt for maggots (Figs 6, 7). Therefore, an efficient way to collect them is to set rotten bamboo traps (Fig. 2). Species of the *Paramichrotus* sometimes may also be found sucking sap around tree wounds (Fig. 8). A similar behaviour was previously described by Hu et al. (2020) on rotting stems of *Alocasia odora* (G. Lodd.) Spach. Species of the subgenus *Hesperosoma* prefer decaying trees with fungi (Figs 3, 4). Members of both subgenera hide from light inside log or fungi crevices in daylight and they are usually spotted by searching logs in dense forests or at night (Fig. 5).

Materials and methods

The specimens, examined in this paper, were collected by searching logs, sifting rotten bamboo or leaf litter and were euthanised with ethyl acetate. For examination of the genitalia, the last three abdominal segments were detached from the body after softening in hot water. The aedeagus or tergite X, together with other dissected pieces, was mounted in Euparal (Chroma Gesellschaft Schmidt, Koengen, Germany) on plastic slides. Photos of sexual characters were taken with a Canon G9 camera attached to an Olympus SZX 16 stereoscope; habitus photos were taken with a Canon macro photo lens MP-E 65 mm attached to a Canon EOS7D camera and stacked with Zerene Stacker.

The specimens treated in this study are deposited in the Department of Biology, Shanghai Normal University, P. R. China (**SHNU**) and Naturhistorisches Museum Wien, Austria (**NMW**).

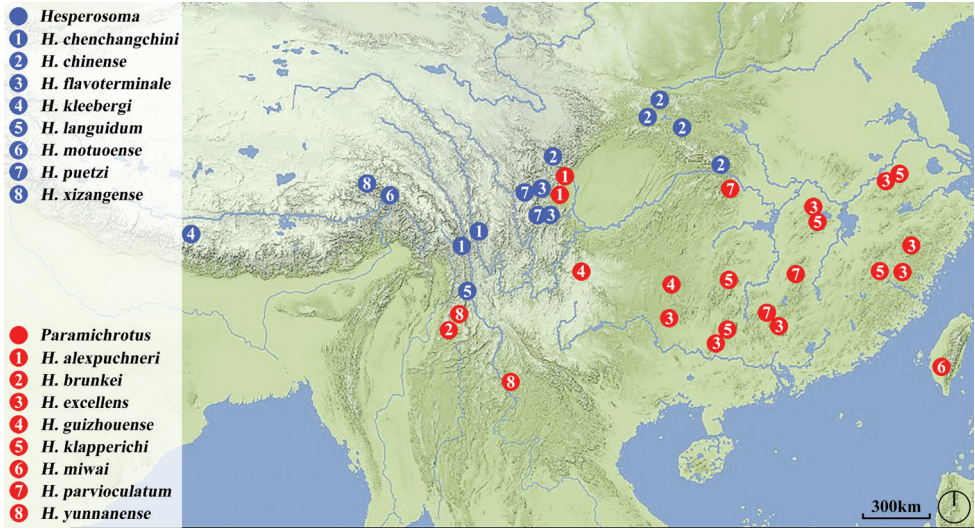


Figure 1. Distribution map of *Hesperosoma* species of China.

Body measurements are abbreviated as follows:

- BL** body length, measured from the anterior margin of the clypeus to the posterior margin of abdominal tergite X;
- EL** length of elytra, measured from humeral angle;
- EW** width of elytra at the widest point;
- EYL** length of eye;
- FL** fore-body length, measured from the anterior margin of the clypeus to the apex of the elytra (apicolateral angle);
- HL** length of head along the mid-line;
- HW** width of head including eyes;
- PL** length of pronotum along the mid-line;
- PW** width of pronotum at the widest point;
- TL** length of tempora.

List of Chinese species

Subgenus *Hesperosoma*

- Hesperosoma chenchangchini* sp. nov.
Hesperosoma chinense Hayashi, 2002
Hesperosoma flavoterminalis Schillhammer, 2004
Hesperosoma kleebergi Schillhammer, 2009
Hesperosoma languidum sp. nov.
Hesperosoma motuoense sp. nov.
Hesperosoma puetzi Schillhammer, 2004
Hesperosoma xizangense sp. nov.



Figures 2–8. **2** rotten bamboo trap (Photo by Mr. Yu-Jie Cai from Guizhou, Leishan County, Xiannütang at 1 May 2021) **3** habitat of *H. flavoterminalis* (Photo by Mr. Qin-Hao Zhao from Sichuan, Dujiangyan City, Mt Qingchengshan at 1 Aug. 2021) **4** living *H. flavoterminalis* on decaying tree (Photo by Mr. Qin-Hao Zhao from Sichuan, Dujiangyan City, Mt Qingchengshan at 1 Aug 2021) **5** living *H. languidum* sp. nov. running on decaying tree with fungi during the night (Photo by Mr. Liang Tang from Yunnan, Lushui County, Yaojiapin at 21 Jun 2010) **6** living *H. excellens* on rotten bamboo (Photo by Mr. Liang Tang from Anhui, Tangkou Town, Jiulongpu at 1 Jul 2020) **7** living *H. guizhouense* hunting for maggots in rotten bamboo (Photo by Mr. Yu-Jie Cai from Guizhou, Leishan County, Xiannütang at 2 May 2021) **8** living *H. klapperichi* sucking tree sap (Photo by Mr. Zhong Peng from Guangxi, Jinxiu County, ‘16 km’ at 13 Jul 2014).

Subgenus *Paramichrotus*

- Hesperosoma alexpuchneri* Schillhammer, 2009
Hesperosoma brunkei Schillhammer, 2015
Hesperosoma excellens (Bernhauer, 1939)
Hesperosoma guizhouense Schillhammer, 2018
Hesperosoma klapperichi Schillhammer, 2004
Hesperosoma miwai (Bernhauer, 1943)
Hesperosoma parvioculatum sp. nov.
Hesperosoma yunnanense Schillhammer, 2009

Key to species of *Hesperosoma* from China

- 1 Elytra entirely dark, always with distinct metallic blue or greenish-blue lustre; aedeagus at least weakly asymmetrical (subgenus *Hesperosoma*) **2**
 – Elytra not metallic, with at least some reddish colouration, usually extensive, rarely reduced to shoulders; aedeagus symmetrical (subgenus *Paramichrotus*) **9**
 2 Fore-body very shiny; punctation less dense, most punctures simple, widely separated..... ***H. motuoense* sp. nov. China (Xizang)**
 – Fore-body rather opaque due to very dense punctation; punctures subumbilicate, almost contiguous..... **3**
 3 First three or four visible abdominal segments reddish **4**
 – First five visible abdominal segments black **5**
 4 Four apical segments of antennae creamy white; abdominal segment VIII entirely reddish-yellow ***H. chenchangchini* sp. nov. China (Yunnan)**
 – Five apical segments of antennae creamy white; abdominal segment VIII blackish-brown with base of the tergite widely yellowish.....
 ***H. chinense* China (Shaanxi, Hubei, Sichuan)**
 5 Five apical segments of antennae creamy white **6**
 – Four apical segments of antennae creamy white **7**
 6 Pronotum deep metallic blue, relatively weak build; pubescence of first three visible tergites entirely golden ***H. flavoterniale* China (Sichuan)**
 – Pronotum brighter metallic blue, more robust build; pubescence of first three visible tergites entirely black..... ***H. kleebergi* Nepal, China (Xizang)**
 7 Head 1.29 times as wide as long; frons with anterior margin emarginate (Fig. 9); mandibles relatively darker ***H. xizangense* sp. nov. China (Xizang)**
 – Head 1.14–1.22 times as wide as long; frons with anterior margin nearly straight (Fig. 8); mandibles relatively lighter **8**
 8 TL/EYL: 1.78; head, pronotum and elytra with dense and faint punctation (Fig. 10); first three visible abdominal tergites with shallower punctures in basal half..... ***H. languidum* sp. nov. China (Yunnan)**
 – TL/EYL: 1.47–1.48; head, pronotum and elytra with dense and coarse punctation (Fig. 8); first three visible abdominal tergites with pit-like punctures in basal half..... ***H. puetzi* China (Sichuan)**

- 9 Pronotum black, procoxae partly and lateral parts of mesoventrite dark brown to black..... **10**
- Pronotum entirely rufous, rarely with darker markings, procoxae and mesoventrite reddish **15**
- 10 Elytra with black marking occupying more than posterior half of each elytron, with elevated, reddish sutural stripe connects with black marking for at least half of its length..... **11**
- Elytra with black marking occupying at most posterior half of each elytron, usually less, marking not reaching elevated reddish sutural stripe or only narrowly, at the postero-sutural angle..... **12**
- 11 TL/EYL: 1.18–1.29; head 1.26–1.40 times as wide as long
..... ***H. yunnanense* China (Yunnan)**
- TL/EYL: 1.35–1.39; head 1.63 times as wide as long
..... ***H. parvioculatum* sp. nov. China (Hubei, Hunan)**
- 12 All tibiae predominantly black..... ***H. miwai* China (Taiwan)**
- Tibiae predominantly reddish or bicoloured **13**
- 13 Paramere with acutely pointed apex ***H. alexpuchneri* China (Sichuan)**
- Paramere bilobed **14**
- 14 Paramere (Fig. 75) with relatively deeper medio-apical emargination
..... ***H. guizhouense* China (Guizhou)**
- Paramere (Fig. 81) with relatively shallower medio-apical emargination.....
..... ***H. klapperichi* China (Anhui, Fujian, Guangxi, Hubei, Hunan)**
- 15 Basal antennomeres 3–4 bright reddish; maxillary palpi entirely reddish
... ***H. excellens* China (Anhui, Fujian, Guangdong, Guangxi, Hubei, Hunan, Zhejiang)**
- Basal antennomeres 3–4 at least partly blackish; segments 2 and 3 of maxillary palpi reddish-brown ***H. brunkei* Laos, Myanmar, China (Yunnan)**

Taxonomy

Subgenus *Hesperosoma*

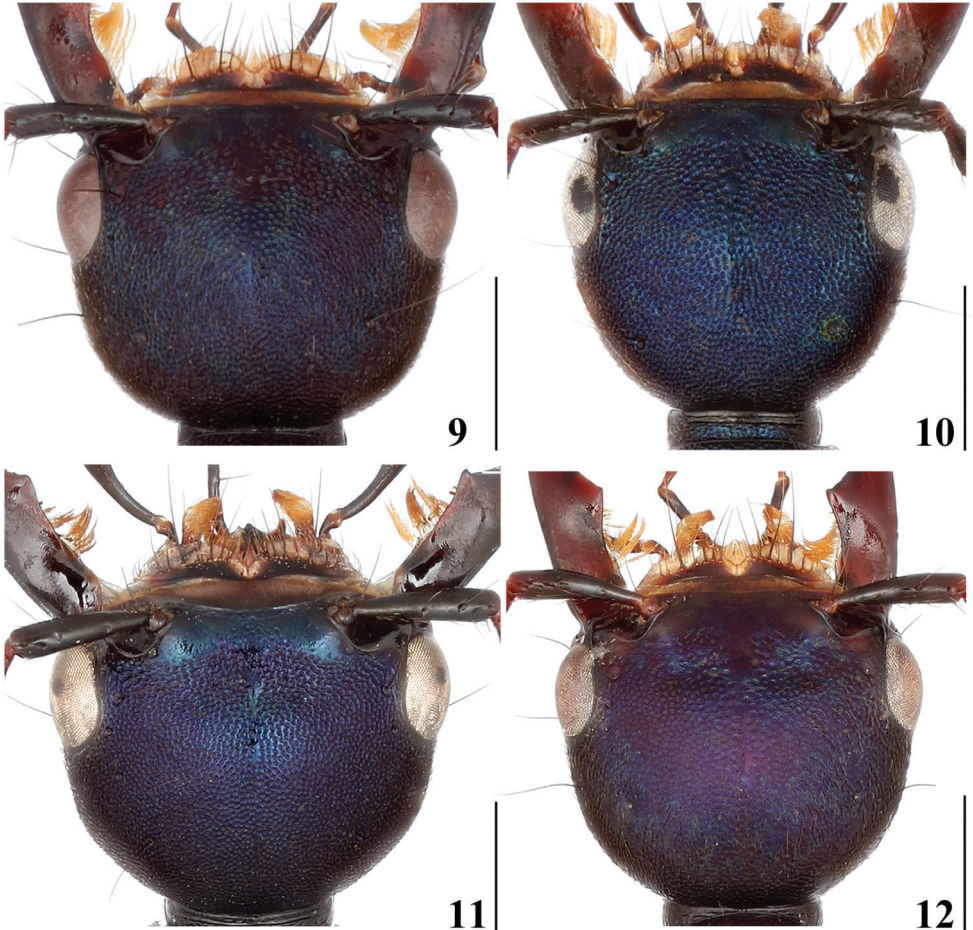
Hesperosoma (s.str.) *chenchangchini* sp. nov.

<http://zoobank.org/D92FFB10-ADD6-4FC8-A13A-3F283D80125E>

Figures 9, 13–18

Material examined. Holotype. CHINA – Yunnan Prov. • ♂; glued on a card with labels as follows: “China: Yunnan Deqin County, Nagu Vill; alt. 2250 m; 11 Jul 2010; Wen-Xuan Bi leg.” “Holotype / *Hesperosoma* (s.str.) *chenchangchini* / Cai, Tang & Schillhammer” [red handwritten label]; SHNU. **Paratypes.** CHINA – Yunnan Prov. • 2♂♂, 1♀; Gongshan County, Heiwadi; alt. 2000 m; 07 Jul 2009; Jian-Qing Zhu leg.; SHNU.

Description. Measurements of male: BL: 12.17–13.87 mm, FL: 6.95–7.63 mm. HL: 1.89–2.07 mm, HW: 2.41–2.79 mm, EYL: 0.65–0.77 mm, TL: 0.96–1.12 mm,



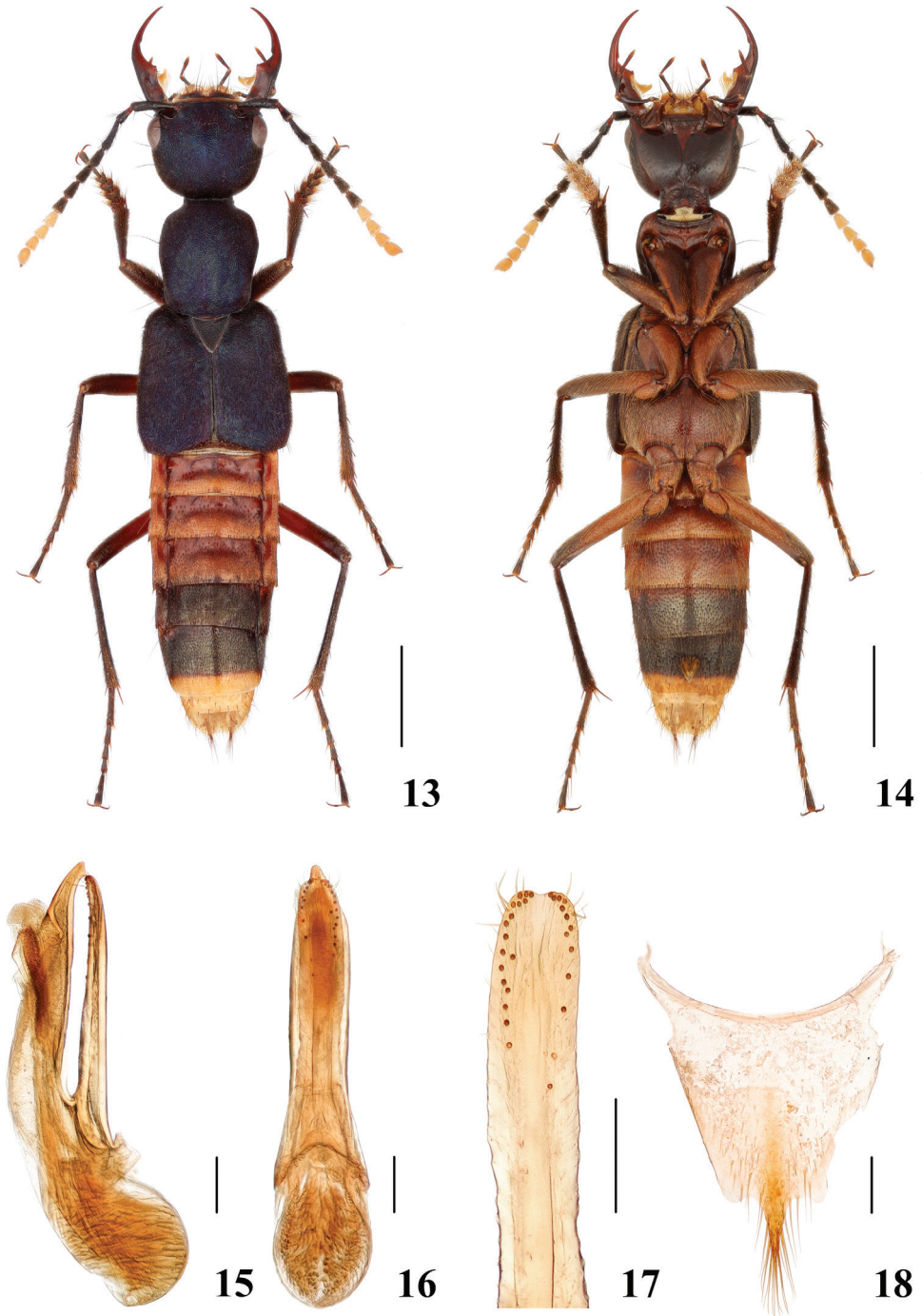
Figures 9–12. Head of species of subgenus *Hesperosoma* **9** *H. chenchangchini* sp. nov. **10** *H. puetzi* **11** *H. xizangense* sp. nov. **12** *H. languidum* sp. nov. Scale bars: 1 mm.

PL: 2.30–2.68 mm, PW: 2.00–2.23 mm, EL: 3.13–3.44 mm, EW: 3.06–3.51 mm. HW/HL: 1.24–1.35, TL/EYL: 1.41–1.48, PL/PW: 1.14–1.20, EL/EW: 0.98–1.02.

Measurements of female: BL: 12.73 mm, FL: 7.06 mm. HL: 1.89 mm, HW: 2.34 mm, EYL: 0.68 mm, TL: 0.90 mm, PL: 2.38 mm, PW: 2.07 mm, EL: 3.17 mm, EW: 3.28 mm. HW/HL: 1.24, TL/EYL: 1.32, PL/PW: 1.15, EL/EW: 0.97.

Head, pronotum and elytra metallic dark blue to violaceous blue; abdomen with segments III–V reddish, VI black with anterior margin narrowly reddish, VII black with posterior margin broadly reddish-yellow, segments VIII and X entirely reddish-yellow, segment IX reddish; antennae black, base and apex of segment 1 and 2 reddish, segments 8–11 creamy white; mandibles dark brown, medial margin and distal portion of mandible dark reddish-brown; maxillary and labial palpi deep black, last segments sometimes slightly paler brownish.

Head (Fig. 9) 1.24–1.35 times as wide as long, rounded trapezoid, tempora narrowed towards neck in regular arc, eyes moderately protruding; surface with dense and



Figures 13–18. *Hesperosoma chenchangchini* sp. nov. 13–14 habitus 15–17 aedeagus, lateral (15) and ventral (16) views, paramere (17) 18 female abdominal tergite X. Scale bars: 2 mm (13–14), 0.2 mm (15–18).

coarse punctation, mostly contiguous; frons impunctate; with short, weakly delimited impunctate mid-line, extending from frons to about half of mid-length; antennae with segments 4–8 markedly oblong, segments 9 and 10 about as long as wide.

Pronotum 1.14–1.20 times as long as wide, widest at level of large lateral seta, narrowed towards base in wide, but shallow concave arc; surface as densely and coarsely punctate as on head, with indistinct, short impunctate mid-line in posterior half; scutellum with dense and pit-like punctation, interstices forming small transverse rugae.

Elytra 0.97–1.02 times as long as wide, exceedingly densely, coarsely punctate, punctures almost contiguous.

Abdominal tergites III–V with basal transverse depression, punctation of abdominal tergites IV–V moderate and sparse at base, abdominal tergite III impunctate at base; posterior halves of abdominal tergites III–V and entire surface of remaining tergites with very fine and dense punctation.

Male. Protarsomeres 1–4 moderately dilated, heart-shaped; sternite VII with patch of yellow setae on median portion and posterior margin broadly emarginate at middle; sternite VIII with posterior margin broadly emarginate at middle; aedeagus (Figs 15–17) with median lobe and paramere slightly asymmetrical, paramere (Fig. 17) shorter than median lobe and slightly bent to left side in ventral view.

Female. Tergite X (Fig. 18) slightly asymmetrical with posterior margin projecting at middle.

Etymology. This species is named in honour of Mr. Chang-Chin Chen who donates lots of staphylinid specimens to the SHNU, including the holotype of the new species.

Distribution. China (Yunnan).

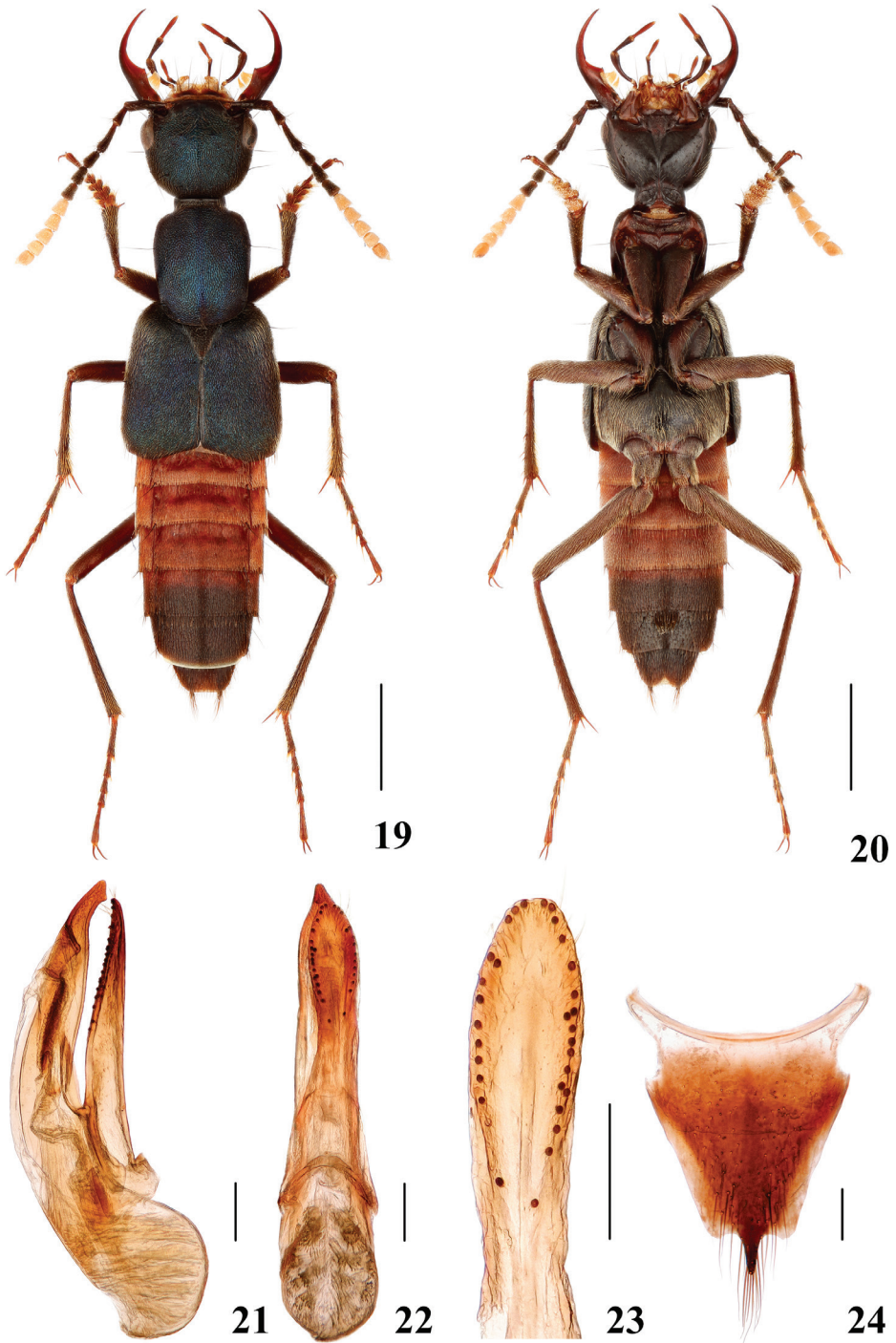
Diagnosis. Amongst the species of the nominal subgenus with reddish abdomen, *H. malaisei* from Myanmar, *H. chinense* (Shaanxi, Hubei, Sichuan) and *H. rufomarginatum* from Vietnam, the new species may be easily recognised by four outer segments of antennae creamy white (five outer segments of antennae creamy white in *H. chinense* and *H. malaisei*), entirely metallic dark blue to violaceous blue elytra (reddish suture and shoulders of elytra in *H. rufomarginatum*).

Hesperosoma (s.str.) *chinense* Hayashi, 2002

Figures 19–24

Hesperosoma chinense Hayashi 2002: 175; Schillhammer 2004: 256; Schillhammer 2009: 84

Material examined. CHINA – Shaanxi Prov. • 1♂; Zhouzhi County, Houzhenzi, Qinling, Qinlingliangxia; 33°48'96"N, 107°44'48"E; alt. 2018 m; 7 May 2008; Hao Huang & Wang Xu leg.; SHNU • 1♂; Zhouzhi County, Houzhenzi, Qinling, Qinlingliangxia; 33°48'97"N, 107°44'48"E; alt. 1820 m; 18 May 2008; Hao Huang & Wang Xu leg.; SHNU • 1♂, 1♀; Zhouzhi County, Houzhenzi, Qinling, West Sangongli Gou; 33°50'613"N, 107°48'524"E; alt. 1336 m; 17–19 May 2008; Hao



Figures 19–24. *Hesperosoma chinense* 19–20 habitus 21–23 aedeagus, lateral (21) and ventral (22) views, paramere (23) 24 female abdominal tergite X. Scale bars: 2 mm (19–20), 0.2 mm (21–24).

Huang & Wang Xu leg.; SHNU • 1♂; Mei County, Taibai-Shan, Kaitianguan; 34°00'69"N, 107°51'41"E; alt. 1850 m; 22–23 May 2008; Hao Huang & Wang Xu leg.; SHNU • 2♂♂, 5♀♀; Ankang City, Ningshan County, Huoditang; 33°44'N, 108°45'E; alt. 1590 m; 19 Jul 2015; Yi-Zhou Liu leg.; SHNU • 1♂; Hanzhong City Mian County; 33°10'24"N, 106°40'13"E; alt. 1800 m; 24 Jun 2020; W-X Bi leg.; SHNU • 9♀♀; Ankang City, Ningshan County, Huodigou; 33°46'N, 108°44'E; alt. 1540 m; 18 Jul 2015; Yi-Zhou Liu leg.; SHNU. – **Sichuan Prov.** • 1♂; Aba Pre, Li County; alt. 1800–2300 m; 29 Jun 2015; Hao Huang leg.; SHNU.

Measurements. Male: BL: 10.45–14.56 mm, FL: 6.06–8.11 mm. HL: 1.72–2.11 mm, HW: 2.00–2.66 mm, EYL: 0.61–0.71 mm, TL: 0.83–1.11 mm, PL: 2.11–2.63 mm, PW: 1.77–2.22 mm, EL: 2.72–3.43 mm, EW: 2.78–3.33 mm. HW/HL: 1.16–1.26, TL/EYL: 1.36–1.68, PL/PW: 1.16–1.23, EL/EW: 0.98–1.03.

Female: BL: 13.06–16.79 mm, FL: 6.95–8.22 mm. HL: 1.94–2.24 mm, HW: 2.27–2.55 mm, EYL: 0.61–0.72 mm, TL: 0.94–1.11 mm, PL: 2.39–2.72 mm, PW: 2.00–2.33 mm, EL: 3.11–3.61 mm, EW: 3.11–3.78 mm. HW/HL: 1.14–1.21, TL/EYL: 1.42–1.64, PL/PW: 1.14–1.20, EL/EW: 0.96–1.03.

Distribution. China (Hubei, Shaanxi and Sichuan).

Diagnosis. Amongst the species of the subgenus with reddish abdomen, *H. chinense* may be readily recognised from *H. chenchangchini* sp. nov. and *H. rufomarginatum* by five outer segments of antennae creamy white (four outer segments of antennae creamy white in *H. chenchangchini* sp. nov. and *H. rufomarginatum*); abdomen reddish in basal four visible segments, segment VIII blackish-brown with base of the tergite broadly yellowish, segment IX blackish-brown (abdomen reddish in basal three visible segments, segments VIII and IX pale yellow in *H. malaisei*).

Hesperosoma (s.str.) *flavoterninale* Schillhammer, 2004

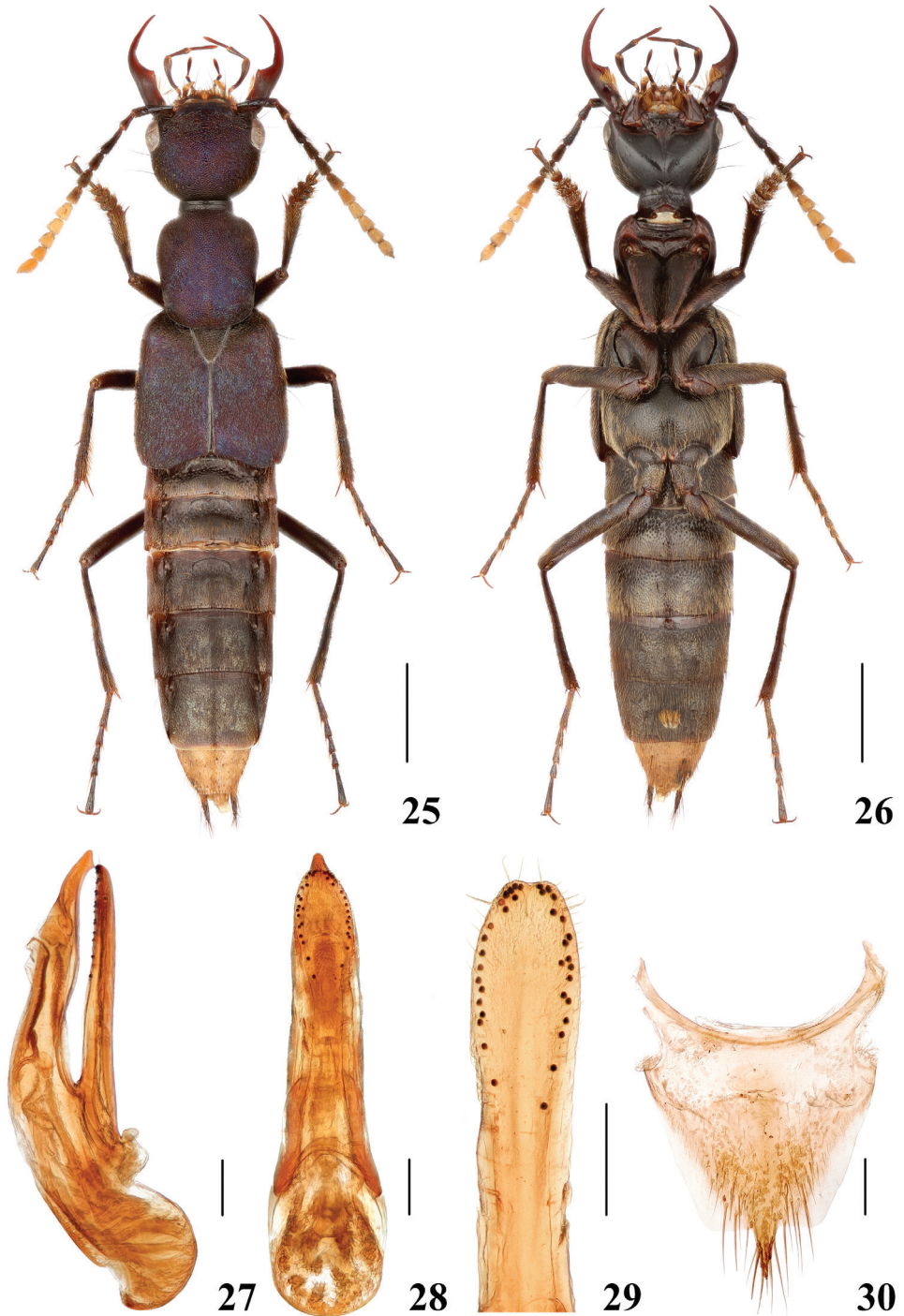
Figures 25–30

Hesperosoma flavoterninale Schillhammer 2004: 257; Schillhammer 2009: 85

Material examined. CHINA – **Sichuan Prov.** • 1♂; Shimian County, Liziping, Zima Village; 28°59'N, 102°16'E; alt. 1800 m; 16 Aug 2012; Peng, Dai & Yin leg.; SHNU • 1♂; Hailuogou, Qingshibangou; alt. 2200 m; 20 Jul 2011; Hao Huang leg.; SHNU • 1♂, 5♀♀; Baoxing County, Fengtongzhai nat. cons., Dashuigou station; 30.57247N, 102.88260E; alt. 1569 m; 29 Jun 2013; Li leg.; by pitfall trap, broadleaf forest; SHNU.

Measurements. Male: BL: 12.62–14.13 mm, FL: 6.85–7.65 mm. HL: 1.89–2.13 mm, HW: 2.32–2.66 mm, EYL: 0.68–0.74 mm, TL: 0.94–1.08 mm, PL: 2.29–2.54 mm, PW: 1.92–2.23 mm, EL: 3.03–3.40 mm, EW: 3.03–3.49 mm. HW/HL: 1.23–1.26, TL/EYL: 1.41–1.46, PL/PW: 1.14–1.23, EL/EW: 0.97–1.04.

Female: BL: 13.33–15.82 mm, FL: 7.29–7.84 mm. HL: 1.98–2.17 mm, HW: 2.35–2.54 mm, EYL: 0.71–0.77 mm, TL: 0.96–1.05 mm, PL: 2.48–2.66 mm, PW:



Figures 25–30. *Hesperosoma flavoterminalis* 25–26 habitus 27–29 aedeagus, lateral (27) and ventral (28) views, paramere (29) 30 female abdominal tergite X. Scale bars: 2 mm (25–26), 0.2 mm (27–30).

2.10–2.23 mm, EL: 3.32–3.51 mm, EW: 3.40–3.62 mm. HW/HL: 1.16–1.19, TL/EYL: 1.25–1.44, PL/PW: 1.14–1.21, EL/EW: 0.97–0.98.

Female characters. Tergite X (Fig. 30) with posterior margin projecting at middle.

Distribution. China (Sichuan).

Diagnosis. Externally, the species is very similar to *H. kleebergi*, but differs mainly in relatively weak build, dark metallic colour, larger eyes, narrow reddish-yellow apical margin of abdominal segment VII and entirely golden pubescence of first three visible tergites (pubescence of first three visible tergites entirely black in *H. kleebergi*).

***Hesperosoma* (s.str.) *kleebergi* Schillhammer, 2009**

Figures 31–35

Hesperosoma kleebergi Schillhammer, 2009: 85

Material examined. CHINA – **Xizang Prov.** • 1♂; Xizang A. R., Nielamu County, Lixin Vill.; alt. 2600 m; 24 Jul 2010; Wen-Xuan Bi leg.; SHNU.

Measurements. Male: BL: 13.19 mm, FL: 7.48 mm. HL: 2.07 mm, HW: 2.60 mm, EYL: 0.71 mm, TL: 1.05 mm, PL: 2.45 mm, PW: 2.15 mm, EL: 3.51 mm, EW: 3.40 mm. HW/HL: 1.26, TL/EYL: 1.48, PL/PW: 1.14, EL/EW: 1.03.

Distribution. China (Xizang) and Nepal. New to China.

Remarks. The collecting locality of the male specimen is about 200 km away from the type locality in Nepal. The specimen fits the original description in all characters. New record for China.

***Hesperosoma* (s.str.) *languidum* sp. nov.**

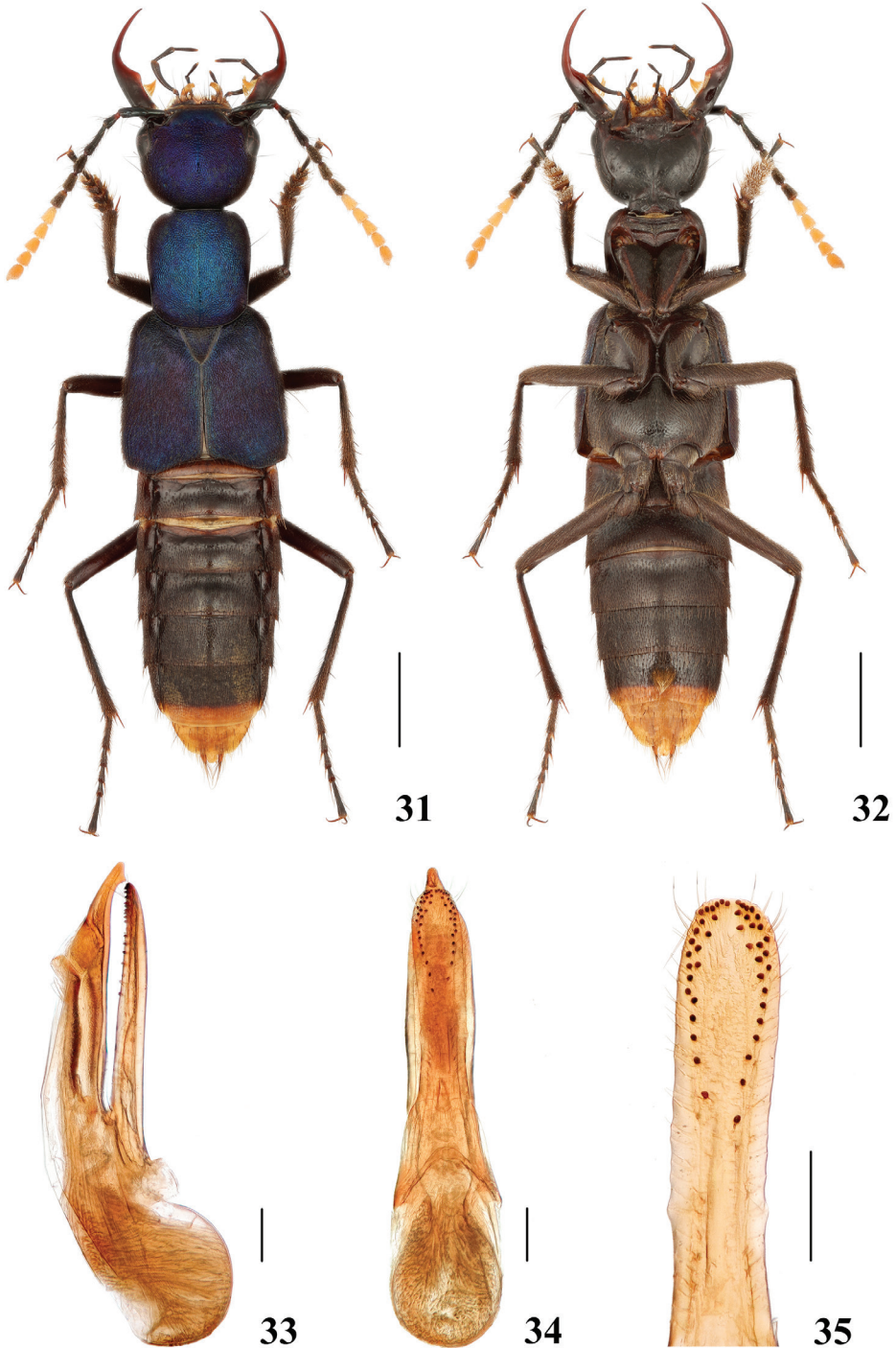
<http://zoobank.org/4E16817A-3DFF-42A4-8519-A49E88436839>

Figures 12, 36–40

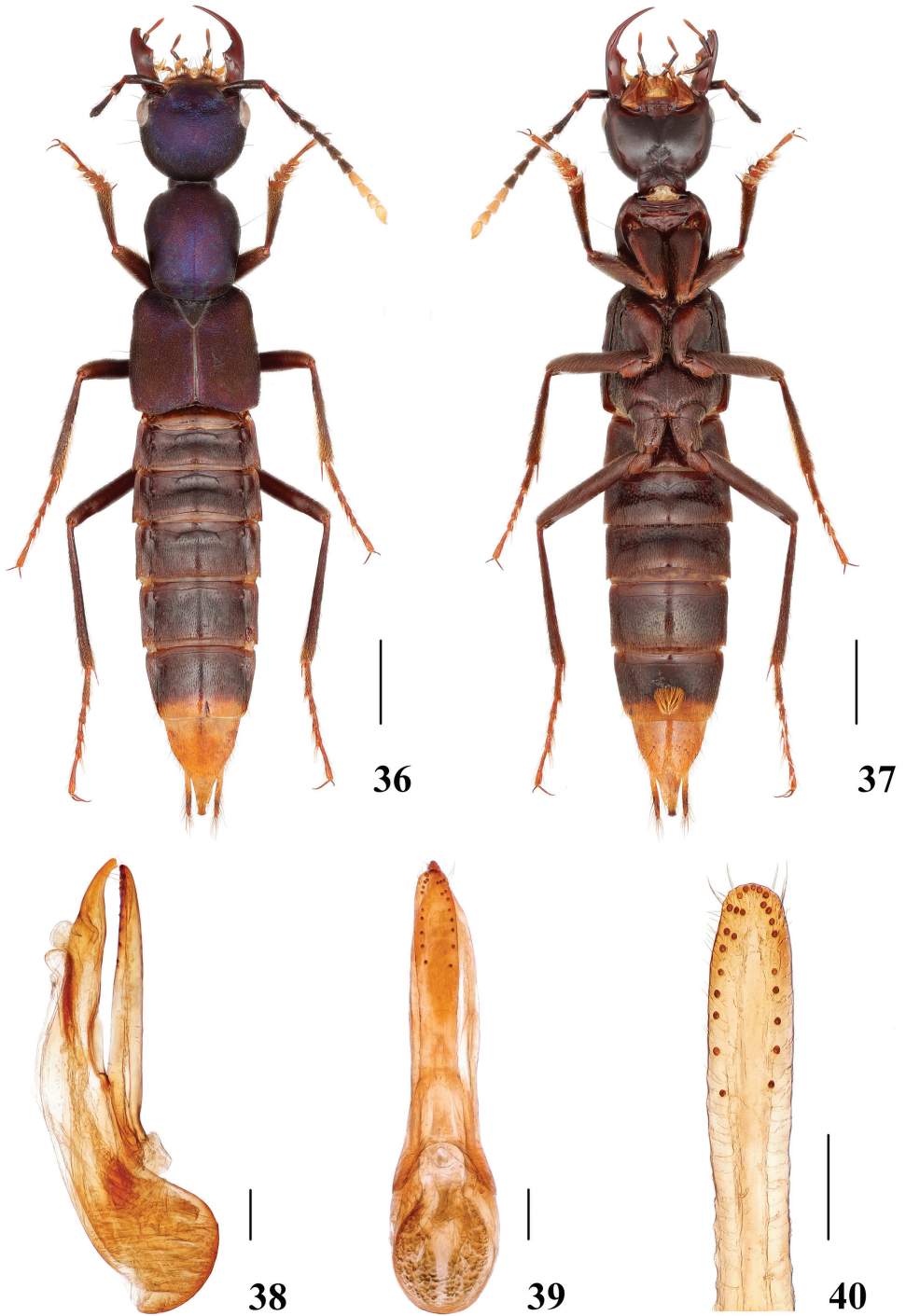
Material examined. Holotype. CHINA – **Yunnan Prov.** • ♂; glued on a card with labels as follows: “China: Yunnan, Lushui County, Yaojiapin; alt. 2540 m; 21 Jun 2010; Liang Tang leg.” “Holotype / *Hesperosoma* (s.str.) *languidum* / Cai, Tang & Schillhammer” [red handwritten label]; SHNU.

Description. Measurements of male: BL: 15.63 mm, FL: 7.48 mm. HL: 2.19 mm, HW: 2.68 mm, EYL: 0.68 mm, TL: 1.21 mm, PL: 2.72 mm, PW: 2.27 mm, EL: 3.06 mm, EW: 3.05 mm. HW/HL: 1.22, TL/EYL: 1.78, PL/PW: 1.20, EL/EW: 1.00.

Head and pronotum metallic violaceous blue to deep blue, elytra dark metallic violaceous blue, usually a bit more opaque than head and pronotum; abdomen with segments III–VI dark red, segment VII dark red with posterior margin broadly reddish-yellow, segments VIII and X entirely reddish-yellow, segment IX reddish-yellow with apical third of latter blackish; antennae black, base and apex of segments 1 and 2 and



Figures 31–35. *Hesperosoma kleebergi* 31–32 habitus 33–35 aedeagus, lateral (33) and ventral (34) views, paramere (35). Scale bars: 2 mm (31–32), 0.2 mm (33–35).



Figures 36–40. *Hesperosoma languidum* sp. nov. 36–37 habitus 38–40 aedeagus, lateral (38) and ventral (39) views, paramere (40). Scale bars: 2 mm (36–37), 0.2 mm (38–40).

base of segment 3 reddish, four outer segments creamy white; mandibles dark reddish-brown; maxillary palpi with segments I–III black, segment IV brown, labial palpi with segments I and II black, segment III brown.

Head (Fig. 12) 1.22 times as wide as long, rounded trapezoid, tempora regularly convex, eyes moderately protruding; surface with dense and shallow punctation, mostly contiguous; frons impunctate; with short, weakly delimited impunctate mid-line, extending from impunctate frons to about half of mid-length; antennae with segments 4–8 markedly oblong, segment 9 slightly oblong.

Pronotum 1.20 times as long as wide, slender, widest at level of large lateral seta, narrowed towards base in wide, but shallow concave arc; surface as densely and shallowly punctate as on head, with indistinct, short impunctate mid-line in posterior third; scutellum with dense and shallow punctation, interstices forming small transverse rugae.

Elytra as long as wide, exceedingly densely, shallowly punctate, punctures almost contiguous.

Abdominal tergites III–V with basal transverse depression, punctation of abdominal tergites III–V feeble at base; posterior halves of abdominal tergites III–V and entire surface of remaining tergites with very fine and dense punctation.

Male. Protarsomeres 1–4 moderately dilated, heart-shaped; sternite VII with patch of long bright yellow setae on median portion; sternite VIII with posterior margin emarginate at middle; aedeagus (Figs 38–40) with median lobe and paramere slightly asymmetrical, paramere (Fig. 40) relatively shorter than median lobe, aedeagus very similar to that of *H. puetzi*, but paramere narrower and apex of the median lobe markedly slender in lateral view.

Female. Unknown.

Etymology. The specific epithet refers to the shallow punctation of the new species

Distribution. China (Yunnan).

Diagnosis. The new species is very similar to *H. puetzi* (Sichuan), but can be easily distinguished from it by smaller eyes with TL/EYL about 1.70 (1.47 in *H. puetzi*); head, pronotum and elytra with dense and shallow punctation (punctation in *H. puetzi* dense and coarse); abdominal tergites III–V without pit-like punctures in basal half. In appearance, it is also similar to *H. flavoterminalis* (Sichuan), *H. tarasovi* from Laos and *H. kleebergi* from China (Xizang) and Nepal, but can be distinguished from *H. flavoterminalis* and *H. kleebergi* by the antennal segments VIII–XI being creamy white (segments VII–XI creamy white in *H. flavoterminalis* and *H. kleebergi*); and from *H. tarasovi* by the narrower head.

***Hesperosoma* (s.str.) *motuoense* sp. nov.**

<http://zoobank.org/43DC52F6-AD98-4328-8E3B-93D67DAC68F1>

Figures 41–46

Material examined. Holotype. CHINA – **Xizang Prov.** • ♂; glued on a card with labels as follows: “China: Xizang A. R., Motuo County, Hanmi; alt. 2100 m; 23 Aug 2011; Wen-Xuan Bi leg.” “Holotype / *Hesperosoma* (s.str.) *motuoense* / Cai, Tang & Schillhammer” [red handwritten label]; SHNU. **Paratypes.** CHINA – **Xizang Prov.** • 3♂♂; Motuo County, 80k; alt. 2100 m; 24 Aug 2011; Wen-Xuan Bi leg.; SHNU, NMW • 2♀♀; same locality,

but 11 Aug 2013, Wen-Xuan Bi leg.; SHNU, NMW • 2♂♂; same locality, but 11 Aug 2013; Wen-Xuan Bi leg.; SHNU • 1♀; same locality, but 22 Jul 2013; Wen-Xuan Bi leg.; SHNU • 1♂; Zhucun-Bangxin; alt. 1850 m; 26 Aug 2013; Wen-Xuan Bi leg.; SHNU.

Measurements. Male: BL: 10.54–14.54 mm, FL: 6.12–7.25 mm. HL: 1.77–2.07 mm, HW: 2.11–2.68 mm, EYL: 0.64–0.75 mm, TL: 0.83–1.05 mm, PL: 2.00–2.45 mm, PW: 1.77–2.19 mm, EL: 2.75–3.21 mm, EW: 2.75–3.28 mm. HW/HL: 1.19–1.34, TL/EYL: 1.25–1.44, PL/PW: 1.11–1.15, EL/EW: 0.94–1.00.

Female: BL: 13.23–15.49 mm, FL: 7.10–7.40 mm. HL: 1.96–2.07 mm, HW: 2.34–2.45 mm, EYL: 0.75–0.79 mm, TL: 0.94–1.02 mm, PL: 2.41–2.45 mm, PW: 2.07–2.15 mm, EL: 3.17–3.40 mm, EW: 3.25–3.40 mm. HW/HL: 1.16–1.20, TL/EYL: 1.25–1.29, PL/PW: 1.14–1.18, EL/EW: 0.96–1.00.

Head and pronotum brilliant metallic green to bluish-green, elytra brighter metallic green, bluish-green at shoulders, along sides and at posterolateral angles; abdomen with segments III–V reddish (in one specimen, abdomen with segments III–V reddish, medio-posterior portion darkened on segments IV and V), segments VI–VII dark brown, but segment VII with apical portion broadly yellow, segments VIII–IX entirely pale yellow; antennae with segments 1–6 black, base of segment 2 reddish, segments 7–11 creamy white; mandibles reddish with narrowly darkened medial and lateral margins; palpi dark reddish-brown with paler reddish tips; legs reddish-brown.

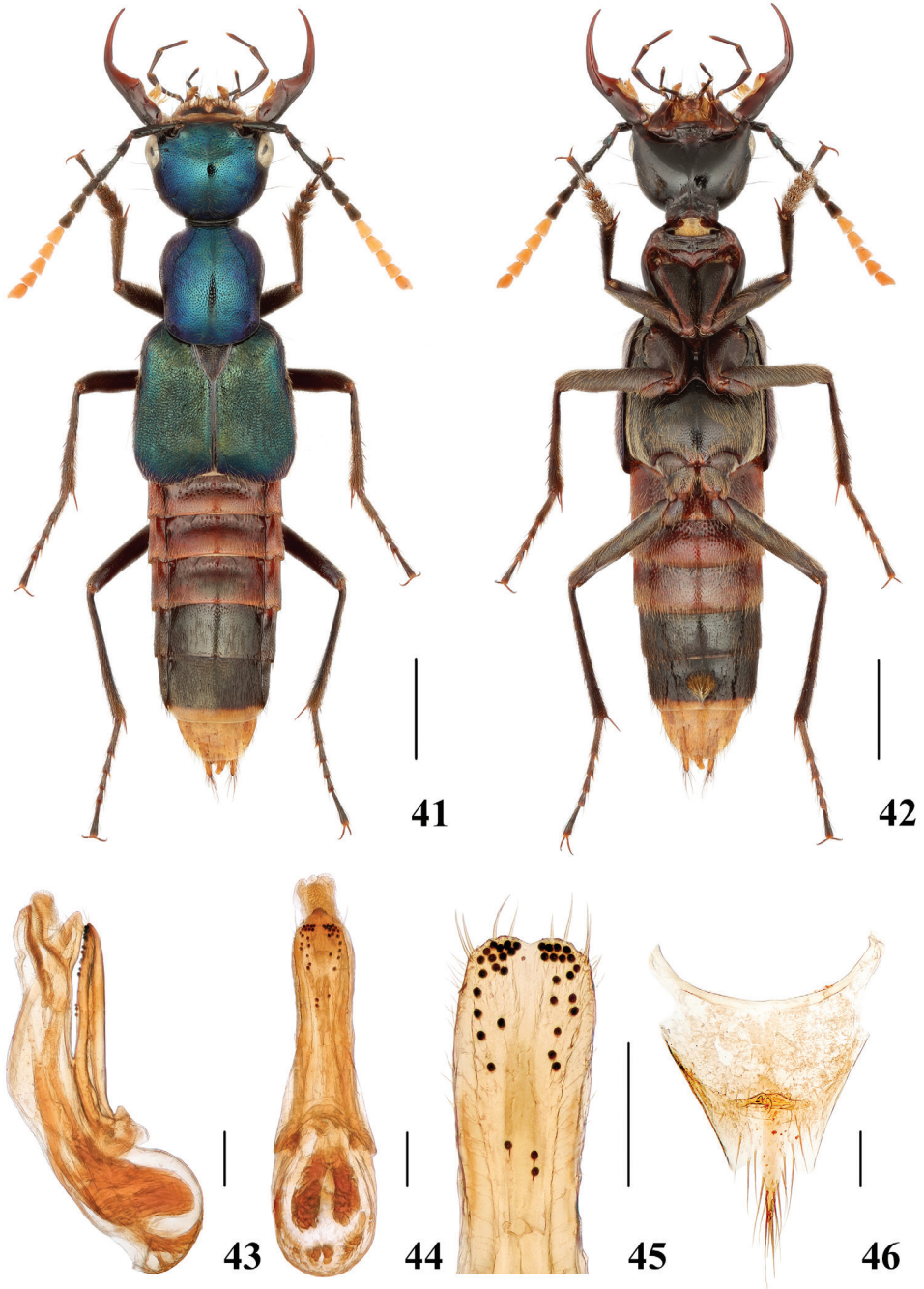
Head 1.16–1.34 times as wide as long, rounded trapezoid, tempora narrowed behind eyes; surface with moderately dense, simple punctation, punctures separated by about 1–2 puncture diameters in transverse direction; narrow anterior portion of frons impunctate; narrow impunctate mid-line extending from frons posteriad to mid-length; pubescence brownish; antennae with segments 4–7 markedly oblong, segments 8 and 9 slightly oblong, segment 10 about as long as wide.

Pronotum 1.11–1.18 times as long as wide, widest at about level of large lateral seta, narrowed towards base in distinct concave arc; punctation of surface similar to that of head, with narrow impunctate mid-line; scutellum densely furnished with pit-like punctures, but punctures, although almost contiguous, well isolated.

Elytra 0.94–1.00 times as long as wide, surface slightly uneven, with distinct depression between shoulders, scutellum and apical margin of elytra, along suture slightly elevated; punctation dense, but punctures not contiguous, separated by less than a puncture diameter in transverse direction; pubescence yellow, long and dense along suture and posterior elytral margin.

Abdominal tergites III–V with basal transverse depression; punctation of abdominal tergites III–V pit-like at base, gradually becoming finer towards apical margin, pit-like punctures occupying more than basal half on tergite III, about basal half on tergite IV and about basal third on tergite V; abdominal tergites VI–VIII with punctures similar in size, interstices smooth.

Male. Protarsomeres 1–4 moderately dilated, heart-shaped; sternite VII with patch of long yellow setae on median portion, posterior margin broadly emarginate at middle; sternite VIII with posterior margin emarginate at middle; aedeagus (Figs 43–45) with median lobe and paramere slightly asymmetrical, paramere (Fig. 45) shorter than median lobe and medio-apically emarginate.



Figures 41–46. *Hesperosoma motuoense* sp. nov. 41–42 habitus 43–45 aedeagus, lateral (43) and ventral (44) views, paramere (45) 46 female abdominal tergite X. Scale bars: 2 mm (41–42), 0.2 mm (43–46).

Female. Tergite X (Fig. 46) slightly asymmetrical with posterior margin projecting at middle.

Etymology. The species is named after the type locality.

Distribution. China (Xizang).

Diagnosis. Externally, the species hardly differs from *H. mishmiense* Schillhammer, 2004 from India, but may be distinguished by the shape of the aedeagus (Figs 43–45): median lobe (lateral view) in *H. motuoense* sp. nov. broader than in *H. mishmiense*, paramere in *H. motuoense* sp. nov. with shallower medio-apical emargination.

***Hesperosoma* (s.str.) *puetzi* Schillhammer, 2004**

Figures 10, 47–52

Hesperosoma puetzi Schillhammer 2004: 256; Schillhammer 2009: 84

Material examined. CHINA – Sichuan Prov. • 1♂; Luding County, Hailuogou, Cao-haizi; alt. 2780 m; 28 Jun 2009; Li-Zhen Li leg.; SHNU • 1♂; Shimian County, Liziping, Yele Dam; 28°55'N, 102°13'E; alt. 2600 m; 15 Jul 2012; Peng, Dai & Yin leg.; SHNU • 1♀; Luding County, Hailuogou, Qingshibangou; alt. 2200 m; 20 Jul 2011; Hao Huang leg.; SHNU.

Measurements. Male: BL: 12.83–13.20 mm, FL: 6.61–6.69 mm. HL: 1.89–1.92 mm, HW: 2.15–2.22 mm, EYL: 0.64–0.65 mm, TL: 0.94–0.96 mm, PL: 2.30–2.32 mm, PW: 1.92 mm, EL: 2.94–3.04 mm, EW: 3.02–3.07 mm. HW/HL: 1.14–1.16, TL/EYL: 1.47–1.48, PL/PW: 1.20–1.21, EL/EW: 0.97–0.99.

Female: BL: 12.30 mm, FL: 7.07 mm. HL: 1.92 mm, HW: 2.29 mm, EYL: 0.74 mm, TL: 0.93 mm, PL: 2.45 mm, PW: 1.98 mm, EL: 3.04 mm, EW: 3.25 mm. HW/HL: 1.19, TL/EYL: 1.26, PL/PW: 1.24, EL/EW: 0.94.

Distribution. China (Sichuan).

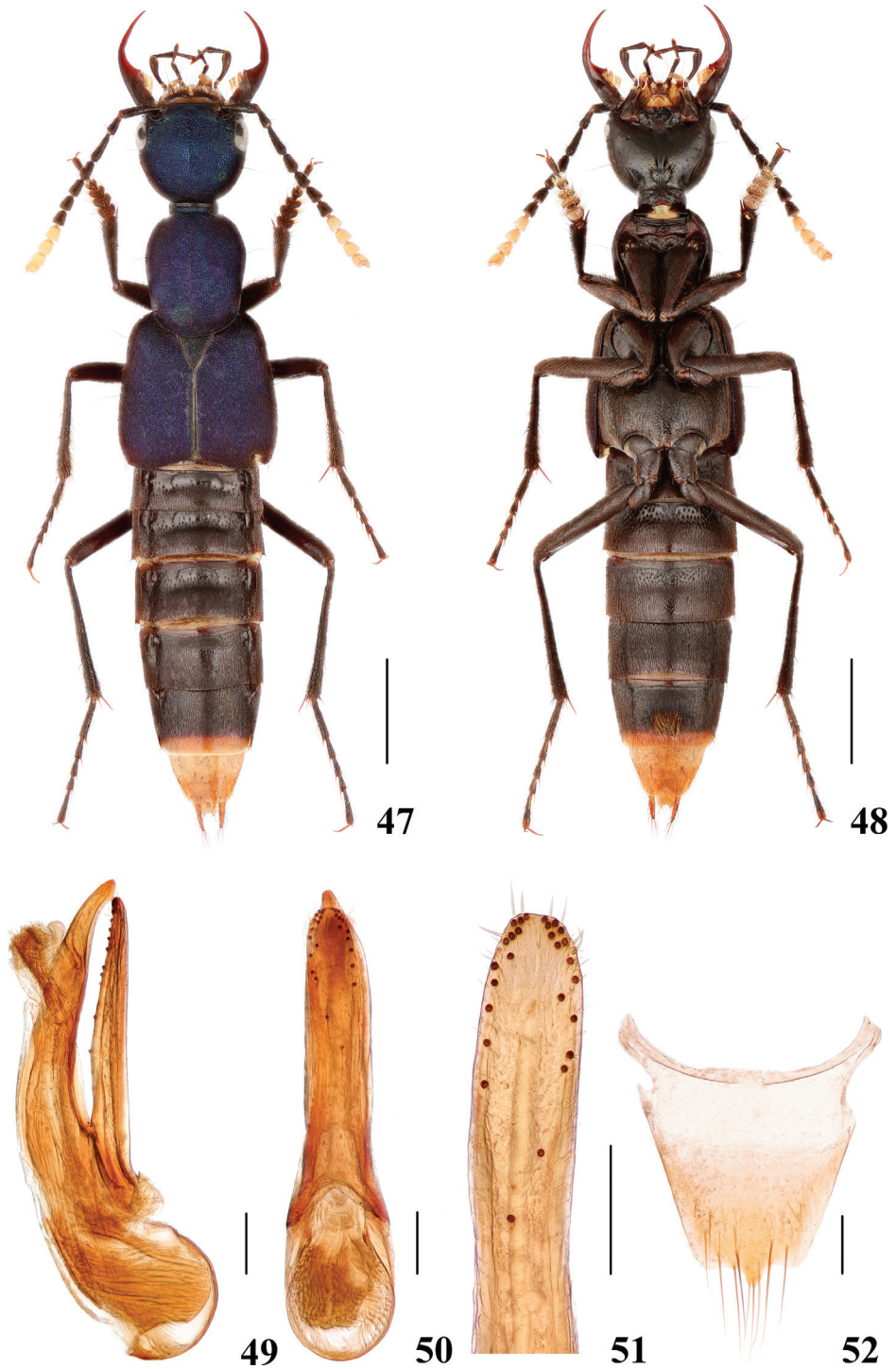
Diagnosis. Amongst the species of the nominal subgenus with four outer segments of antennae creamy white, *H. puetzi* may be easily recognised by the narrower head (HW/HL: 1.14–1.16 in *H. puetzi*, HW/HL: 1.22 in *H. languidum*, HW/HL: 1.29 in *H. xizangense*, HW/HL: 1.24–1.35 in *H. chenchangchini*) and other differences (see diagnoses in *Hesperosoma* (s.str.) *xizangense* sp. nov. and *Hesperosoma* (s.str.) *languidum* sp. nov.).

***Hesperosoma* (s.str.) *xizangense* sp. nov.**

<http://zoobank.org/30F6B5FA-7004-4F4C-BA23-F0DB3E3A1971>

Figures 11, 53–57

Material examined. Holotype. CHINA – Xizang Prov. • ♂; glued on a card with labels as follows: “China: Xizang, Bomi County, Yigong; alt. 2397 m; 27 Jul 2016; Yan-Quan Lu leg.; mixed forest.” “Holotype / *Hesperosoma* (s.str.) *xizangense* / Cai, Tang & Schillhammer” [red handwritten label]; SHNU.



Figures 47–52. *Hesperosoma puetzi* 47–48 habitus 49–51 aedeagus, lateral (49) and ventral (50) views, paramere (51) 52 female abdominal tergite X. Scale bars: 2 mm (47–48), 0.2 mm (49–52).

Description. Measurements of male: BL: 13.67 mm, FL: 8.12 mm. HL: 2.26 mm, HW: 2.91 mm, EYL: 0.74 mm, TL: 1.24 mm, PL: 2.75 mm, PW: 2.34 mm, EL: 3.55 mm, EW: 3.59 mm. HW/HL: 1.29, TL/EYL: 1.68, PL/PW: 1.18, EL/EW: 0.99.

Head metallic dark blue to violaceous blue, pronotum and elytra metallic dark blue to violaceous with purplish hue; abdomen with segments III–VI black, segment VII black with posterior margin broadly reddish-yellow, segments VIII and X entirely reddish-yellow, segment IX reddish-yellow with apical half of latter blackish; antennae black, base and apex of segment 1 and 2 reddish, four outer segments creamy white; mandibles black, medial margin and distal portion of mandible dark reddish-brown; maxillary and labial palpi deep black, last segments sometimes slightly paler brownish.

Head (Fig. 11) 1.29 times as wide as long, rounded trapezoid, tempora narrowed towards neck in regular arc, eyes moderately protruding; surface with dense and coarse punctation, mostly contiguous; with short, weakly delimited impunctate mid-line, extending from frons to about half of mid-length; antennae with segments 4–8 markedly oblong, segments 9 and 10 about as long as wide.

Pronotum 1.18 times as long as wide, widest at level of large lateral seta, narrowed towards base in wide, but shallow concave arc; surface as densely and coarsely punctate as on head, with indistinct, short impunctate mid-line in posterior third; scutellum with dense and pit-like punctation, interstices forming small transverse rugae.

Elytra as long as wide, exceedingly densely, coarsely punctate, punctures almost contiguous.

Abdominal tergites III–V with basal transverse depression, punctation of abdominal tergites III–V large, but feeble at base; posterior halves of abdominal tergites III–V and entire surface of remaining tergites with very fine and dense punctation.

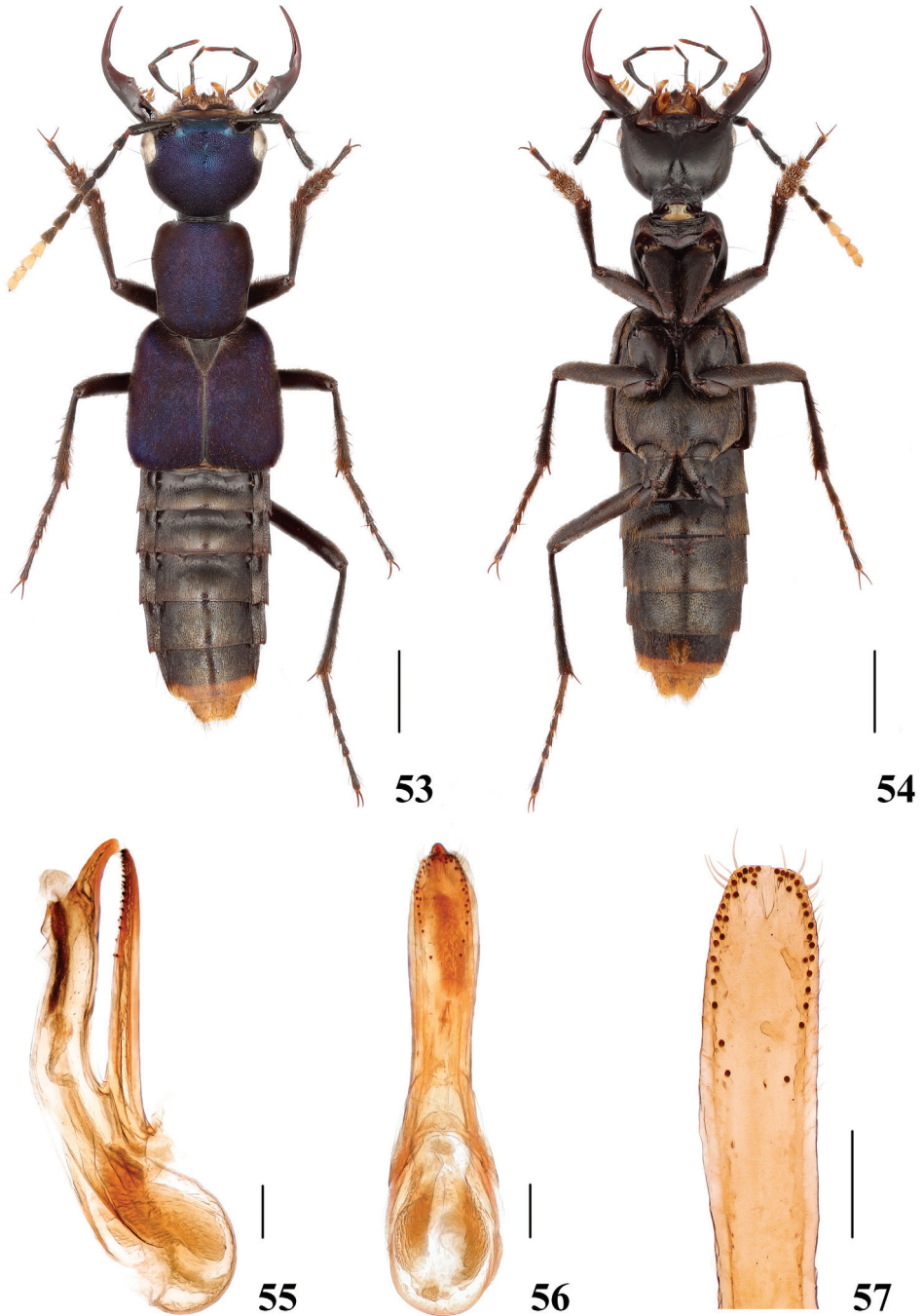
Male. Protarsomeres 1–4 moderately dilated, heart-shaped; sternite VII with patch of long yellow setae on median portion and posterior margin broadly emarginate at middle; sternite VIII with posterior margin emarginate at middle; aedeagus (Figs 55–57) very similar to that of *H. puetzi* and *H. xizangense* sp. nov., but markedly larger, median lobe and paramere slightly asymmetrical, paramere (Fig. 57) shorter than median lobe and slightly bent to left side in ventral view.

Female. Unknown.

Etymology. The species is named after the type locality

Distribution. China (Xizang).

Diagnosis. The new species is very similar externally to *H. languidum* sp. nov. (Yunnan) and *H. puetzi* (Sichuan), but can be recognised by the emarginated anterior margin of frons (Figs 8–9), as well as by the different shape of the aedeagus, especially the paramere, which is broad and truncate apically. Additionally, the head is wider, 1.29 times as wide as long (1.14–1.16 in *H. puetzi*, 1.22 in *H. languidum* sp. nov.), the mandibles are relatively darker (relatively lighter in *H. puetzi* and *H. languidum* sp. nov.) and the legs are relatively darker (relatively lighter in *H. puetzi* and *H. languidum* sp. nov.).



Figures 53–57. *Hesperosoma xizangense* sp. nov. **53–54** habitus **55–57** aedeagus, lateral (**55**) and ventral (**56**) views, paramere (**57**). Scale bars: 2 mm (**53–54**), 0.2 mm (**55–57**).

Subgenus *Paramichrotus****Hesperosoma (Paramichrotus) alexpuchneri* Schillhammer, 2009**

Figures 58–60

Hesperosoma alexpuchneri Schillhammer 2009: 87; Schillhammer 2014: 208*Hesperosoma (Hemihesperosoma) alexpuchneri* Schillhammer 2015: 127

Material examined. CHINA – Sichuan Prov. • 1♀; Tianquan County, Lianglu Countryside; alt. 1400 m; 1 Aug 2011; Hao Huang leg.; SHNU.

Measurements. Female. BL: 10.89 mm, FL: 5.28 mm. HL: 1.48 mm, HW: 1.89 mm, EYL: 0.56 mm, TL: 0.71 mm, PL: 1.76 mm, PW: 1.61 mm, EL: 2.29 mm, EW: 2.54 mm. HW/HL: 1.28, TL/EYL: 1.27, PL/PW: 1.09, EL/EW: 0.90.

Female characters. Tergite X (Fig. 60) indistinctly asymmetrical with short apex.

Distribution. China (Sichuan).

Diagnosis. The collecting locality of the female specimen is about 68 km away from the type locality. The specimen corresponds with the original description and is, thus, temporarily assigned to *H. alexpuchneri*.

***Hesperosoma (Paramichrotus) brunkei* Schillhammer, 2015**

Figures 61–66

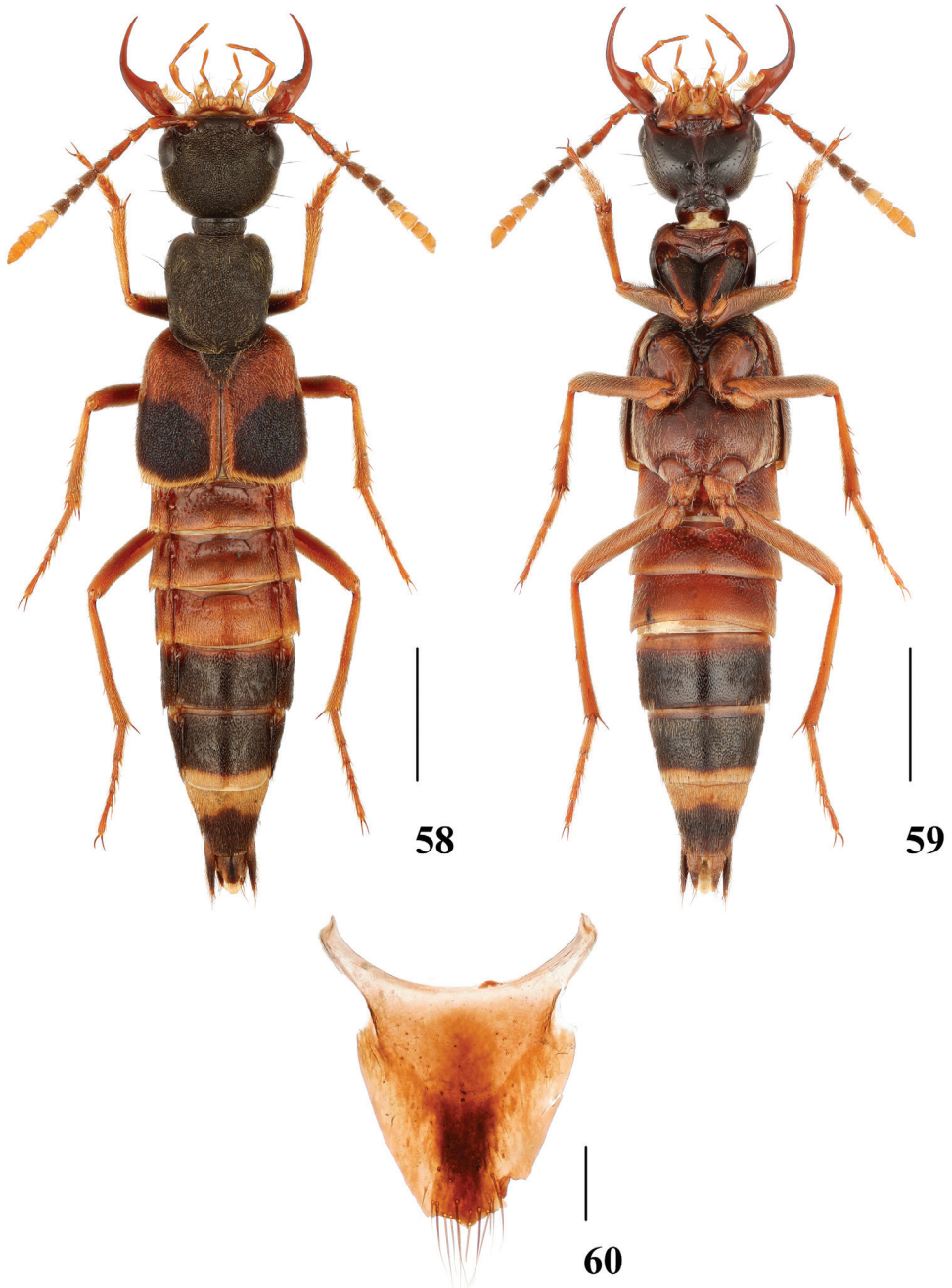
Hesperosoma (Hemihesperosoma) brunkei Schillhammer 2015: 133

Material examined. CHINA – Yunnan Prov. • 1♂; Dehon District, Ruili City, Ruili Botanical Garden; alt. 1100 m; 03 May 2013; Wen-Xuan Bi leg.; SHNU • 1♀; Dehongmang, Yingjiang County, Tongbiguan Town, near Mangna Road; 24°36'59"N, 97°44'30"E; alt. 1550 m; 29 Jul 2019; Cheng & Shen leg.; mixed leaf litter; sifted; SHNU • 1♀; Dehongmang, Yingjiang County, Xima Town, near Yingxi Road; 24°37'53"N, 97°45'39"E; alt. 1469 m; 1 Aug 2019; Cheng & Shen leg.; mixed leaf litter; sifted; SHNU • 1♀; Nabanhe N. R., Chuguohe, Bengganhani; alt. 1750 m; 28 Apr 2009; Jia-Yao Hu & Zi-Wei Yin leg.; SHNU.

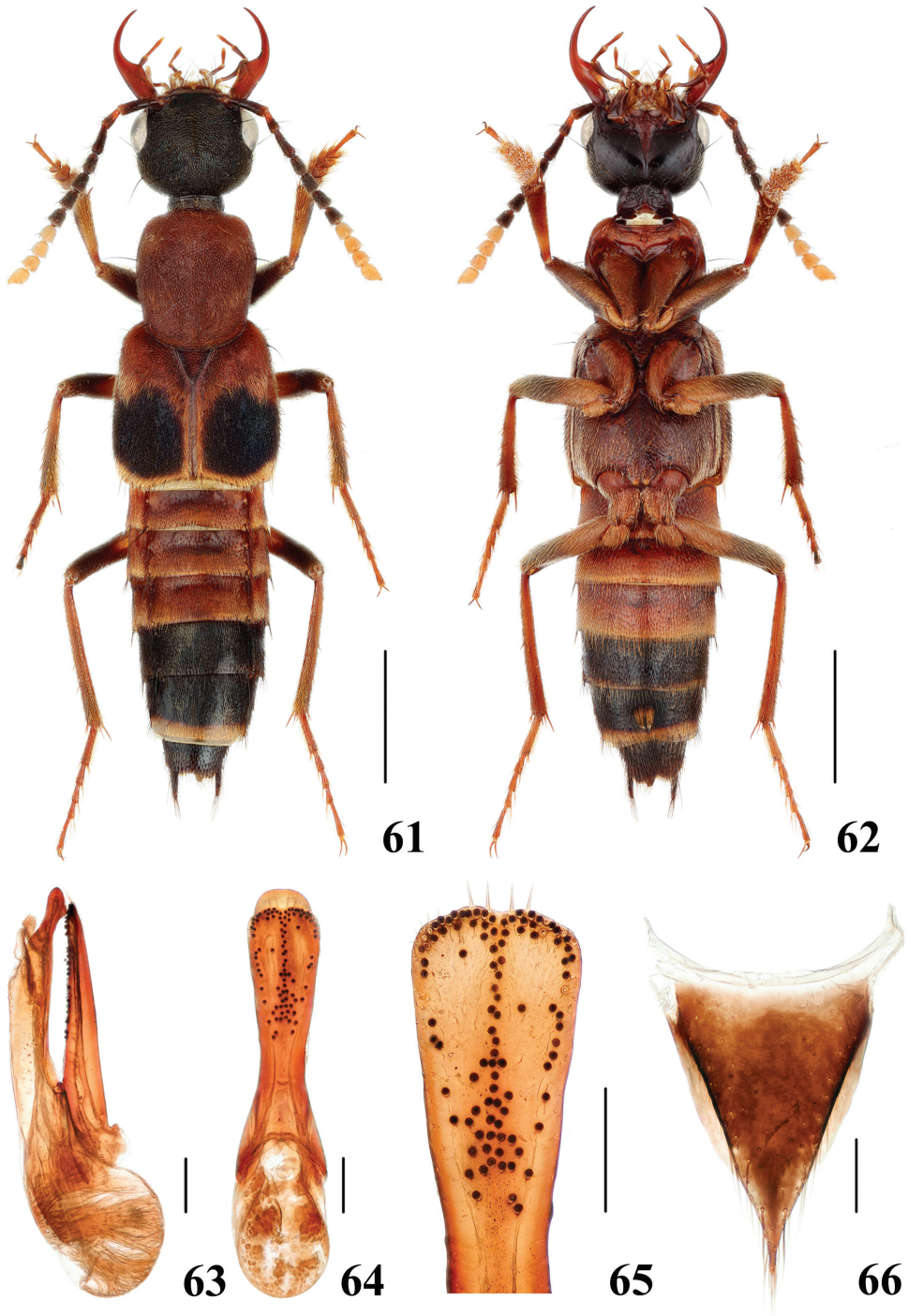
Measurements. Male. BL: 9.77 mm, FL: 5.59 mm. HL: 1.51 mm, HW: 1.92 mm, EYL: 0.64 mm, TL: 0.64 mm, PL: 2.04 mm, PW: 1.81 mm, EL: 2.45 mm, EW: 2.45 mm. HW/HL: 1.27, TL/EYL: 1.00, PL/PW: 1.13, EL/EW: 1.00.

Female. BL: 8.95–10.58 mm, FL: 5.85–6.19 mm. HL: 1.51–1.58 mm, HW: 1.89–2.04 mm, EYL: 0.68–0.71 mm, TL: 0.60–0.68 mm, PL: 2.07–2.19 mm, PW: 1.77–1.89 mm, EL: 2.57–2.72 mm, EW: 2.68–2.87 mm. HW/HL: 1.25–1.30, TL/EYL: 0.85–1.00, PL/PW: 1.14–1.17, EL/EW: 0.92–0.96.

Distribution. China (Yunnan), Laos and Myanmar. New to China.



Figures 58–60. *Hesperosoma alexpuchneri* **58–59** habitus **60** female abdominal tergite X. Scale bars: 2 mm (**58–59**), 0.2 mm (**60**).



Figures 61–66. *Hesperosoma brunkei* 61–62 habitus 63–65 aedeagus, lateral (63) and ventral (64) views, paramere (65) 66 female abdominal tergite X. Scale bars: 2 mm (61–62), 0.2 mm (63–66).

Diagnosis. The collecting locality of the male specimen is about 760 km away from the holotype locality in north-eastern Laos and about 210 km away from the paratype locality in Myanmar. The specimen fits the original description in all characters, but the medio-apical margin of the paramere looks slightly different as well as the apex of the median lobe in lateral view. The ventral view of the median lobe as depicted here is more representative of the species, as it is matching that of the other specimens of the type series. The shape of the paramere is here considered as within the variability range of this widespread species. The females correspond with the original description in all characters.

***Hesperosoma (Paramichrotus) excellens* (Bernhauer, 1939)**

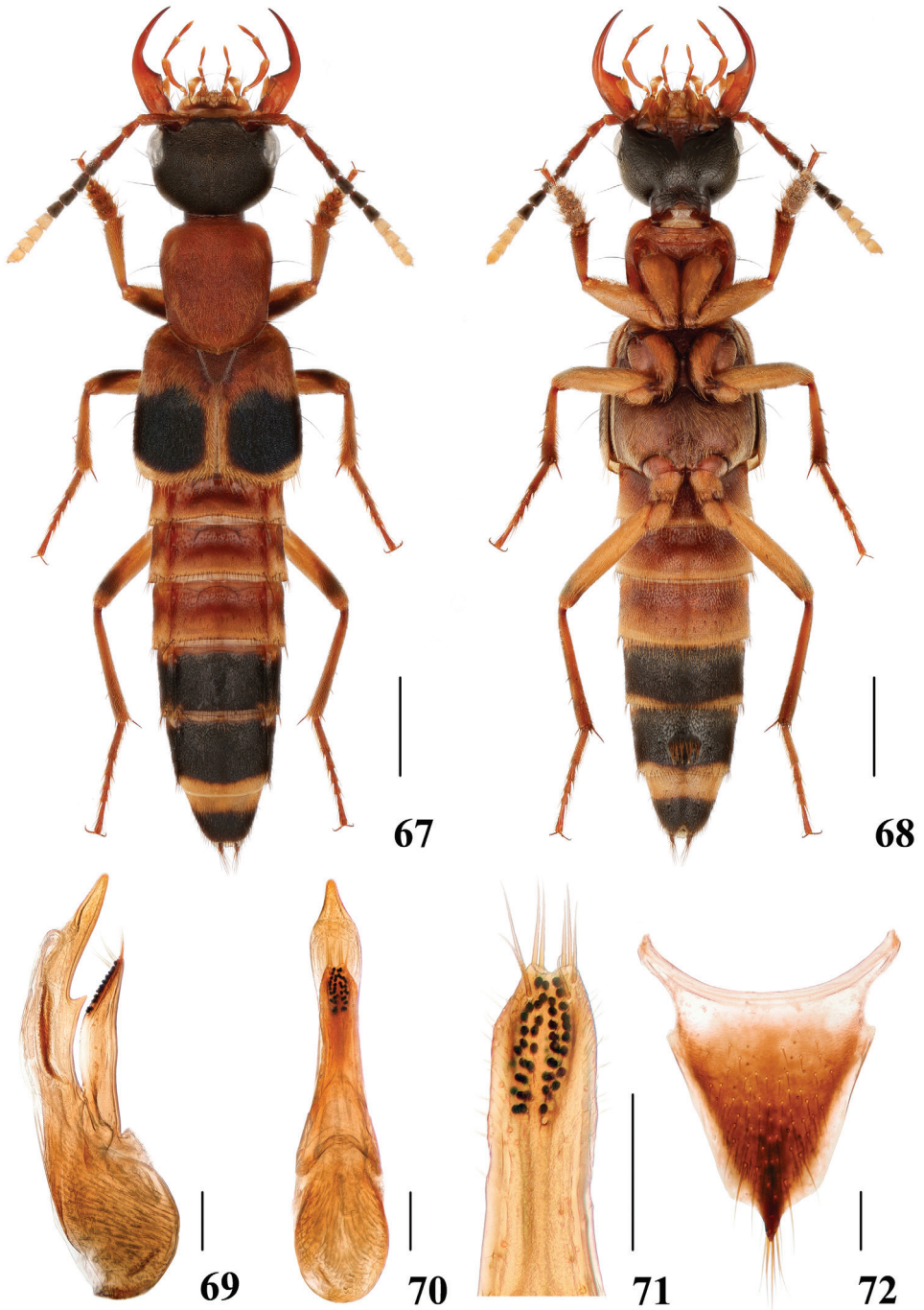
Figures 67–72

Amichrotus excellens Bernhauer 1939: 100

Hesperosoma (Euhesperosoma) excellens Hayashi 2002: 178; Schillhammer 2004: 261; Schillhammer 2009: 86

Hesperosoma (Hemihesperosoma) excellens Schillhammer, 2015: 134

Material examined. CHINA – **Anhui Prov.** • 1♂; Huangshan, Tangkou Town, Jiulongpu; 30°6'41.12"N, 118°12'37.74"E; alt. 760 m; 01 Jul 2020; Tang, Li & Zhou leg.; sifted; SHNU • 1♀; Huangshan, Tangkou Town, Hougu; 30°5'3.48"N, 118°8'45.96"E; alt. 569–688 m; 29 Jun –7 Jul 2020; Tang, Li & Zhou leg.; sifted; SHNU. – **Fujian Prov.** • 1♂; Wuyishan City, Guadun Vill; 27°44'N, 117°38'E; alt. 1200–1300 m; 24 May 2012; Peng & Dai leg.; SHNU • 1♂, 1♀; same collection data as for the preceding; but alt. 1200–1500 m; 25 May 2012 • 2♂♂; same collection data as for the preceding; but alt. 1200–1500 m; 26 May 2012 • 1♂; same collection data as for the preceding; but alt. 1300–1500 m; 27 May 2012. – **Guangdong Prov.** • 3♂♂; Ruyuan County, Nanling N. R., Qingshui Valley; 24°54'57"N, 113°01'55"E; alt. 900 m; 04 May 2015; Peng, Tu & Zhou leg.; mixed forest, leaf litter, sifted; SHNU • 1♀; Ruyuan County, Nanling N. R., Babaoshan station; 24°55'43"N, 113°00'58"E; alt. 1030 m; 25 Apr 2015; Z Peng, YY Tu & ZD Zhou leg.; decaying log; SHNU. – **Guangxi Prov.** • 1♂; Jinxiu County, '16 km'; 24°08'11"N, 110°14'28"E; alt. 960 m; 25 Jul 2014; Peng, Song, Yu & Yan leg.; forest, leaf litter, sifted; SHNU • 1♂, 1♀; Jinxiu County, '16 km'; 24°08'25"N, 110°15'38"E; alt. 960 m; 13 Jul 2014; Peng, Song, Yu & Yan leg.; beech forest, leaf litter, humus, sifted; SHNU. – **Hunan Prov.** • 1♂, 1♀; Yizhang County, Mang Mt.; 24°55'39"N, 112°59'28"E; alt. 1000–1200 m; 10 May 2020; Li & Wang leg.; FIT; SHNU. – **Zhejiang Prov.** • 1♂; Wuyanling; alt. 700 m; 9 May 2004; Hu, Tang & Zhu leg.; SHNU • 2♂♂; Longquan, Fengyang Mt., Guan Yin Tai; 27°55'23"N, 119°11'26"E; alt. 1100 m; 11 May 2019; Tang & Zhao leg.; sifted; SHNU • 1♂; Longquan, Fengyang Mt., Mihou Valley; 27°55'2"N, 119°11'37"E; alt. 950 m; 09 May 2019; Tang & Zhao leg.; sifted; SHNU • 1♂; same



Figures 67–72. *Hesperosoma excellens* 67–68 habitus 69–71 aedeagus, lateral (69) and ventral (70) views, paramere (71) 72 female abdominal tergite X. Scale bars: 2 mm (67–68), 0.2 mm (69–72).

collection data as for the preceding; but 11 May 2019 • 1♀; Longquan City, Fengyangshan N. R., Lu'aocun Village; 27°55'19.66"N, 119°11'38.86"E; alt. 1076 m; 04 May 2016; Jiang, Liu & Zhou leg.; SHNU.

Measurements. Male. BL: 10.23–13.98 mm, FL: 5.85–7.10 mm. HL: 1.61–1.89 mm, HW: 2.01–2.57 mm, EYL: 0.68–0.77 mm, TL: 0.68–0.86 mm, PL: 2.17–2.60 mm, PW: 1.76–2.23 mm, EL: 2.51–3.17 mm, EW: 2.57–3.32 mm. HW/HL: 1.25–1.36, TL/EYL: 1.00–1.16, PL/PW: 1.14–1.23, EL/EW: 0.95–0.99.

Female. BL: 11.72–13.36 mm, FL: 6.48–7.22 mm. HL: 1.71–1.92 mm, HW: 2.23–2.41 mm, EYL: 0.71–0.77 mm, TL: 0.77–0.83 mm, PL: 2.32–2.60 mm, PW: 2.01–2.23 mm, EL: 2.85–3.32 mm, EW: 2.91–3.32 mm. HW/HL: 1.25–1.30, TL/EYL: 1.00–1.13, PL/PW: 1.14–1.17, EL/EW: 0.96–1.00.

Distribution. China (Anhui, Fujian, Guangdong, Guangxi, Hubei and Zhejiang). New to Anhui, Guangdong, Guangxi and Zhejiang.

Diagnosis. Externally, the species hardly differs from *H. meghalayense* from India, but may be distinguished by the very different aedeagus (Figs 67–69) and, to some extent, geographically. From *H. brunkei*, it differs in the proximal antennomeres 3 and 4 being bright reddish and segments I–IV of maxillary palpi reddish.

Hesperosoma (Paramichrotus) guizhouense Schillhammer, 2018

Figures 73–78

Hesperosoma guizhouense Schillhammer 2018: 44

Material examined. CHINA – **Guizhou Prov.** • 1♂; Rongjiang County, Xiaodanjiang; 26°20'16.09"N, 108°20'23.34"E; alt. 700 m; 5 May 2021; De-Yao Zhou leg.; SHNU • 1♀; Leishan County, Leigong Mt., Xiannütang; 26°22'22.11"N, 108°11'52.12"E; alt. 1550 m; 30 Apr 2021; Tang, Peng, Cai & Song leg.; SHNU.

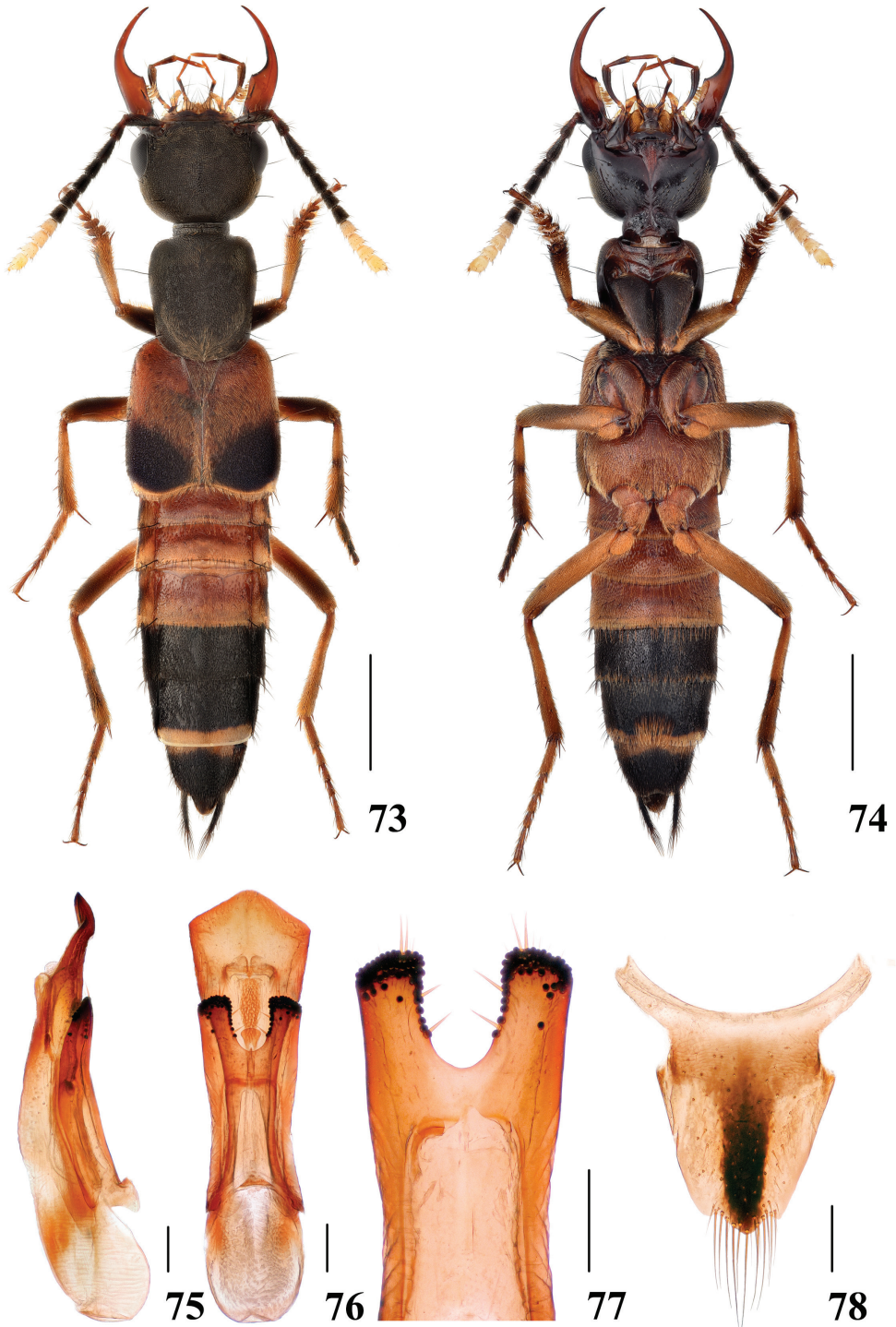
Measurements. Male. BL: 11.19 mm, FL: 6.17 mm. HL: 1.67 mm, HW: 2.29 mm, EYL: 0.71 mm, TL: 0.74 mm, PL: 2.17 mm, PW: 1.86 mm, EL: 2.76 mm, EW: 2.66 mm. HW/HL: 1.37, TL/EYL: 1.04, PL/PW: 1.17, EL/EW: 1.04.

Female. BL: 11.47 mm, FL: 6.11 mm. HL: 1.67 mm, HW: 2.17 mm, EYL: 0.65 mm, TL: 0.83 mm, PL: 2.11 mm, PW: 1.86 mm, EL: 2.69 mm, EW: 2.76 mm. HW/HL: 1.30, TL/EYL: 1.28, PL/PW: 1.13, EL/EW: 0.97.

Female characters. Tergite X (Fig. 78) slightly asymmetrical with blunt apex.

Distribution. China (Guizhou).

Diagnosis. *Hesperosoma guizhouense* does not differ externally from two allopatric species, *H. klapperichi* and *H. alexpuchneri*, but it may be distinguished only by the shape of the aedeagus (Figs 73–75): paramere in *H. guizhouense* with relatively deeper medio-apical emargination, in *H. klapperichi* with relatively shallower medio-apical emargination and in *H. alexpuchneri* with acutely pointed apex. In one examined male specimen, the suture is reddish, which may be explained by the variability of the species.



Figures 73–78. *Hesperosoma guizhouense* 73–74 habitus 75–77 aedeagus, lateral (75) and ventral (76) views, paramere (77) 78 female abdominal tergite X. Scale bars: 2 mm (73–74), 0.2 mm (75–78).

***Hesperosoma (Paramichrotus) klapperichi* Schillhammer, 2004**

Figures 79–84

Hesperosoma klapperichi Schillhammer 2004: 260*Hesperosoma (Hemihesperosoma) klapperichi* Schillhammer, 2015: 126

Material examined. CHINA – **Anhui Prov.** • 2♂♂, 1♀; Huangshan, Tangkou Town, Hougu; 30°5'3.48"N, 118°8'45.96"E; alt. 569–688 m; 29 Jun –3 Jul 2020; Chong Li leg.; pitfall trapped; SHNU. – **Fujian Prov.** • 1♂; Wuyishan City, Guadun Vill; 27°44'N, 117°38'E; alt. 1200–1500 m; 26 May 2012; Peng & Dai leg.; SHNU. – **Guangxi Prov.** • 7♂♂, 1♀; Jinxiu County, '16 km'; 24°08'25"N, 110°15'38"E; alt. 960 m; 13 Jul 2014; Peng, Song, Yu & Yan leg.; beech forest, mixed leaf litter, humus, shifted; SHNU • 1♀; Jinxiu County, '16 km'; 24°08'11"N, 110°14'28"E; alt. 960 m; 25 Jul 2014; Peng, Song, Yu & Yan leg.; forest, leaf litter, shifted; SHNU • 1♂, 1♀; Jinxiu County, Laoshan Forest Farm; 24°07'17"N, 110°11'54"E; alt. 840 m; 18 Jul 2014; Peng, Song, Yu & Yan leg.; beech forest, mixed leaf litter, humus, shifted; SHNU • 1♀; Lingui County, Huaping, Anjiangping; alt. 1200 m; 16 Jul 2011; L Tang & W-J He leg.; SHNU • 2♂♂; Jinxiu County, Dayaoshan, Luoyingou; alt. 1200 m; 15 Jul 2016; Jin-Teng Zhao leg.; SHNU • 1♀; Jinxiu County, Yinshan Conservation Station; 24°10'01"N, 110°14'38"E; alt. 1200 m; 10 Jul 2014; Peng, Song, Yu & Yan leg.; beech forest, mixed leaf litter, shifted; SHNU. – **Hunan Prov.** • 1♀; Xinning County, Shunhuang Mt., Yangheping; 26°23'41.58"N, 111°00'08.16"E; alt. 820 m; 2 May 2021; Yin, Zhang, Pan & Shen leg.; SHNU.

Measurements. Male. BL: 9.51–12.15 mm, FL: 5.82–6.69 mm. HL: 1.55–1.82 mm, HW: 2.20–2.79 mm, EYL: 0.65–0.74 mm, TL: 0.71–0.93 mm, PL: 2.07–2.32 mm, PW: 1.79–2.13 mm, EL: 2.57–3.07 mm, EW: 2.51–3.01 mm. HW/HL: 1.39–1.53, TL/EYL: 1.04–1.31, PL/PW: 1.09–1.17, EL/EW: 1.00–1.02.

Female. BL: 10.14–12.77 mm, FL: 6.07–6.66 mm. HL: 1.61–1.79 mm, HW: 2.13–2.38 mm, EYL: 0.65–0.74 mm, TL: 0.74–0.86 mm, PL: 2.13–2.38 mm, PW: 1.89–2.07 mm, EL: 2.54–2.97 mm, EW: 2.69–3.10 mm. HW/HL: 1.30–1.44, TL/EYL: 1.08–1.17, PL/PW: 1.13–1.16, EL/EW: 0.94–0.98.

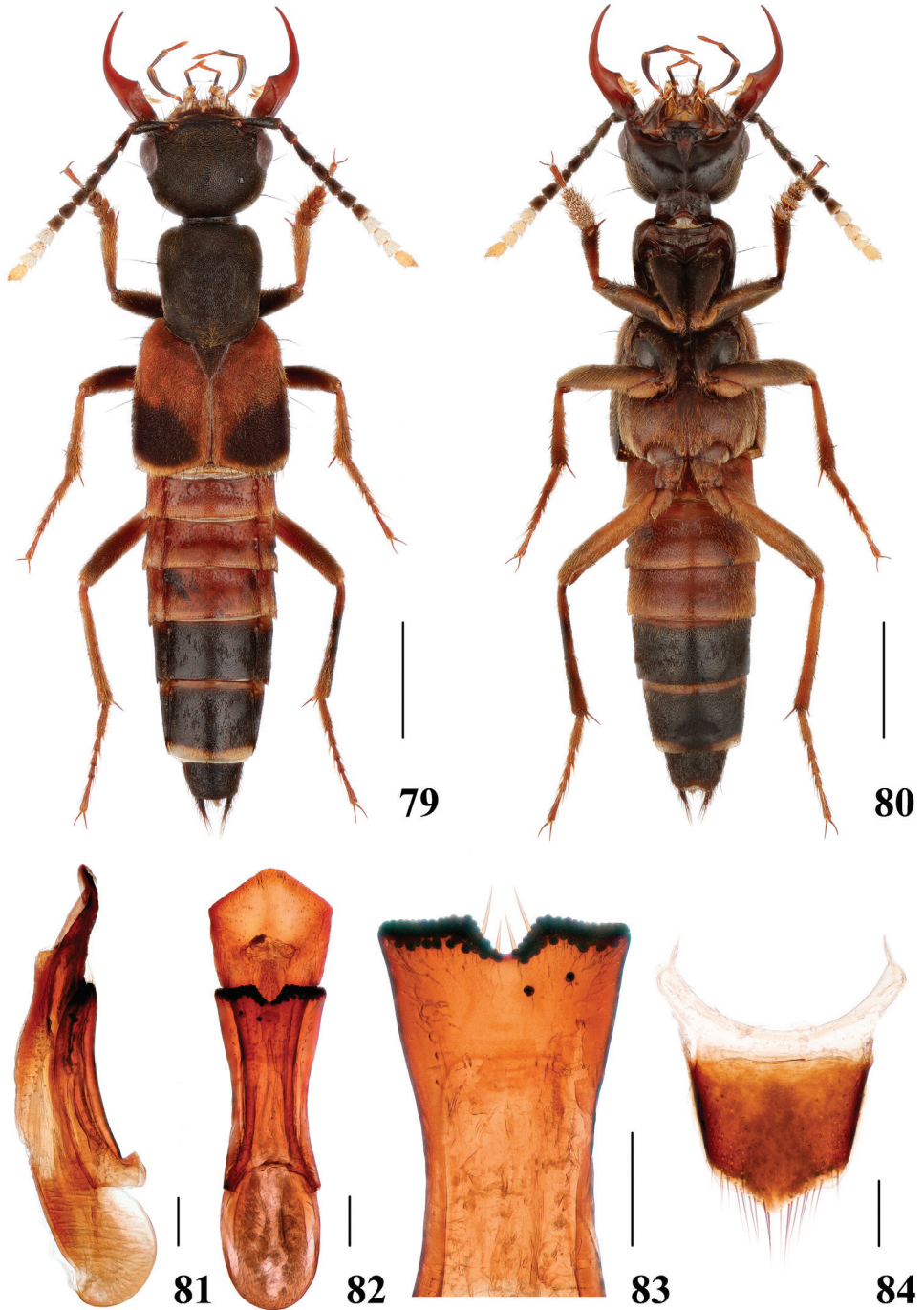
Distribution. China (Anhui, Fujian, Guangxi, Hubei and Hunan). New to Anhui, Guangxi and Hunan.

Diagnosis. The species is very similar to *H. miwai*, but may be distinguished by the paler, almost entirely reddish tibiae. From *H. guizhouense* and *H. alexpuchneri*, the main distinguishing character is the aedeagus (Figs 81–83) (see diagnosis in *H. guizhouense*).

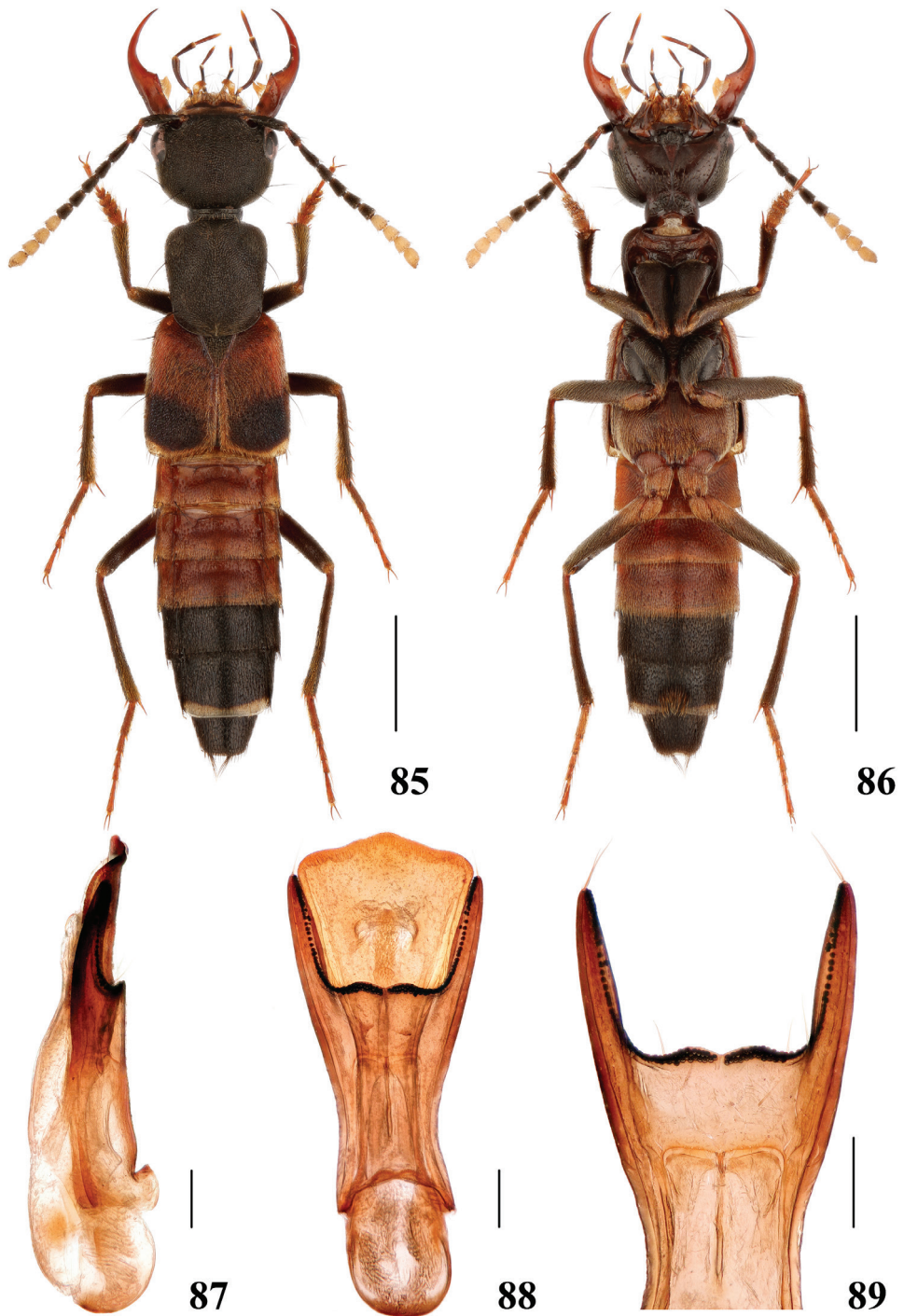
***Hesperosoma (Paramichrotus) miwai* (Bernhauer, 1943)**

Figures 85–89

Amichrotus miwai Bernhauer 1943: 177; Shibata 1976: 11*Hesperosoma miwai* Hayashi 1993a: 290; Hayashi 2002: 177; Schillhammer 2009: 86*Hesperosoma (Hemihesperosoma) miwai* Schillhammer, 2015: 125



Figures 79–84. *Hesperosoma klapperichi* 79–80 habitus 81–83 aedeagus, lateral (81) and ventral (82) views, paramere (83) 84 female abdominal tergite X. Scale bars: 2 mm (79–80), 0.2 mm (81–84).



Figures 85–89. *Hesperosoma miwai* 85–86 habitus 87–89 aedeagus, lateral (87) and ventral (88) views, paramere (89). Scale bars: 2 mm (85–86), 0.2 mm (87–89).

Hesperosoma miwai nashanchiana Hayashi, 1993b: 123; Schillhammer 2009: 86

Hesperosoma sakoi Hayashi, 1993b: 124; Schillhammer 2009: 86

Material examined. CHINA – **Taiwan** • 1♂; Pingtung, Tai-wu, Pei-ta-wu-shan; 22°37'47"N, 120°45'32"E; alt. 1300 m; 10 Oct 2017; Chung leg.; SHNU.

Measurements. Male. BL: 10.73 mm, FL: 5.82 mm. HL: 1.62 mm, HW: 2.15 mm, EYL: 0.64 mm, TL: 0.79 mm, PL: 1.96 mm, PW: 1.77 mm, EL: 2.49 mm, EW: 2.41 mm. HW/HL: 1.33, TL/EYL: 1.23, PL/PW: 1.11, EL/EW: 1.03.

Distribution. China (Taiwan).

Diagnosis. Externally, the species is very similar to *H. guizhouense*, *H. klapperichi* and *H. alexpuchneri*, both in colouration and shape, but it differs mainly, in addition to the aedeagus (Figs 87–89) and geography, by all tibiae being predominantly black.

***Hesperosoma (Paramichrotus) parvioculatum* sp. nov.**

<http://zoobank.org/616E3B86-58DA-4D44-BEBD-C30DE0FEB289>

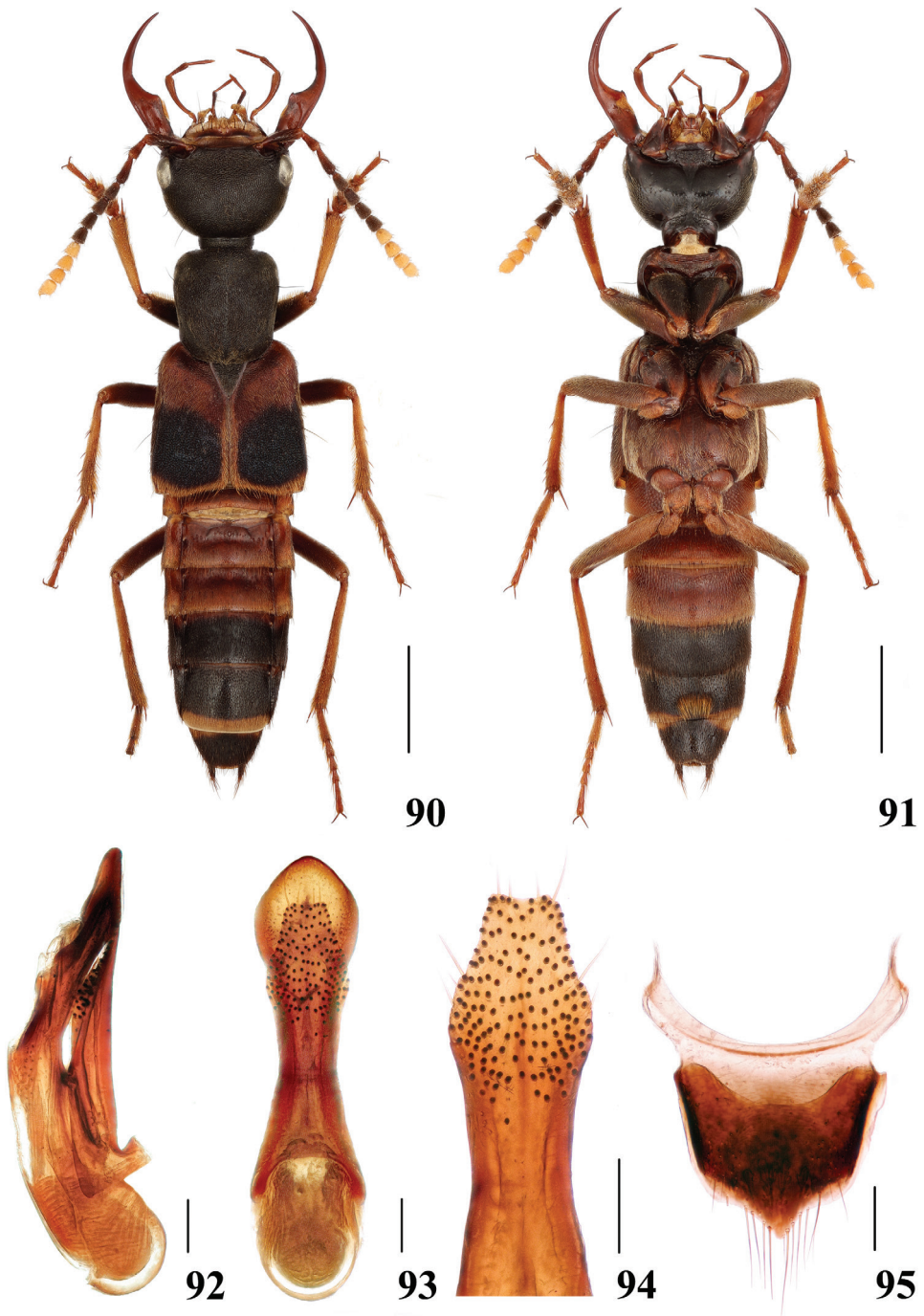
Figures 90–95

Material examined. Holotype. CHINA – **Hunan Prov.** • 1♂; glued on a card with labels as follows: “China: Hunan, Yanling County, Nanfengmian; 26°18'10"N, 114°00'12"E; alt. 1620 m; 26 May 2014; Peng, Shen, Yu & Yan leg.; mixed forest, leaf litter, wood sifted” “Holotype / *Hesperosoma (Paramichrotus) parvioculatum* / Cai, Tang & Schillhammer” [red handwritten label]; SHNU. **Paratypes.** CHINA – **Hunan Prov.** • 1♂; Yizhang County, Mang Mt.; 24°55'39"N, 112°59'28"E; alt. 1000–1200 m; 10 May 2020; Li & Wang leg.; FIT; NMW • 1♀; same collection data as for the preceding; but 17 Jul 2020; SHNU. – **Hubei Prov.** • 1♂, Wufeng County, Houhe Natural Reserve; 30°05'09"N, 110°33'05"E; alt. 1160 m; 08 Jul 2013; Dai, Peng & Xie leg.; along path in a mixed forest; bamboo; leaf litter; sifted; SHNU.

Description. Measurements of male: BL: 10.61–13.33 mm, FL: 6.35–6.73 mm. HL: 1.58–1.79 mm, HW: 2.57–2.79 mm, EYL: 0.62–0.71 mm, TL: 0.86–0.96 mm, PL: 2.15–2.38 mm, PW: 1.95–2.11 mm, EL: 2.85–3.04 mm, EW: 2.83–3.10 mm. HW/HL: 1.48–1.63, TL/EYL: 1.35–1.39, PL/PW: 1.08–1.13, EL/EW: 0.98–1.01.

Measurements of female: BL: 13.79 mm, FL: 6.82 mm. HL: 1.83 mm, HW: 2.384 mm, EYL: 0.71 mm, TL: 0.92 mm, PL: 2.42 mm, PW: 2.07 mm, EL: 3.01 mm, EW: 3.13 mm. HW/HL: 1.30, TL/EYL: 1.30, PL/PW: 1.17, EL/EW: 0.96.

Head, pronotum and scutellum black; elytra red, with a large black patch with faint bluish hue, nearly occupying posterior two thirds, continuing on to hypomeron, but not reaching ventro-lateral margin, posterior margin and suture narrowly yellowish-red; abdomen with segments III–V reddish, VI black with anterior margin narrowly reddish, VII black with posterior margin narrowly yellowish, VIII with proximal half yellowish and distal half black, IX dark brown, X black, narrowly, obscurely reddish at base; antennae with segments 1–7 black, base and apex of segment 1, 2 and base



Figures 90–95. *Hesperosoma parvioculatum* sp. nov. 90–91 habitus 92–94 aedeagus, lateral (92) and ventral (93) views, paramere (94) 95 female abdominal tergite X. Scale bars: 2 mm (90–91), 0.2 mm (92–95).

of segment 3 reddish, segments 8–11 creamy white; mandibles dark reddish-brown; maxillary palpi reddish, labial palpi with segments 1 and 3 reddish, segment 2 black brown; legs reddish-yellow, femora reddish-brown.

Head 1.48–1.63 times as long as wide, rounded trapezoid, tempora narrowed behind eyes; dorsal surface coarsely and very densely punctate, punctures contiguous, including clypeus; antennae rather short, antennae with segments 4–7 weakly oblong, segments 8 and 10 about as long as wide.

Pronotum 1.08–1.13 times as long as wide, widest at about level of large antero-lateral seta, narrowed towards base in weak concave arc, surface with dense and coarse punctation similar to that on head, with narrow impunctate mid-line, ground pubescence slightly more obvious than that on head; scutellum uniformly, densely punctate, space between punctures with very fine wavy microsculpture.

Elytra as long as wide, along sides distinctly longer than pronotum, with slightly uneven surface, densely punctate and pubescent, with distinct depression between shoulders, scutellum and apical margin of elytra; pubescence yellow, long and dense along suture and posterior elytral margin.

Abdominal tergites III–V with transverse basal depression and pair of short oblique basal carinae, punctation very sparse and rather coarse basally and laterally, gradually becoming finer towards apical margin, tergites VI–VIII entirely with fine and uniform punctation and pubescence, colour of pubescence corresponding with colour of integument underneath; legs long and slender.

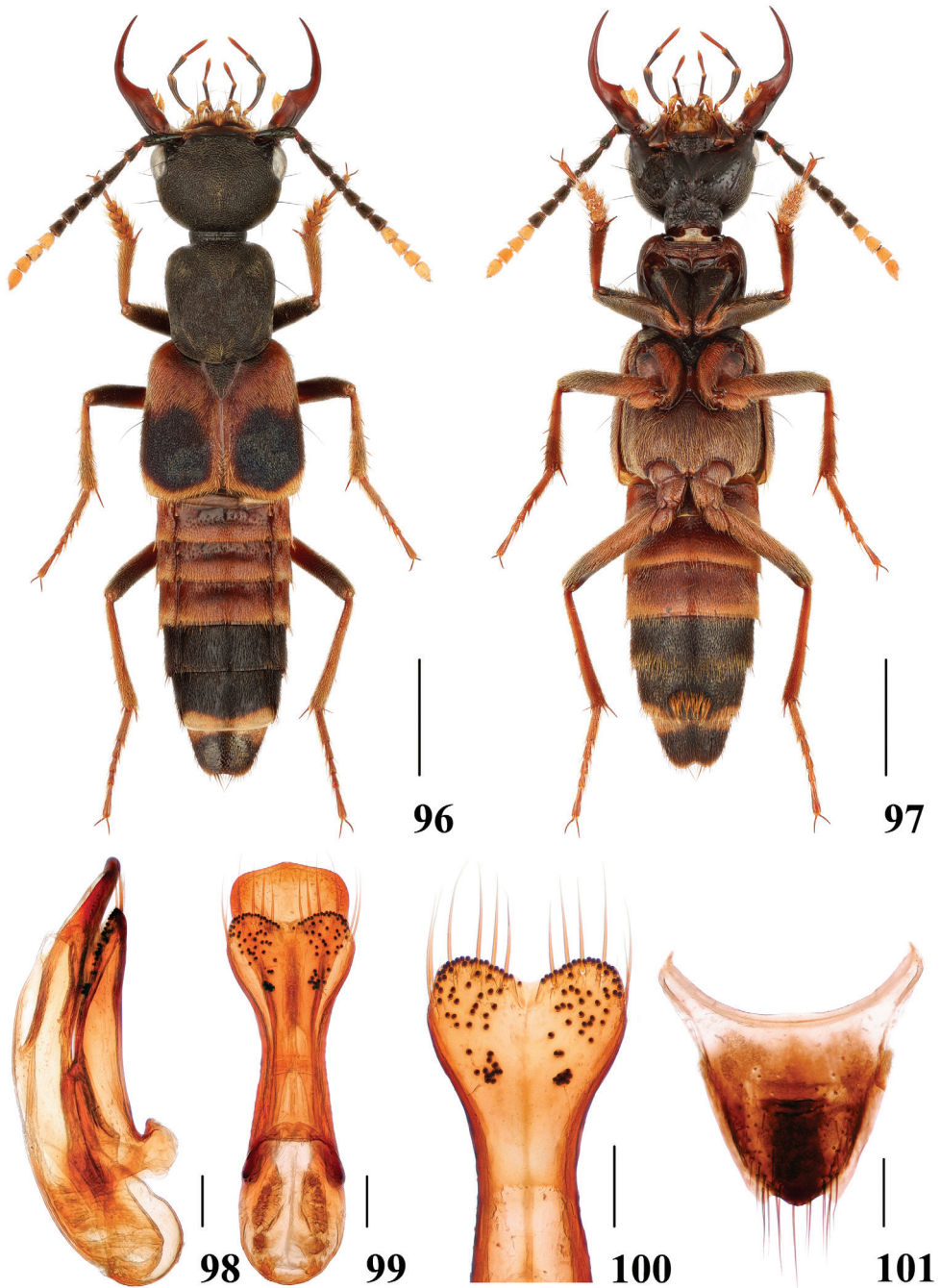
Male. Protarsomeres 1–4 moderately dilated, heart-shaped; sternite VII with the usual setose groove and patch of long yellow setae on median portion, posterior margin broadly emarginate at middle; sternite VIII with posterior margin emarginate at middle; aedeagus (Figs 92–94) with apex of median lobe broad, anterior margin with gibbosities at middle (ventral view); paramere (Fig. 94) with narrow apical portion, shorter than median lobe.

Female. Tergite X (Fig. 95) slightly asymmetrical with short apex.

Etymology. The specific epithet refers to the small eyes of the new species.

Distribution. China (Hubei and Hunan).

Diagnosis. Externally, *H. parvioculatum* sp. nov. is virtually identical to *H. nigricolle* from Myanmar, but differs mainly, aside from the distribution, by the shape of the aedeagus: paramere with narrow apical portion (paramere with broad apical portion, distinctly bilobed in *H. nigricolle*); the wider head with HW/HL about 1.48–1.63 (1.35 in *H. nigricolle*); posterior angles of the head being rounded (slightly prominent in *H. nigricolle*); legs reddish-yellow, femora reddish-brown (legs reddish to yellowish-red, distal halves of femora black in *H. nigricolle*). In appearance, it is also similar to *H. klapperichi*, *H. alexpuchneri*, *H. guizhouense* and *H. yunnanense*, but can be distinguished from *H. klapperichi*, *H. alexpuchneri* and *H. guizhouense* by the larger black elytral patch, occupying more than half of the elytral disc. From *H. yunnanense*, it is distinguished by the smaller eyes with TL/EYL about 1.35–1.39 (1.18–1.29 in *H. yunnanense*) and the wider head with HW/HL about 1.48–1.63 (1.26–1.40 in *H. yunnanense*).



Figures 96–101. *Hesperosoma yunnanense* 96–97 habitus 98–100 aedeagus, lateral (98) and ventral (99) views, paramere (100) 101 female abdominal tergite X. Scale bars: 2 mm (96–97), 0.2 mm (98–101).

***Hesperosoma (Paramichrotus) yunnanense* Schillhammer, 2009**

Figures 96–101

Hesperosoma yunnanense Schillhammer 2009: 88; Schillhammer 2014: 208*Hesperosoma (Hemihesperosoma) yunnanense* Schillhammer 2015: 128

Material examined. CHINA – Yunnan Prov. • 1♂, 1♀; Yinjiang County, Sudian Town, Maocaozhaicun; 25°08'10"N, 97°52'44"E; alt. 1900 m; 15–18 May 2020; Lu Qiu leg.; SHNU • 1♂; Baoshan City, Baihualing; 25°16'46"N, 98°47'20"E; alt. 1350–1450 m; 22 Apr 2013; Song, Peng & Dai leg.; SHNU • 1♂; Nabanhe N. R., Bengganghani, Nanmugaha; alt. 1650 m; 30 Apr 2009; Jia-Yao Hu & Zi-Wei Yin leg.; SHNU • 1♂; Lingcang City., Wumulong, Xinfangzi; 25.17N, 99.69E; alt. 2450 m; 16 Jun 2015; Mao Ye leg.; SHNU • 1♀; Nabanhe N. R., Bengganghani; alt. 2000 m; 29 Apr 2009; Jia-Yao Hu & Zi-Wei Yin leg.; SHNU.

Measurements. Male. BL: 9.76–10.73 mm, FL: 5.51–6.01 mm. HL: 1.45–1.67 mm, HW: 1.89–2.33 mm, EYL: 0.55–0.68 mm, TL: 0.71–0.89 mm, PL: 1.89–2.11 mm, PW: 1.70–1.92 mm, EL: 2.35–2.78 mm, EW: 2.38–2.79 mm. HW/HL: 1.30–1.40, TL/EYL: 1.18–1.38, PL/PW: 1.08–1.13, EL/EW: 0.96–1.00.

Female. BL: 10.72–11.56 mm, FL: 6.07–6.11 mm. HL: 1.58–1.64 mm, HW: 2.01–2.10 mm, EYL: 0.62–0.65 mm, TL: 0.77–0.80 mm, PL: 2.04–2.13 mm, PW: 1.88–1.89 mm, EL: 2.69–2.72 mm, EW: 2.79–2.82 mm. HW/HL: 1.27–1.28, TL/EYL: 1.18–1.29, PL/PW: 1.08–1.13, EL/EW: 0.95–0.96.

Distribution. China (Yunnan).

Diagnosis. Externally, the species is similar to *H. miwai*, *H. klapperichi*, *H. guizhouense* and *H. alexpuchneri*, both in colouration and shape and differs mainly in the much larger black elytral spot, occupying the apical two thirds of each elytron. For differences with *H. parvioculatum*, see diagnosis under that species.

Acknowledgements

We express our sincere gratitude to Mr. Chang-Chin Chen who donates lots of staphylinid specimens to us and to all the collectors mentioned in the paper especially Dr. Zhong Peng, Mr. Wen-Xuan Bi, Mr. Hao Huang, Mr. Yi-Zhou Liu, Mr. Yan-Quan Lu, Dr. Lu Qiu, Mr. De-Yao Zhou, Mr. Xiao-Bin Song and Mr. Qin-Hao Zhao.

References

- Hayashi Y (2002) Studies on the Asian Staphylininae, V (Coleoptera, Staphylinidae). Entomological Review of Japan 57(2): 169–179.
- Hu F-S, Liu R-H, Chen G-R, Yu S-T (2020) Taxonomic Notes of *Hesperosoma* (Hemihesperosoma) *miwai* (Bernhauer, 1943) with Observations of Uncommon Behavior (Coleoptera: Staphylinidae). Taiwanese Journal of Entomological Studies 5(2): 12–17.

- Ito T (2011) Notes on the Species of Staphylinidae (Coleoptera) from Asia, IV. *Elytra* 1(1): 57–65.
- Schillhammer H (2004) Critical notes on the subtribe Anisolinina with descriptions of nine new species (Coleoptera: Staphylinidae: Staphylininae). *Koleopterologische Rundschau* 74: 251–277.
- Schillhammer H (2009) Additional notes on the subtribe Anisolinina, with descriptions of seven new species (Coleoptera: Staphylinidae: Staphylininae). *Koleopterologische Rundschau* 79: 83–96.
- Schillhammer H (2014) An update on *Philomyceta* CAMERON and *Hesperosoma* SCHEERPELTZ (Coleoptera: Staphylinidae: Staphylininae). *Koleopterologische Rundschau* 84: 201–208.
- Schillhammer H (2015) Subgenus *Hemihesperosoma* HAYASHI of *Hesperosoma* SCHEERPELTZ reinstated and revised (Coleoptera: Staphylinidae: Staphylininae). *Koleopterologische Rundschau* 85: 121–165.
- Schillhammer H (2018) Five new species of the subtribe Anisolinina (Coleoptera: Staphylinidae: Staphylininae). *Koleopterologische Rundschau* 88: 43–57.

A contribution to the knowledge of cave-adapted ground beetles from Guiyang, central Guizhou Province, southwestern China (Coleoptera, Carabidae, Trechini)

Mingyi Tian¹, Guangyuan Cheng², Sunbin Huang^{1,3}

1 Department of Entomology, College of Plant Protection, South China Agricultural University, 483 Wushan Road, Guangzhou, 510642, China **2** Haixia Caving, Bureau of Ecology and Environment, no. 7 Building, Financial City, Guanshanhu, Guiyang, Guizhou, 550081, China **3** Mécanismes adaptatifs et évolution (MECADEV), UMR 7179 CNRS–MNHN, Muséum national d'Histoire naturelle, CP50, 57 Rue Cuvier, F–75005 Paris, France

Corresponding author: Mingyi Tian (mytian@scau.edu.cn)

Academic editor: T. Assmann | Received 21 August 2021 | Accepted 17 November 2021 | Published 7 December 2021

<http://zoobank.org/E78D8970-2BE5-424F-A4F1-B77E009B4154>

Citation: Tian M, Cheng G, Huang S (2021) A contribution to the knowledge of cave-adapted ground beetles from Guiyang, central Guizhou Province, southwestern China (Coleoptera, Carabidae, Trechini). ZooKeys 1075: 175–198. <https://doi.org/10.3897/zookeys.1075.73318>

Abstract

A new genus and two new species of cavernicolous trechines are reported from central Guizhou Province, southwestern China. *Haixiaphaenops* **gen. nov.** is established to place a new species discovered in two limestone caves in northern Qingzhen Shi: *H. jinxiaohongae* **sp. nov.** (Dawan Dong cave and Changtu Dong and Dawan Dong caves). This new genus is allied to *Zhijinaphaenops* Uéno & Ran, 2002. *Zhijinaphaenops zhaofei* **sp. nov.** is described from Zhangkou Dong cave in northern Jiuzhuang Zhen of Xifeng County. In addition, two new localities of the species *Zhijinaphaenops jingliae* Deuve & Tian, 2015, and two new localities of *Sinaphaenops chengguangyuani* Ma et al. 2020 are provided. A distribution map for all cavernicolous trechine beetles known in Guiyang is provided.

Keywords

Hypogean, new genus, new species, semi-aphaenopsian, trechines

Introduction

Undoubtedly, Guizhou is the province harbouring the richest cave specific diversity in China in terms of hypogean trechine beetles (Tian et al. 2016, 2020; Chen et al. 2017; Huang et al. 2020; Tian et al. 2021). Of the 168 cave species of trechines known in China, 62 are occurring in Guizhou Province. But the subterranean fauna of ground beetles is poorly studied in Guiyang Shi, central Guizhou. Only three species in two genera of cave-adapted trechines have been reported from this area. The genus *Zhijinaphaenops* Uéno & Ran, 2002 was formerly described from Zhijin County, Bijie Shi, central Guizhou, then reported from several other counties, viz. Dafang, Xifeng, Zunyi, and Weng'an. Nine species are included in the genus so far (Uéno and Ran 2002; Deuve and Tian 2015, 2018). Among them, two species were recorded from Xifeng County, Guiyang Shi: *Zhijinaphaenops jingliae* Deuve & Tian, 2015 and *Z. liuae* Deuve & Tian, 2015.

Sinaphaenops Uéno & Wang, 1991 is a large genus, composed of 13 species so far, ranging in southern Guizhou and also extending to Huanjiang County, northernmost Guangxi (Uéno and Wang 1991; Uéno and Ran 1998; Uéno 2002; Deuve and Tian 2014; Chen et al. 2017; Ma et al. 2020). Amongst them, only *S. lipoi* Chen et al. 2020 is known from Guiyang (Chen et al. 2020).

Led by Guanyuan Cheng, the second author, the local cavers from the Haixia Caving (a cave exploration team in Guiyang) have begun to carry out biological surveys in recent years. They have visited many limestone caves in central Guizhou Province and discovered some interesting cavernicolous ground beetles (Fig. 1). For instance, *Sinaphaenops chengguangyuani* Ma et al. 2020 was formerly found by them in a limestone cave in Longli County of Qiannan Buyi & Maiao Autonomous Prefecture, close to Guiyang (Ma et al. 2020). Two more localities, from Guiyang and Longli respectively, of this beautiful species are now confirmed. In Xifeng County, they discovered two other caves where *Zhijinaphaenops jingliae* is living. In Qingzhen Shi, they found two beetle individuals in the cave Dawan Dong and another beetle in the cave Changtu Dong. These beetles are members of an undescribed species belonging to an unknown genus allied to *Zhijinaphaenops*.

Hence, we establish a new genus to accommodate the new species found in the caves Dawan Dong and Changtu Dong, describe a new *Zhijinaphaenops* species from the cave Zhangkou Dong in Xifeng County and provide new localities for *Zhijinaphaenops jingliae* and *Sinaphaenops chengguangyuani* in the suburbs of Guiyang, the capital city of Guizhou Province.

Materials and methods

The beetle specimens were collected in caves by hand or by using an aspirator, and kept in vials with 50% ethanol. One exemplar of each species was placed into 95% ethanol for DNA sequencing. Dissections and observations were made by using a Leica MZ75 dissecting stereomicroscope (Wetzlar, Germany). Dissected genitalia, including the

median lobe and parameres of aedeagus, were glued on small transparent plastic cards and pinned under the specimen from which they were removed. Digital pictures were taken using a Canon EOS 5D Mark III camera (Tokyo, Japan), and then processed by means of Adobe Photoshop CS5 software (Adobe System Incorporated, California, USA).

Measurements and terminologies used in the text follow Tian et al. (2016). The abbreviations used in the text are as follow:

- HLm** length of head including mandibles, from apex of right mandible to occipital suture;
HLI length of head excluding mandibles, from front of labrum to occipital suture;
HW maximum width of head;
PrL length of prothorax, along the median line;
PnL length of pronotum, as above;
PrW maximum width of prothorax;
PnW maximum width of pronotum;
PfW width of pronotum at front;
PbW width of pronotum at base;
EL length of elytra, from base of scutellum to elytral apex;
EW maximum width of combined elytra.

All material is deposited in the insects collection of South China Agricultural University, Guangzhou, China (SCAU).

Taxonomy

Tribe Trechini Bonelli, 1810

Haixiaphaenops gen. nov.

<http://zoobank.org/7BBA8EF9-21D8-460D-A361-CC134DF019CD>

(Chinese name: 海峡盲步甲属)

Type species: *Haixiaphaenops jinxiiahongae* sp. nov. (caves Dawan Dong and Changtu Dong, Qingzhen, Guiyang)

Generic characteristics. Medium-sized cave trechine, depigmented and eyeless, semi-aphaenopsian; body stout though fore body elongated, with moderately elongated appendages. Head longer than wide, 2 pairs of supraorbital setiferous pores present; frontal furrows rather long, incomplete, parallel-sided in most part, divergent posteriad; mandibles thin and very elongated, moderately hooked apically, right mandibular tooth bidentate though with 2 additional tiny denticles medially; labial suture absent; mentum 2-setose, base widely concave, submentum 10-setose; antennae thin and rather long, extending to apical 1/3 to 1/4 of elytra. Prothorax strongly convex and propleura notably visible from above; pronotum, much longer than wide,

subparallel sided, disc covered with long setae, presence of only anterior lateral setae. Elytra elongated ovate, much wider than fore body; widest before middle, without humeral angles; base bordered, lateral margins well-bordered and ciliate throughout; disc extremely convex and tumid, partly concealing lateral margins; striae noticeable though punctures faint, intervals slightly convex; 3 discal setiferous pores present on each elytron, the preapical pores absent; the humeral group of the marginal umbilicate pores not aggregated, 1st pore inwardly and backwardly shifted, 5th and 6th pores (middle group) moderately spaced. 1st protarsomere dilated and elongated in male, inwardly spurred at apex; abdominal ventrite VII 6-setose in male.

Remarks. *Haixiaphaenops* gen. nov. is allied to the genus *Zhijinaphaenops* Uéno & Ran, 2002 by sharing the following characteristics: (1) mentum and submentum completely fused; (2) prothorax strongly dilated and propleura notably visible from above, pronotum with only anterior latero-marginal setae; (3) only protarsomere 1 modified in male, which is long and inwardly spurred at apex; (4) pronotum covered with long setae; (5) elytra shortly pubescent, with hardly distinguishable striae, and the 1st marginal umbilicate pore inwardly and backwardly shifted, located behind the level of the 3rd pore. However, *Haixiaphaenops* gen. nov. readily differs from *Zhijinaphaenops* in several generic-level characters, such as: (1) 2 pairs of frontal pores present in *Haixiaphaenops* gen. nov., versus only the posterior pores present in *Zhijinaphaenops*; (2) antennae much shorter in *Haixiaphaenops* gen. nov., only extending at most to apical 1/4 of elytra, versus longer, projection over apices of elytra in *Zhijinaphaenops*; (3) pronotum elongated quadrate, nearly parallel-sided in *Haixiaphaenops* gen. nov., versus subcordate, not parallel-sided in *Zhijinaphaenops*; (4) elytra much stouter and more convex in *Haixiaphaenops* gen. nov., partly concealing lateral margins in median portion, versus more elongated and less convex in *Zhijinaphaenops*, with whole lateral margins visible from above; (5) base of elytra bordered in *Haixiaphaenops* gen. nov., versus unbordered in *Zhijinaphaenops*; and (6) male genitalia are small and stout, slightly bent medially, and widely rounded at apex in *Haixiaphaenops* gen. nov., versus large and slender, strongly arcuate medially, and more or less sharpened at apex in *Zhijinaphaenops*.

Etymology. “Haixia” + “Aphaenops”, dedicated to Haixia Caving, a cave exploration team in Guiyang. Gender masculine.

Range. China (Guizhou). Only one species of the genus was found in the limestone caves Dawan Dong and Changtu Dong in Qingzhen, northern Guiyang Shi (Fig. 1).

***Haixiaphaenops jinxiaohongae* sp. nov.**

<http://zoobank.org/701ACD12-A45D-4794-9994-BF58B3BE90D4>

(Chinese name: 晓红盲步甲)

Figures 2–7

Type material. *Holotype* male: Guizhou, Qingzhen, Anliu, Yangtianwo, Dawan Dong cave (贵州省清镇市暗流镇大湾洞), 26°52'N, 106°24'E, 941 m, 2020–IV–19, leg. Xiaohong Jin & Guangyuan Cheng, in SCAU; *Paratypes*: 1 male, same cave as holotype, 2021–VI–23, leg. Chenggang Wang; 1 male, Guizhou, Qingzhen, Anliu, Ximi,

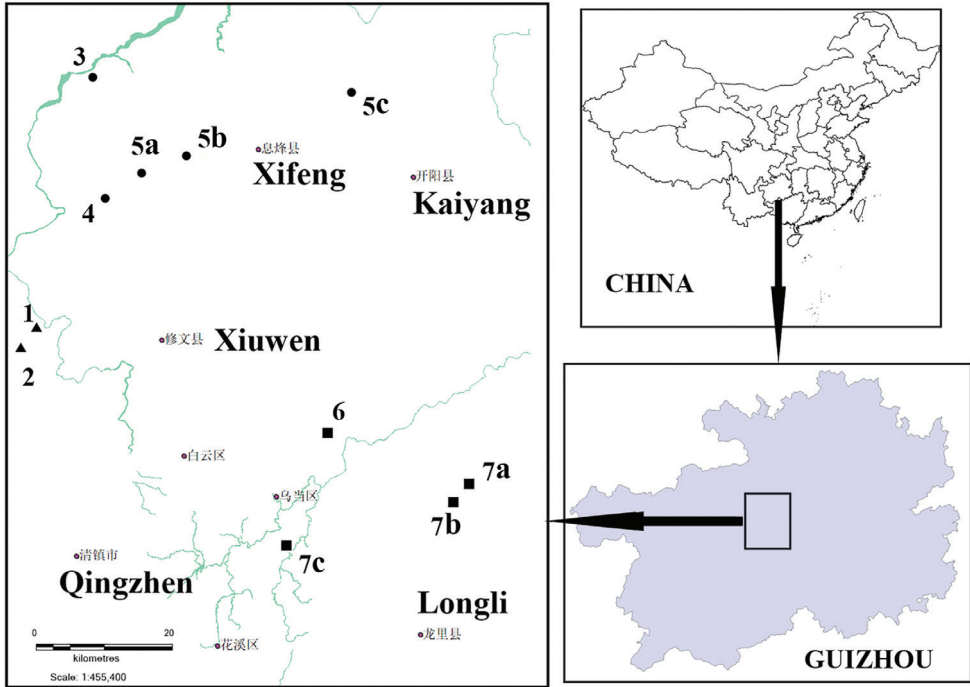


Figure 1. A distribution map of cavernicolous trechine beetles in Guiyang, central Guizhou Province. Triangles: *Haixiaphaenops* gen. nov.; dots: *Zbijinaphaenops*; squares: *Sinaphaenops* **1** *H. jinxiaohongae* sp. nov. / Changtu Dong **2** *H. jinxiaohongae* sp. nov. / Dawan Dong **3** *Z. zhaofei* sp. nov. / Zhangkou Dong **4** *Z. liuae* Deuve & Tian, 2015 / Hejia Dong **5a** *Z. jingliae* Deuve & Tian, 2015 / Zhangkou Dong **5b** *Z. jingliae* / Mafen Dong **5c** *Z. jingliae* / Wenquan Dong **6** *S. lipoi* Chen et al. 2020 / Da Dong **7a** *S. chengguangyuani* Ma et al. 2020 / Shuijing Dong **7b** *S. chengguangyuani* / Duocai Dong **7c** *S. chengguangyuani* / Jianlong Dong.

Changtu Dong cave (贵州省清镇市暗流镇长土洞), 26°51'N, 106°21'E, 1249 m, 2020–VI–27, leg. Chenggang Wang, Xiaohong Jing, Guangyuan Cheng, Yi Zhao & Mingyi Tian, both in SCAU.

Description. Length: 6.5–6.8 mm (including mandibles); width: 1.0–1.1 mm. Habitus as in Figures 2, 3.

Head and pronotum dark brown (in holotype) or brown (in paratypes), elytra, femora and tibiae lighter, antennae, palps, and tarsi yellow. Head glabrous on upper surface, pronotum covered with long setae, elytra with short pubescence, ventral head covered with several setae; prosternum, meso- and metasterna and fore coxae glabrous, abdominal ventrites with dense and short pubescence, in particular on median portion. Microsculptural engraved meshes strongly transverse on head and pronotum, irregular isodiametric on elytra. Body moderately elongated, fore body (including mandibles) shorter than elytra.

Head (Fig. 4A, B) moderately elongated, distinctly longer than wide, HLm/HW= 2.27, HLI/HW= 1.56; widest at about middle of head from labrum; frons and vertex moderately convex, genae gently expanded anteriad (but hardly expanded in paratype



Figure 2. Habitus of *Haixiaphaenops jinxiaohongae* gen. nov., sp. nov., holotype, male



Figure 3. Habitus of *Haixiaphaenops jinxiaohongae* gen. nov., sp. nov., paratype male, from the Cave Changtu Dong

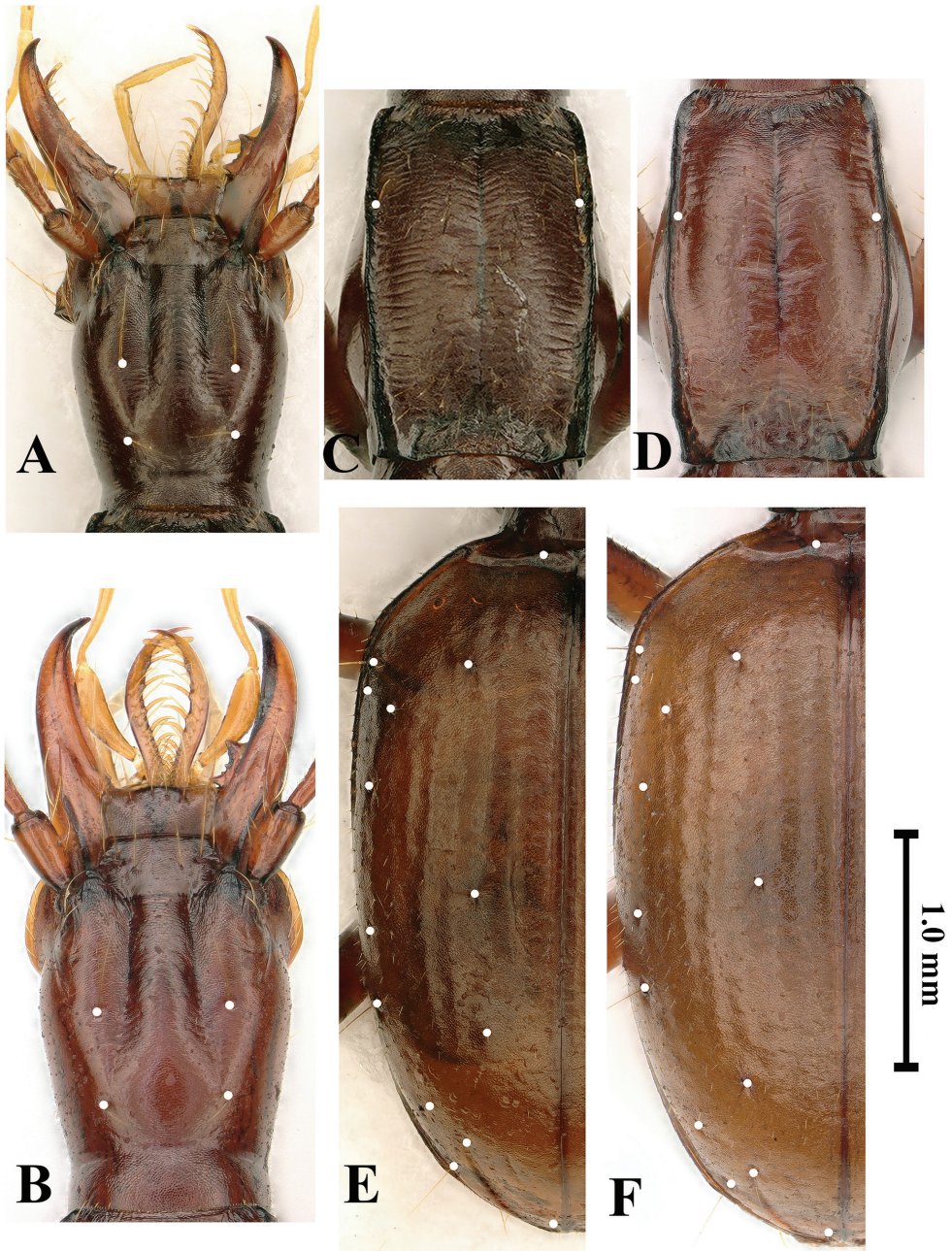


Figure 4. Shapes and chaetotaxy of head, pronotum and elytra of *Haixiaphaenops jinxiabongae* gen. nov., sp. nov. **A, C, E** holotype from Dawan Dong **B, D, F** paratype from Changtu Dong **A, B** head **C, D** pronotum **E, F** elytra. Scale bar: 1.0 mm (**A–F**).

specimens); frontal furrows nearly parallel-sided in anterior 2/3, then strongly divergent posteriad, ending before posterior supraorbital pores; clypeus transverse, 6-setose, with an additional short seta medially; labrum transverse, nearly straight at front margin,

6-setose; mandibles thin, gently unciform at apex; labial suture absent; mentum 2-setose on each side of tooth at base, mentum base widely concave; labial tooth short, thin and bifid at tip, about half length of lateral lobe; submentum 10-setose; ligula bisetose, paraglossae pubescent; palpomeres moderately elongate, all glabrous except 2nd labial palpomere which is 4-setose (2 on inner margin and other 2 on outer margin at middle); the 2nd labial palpomere 1.3 times as long as 3rd; 3rd maxillary palpomere 1.2 times longer than 4th; suborbital pores near neck constriction; antennae slender and filiform, extending at about apical 1/4 of elytra, densely pubescent from pedicle to 11th antennomere; scape thick, fusiform, smooth but with several rather long setae, slightly shorter than pedicle; 5th and 6th antennomeres longest; antennal ratio (relative length of each antennomere compared with scape in the holotype) as follows: 1st (1.0), 2nd (1.25), 3rd (2.0), 4th (2.0), 5th (2.25), 6th (2.25), 7th (2.0), 8th (2.75), 9th (1.85), 10th (1.5) and 11th (2.0).

Prothorax (Fig. 4C, D) longer than wide, PrL/PrW = 1.25–1.45; distinctly wider than pronotum, PrW/PnW = 1.14–1.23; much shorter than head including mandibles, PrL/HLm = 0.6–0.70, or as long as head excluding mandibles; propleura tumid, widest at about 2/5 from base. Pronotum as wide as head; much longer than wide, PnL/PnW = 1.51–1.64, widest at about middle, sides nearly parallel-sided; lateral margins distinctly reflexed throughout, front angles obtusely rectangular, hind angles sharply angulate; anterior lateral setae at about 2/7 from front margin, posterior setae absent; both base and front unbordered, the former anterior margin is subrectilinear, basal margin emarginate medially, convex laterally; disc slightly convex, surface with short and transversal striations; basal foveae large and deep, reverse triangular in shape. Scutellum short and wide.

Elytra (Fig. 4E, F) ovate and stout, much wider than prothorax, EW/PrW = 2.10–2.18, much longer than wide, EL/EW = 1.52–1.60, widest at about basal 1/3 of elytra, extraordinarily convex, lateral margins of subapical portion invisible from above; humeri broadly rounded; lateral margins ciliate throughout; base bordered; striae easily traceable though punctures absent, apical striole well marked, ended at about apical 1/7 of elytra, in the joint area of 5th and 6th striae; intervals convex; chaetotaxy: basal pores present, along both sides of scutellum at apex; three discal pores present near position of 4th stria, anterior and posterior pores at about 1/5 and 2/7 of elytra from base and from apex respectively, median pore near middle of elytra; humeral set of marginal umbilicate pores not aggregated, only 2nd and 3rd pores close to marginal gutter; 1st pore transversely and backwardly shifted to site of 6th interval, far behind level of 3rd pore, making 4th pore closer to 1st than to 3rd; locations of middle set (5th and 6th pores) behind middle of elytra, not close to each other; umbilicate seta 8 clearly visible; angulo-apical pore present.

Legs quite stout, tibiae not longitudinally furrowed; protarsi short, 1st protarsomere elongated and widened, denticulate on inner side of apex in male; 1st tarsomere shorter than, subequal to, and longer than 2nd–4th tarsomeres combined in pro-, meso- and metatarsi, respectively.

Ventrites IV with a pair, V–VI each with two pairs of paramedial setae, VII 6-setose apically in male.

Male genitalia (Fig. 5): Median lobe of aedeagus short and stout, moderately sclerotized, with a large sagittal aileron and a large and elongated copulatory piece; ventral

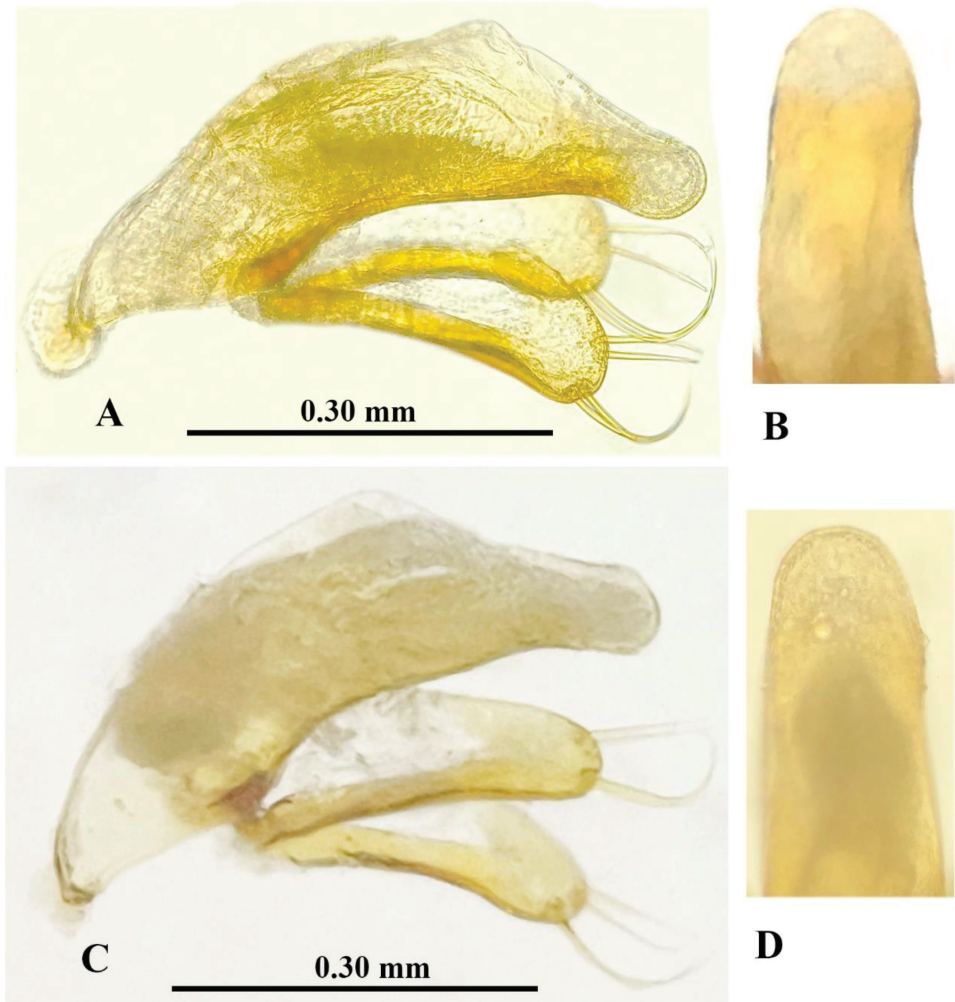


Figure 5. Male genitalia of *Haixiaphaenops jinxiaohongae* gen. nov., sp. nov. **A, B** holotype from Dawan Dong **C, D** paratype from Changtu Dong.

margin hardly sinuate, base opening wide, apex broadly rounded; parameres long and broad, but shorter than median lobe, each with four long setae at apex; in dorsal view, apical lobe rounded at apex, nearly as long as wide.

Female: unknown.

Etymology. This species is dedicated to Ms Xiaohong Jin, an active member of Haixia Caving, Guiyang, who found and collected the unique known specimen.

Variations. Both of the paratype specimens have a slightly thinner head than the holotype, and whole body concolorous brown instead of dark brown. Presently, we deal

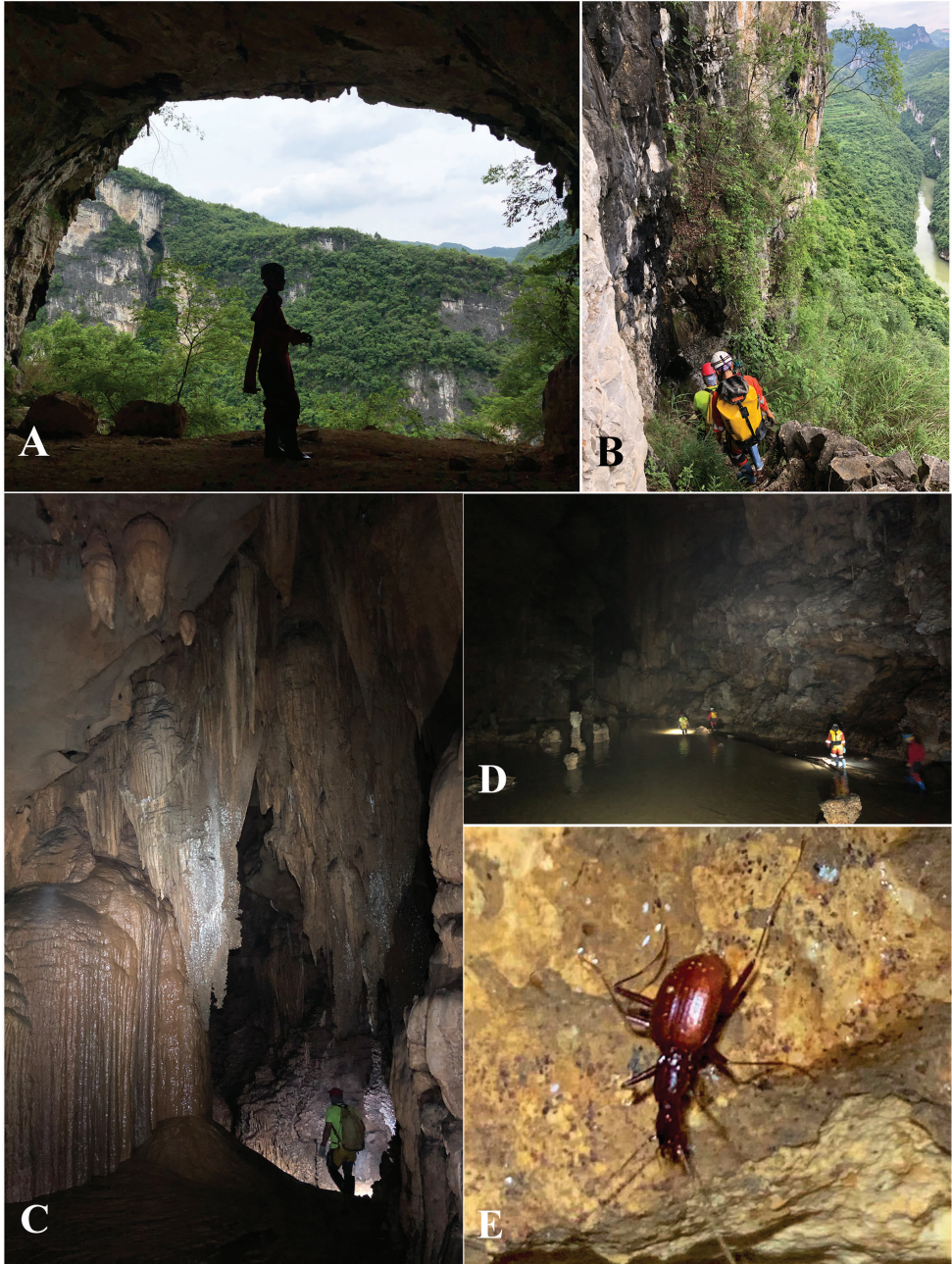


Figure 6. Dawan Dong cave, the type locality of *Haixiaphaenops jinxiabongae* gen. nov., sp. nov. **A, B** Entrances and environs **C, D** scenes inside the cave **E** a running individual of *H. jinxiabongae* sp. nov. in the cave, courtesy of Mr Chengang Wang.

with the differences as individual variations regarding the facts that the similarities of morphological and genital structures, and the caves Dawan Dong and Changtu Dong are close to each other. Molecular analysis would be helpful to clarify their relationship.

Distribution. China (Guizhou). Known from two limestone caves: Dawan Dong and Changtu Dong in the suburb of Guiyang (Fig. 1).

Located in the northern most part of Qingzhen Shi, about 45 km from the main town, Dawan Dong (Fig. 6A) in openings of a cliff of the Maotiaohe valley, on the western side of the river (Fig. 6B). This beautiful cave is 2026 m long, 10–30 m wide and 10–50 m high (Zhao Fei, pers. comm.), with large galleries and several huge chambers (Fig. 6C, D). The single specimen was found running on the ground in a moist and dark area about 500 m from the entrance (Fig. 6 E). Other cave invertebrates found in this cave were woodlice, harvestmen and crickets.

Cave Changtu Dong (Fig. 7) is located about 3.5 km from Dawan Dong in the west, and about half a kilometre from Ximi Village. The cave has two entrances, its length is still unknown. It has been badly impacted and not so pristine as Dawan Dong. Most of the main passage from the smaller entrance is wet and favourable for cave fauna (Fig. 7A, B). The single specimen of *H. jinxiaohongae* gen. nov., sp. nov. was collected together with harvestmen, moths, and millipedes of the genera *Pacidesmus* and *Glyphiulus* along the main passage (Fig. 7C–G).

Genus *Zhijinaphaenops* Uéno & Ran, 2002

Zhijinaphaenops zhaofei sp. nov.

<http://zoobank.org/4A45AFCB-A77F-41B0-A2E8-5E57CDCAFF35>

(Chinese name: 赵飞盲步甲)

Figures 8, 9A, E, 10A, B, 11

Type material. *Holotype* male: Guizhou, Guiyang, Xifeng, Jiuzhuang, Changtu Dong cave (贵州省贵阳市息烽县九庄镇张口洞), 27°11'N, 106°29'E, 1008 m, 2019–VI–08, leg. Jingli Cheng & Mingyi Tian.

Diagnosis. A medium-sized *Zhijinaphaenops* species, body concolorous reddish brown, antennae very long, extending over elytral apices.

Description. Length: 5.8 mm (including mandibles); width: 1.7 mm. Habitus as in Figure 8.

Body reddish brown, palps and tarsi pale. Head covered with sparse and short hairs, whole disc of pronotum covered with dense and long setae; elytra densely pubescent, except glabrous at apical portion; genae, ventral head and prosternum with a few setae; meso- and metasterna and hind coxae dense setose; abdominal ventrites covered with dense and short pubescence.

Microsculptural engraved meshes isodiametric on labrum and base of frons, moderately transverse on vertex and more or less transversally striate on pronotum and elytra. Elytra rather stout, fore body (including mandibles) as long as elytra.

Head (Fig. 9A) moderately elongated, distinctly longer than wide, HLm/HW = 2.25, Hll/HW = 1.66; widest at about middle; sub-parallel-sided, frons and ver-

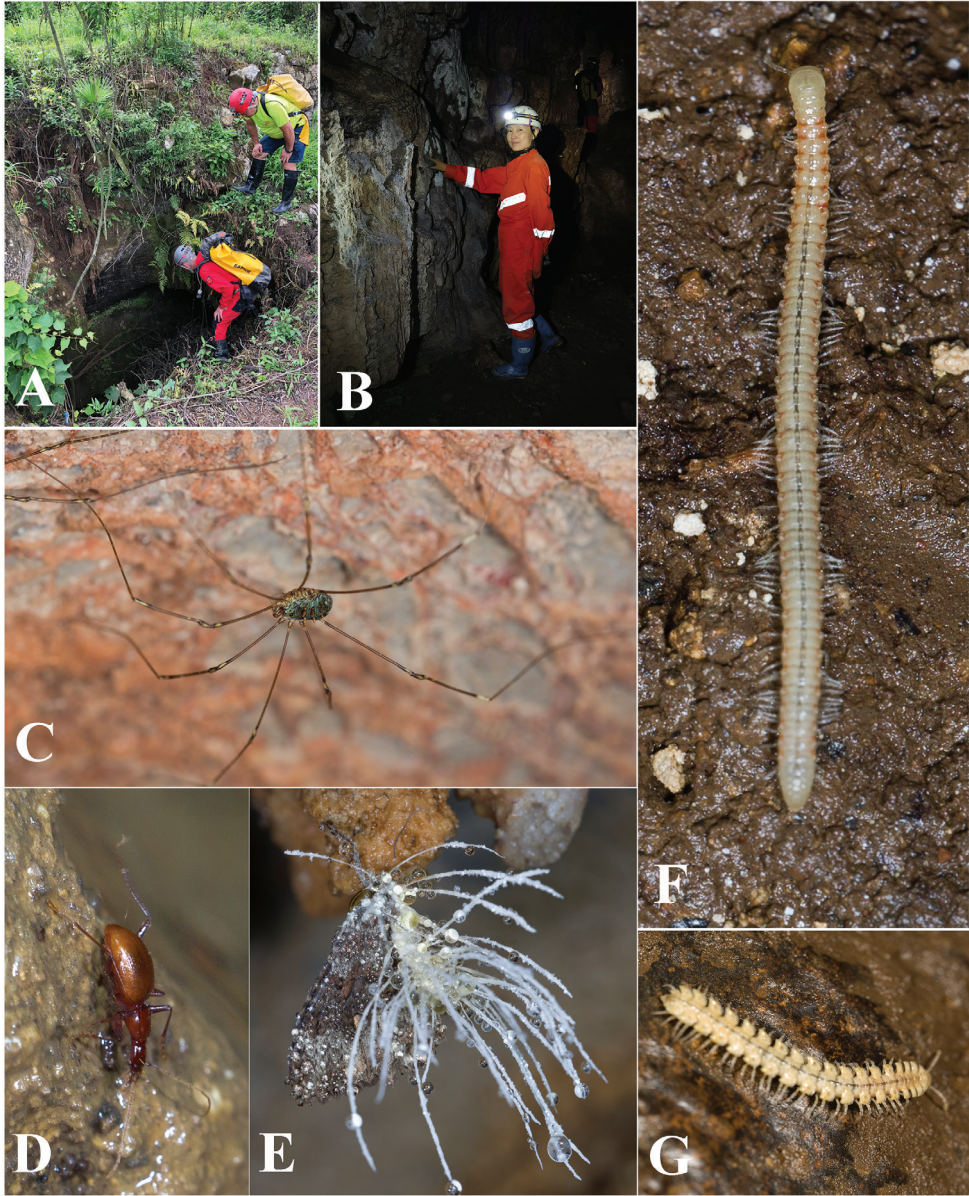


Figure 7. Changtu Dong cave, another locality of *Haixiaphaenops jinxiaohongae* gen. nov., sp. nov. **A** one of the entrances **B** Xiaohong Jin is collecting in the cave **C** a harvestman **D** a running individual of *H. jinxiaohongae* gen. nov., sp. nov. **E** *Cordyceps* fungus growing on a *Triphosa* moth **F** millipede *Glyphiulus* sp. **G** millipede *Pacidesmus* sp.

tex moderately convex; frontal furrows nearly parallel-sided in anterior 2/3, then strongly divergent posteriad, ending before posterior supraorbital pores; anterior supraorbital pores absent; clypeus transverse, 6-setose; labrum transverse, front margin shallowly bisinuate, 6-setose; mandibles thickened, feebly unciform at apex, right



Figure 8. Habitus of *Zbijnaphaenops zhaofei* sp. nov., holotype, male.

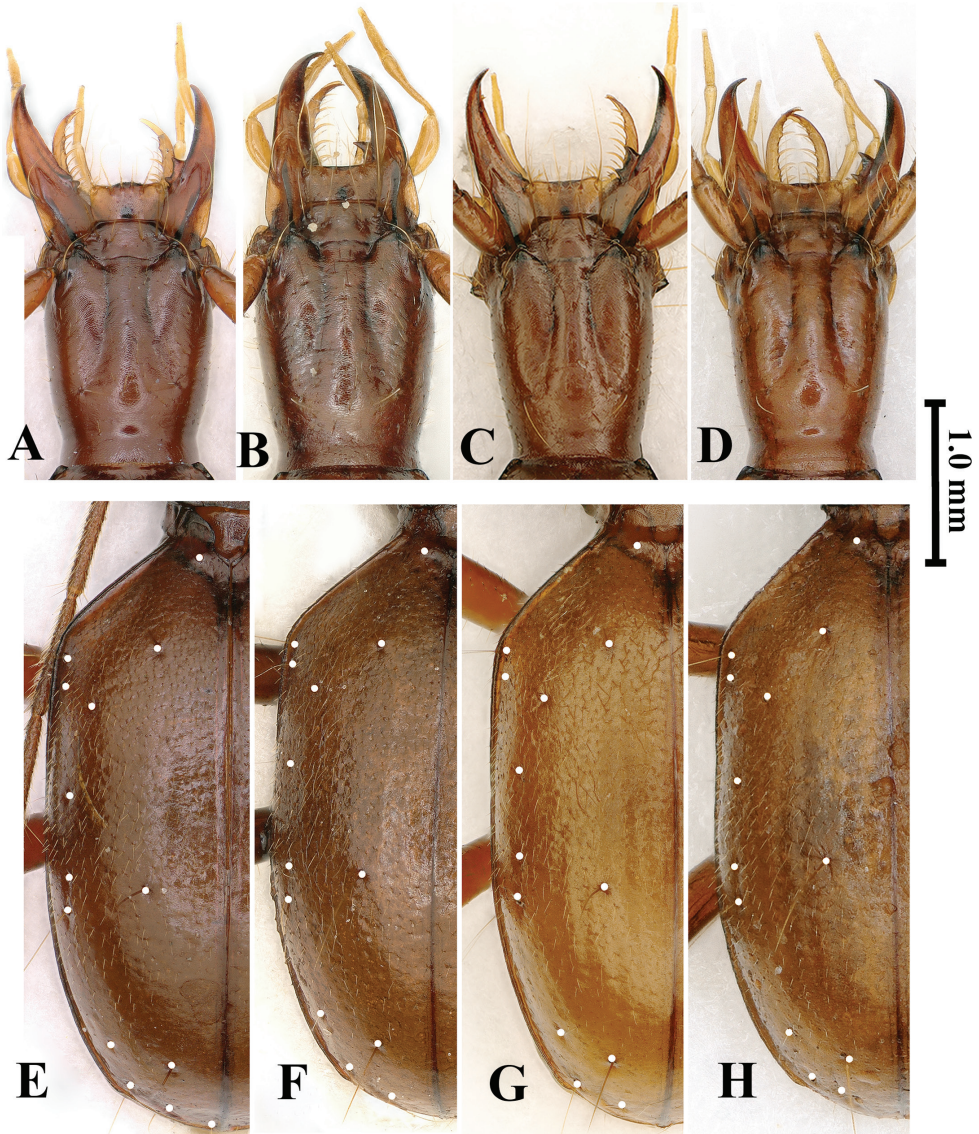


Figure 9. Head (**A–D**) and elytral chaetotaxy (**E–H**) of *Zhijinaphaenops* species **A, E** *Z. zhaofeii* sp. nov. **B–D, F–H** *Z. jingliae* **B, F** from Zhangkou Dong in Musan, type locality **C, G** from Mafen Dong **D, H** from Wenquan Dong. Scale bar: 1.0 mm (**A–H**).

mandibular tooth bidentate; labial suture completely disappeared; mentum 2-setose, base widely concave, tooth short, thin and bifid at tip; submentum 9-setose; ligula 2-setose at apex; palpomeres moderately long and slender, glabrous except 2nd labial palpomere bisetose on inner margin, with an additional seta on outer margin near apex; 2nd labial palpomere 1.15 times as long as 3rd, whereas 3rd maxillary one 1.20 times longer than 4th; suborbital setae close to base of head; antennae slender

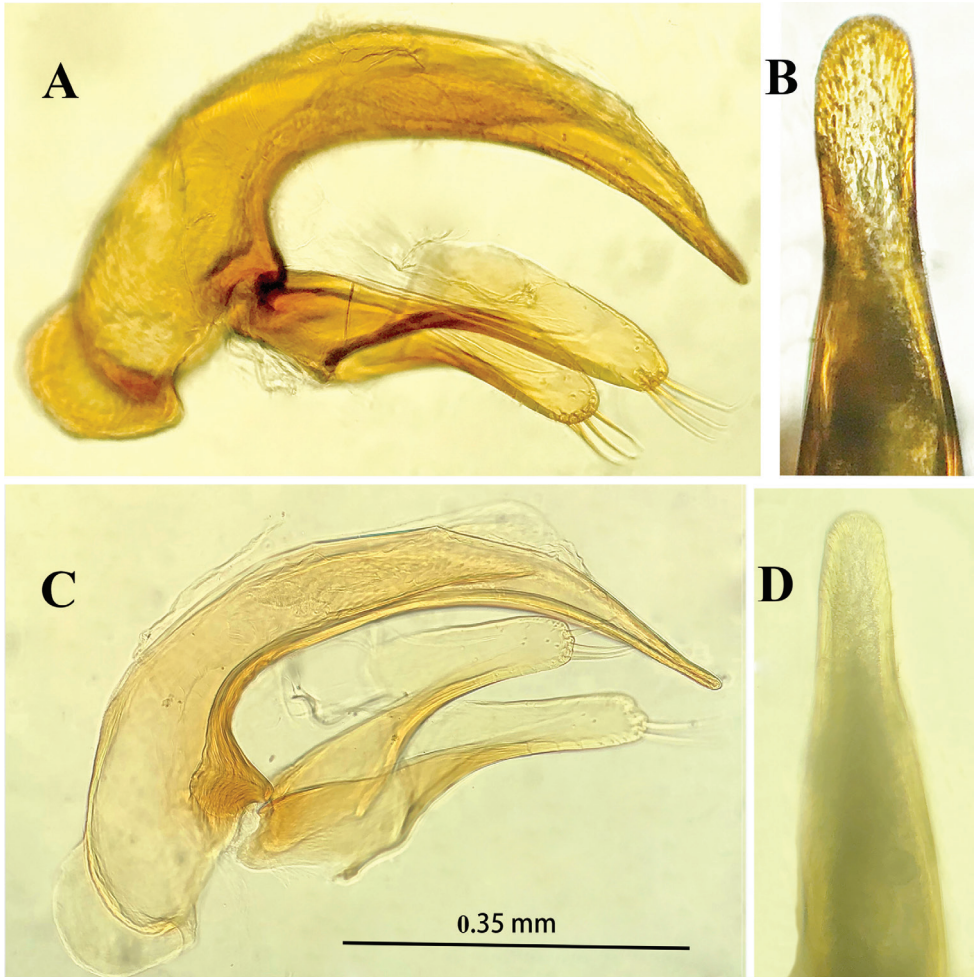


Figure 10. Male genitalia of *Zhijinaphaenops* species, lateral view and apical lobe in dorsal view **A, B** *Z. zhaofei* sp. nov. **C, D** *Z. jingliae* Deuve & Tian, 2015. Scale bar for **A–D**.

and elongate, 11th antennomere and part of 10th antennomere extending over elytral apices; scape thick, fusiform, with several rather long setae, pedicle the shortest; antennomeres densely pubescent from pedicle to 11th; 3rd antennomeres longest; relative length of each antennomere compared with pedicle in the holotype as follows: 1st (1.27), 2nd (1.00), 3rd (2.57), 4th (2.38), 5th (2.46), 6th (2.22), 7th (2.10), 8th (1.83), 9th (1.75), 10th (1.60) and 11th (1.89).

Prothorax longer than wide, PrL/PrW = 1.14; distinctly wider than pronotum, PrW/PnW = 1.19; shorter than head, PrL/HLm = 0.68, PrL/HLl = 0.92, propleura

strongly tumid, widest at about 2/5 from base. Pronotum wider than head, PnW/HW = 1.15; longer than wide, PnL/PnW = 1.35, sides bordered and reflexed throughout, more reflexed near base, widest at about 3/5 from base, more constricted anteriorly, gently contracted backwards, then shallowly sinuate before hind angles; fore angles obtuse, hind angles rectangular; base and front straight, unbordered, and subequal in width; anterior lateral setae at about 1/4 from front, posterior setae absent; disc slightly convex, basal foveae large and deep. Scutellum moderate in size.

Elytra (Fig. 9E) elongated ovate, strongly convex though lateral margins visible throughout from above; much wider than prothorax, EW/PrW = 1.88, much longer than wide, EL/EW = 1.64, widest at about middle; humeral angles broadly rounded; lateral margins finely bordered throughout, smooth, not ciliate; base unbordered, apical striole absent; striae not easily traceable; intervals faintly convex; chaetotaxy (Fig. 9E), anterior discal pore located at about basal 1/6 of elytra, posterior one at about apical 2/5 of elytra; 7th and 8th pores well marked; angulo-apical pore present.

Legs rather long for a *Zhijinaphaenops* species, fore and middle tibiae longitudinally furrowed; the 1st protarsomere in male elongated and widened, denticulate on inner side of apex; 1st tarsomere as long as 2nd–4th tarsomeres combined in all legs.

Ventrites IV with 2 pairs, V and VI each with 3 pairs of paramedial setae, VII 6-setose apically.

Male genitalia (Fig. 10A, B): Median lobe of aedeagus short, moderately sclerotized, with a large sagittal aileron and a large and elongated copulatory piece which is about 1/4 of median lobe in length; ventral margin strongly sinuate, then tapering toward apex which is blunt; base opening rather narrow, apical lobe narrow, much longer than wide, broadly rounded at apex; parameres long and broadly widened, but shorter than median lobe, each with 3 long setae at apex.

Female: unknown.

Remarks. Similar to *Zhijinaphaenops jingliae* Deuve & Tian, 2015, but *Z. zhaofeii* sp. nov. differs in having a wider head, with labrum bisinuate instead of nearly straight, mandibles less hooked at tips and a median lobe with a broader apex in dorsal view.

Etymology. In honor of Mr Fei Zhao, a young active caver in Guiyang.

Distribution. China (Guizhou). Known only from limestone cave Zhangkou Dong, in the suburb of Guiyang (Fig. 1).

Located in the northwestern part of Xifeng County, Zhangkou Dong (Fig. 11) on the southern bank of the Wujiang River. The entrance (Fig. 11A) is close to the main road from Jiuzhuang town to the dock. The passage goes obliquely down to the inner part of the cave, with a small creek inside. It is a rather beautiful cave, but partly damaged by the villagers. The habitat remains favourable for cave animals (Fig. 11B, C). The single beetle was found under a stone in a muddy area about 100 m from the entrance (Fig. 11D). Other cave invertebrates found in this cave were millipedes of *Pacidesmus* and *Glyphiulus* (Fig. 11E, F), a mite (Fig. 11G), moths and crickets.

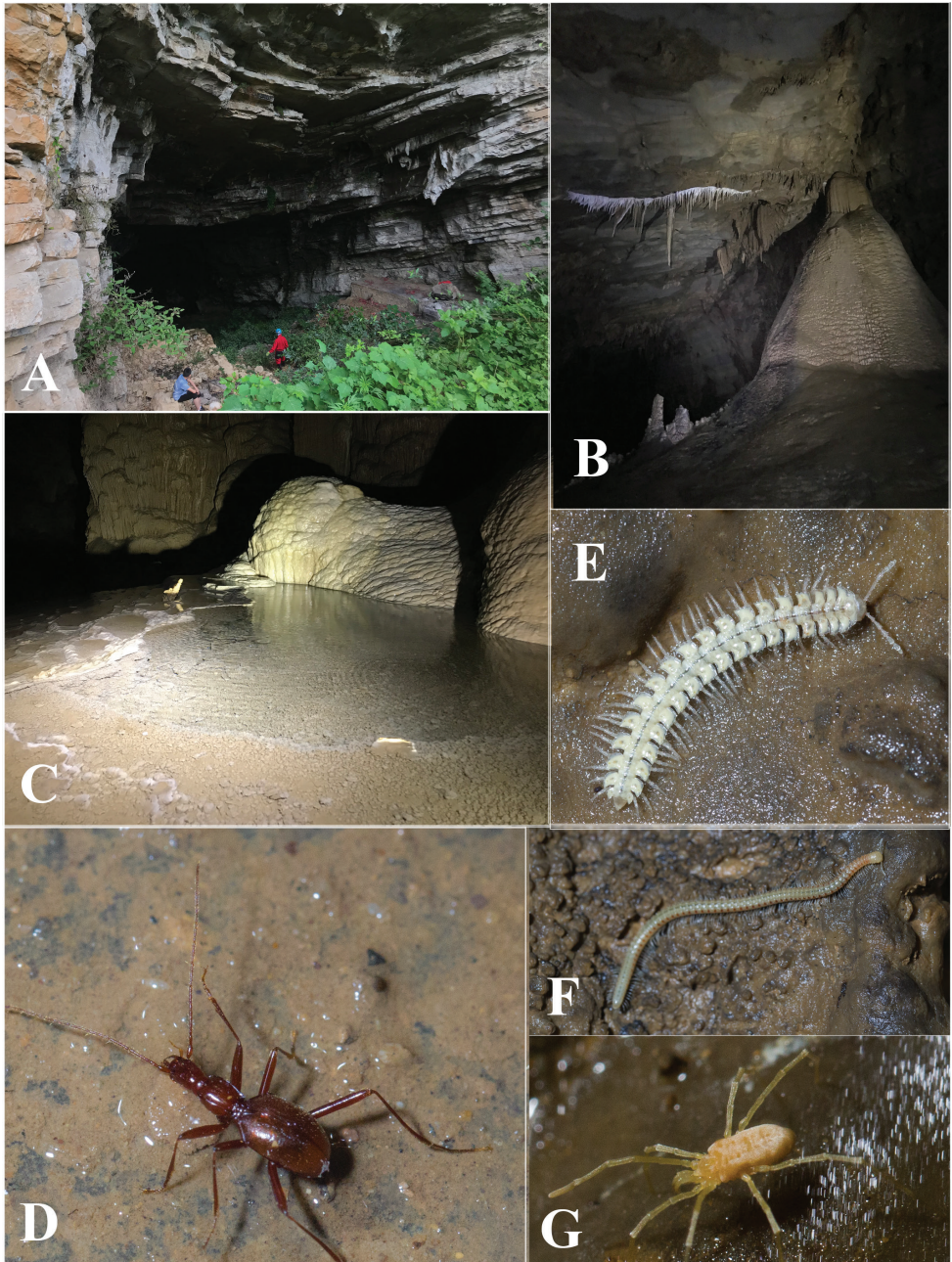


Figure 11. Zhangkou Dong cave, type locality of *Zhijinaphaenops zhaofei* sp. nov. **A** entrance **B, C** scenes inside the cave **D** a running individual of *Zhijinaphaenops zhaofei* sp. nov. **E** millipede *Pacidesmus* sp. **F** millipede *Glyphiulus* sp. **G** a mite.

***Zhijinaphaenops jingliae* Deuve & Tian, 2015**

(Chinese name: 景丽织盲步甲)

Figures 1, 9B–D, F–H, 10C, D, 12, 13

Zhijinaphaenops jingliae Deuve & Tian, 2015: 397

Material. 2 males & 1 female, Guizhou: Guiyang, Xifeng, Xishan, Shenli, Mafen Dong cave (息烽县西山镇马粪洞), 27°04'N, 106°37'E, 1157 m, 2020–II–29, leg. Guangyuan Cheng; 1 male, Guizhou, Guiyang, Xifeng, Xinlong, Wenquan Dong (息烽县温泉镇温泉洞), 27°11'N, 106°49'E, 916 m, 2020–VII–18, leg. Jingli Cheng.

Diagnosis. A medium-sized *Zhijinaphaenops* species, wholly brown and pubescent, head narrow, with thin and very long antennae which extend beyond of elytral apices. Habitus as in Figure 12 A.

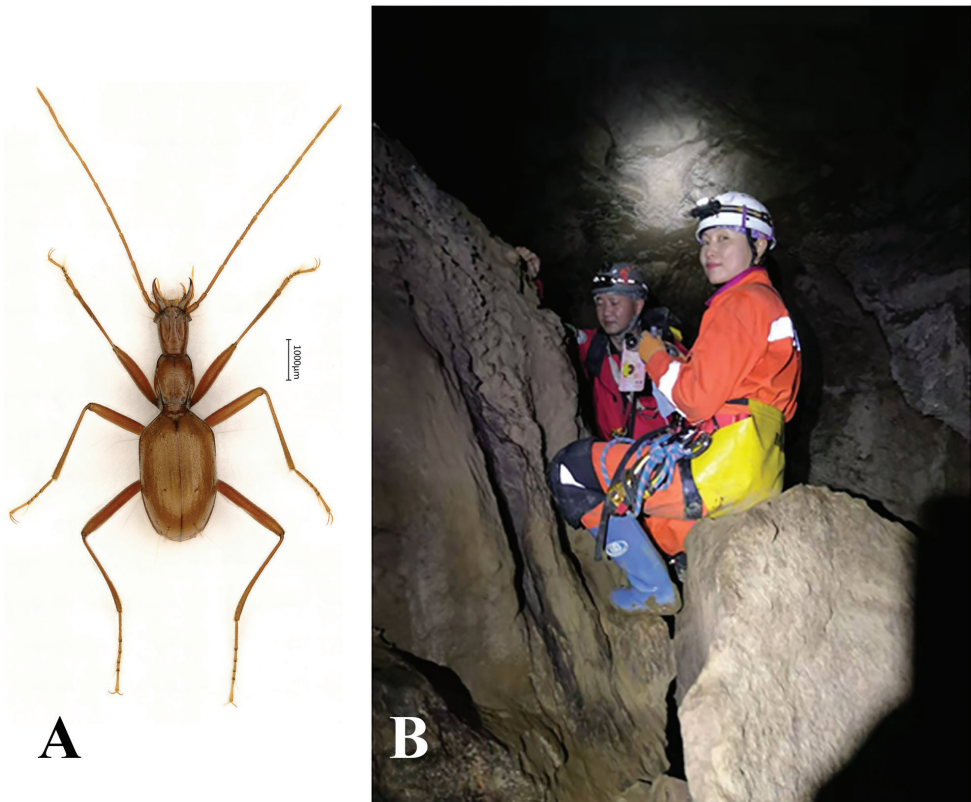


Figure 12. Mafen Dong cave, a new locality of *Zhijinaphaenops jingliae* Deuve & Tian, 2015 **A** habitus of a male beetle discovered in Mafen Dong **B** place where beetles were discovered.

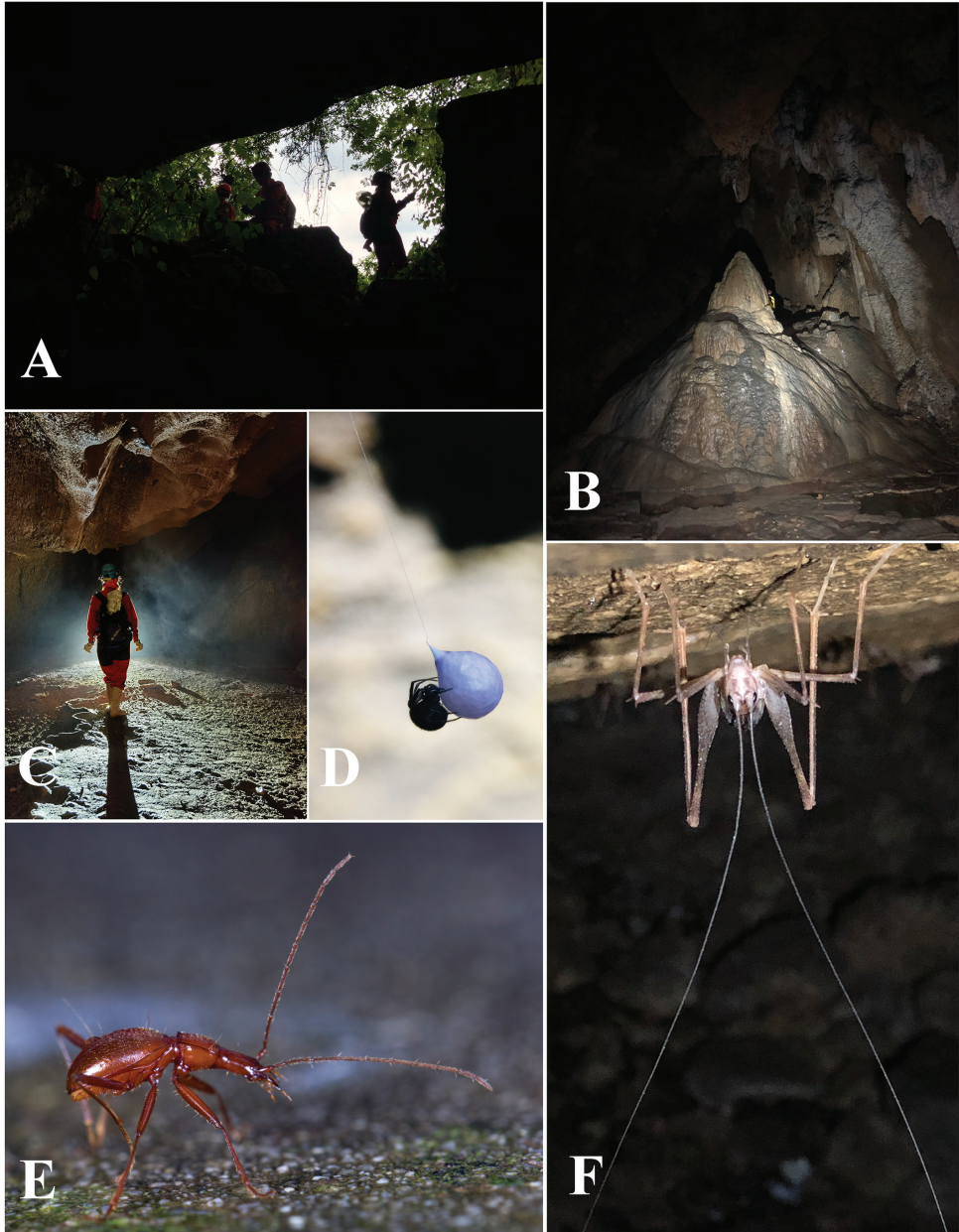


Figure 13. Wenquan Dong cave, a locality of *Zhijinapbaenops jingliae* Deuve & Tian, 2015 and its sympatric arthropods **A** entrance **B, C** environ inside cave **D** a spider with an egg sac **E** a running individual of *Z. jingliae* **F** a *Tachycines* cricket.

Remarks. *Zhijinaphaenops jingliae* was recorded from Zhangkou Dong cave near Musa village, Shidong Zhen, Xifeng County (Deuve and Tian 2015). In 2020, this species was found in two caves of the same county, Mafen Dong (Xishan Zhen) and Wenquan Dong (Wenquan Zhen). Morphological characteristics including male genitalia of individuals from the above two caves are identical to the holotype specimen (Figs 9B–D, F–H, 10C, D).

Distribution. China (Guizhou). Known from three limestone caves in Xifeng County, northern Guiyang (Fig. 1).

Mafen Dong cave (Fig. 12B) is about 600 m from Mafen village, only 5 km away Zhangkou Dong cave in the east. The individuals of *Z. jingliae* were found running on the ground in a dark area not far from the entrance.

Wenquan Dong cave is near Xinglong village, about 30 km from Zhangkou Dong. It opens via quite large entrance in a small hill of a valley and is surrounded by bushes, (Fig. 13A). There are two large chambers inside and a main passage about two hundred meters long. There is a pool at the bottom of the first chamber. A large part of the cave is moist and maintains good conditions for cave animals (Fig. 13B, C). Apart from the single beetle of *Zhijinaphaenops jingliae*, other cave arthropod animals found in this cave were spiders and crickets (Fig. 13D–F).

Genus *Sinaphaenops* Uéno & Wang, 1991

Sinaphaenops chengguangyuani Ma et al. 2020

(Chinese name: 程广源华盲步甲)

Figures 1, 14, 15

Sinaphaenops chengguangyuani Ma et al. 2020: 582

Material. 1 male & 4 females, Guizhou, Guiyang, Nanming, Yunguan, Jianlonglu, Jianlong Dong cave (贵州省贵阳市南明区见龙洞), 26°32'N, 106°46'E, 1094 m, 2020–VI–26, leg. Guangyuan Cheng, Xiaohong Jin, Chenggang Wang, Yi Zhao & Mingyi Tian; 1 female & 1 male, Guizhou, Qiannan Miao & Buyi Autonomous Prefecture, Longli, Duocai Dong (贵州省黔南布依族苗族自治州龙里县多彩洞), 26°34'N, 106°59'E, 1555 m, 2021–VIII–14, leg. Guangyuan Cheng.

Distribution. China (Guizhou). Known from three limestone caves in Guiyang Shi and Longli County, Qiannan Buyi & Miao Autonomous Prefecture (Fig. 1).

This species was described from Shuijing Dong cave, Longli County, Qiannan Buyi & Miao Autonomous Prefecture (Ma et al. 2020). Then it was found in Jianlong Dong, Guiyang and Duocai Dong, Longli.

Jianlong Dong cave (Fig. 14) is located at the eastern suburb of Guiyang, about 40 km from Shuijing Dong, the type locality of *S. chengguangyuani*. This cave is a municipal protected area because of the engraved inscriptions on the precipices inside dating from

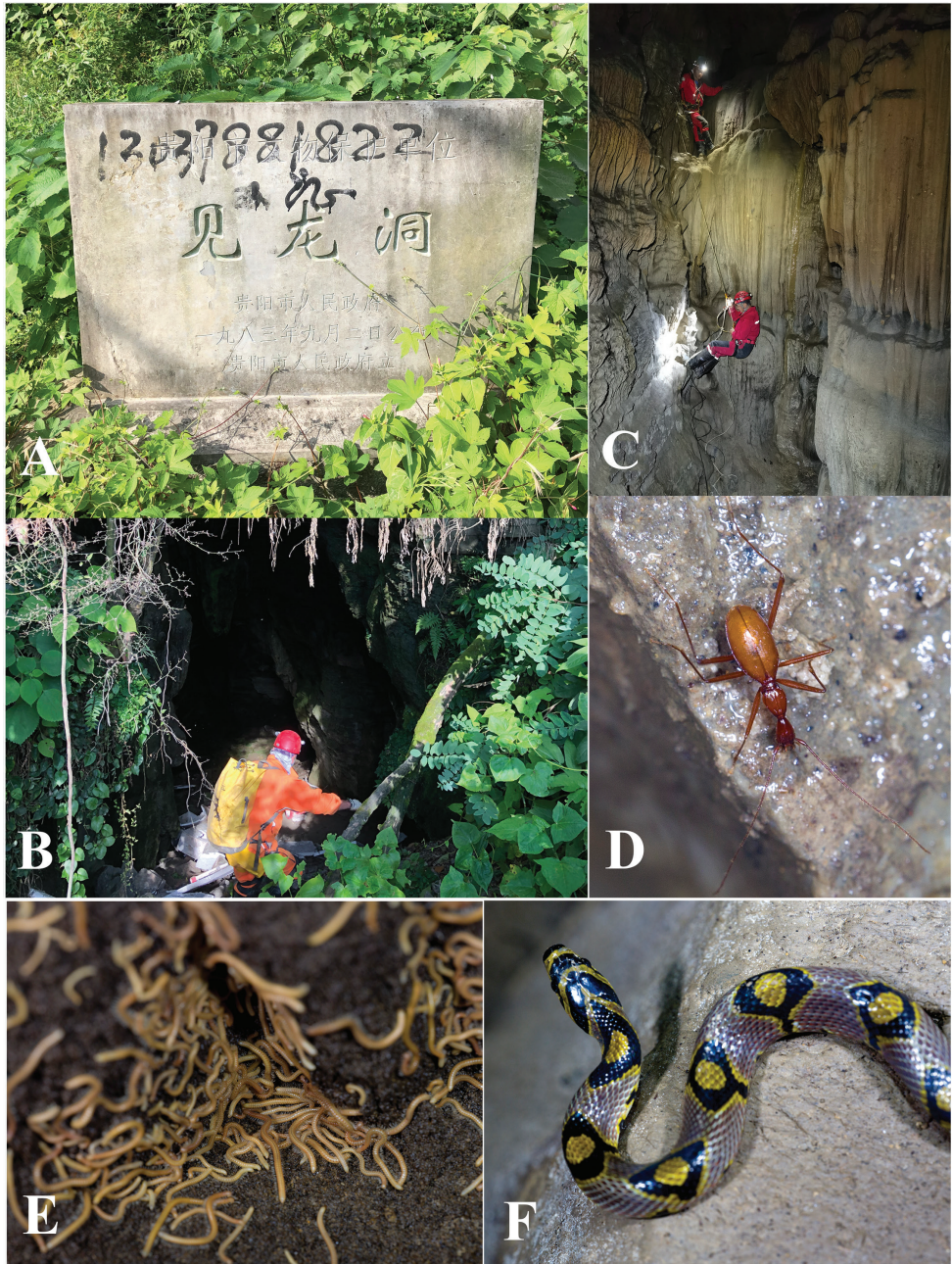


Figure 14. Jianlong Dong cave, a new locality of *Sinaphaenops chengguangyuani* Ma et al. 2020 **A** a monument indicating that the cave is under protection **B** entrance **C** stalagmites in the inner chamber **D** a running beetle of *S. chengguangyuani* **E** millipedes of *Glyphiulus* sp. **F** a snake *Elaphe mandarina* (Cantor, 1842).



Figure 15. A running individual of *Sinaphaenops chengguangyuani* Ma et al. 2020 inside Duocai Dong cave.

the Ming Dynasty, over 400 years ago (Fig. 14A). The rather large entrance is just on the side of the road Jianlonglu (Fig. 14B). The cave is about 100 m long, with two chambers inside. The first half part is rather dry, then becomes wet in the inner part (Fig. 14C). All of the beetle individuals were collected in the inner part, running on the ground or on the wall. Other cave animals observed in this cave were millipedes (*Glyphiulus* sp., Fig. 14E), a snake (*Elaphe mandarina* Cantor, 1842; Fig. 14F), crickets and moths.

Duocai Dong is a stalagmite-rich cave, about 5 km from Shuijing Dong in straight line. The two individuals were collected in dark zone, running on the wall (Fig. 15).

Acknowledgements

First of all, we are grateful to Ms Xiaohong Jin, Mr Chenggang Wang (both are senior members of Haixia Caving, Guiyang) and Ms Yi Zhao (SCAU team member, Guangzhou) for their efforts and assistance during the biological surveys. We thank Mr Fei Zhao (an active caver in Guiyang) for providing useful information about caves Dawan Dong and Zhangkou Dong. We thank also Drs Arnaud Faille (Stuttgart State Museum of Natural History, Stuttgart), Igor A. Belousov and Ilya I. Kabak (All-Russian Institute of Plant Protection, St. Petersburg,) for their critical remarks and constructive suggestions to improve the quality of the manuscript.

This study was sponsored by a project of the National Foundation of Natural Science of China (NSFC, Grant no. 41871039).

References

- Chen JJ, Tang MR, Yang PJ, Tian MY (2017). Contribution to the knowledge of the aphaenopsian genus *Sinaphaenops* Uéno et Wang, 1991 (Coleoptera: Carabidae: Trechini). *Zootaxa* 4227(1): 106–118. <https://doi.org/10.11646/zootaxa.4227.1.6>
- Chen MZ, Huang SB, Tian MY (2020) A new species of the aphaenopsian genus *Sinaphaenops* Uéno and Wang, with notes on male genitalia of *S. orthogenys* Uéno (Coleoptera: Carabidae: Trechini). *The Coleopterists Bulletin* 74(2): 1–8. <https://doi.org/10.1649/0010-065X-74.2.343>
- Deuve T, Tian MY (2014) Un nouveau Trechini aphénopsien dans l'ouest du Guizhou (Coleoptera, Caraboidea). *Bulletin de la Société entomologique de France*, 119(3): 319–322. <https://doi.org/10.3406/bsef.2014.2448>
- Deuve T, Tian MY (2015) Trois nouveaux Trechidae troglobies anophtalmes des karsts du Guizhou et du Zhejiang, en Chine (Coleoptera, Caraboidea). *Bulletin de la Société entomologique de France* 120(3): 397–402. <https://doi.org/10.3406/bsef.2015.2259>
- Deuve T, Tian MY (2018) Nouveaux Trechini cavernicoles du Guizhou nord-occidental des genres *Zhijinaphaenops* et *Guizhaphaenops* (Coleoptera, Trechidae). *Bulletin de la Société Entomologique de France* 123(3): 333–339. https://doi.org/10.32475/bsef_2039
- Huang SB, Tian MY, Faille A (2020) Three new species of the aphaenopsian trechine genus *Pilosaphaenops* Deuve & Tian, 2008 from South China Karst (Coleoptera: Carabidae: Trechinae). *Annales de la Société entomologique de France (N. S.)* 56(3): 203–214. <https://doi.org/10.1080/00379271.2020.1771203>
- Ma ZJ, Huang SB, Tian MY (2020) Two new species of cavernicolous trechines from central Guizhou and northwestern Guangxi, China (Coleoptera: Carabidae: Trechinae). *Zootaxa* 4861(4): 581–593. <https://doi.org/10.11646/zootaxa.4861.4.6>
- Tian MY, Huang SB, Wang XH, Tang MR (2016) Contributions to the knowledge of subterranean trechine beetles in southern China's karsts: five new genera (Insecta: Coleoptera: Carabidae: Trechini). *ZooKeys* 564: 121–156. <https://doi.org/10.3897/zookeys.564.6819>
- Tian MY, Chen MZ, Ma ZJ (2020) A new anophthalmic trechine genus and two new species from southern Guizhou, China (Coleoptera: Carabidae: Trechini). *Zootaxa* 4766(4): 575–587. <https://doi.org/10.11646/zootaxa.4766.4.4>
- Tian MY, Huang SB, Ma ZJ (2021) Two remarkable new genera and species of cavernicolous ground beetles from Guizhou Province, southwestern China (Coleoptera: Carabidae: Trechinae). *Annales de la Société entomologique de France (N.S.)*, 57(2): 165–172. <https://doi.org/10.1080/00379271.2021.1881917>
- Uéno SI (2002) New *Sinaphaenops* (Coleoptera, Trechinae) from southern Guizhou, with notes on *Thaumastaphaenops pulcherrimus*. *Elytra* 30: 57–72.
- Uéno SI, Wang FX (1991) Discovery of a highly specialized cave trechine (Carabidae, Trechinae) in Southeast China. *Elytra* 19(1): 127–135.
- Uéno SI, Ran JC (1998) Notes on *Sinaphaenops* (Coleoptera, Trechinae), with descriptions of two new species. *Elytra* 26: 51–59.
- Uéno SI, Ran JC (2002) A new genus with three new species of aphaenopsoid trechine beetles (Coleoptera, Trechinae) from Western Guizhou, South China. *Journal of the speleological Society of Japan* 27: 42–59.